

**EFFICACY OF GREEN TEA POLYPHENOL- EPIGALLOCATECHIN
GALLATE (EGCG) FOR THE MANAGEMENT OF DIABETES
MELLITUS IN ZEBRAFISH MODEL**

by

AJUNGLA JAMIR

Reg. No. 00289/2018



Submitted to

NAGALAND UNIVERSITY

*In Partial Fulfilment of the Requirements for
Award of the Degree of*

**DOCTOR OF PHILOSOPHY
IN ZOOLOGY**

**DEPARTMENT OF ZOOLOGY
SCHOOL OF SCIENCES
NAGALAND UNIVERSITY
LUMAMI – 798627
NAGALAND, INDIA**

MAY, 2024



नागालैण्ड विश्वविद्यालय

NAGALAND UNIVERSITY

(संसद द्वारा पारित अधिनियम 1989, क्रमांक 35 के अंतर्गत स्थापित केंद्रीय विश्वविद्यालय)

(A Central University established by an Act of Parliament No. 35 of 1989)

मुख्यालय : लुमामी, जिला : जुन्हेबोटो (नागालैण्ड), पिनकोड – 798627

Hqrs: Lumami, Dist. Zunheboto (Nagaland), PIN Code – 798627

DEPARTMENT OF ZOOLOGY / प्राणी विज्ञान विभाग

Dr. Pranay Punj Pankaj / डॉ. प्रणय पुंज पंकज

Mobile: +91-977116290

Associate Professor / सह प्राध्यापक

E-mail: pranaypunj@gmail.com

CERTIFICATE

This is to certify that the work presented in this thesis titled, “**Efficacy of green tea polyphenol-epigallocatechin gallate (EGCG) for the management of diabetes mellitus in zebrafish model**” submitted to Nagaland University, Lumami, is an authentic record of the research work carried out by **Ms. Ajungla Jamir**, under my supervision in the Department of Zoology, and that the work has not been submitted for the award of any other degree or diploma from any other university.

Dated: 31/05/2024

Place: NU, Lumami

Dr. Pranay Punj Pankaj

Associate Professor

Department of Zoology

Nagaland University, Lumami

Nagaland- 798627



नागालैण्ड विश्वविद्यालय

NAGALAND UNIVERSITY

(संसद द्वारा पारित अधिनियम 1989, क्रमांक 35 के अंतर्गत स्थापित केंद्रीय विश्वविद्यालय)

(A Central University established by an Act of Parliament No. 35 of 1989)

मुख्यालय : लुमामी, जिला : जुन्हेबोटो (नागालैण्ड), पिनकोड – 798627

Hqrs: Lumami, Dist. Zunheboto (Nagaland), PIN Code – 798627

DEPARTMENT OF ZOOLOGY / प्राणी विज्ञान विभाग

DECLARATION

I, **Ms. Ajungla Jamir** bearing Ph.D registration No. 00289/2018, hereby declare that the thesis entitled “**Efficacy of green tea polyphenol-epigallocatechin gallate (EGCG) for the management of diabetes mellitus in zebrafish model**” is a record of work done by me under the supervision of **Dr. Pranay Punj Pankaj**, Associate Professor, Department of Zoology, Nagaland University, Lumami - 798627, and that the thesis has not been submitted, in whole or in part, in any previous application for the award of any degree or diploma of this university or any other university.

Dated: **31.05.2024**

Place: NU, Lumami

(Ms. Ajungla Jamir)

Research Scholar

Department of Zoology

(Prof. Bendang Ao)

Head of Department

Department of Zoology

Nagaland University

Lumami-798627

(Dr. Pranay Punj Pankaj)

Associate Professor

Department of Zoology

Nagaland University

Lumami-798627

विभागध्यक्ष / Head
प्राणि विज्ञान विभाग / Department of Zoology
नागालैण्ड विश्वविद्यालय / Nagaland University
लुमामी / Lumami - 798627

Dr. Pranay P Pankaj
Department of Zoology
Nagaland University

(संसद द्वारा पारित अधिनियम 1989, क्रमांक 35 के अंतर्गत स्थापित केंद्रीय विश्वविद्यालय)
(A Central University established by an Act of Parliament No.35 of 1989)

मुख्यालय : लुमामी | Headquarters : Lumami

PLAGIARISM FREE UNDERTAKING

साहित्यिक चोरी मुक्त शपथ-पत्र

Name of Research Scholar शोधार्थी का नाम	Ms. Ajungla Jamir
Ph.D Registration Number पीएच.डी पंजीयन संख्या	Reg. No. Ph.D/00289/2018
Title of Ph.D thesis पीएच.डी थीसिस का शीर्षक	Efficacy of green tea polyphenol- epigallocatechin gallate (EGCG) for the management of diabetes mellitus in zebrafish model
Name & Institutional Address of the Supervisor शोध-निर्देशक का नाम व संस्थानिक पता	Dr. Pranay Punj Pankaj Department of Zoology, Nagaland University HQ: Lumami-798627, Nagaland
Name of the Department/School विभाग/संकाय का नाम	Department of Zoology/ School of Sciences
Date of Submission प्रस्तुत करने की तिथि	31-05-2024
Date of Plagiarism Check साहित्यिक चोरी की जांच की तारीख	31 May 2024
Percentage of similarity detected by the DrillBit software ड्रिलबिट सॉफ्टवेयर द्वारा खोजी गई समानता का प्रतिशत	4%

I hereby declare/certify that the Ph.D Thesis submitted by me is complete in all respect, as per the guidelines of Nagaland University (NU) for this purpose. I also certify that the Thesis (soft copy) has been checked for plagiarism using **DrillBit** similarity check software. It is also certified that the contents of the electronic version of the thesis are the same as the final hard copy of the thesis. A copy of the Report generated by the **DrillBit** software is also enclosed.

मैं एतद् द्वारा घोषित/प्रमाणित करता/करती हूँ कि पीएच.डी. थीसिस/एम.फिल. इस उद्देश्य के लिए नागालैण्ड विश्वविद्यालय (एनयू) के दिशा-निर्देशों के अनुसार मेरे द्वारा प्रस्तुत शोध प्रबंध सभी प्रकार से पूर्ण है। मैं यह भी प्रमाणित करता/करती हूँ कि थीसिस/शोध-प्रबंध (सॉफ्ट कॉपी) को **ड्रिलबिट** समानता जाँच सॉफ्टवेयर का उपयोग करके साहित्यिक चोरी के लिए जाँचा गया है। यह भी प्रमाणित किया जाता है कि थीसिस / शोध-प्रबंध के इलेक्ट्रॉनिक संस्करण की सामग्री थीसिस / शोध-प्रबंध की अंतिम हार्डकॉपी के समान है। **ड्रिलबिट** सॉफ्टवेयर द्वारा तैयार की गई रिपोर्ट की प्रति भी संलग्न है।

Date/दिनांक: 31.05.2024

Place/स्थान: NU, Lumami

Ajungla
(Ajungla Jamir)

(Name & Signature of the Scholar)
(शोधार्थी का नाम व हस्ताक्षर)

Pranay Punj Pankaj

Dr. Pranay Punj Pankaj

Name & Signature of the Supervisor (With Seal):

शोध-निर्देशक का नाम व हस्ताक्षर (मुहर सहित)

Dr. Pranay P Pankaj
Department of Zoology
Nagaland University



The Report is Generated by DrillBit Plagiarism Detection Software

Submission Information

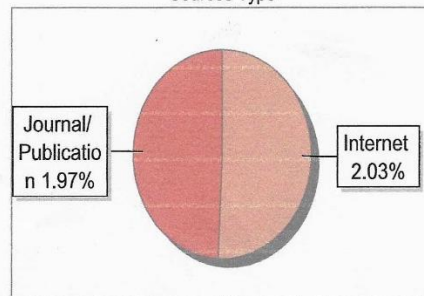
Author Name	Ms. Ajungla Jamir
Title	EFFICACY OF GREEN TEA POLYPHENOL - EPIGALLOCATECHIN GALLATE (EGCG) FOR THE MANAGEMENT OF DIABETES MELLITUS IN ZEBRAFISH MODEL
Paper/Submission ID	1910877
Submitted by	pranaypunj@nagalanduniversity.ac.in
Submission Date	2024-05-31 11:52:09
Total Pages, Total Words	198, 38715
Document type	Thesis

Result Information

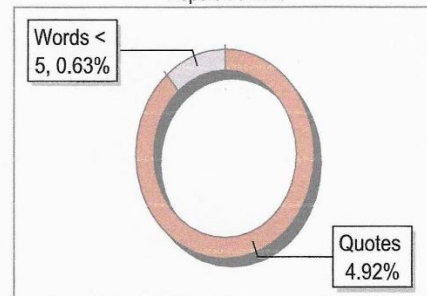
Similarity 4 %



Sources Type



Report Content



Exclude Information

Quotes	Excluded
References/Bibliography	Excluded
Source: Excluded < 5 Words	Excluded
Excluded Source	0 %
Excluded Phrases	Excluded

Database Selection

Language	English
Student Papers	Yes
Journals & publishers	Yes
Internet or Web	Yes
Institution Repository	Yes

A Unique QR Code use to View/Download/Share Pdf File





DrillBit Similarity Report

4

SIMILARITY %

81

MATCHED SOURCES

A

GRADE

A-Satisfactory (0-10%)
B-Upgrade (11-40%)
C-Poor (41-60%)
D-Unacceptable (61-100%)

LOCATION	MATCHED DOMAIN	%	SOURCE TYPE
1	Thesis Submitted to Shodhganga Repository	<1	Publication
2	Thesis Submitted to Shodhganga Repository	<1	Publication
3	Thesis Submitted to Shodhganga Repository	<1	Publication
4	www.ncbi.nlm.nih.gov	<1	Internet Data
5	healthdocbox.com	<1	Internet Data
6	www.ncbi.nlm.nih.gov	<1	Internet Data
8	japsonline.com	<1	Internet Data
9	52.172.27.147 8080	<1	Publication
10	Thesis Submitted to Shodhganga Repository	<1	Publication
12	Therapeutic potential of octyl gallate isolated from fruits of by Latha-2013	<1	Publication
13	Thesis Submitted to Shodhganga Repository	<1	Publication
14	econjournals.com	<1	Internet Data
15	docobook.com	<1	Internet Data
16	www.hvm.bioflux.com.ro	<1	Publication

EXCLUDED PHRASES

- 1 diabetes mellitus
- 2 type 1 diabetes mellitus
- 3 type 2 diabetes mellitus
- 4 materials and methods
- 5 graphpad prism
- 6 blood glucose levels
- 7 one-way analysis of variance



नागालैण्ड विश्वविद्यालय

NAGALAND UNIVERSITY

(संसद द्वारा पारित अधिनियम 1989, क्रमांक 35 के अंतर्गत स्थापित केंद्रीय विश्वविद्यालय)

(A Central University established by an Act of Parliament No.35 of 1989)

मुख्यालय : लुमामी, जिला : जुन्हेबोटो (नागालैण्ड), पिनकोड – 798627

Hqrs: Lumami, Dist. Zunheboto (Nagaland), Pin Code – 798627

DEPARTMENT OF ZOOLOGY / प्राणी विज्ञान विभाग

CERTIFICATE

This is to certify that the thesis entitled “Efficacy of green tea polyphenol-epigallocatechin gallate (EGCG) for the management of diabetes mellitus in zebrafish model” has been approved by the Institutional Animal Ethics Committee (IAEC), Nagaland University.


17/9/2020

(Prof. L.N. Kakati)

Name of Member Secretary IAEC

Signature with date


17/9/2020

(Dr. Bendang Ao)

Name of Chariman

Signature with date


17/9/2020

(Prof. L.N. Kakati)

Name of Member Secretary IAEC

Signature with date


17/9/2020

(Dr. Bendang Ao)

Name of Chariman

Signature with date

IAEC approval No.

NU/ZOO/IAEC/Meeting No.01/2020
Protocol No. 04

Acknowledgement

I am immensely thankful to my research supervisor, Dr. Pranay Punj Pankaj, Associate Professor, Department of Zoology, Nagaland University, Lumami, for his continual support, corrections, and advice during the study. His guidance, insightful remarks, constructive criticism, patience, and genuine support enabled me to complete the work.

I would also like to acknowledge my gratitude to Prof. Bendang Ao, Head of the Department, and the department's teaching staff members, Prof. Sarat Chandra Yeniseti, Prof. Ranjit Kumar, Mr. Rajesh Singh, Dr. Lobeno Mozhui, and Dr. Ramita Sougrak Pam for their encouragement and assistance. My sincere appreciation also goes to the non-teaching staffs of this department for their continual support in completing this study. I am also thankful to the authorities of Nagaland University, Lumami, for providing the necessary facilities on the campus.

Additionally, I want to express my sincere gratitude to my lab mates Dr. Sophiya Ezung, Ms. Metevinu Kechu, Dr. Sentiyanger Longkumer, Mr. Rejuba Pongen, and Ms. Veselu Khesoh, with whom I had the opportunity to spend the better part of the academic duration, and the experience of working together has been an incredible learning curve. I am thankful for your constant assistance and validation.

I would also like to acknowledge my batch mates, Dr. Lirikhum Jing, Mr. Kelevikho Neikha, Ms. Tezenle Magh, Ms. Patricia Kiewhuo, Mr. Rahul Chaurasia, and Mr. Shumbenthung Odyuo, and all the other departmental research scholars, for their friendship and support.

Furthermore, I want to thank Dr. Vikas Kumar Roy, Associate Professor, Department of Zoology, Mizoram University, and his students, in particular Dr. Jeremy Malsamhriatzuala and Dr. Annie Lalrawngbawli, for offering a week of in-

Acknowledgement

depth instruction in fundamental histology as well and immunohistochemistry techniques.

I sincerely thank Prof. Chitta Ranjan Deb, Department of Botany, Nagaland University Lumami, and fellow scholar Ms. Bendangsenla Pongen for providing me with the necessary assistance for using the microscope during the early phases of my research endeavour.

I am deeply grateful to my friends Dr. Zevivonu Thakro, Dr. Ranjoy Wangkhem, Dr. Watitemjen, Ms. Betokali Zhimomi, Ms. Tsathrongla Sangtam, and Ms. Nungshisangla Jamir for their assistance during the micrography and application of the software. I also thank Nagaland University for granting me the UGC Non-NET fellowship, which helped me financially throughout my research period.

Finally, I am forever grateful to my parents, siblings, and relatives for their love, care, unwavering support, and prayers. Their encouragement has provided the entire journey with a greater sense of purpose.

To God alone be the glory

AJUNGLA JAMIR

DEDICATED

To

My Parents

lt. Imtímeren Jamír &

Watínaro Imchen

My Siblings

Meyasangla, Arentíba

& Achíla

Contents

	Titles	Page No.
List of Tables	I-VI
List of Figures	VII-XVII
Abbreviations	XVIII-XIX
Chapter-1	General Introduction	1-18
1.1	Diabetes mellitus	1
1.2	Global burden of diabetes	1
1.3	Classification of diabetes	2-7
1.3.1	Type 1 diabetes mellitus (T1DM)	3
1.3.1.1	Causes of T1DM	3-4
1.3.2	Type 2 diabetes mellitus (T2DM)	4
1.3.2.1	Causes of T2DM	4-6
1.3.2.1.1	Obesity and physical inactivity	5
1.3.2.1.2	Genetic susceptibility	5
1.3.2.1.3	Insulin resistance	5-6
1.3.2.1.4	Metabolic syndrome	6
1.3.2.1.5	Abnormal glucose production by the liver	6
1.3.3	Gestational diabetes mellitus	6-7
1.3.4	Other types of diabetes	7
1.4	Diabetes and its complications	7-10
1.4.1	Pathogenesis of diabetic complications	8
1.4.1.1	Acute complications	8
1.4.1.2	Chronic complications	8-10
1.4.1.2.1	Diabetic hepatopathy	9
1.4.1.2.2	Diabetic nephropathy	9
1.4.1.2.3	Diabetic wound	10
1.5	Biochemistry of diabetic complications	10
1.6	Factors affecting diabetic complications	10-12
1.6.1	Activation of protein kinase-C	11
1.6.2	Non-enzymatic glycation	11
1.6.3	Polyol pathway	11

Contents

1.6.4	Oxidative stress	11-12
1.7	Epigallocatechin gallate in biomedical research	12-14
1.7.1	Anti-diabetic effect of EGCG	13
1.7.2	Protective effects of EGCG	13
1.7.3	Antioxidative effect of EGCG	13-14
1.8	Zebrafish in pharmaceutical research	14-16
1.8.1	Biology of zebrafish	14-15
1.8.2	Zebrafish as an animal model	15-16
1.9	Scope and objectives of the study	17-18
Chapter-2	Acute toxicity study and behavioural responses in zebrafish model treated with EGCG	19-43
2.1	Introduction	19-21
2.2	Materials and methods	22-27
2.2.1	Chemicals	22
2.2.2	Characterisation of EGCG	22
2.2.3	Acclimatization of zebrafish	22
2.2.4	Physico – chemical parameters of fish tanks	22
2.2.5	Assessment of acute toxicity	23
2.2.6	Behavioural study	23-24
2.2.7	Histopathological study	24
2.2.8	Analysis of histological sections	24-26
2.2.8.1	Fixation	24
2.2.8.2	Washing	24
2.2.8.3	Dehydration	24
2.2.8.4	Clearing	24
2.2.8.5	Infiltration	24
2.2.8.6	Embedding	24
2.2.8.7	Sectioning	25
2.2.8.8	Staining	25-26
2.2.9	Statistical analysis	26-27
2.3	Results	28-39
2.3.1	Characterisation of EGCG	28

Contents

2.3.1.1 Spectral property of EGCG fluorescence dissolved in water	28-29
2.3.2 Acclimatization of zebrafish	29-30
2.3.3 Physico-chemical parameters of fish tank	31
2.3.4 Assessment of acute toxicity	31-33
2.3.5 Behavioural response	34-35
2.3.6 Histopathological study	36-39
2.3.6.1 Effects of EGCG on the liver of experimental zebrafish	36
2.3.6.2 Effects of EGCG on the kidney of experimental zebrafish	36
2.3.6.3 Effects of EGCG on gills of experimental zebrafish	36-37
2.4 Discussion	40-43
Chapter-3 Estimation of the minimum effective dose for EGCG, assessment of general physiological status and fin regeneration in experimental zebrafish	44-73
3.1 Introduction	44-47
3.2 Materials and methods	48-54
3.2.1 Chemicals	48
3.2.2 Acclimatization of zebrafish	48
3.2.3 Induction of diabetes	48-49
3.2.4 Minimum effective dose determination	49-50
3.2.5 Blood glucose levels determination	50-51
3.2.6 Grouping of experimental subjects	51
3.2.7 EGCG: Dose and period	52
3.2.8 Estimation of body weight	52
3.2.9 Estimation of body length	52
3.2.10 Estimation of body mass index	52
3.2.11 Caudal fin regeneration	53-54
3.2.12 Statistical analysis	54
3.3 Results	55-70
3.3.1 Determination of minimum effective dose	55

Contents

3.3.2	Body weight	55
3.3.3	Body length	56
3.3.4	Body mass index	56
3.3.5	Effect of EGCG on caudal fin regeneration	56-57
3.4	Discussion	67-72
Chapter-4	Effect of EGCG on lipid profiles and metabolic enzymes activity in the experimental zebrafish	73-127
4.1	Introduction	73-78
4.2	Materials and methods	79-96
4.2.1	Chemicals	79
4.2.2	Experimental design	79
4.2.3	Blood collection for lipid profiles	79-80
4.2.4	Tissue preparation	80
4.2.5	Biochemical analysis	81
4.2.6	Total cholesterol (TC)	81-82
4.2.7	Triglycerides (TG)	83-85
4.2.8	Very low-density lipoprotein (VLDL)	85
4.2.9	Low density lipoprotein (LDL)	85-87
4.2.10	High density lipoprotein (HDL)	88-90
4.2.11	Alanine aminotransferase (ALT) activity	90-91
4.2.12	Aspartate aminotransferase (AST) Activity	92-93
4.2.13	Alkaline phosphatase (ALP) activity	94-95
4.2.14	Statistical analysis	96
4.3	Results	97-123
4.3.1	Total cholesterol (TC)	97
4.3.2	Triglycerides (TG)	97
4.3.3	Very low-density lipoprotein (VLDL)	97-98
4.3.4	Low-density lipoprotein (LDL)	98
4.3.5	High density lipoprotein (HDL)	99
4.3.6	Hepatic tissue alanine aminotransferase (ALT) activity	99-100
4.3.7	Gill tissue alanine aminotransferase (ALT) activity	10-101

Contents

4.3.8 Renal tissue alanine aminotransferase (ALT) activity	101-102
4.3.9 Hepatic tissue aspartate aminotransferase (AST) activity	102
4.3.10 Gills tissue aspartate aminotransferase (AST) activity	102-103
4.3.11 Renal tissue aspartate aminotransferase (AST) activity	103-104
4.3.12 Hepatic tissue alkaline phosphatase (ALP) activity	104-105
4.3.13 Renal tissue alkaline phosphatase (ALP) activity	105
4.4 Discussion	124-127
Chapter-5 Evaluation of therapeutic efficacy of EGCG on oxidative stress and histopathological changes in zebrafish model	128-158
5.1 Introduction	128-130
5.2 Materials and methods	131-137
5.2.1 Chemicals	131
5.2.2 Acclimatization of zebrafish	131
5.2.3 Experimental design	131-132
5.2.4 Induction of diabetes mellitus	132
5.2.5 Tissue preparation	132
5.2.6 Biochemical assay	133
5.2.6.1 Superoxide dismutase (SOD) (EC.1.15.1.1)	133
5.2.6.2 Catalase assay (CAT) (E.C. 1.11.1.6)	133
5.2.7 Histopathology	134-135
5.2.8 Determination of histological alteration index (HAI) in liver, kidney, and gills	135-136
5.2.9 Statistical analysis	137
5.3 Results	138-150

Contents

5.3.1	SOD and CAT activity in the liver	138
5.3.2	SOD and CAT activity in the kidney	138-139
5.3.3	SOD and CAT activity in the gills	139-140
5.3.4	Histology of liver	140
5.3.5	Histology of kidney	141
5.3.6	Histology of gills	141-142
5.4	Discussion	151-157
Chapter-6	Effect of EGCG on diabetes-induced reproductive performance and developmental deformities in zebrafish model	158-187
6.1	Introduction	158-159
6.2	Materials and methods	160-163
6.2.1	Chemicals	160
6.2.2	Induction of diabetes	160
6.2.3	Acclimatization of zebrafish	160
6.2.4	Experimental design	160-161
6.2.5	Larval rearing	161
6.2.6	Determination of gonadosomatic index (GSI) and hepatosomatic index (HSI)	161-162
6.2.7	Assessment of reproductive parameters	162
6.2.8	Deformity assessment	162-163
6.2.9	Histopathological study	163
6.2.10	Image pre-processing and processing	163
6.2.11	Statistical analysis	163
6.3	Results	164-182
6.3.1	GSI and HSI in female subjects	164
6.3.2	GSI and HSI in male subjects	164-165
6.3.3	Assessment of reproductive parameters	165-169
6.3.3.1	Normal development of zebrafish embryo	165-166
6.3.3.2	Average fecundity	167
6.3.3.3	Percentage fertilization	167-168
6.3.3.4	Percentage hatchability	168
6.3.3.5	Percentage survival	168-169

Contents

6.3.3.6 Deformity assessment	169
6.3.4 Histopathological study	169-170
6.3.4.1 Histopathology of ovary	169-170
6.3.4.2 Histopathology of testis	170
6.4 Discussion	183-187
Chapter-7 Summary and conclusion	188-194
References	195-231
Appendix	i-xv
List of publications	i-vii
Patents	vii-ix
Research paper presentation	ix-xiii
Seminars/workshops/training attended	xiv-xv

List of Tables

Table No.	Description	Page No.
2.1	Tissue block preparation	25-26
2.2	Haematoxylin and eosin staining	26
2.3	Physico-chemical parameters of the test water	31
2.4	LC50 of EGCG for various duration (24-hours, 48-hours, 72-hours and 96-hours) in zebrafish model.	32
3.1	Grouping of experimental models for minimum effective dose determination	50
3.2	Grouping of experimental zebrafish	51
3.3	Blood glucose levels of different experimental groups. Group-I - Control; Group-II – diabetic; Group-IIIa - diabetic zebrafish treated with 1 mg/L of EGCG; Group-IIIb - diabetic zebrafish treated with 2 mg/L of EGCG; Group-IIIc - diabetic zebrafish treated with 4 mg/L of EGCG; Group-IIId - diabetic zebrafish treated with 6 mg/L of EGCG; Group-IIIE - diabetic zebrafish treated with 8 mg/L of EGCG. Data are represented as mean \pm SD; (n=6).	58
3.4	Effect of diabetes on body weight and its treatment with EGCG in zebrafish model. Group-I – control; Group-II – diabetic; Group-III – diabetic + EGCG; Group-IV – control + EGCG. Data are represented as mean \pm SD; (n=6). Different superscripts denote significant (p<0.001) differences; the same superscripts denote insignificant (p>0.05) results between the columns of the treatment groups.	59
3.5	Effect of diabetes on body length and its treatment with EGCG in zebrafish model. Group-I – control; Group-II – diabetic; Group-III – diabetic + EGCG; Group-IV – control + EGCG. Data are represented as mean \pm SD; (n=6). Different superscripts denote significant (p<0.001) differences; the same superscripts denote insignificant (p>0.05) results between the columns of the treatment	

List of Tables

groups.	
3.6 Effect of diabetes on body mass index and its treatment with EGCG in zebrafish model. Group-I – control; Group-II – diabetic; Group-III – diabetic + EGCG; Group-IV – control + EGCG. Data are represented as mean \pm SD; (n=6). Different superscripts denote significant ($p<0.001$) differences; the same superscripts denote insignificant ($p>0.05$) results between the columns of the treatment groups.	59
4.1 Effect of diabetes on the cholesterol level in zebrafish model. Group-I – control; Group-II – diabetic; Group-III – diabetic + EGCG; Group-IV – control + EGCG. Data are expressed as mean \pm SD (n=6). Different superscripts denote significant ($p<0.001$) differences; the same superscripts denote insignificant ($p>0.05$) results between the columns of the exposure groups.	106
4.2 Effect of diabetes on the triglyceride level in zebrafish model. Group-I – control; Group-II – diabetic; Group-III – diabetic + EGCG; Group-IV – control + EGCG. Data are expressed as mean \pm SD (n=6). Different superscripts denote significant ($p<0.001$) differences; the same superscripts denote insignificant ($p>0.05$) results between the columns of the exposure groups.	106
4.3 Effect of diabetes on the very low-density lipoprotein in zebrafish model. Group-I – control; Group-II – diabetic; Group-III – diabetic + EGCG; Group-IV – control + EGCG. Data are expressed as mean \pm SD (n=6). Different superscripts denote significant ($p<0.001$) differences; the same superscripts denote insignificant ($p>0.05$) results between the columns of the exposure groups.	107
4.4 Effect of diabetes on the low-density lipoprotein in zebrafish model. Group-I – control; Group-II – diabetic; Group-III –	107

List of Tables

- diabetic + EGCG; Group-IV – control + EGCG. Data are expressed as mean \pm SD (n=6). Different superscripts denote significant ($p<0.001$) differences; the same superscripts denote insignificant ($p>0.05$) results between the columns of the exposure groups.
- 4.5** Effect of diabetes on the high-density lipoprotein in zebrafish model. Group-I – control; Group-II – diabetic; Group-III – diabetic + EGCG; Group-IV – control + EGCG. Data are expressed as mean \pm SD (n=6). Different superscripts denote significant ($p<0.001$) differences; the same superscripts denote insignificant ($p>0.05$) results between the columns of the exposure groups. 108
- 4.6** Effect of diabetes on the hepatic ALT activity and its treatment with EGCG in zebrafish model. Group-I – control; Group-II – diabetic; Group-III – diabetic + EGCG; Group-IV – control + EGCG. Data are expressed as mean \pm SD (n=6). Different superscripts denote significant ($p<0.001$) differences; the same superscripts denote insignificant ($p>0.05$) results between the columns of the exposure groups. 108
- 4.7** Effect of diabetes on the gills ALT activity and its treatment with EGCG in zebrafish model. Group-I – control; Group-II – diabetic; Group-III – diabetic + EGCG; Group-IV – control + EGCG. Data are expressed as mean \pm SD (n=6). Different superscripts denote significant ($p<0.001$) differences; the same superscripts denote insignificant ($p>0.05$) results between the columns of the exposure groups. 109
- 4.8** Effect of diabetes on the renal ALT activity and its treatment with EGCG in zebrafish model. Group-I – control; Group-II – diabetic; Group-III – diabetic + EGCG; Group-IV – control + EGCG. Data are expressed as mean \pm SD (n=6). 109

List of Tables

- Different superscripts denote significant ($p<0.001$) differences; the same superscripts denote insignificant ($p>0.05$) results between the columns of the exposure groups.
- 4.9** Effect of diabetes on the hepatic AST activity and its treatment with EGCG in zebrafish model. Group-I – control; Group-II – diabetic; Group-III – diabetic + EGCG; Group-IV – control + EGCG. Data are expressed as mean \pm SD ($n=6$). Different superscripts denote significant ($p<0.001$) differences; the same superscripts denote insignificant ($p>0.05$) results between the columns of the exposure groups. 110
- 4.10** Effect of diabetes on the gills AST activity and its treatment with EGCG in zebrafish model. Group-I – control; Group-II – diabetic; Group-III – diabetic + EGCG; Group-IV – control + EGCG. Data are expressed as mean \pm SD ($n=6$). Different superscripts denote significant ($p<0.001$) differences; the same superscripts denote insignificant ($p>0.05$) results between the columns of the exposure groups. 110
- 4.11** Effect of diabetes on the renal AST level and its treatment with EGCG in zebrafish model. Group-I – control; Group-II – diabetic; Group-III – diabetic + EGCG; Group-IV – control + EGCG. Data are expressed as mean \pm SD ($n=6$). Different superscripts denote significant ($p<0.001$) differences; the same superscripts denote insignificant ($p>0.05$) results between the columns of the exposure groups. 111
- 4.12** Effect of diabetes on the hepatic ALP level and its treatment with EGCG in zebrafish model. Group-I – control; Group-II – diabetic; Group-III – diabetic + EGCG; Group-IV – control + EGCG. Data are expressed as mean \pm SD ($n=6$). 111

List of Tables

	Different superscripts denote significant ($p < 0.001$) differences; the same superscripts denote insignificant ($p > 0.05$) results between the columns of the exposure groups.	
4.13	Effect of diabetes on the renal ALP level and its treatment with EGCG in zebrafish model. Group-I – control; Group-II – diabetic; Group-III – diabetic + EGCG; Group-IV – control + EGCG. Data are expressed as mean \pm SD ($n=6$). Different superscripts denote significant ($p < 0.001$) differences; the same superscripts denote insignificant ($p > 0.05$) results between the columns of the exposure groups.	112
5.1	Stages of histological alteration in liver, kidney and gills.	136
5.2	Effect of diabetes on the antioxidant enzyme activity in the liver of zebrafish model. Group-I – control; Group-II – diabetic; Group-III – diabetic + EGCG; Group-IV – control + EGCG. Data are expressed as mean \pm SD ($n=6$). Different superscripts denote significant ($p < 0.001$) differences; the same superscripts denote insignificant ($p > 0.05$) results between the columns of the exposure groups on day 21.	143
5.3	Effect of diabetes on the antioxidant enzyme activity in the kidney of zebrafish model. Group-I – control; Group-II – diabetic; Group-III – diabetic + EGCG; Group-IV – control + EGCG. Data are expressed as mean \pm SD ($n=6$). Different superscripts denote significant ($p < 0.001$) differences; the same superscripts denote insignificant ($p > 0.05$) results between the columns of the exposure groups on day 21.	143
5.4	Effect of diabetes on the antioxidant enzyme activity in the gills of zebrafish model. Group-I – control; Group-II – diabetic; Group-III – diabetic + EGCG; Group-IV – control + EGCG. Data are expressed as mean \pm SD ($n=6$). Different superscripts denote significant ($p < 0.001$) differences; the	144

List of Tables

	same superscripts denote insignificant ($p>0.05$) results between the columns of the exposure groups on day 21.	
6.1	Changes in GSI and HSI of female experimental zebrafish model. Group-I – control; Group-II – diabetic; Group-III – diabetic + EGCG; Group IV – control + EGCG. Data are expressed as mean \pm SD ($n=6$). Different superscripts denote significant ($p<0.001$) differences; the same superscripts denote insignificant ($p>0.05$) results between the columns of the exposure groups.	171
6.2	Changes in GSI and HSI of male experimental zebrafish model. Group-I – control; Group-II – diabetic; Group-III – diabetic + EGCG; Group IV – control + EGCG. Data are expressed as mean \pm SD ($n=6$). Different superscripts denote significant ($p<0.001$) differences; the same superscripts denote insignificant ($p>0.05$) results between the columns of the exposure groups.	171-172
6.3	Normal development of zebrafish embryo	172
6.4	Average fecundity, % fertilization, % hatchability and % survival of the F_1 generation. Group-I – control; Group-II – diabetic; Group-III – diabetic + EGCG; Group IV – control + EGCG. Data are expressed as mean \pm SD ($n=6$). Different superscripts denote significant ($p<0.001$) differences; the same superscripts denote insignificant ($p>0.05$) results between the columns of the exposure groups.	173
6.5	Percentage deformities of the F_1 generation. Groups: (I) – control; (II) – diabetic; (III) – diabetic + EGCG; (IV) – control + EGCG. Data are expressed as mean \pm SD ($n=6$). Different superscripts denote significant ($p<0.001$) differences; the same superscripts denote insignificant ($p>0.05$) results between the columns of the exposure groups.	173

List of Figures

Figure No.	Description	Page No.
1.1	(A) Estimated global diabetes prevalence in 2019 and projection for 2045 (B) Countries with a maximum diabetic population.	2
1.2	Classification of diabetes mellitus	3
1.3	Morphology of zebrafish. (A) Female (B) Male	14
2.1	Chemical structure of EGCG	28
2.2	Emission spectra of EGCG dissolved in distilled water	29
2.3	Schematic representation of zebrafish housing system	30
2.4	Dose response curve of EGCG (mg/L) after exposure to various periods (24 hours, 48 hours, 72 hours and 96 hours) in the zebrafish model.	32
2.5	Mortality percentage at different durations of EGCG exposure. (A) 24 hours (B) 48 hours (C) 72 hours (D) 96 hours.	33
2.6	Behavioural response in experimental zebrafish under treatment with different doses of EGCG.	35
2.7	Morphological changes in zebrafish model treated with EGCG. (A) Control zebrafish (B) Zebrafish treated with 12 mg/L EGCG exhibiting blood aggregation resulting in red coloration in the opercular area (OP) (C-D) Zebrafish treated with 30 mg/L EGCG exhibited hyperaemia towards the anal fin (HA), increased red coloration in the opercular region (OP), serious edema and necrosis in the thorax area (EN), highly dyspigmentation of the body (DP).	35
2.8	Histological changes in zebrafish model treated with EGCG. (A) Control Liver (0.0 mg/L EGCG) (B) Liver treated with 12 mg/L EGCG exhibiting atrophy (SE), necrosis (N), vacuolar degeneration (CV) (C) Liver treated with 30 mg/L EGCG exhibited cell hypertrophy	38

List of Figures

	(HS), atrophy (SE), vacuolar degeneration (CV), necrosis (N).	
	(Figures captured at 40X magnification)	
2.9	Histological changes in zebrafish model treated with EGCG. (A) Control Kidney (0mg/gm/L) (B) Kidney treated with 12 mg/L EGCG exhibiting tubular degeneration (TD), glomerular shrinkage (GD), dilation of bowman's space (DC) (C) kidney treated with 30 mg/L EGCG glomerular shrinkage (GD), vacuolation (CV), vacuolar degeneration (VG), hemorrhage (HR), bowman's space dilation (DC), and necrosis (N). (Figures captured at 40X magnification)	38-39
2.10	Histological changes in zebrafish model treated with EGCG. (A) Control gills (0mg/L) (B) Gills treated with 12 mg/L EGCG exhibiting epithelial lifting (EP), hyperplasia (HP), fusion of secondary lamella (SL) (C-D) Gills treated with 30 mg/L EGCG exhibiting epithelial lifting (EP), epithelial hyperplasia (HP), curling of lamella (CR), mucus secretion (MS), lamellar synechieae (LS), fusion with secondary and adjacent lamella (AD), and shortening of secondary lamella (SH). (Figures captured at 40X magnification)	39
3.1	Diagrammatic representation of diabetes induction in zebrafish	49
3.2	Grouping of experimental subjects	51
3.3	Diagrammatic representation of assessment of fin regeneration.	54
3.4	Blood glucose levels of different experimental groups. Group-I - Control; Group-II – diabetic; Group-IIIa - diabetic zebrafish treated with 1 mg/L of EGCG; Group-IIIb - diabetic zebrafish treated with 2 mg/L of EGCG; Group-IIIc - diabetic zebrafish treated with 4 mg/L of	60

List of Figures

- EGCG; Group-III_d - diabetic zebrafish treated with 6 mg/L of EGCG; Group-III_e - diabetic zebrafish treated with 8 mg/L of EGCG. (A) Day 1 (B) Day 7 (C) Day 14 (D) Day 21. Data are represented as mean \pm SD; (n=6) and analysed by one-way ANOVA followed by Tukey's post-hoc test. Different superscripts denote significant ($p<0.001$) differences; the same superscripts denote insignificant ($p>0.05$) results between the treatment groups.
- 3.5** Blood glucose levels of different experimental groups. 61
Group-I: control; Group-II: diabetic; Group-III_a: diabetic zebrafish treated with 1 mg/L of EGCG; Group-III_b: diabetic zebrafish treated with 2 mg/L of EGCG; Group-III_c: diabetic zebrafish treated with 4 mg/L of EGCG; Group-III_d: diabetic zebrafish treated with 6 mg/L of EGCG; Group-III_e: diabetic zebrafish treated with 8 mg/L of EGCG.
- 3.6** Effect of diabetes on body weight and its treatment with EGCG in zebrafish model. Group-I – control; Group-II – diabetic; Group-III – diabetic + EGCG; Group-IV – control + EGCG. (A) Day 1 (B) Day 7 (C) Day 14 (D) Day 21. Data are represented as mean \pm SD; (n=6) and analysed by one-way ANOVA followed by Tukey's post-hoc test. Asterisk represents a significant difference, * $p<0.05$; ** $p<0.01$; *** $p<0.001$. 62
- 3.7** Effect of diabetes on body length and its treatment with EGCG in zebrafish model. Group-I – control; Group-II – diabetic; Group-III – diabetic + EGCG; Group-IV – control + EGCG. (A) Day 1 (B) Day 7 (C) Day 14 and (D) Day 21. Data are represented as mean \pm SD; (n=6) and analysed by one-way ANOVA followed by Tukey's post 63

List of Figures

- hoc test. Asterisk represents a significant difference, * $p < 0.05$; ** $p < 0.01$; *** $p < 0.001$.
- 3.8** Effect of diabetes on body mass index and its treatment with EGCG in zebrafish model. Group-I – control; Group-II – diabetic; Group-III – diabetic + EGCG; Group-IV – control + EGCG. (A) Day 1 (B) Day 7 (C) Day 14 (D) Day 21. Data are represented as mean \pm SD; (n=6) and analysed by one-way ANOVA followed by Tukey's post-hoc test. Asterisk represents a significant difference, * $p < 0.05$; ** $p < 0.01$; *** $p < 0.001$. 64
- 3.9** Caudal fin regeneration in experimental zebrafish on day 0 (pre amputation), day 1 (initial cut), day 7, day 14 and day 21. (a-e) Control caudal fin, (f-j) Caudal fin of diabetic zebrafish, (k-o) Caudal fin of diabetic zebrafish treated with EGCG, (p-t) Caudal fin of control zebrafish treated with EGCG. (Image captured at 5X magnification) 65
- 3.10** Average percentage growth of the caudal fin of zebrafish. Group-I – control; Group-II – diabetic; Group-III – diabetic + EGCG; Group-IV – control + EGCG. (A) Day 7 (B) Day 14 (C) Day 21. Data are represented as mean \pm SD; (n=6) and analysed by one-way ANOVA followed by Tukey's post-hoc test. Asterisk represents a significant difference, * $p < 0.05$; ** $p < 0.01$; *** $p < 0.001$. 66
- 4.1** Diagrammatic representation of blood collection for lipid profile in zebrafish model 80
- 4.2** Experimental design for tissue collection and studying metabolic activities. 80
- 4.3** Effect of diabetes on the cholesterol level in zebrafish model. Group-I – control; Group-II – diabetic; Group-III – diabetic + EGCG; Group-IV – control + EGCG. (A) Day 1 (B) Day 21. Data are represented as mean \pm SD 113

List of Figures

- (n=6) and analysed by one-way ANOVA followed by Tukey's post-hoc test. Asterisk represents a significant difference, *p<0.05, **p<0.01, ***p<0.001.
- 4.4** Effect of diabetes on the triglyceride level in zebrafish model. Group-I – control; Group-II – diabetic; Group-III – diabetic + EGCG; Group-IV – control + EGCG. (A) Day 1 (B) Day 21. Data are represented as mean ± SD (n=6) and analysed by one-way ANOVA followed by Tukey's post-hoc test. Asterisk represents a significant difference, *p<0.05, **p<0.01, ***p<0.001. 113
- 4.5** Effect of diabetes on the very low-density lipoprote in zebrafish model. Group-I – control; Group-II – diabetic; Group-III – diabetic + EGCG; Group-IV – control + EGCG. (A) Day 1 (B) Day 21. Data are represented as mean ± SD (n=6) and analysed by one-way ANOVA followed by Tukey's post-hoc test. Asterisk represents a significant difference, *p<0.05, **p<0.01, ***p<0.001. 114
- 4.6** Effect of diabetes on the low-density lipoprotein in zebrafish model. Group-I – control; Group-II – diabetic; Group-III – diabetic + EGCG; Group-IV – control + EGCG. (A) Day 1 (B) Day 21. Data are represented as mean ± SD (n=6) and analysed by one-way ANOVA followed by Tukey's post-hoc test. Asterisk represents a significant difference, *p<0.05, **p<0.01, ***p<0.001. 114
- 4.7** Effect of diabetes on the high-density lipoprotein in zebrafish model. Group-I – control; Group-II – diabetic; Group-III – diabetic + EGCG; Group-IV – control + EGCG. (A) Day 1 (B) Day 21. Data are represented as mean ± SD (n=6) and analysed by one-way ANOVA followed by Tukey's post-hoc test. Asterisk represents a significant difference, *p<0.05, **p<0.01, ***p<0.001. 115

List of Figures

- 4.8** Effect of diabetes on the hepatic ALT activity and its treatment with EGCG in zebrafish model. Group-I - control; Group-II - diabetic; Group-III - diabetic + EGCG; Group-IV - control + EGCG. (A) Day 1 (B) Day 7 (C) Day 14 (D) Day 21. Data are represented as mean \pm SD (n=6) and analysed by one-way ANOVA followed by Tukey's post-hoc test. Asterisk represents a significant difference, *p<0.05, **p<0.01, ***p<0.001. 116
- 4.9** Effect of diabetes on the gills ALT activity and its treatment with EGCG in zebrafish model. Group-I - control; Group-II - diabetic; Group-III - diabetic + EGCG; Group-IV - control + EGCG. (A) Day 1 (B) Day 7 (C) Day 14 (D) Day 21. Data are represented as mean \pm SD (n=6) and analysed by one-way ANOVA followed by Tukey's post-hoc test. Asterisk represents a significant difference, *p<0.05, **p<0.01, ***p<0.001. 117
- 4.10** Effect of diabetes on the renal ALT activity and its treatment with EGCG in zebrafish model. Group-I - control; Group-II - diabetic; Group-III - diabetic + EGCG; Group-IV - control + EGCG. (A) Day 1 (B) Day 7 (C) Day 14 (D) Day 21. Data are represented as mean \pm SD (n=6) and analysed by one-way ANOVA followed by Tukey's post-hoc test. Asterisk represents a significant difference, *p<0.05, **p<0.01, ***p<0.001. 118
- 4.11** Effect of diabetes on the hepatic AST activity and its treatment with EGCG in zebrafish model. Group-I - control; Group-II - diabetic; Group-III - diabetic + EGCG; Group-IV - control + EGCG. (A) Day 1 (B) Day 7 (C) Day 14 (D) Day 21. Data are represented as mean \pm SD (n=6) and analysed by one-way ANOVA followed by Tukey's post-hoc test. Asterisk represents a significant difference, *p<0.05, **p<0.01, ***p<0.001. 119

List of Figures

- 4.12** Effect of diabetes on the gills AST activity and its treatment with EGCG in zebrafish model. Group-I - control; Group-II - diabetic; Group-III - diabetic + EGCG; Group-IV - control + EGCG. (A) Day 1 (B) Day 7 (C) Day 14 (D) Day 21. Data are represented as mean \pm SD (n=6) and analysed by one-way ANOVA followed by Tukey's post-hoc test. Asterisk represents a significant difference, *p<0.05, **p<0.01, ***p<0.001. 120
- 4.13** Effect of diabetes on the renal AST level and its treatment with EGCG in zebrafish model. Group-I - control; Group-II - diabetic; Group-III - diabetic + EGCG; Group-IV - control + EGCG. (A) Day 1 (B) Day 7 (C) Day 14 (D) Day 21. Data are represented as mean \pm SD (n=6) and analysed by one-way ANOVA followed by Tukey's post-hoc test. Asterisk represents a significant difference, *p<0.05, **p<0.01, ***p<0.001. 121
- 4.14** Effect of diabetes on the hepatic ALP level and its treatment with EGCG in zebrafish model. Group-I - control; Group-II - diabetic; Group-III - diabetic + EGCG; Group-IV - control + EGCG. (A) Day 1 (B) Day 7 (C) Day 14 (D) Day 21. Data are represented as mean \pm SD (n=6) and analysed by one-way ANOVA followed by Tukey's post-hoc test. Asterisk represents a significant difference, *p<0.05, **p<0.01, ***p<0.001. 122
- 4.15** Effect of diabetes on the renal ALP level and its treatment with EGCG in zebrafish model. Group-I - control; Group-II - diabetic; Group-III - diabetic + EGCG; Group-IV - control + EGCG. (A) Day 1 (B) Day 7 (C) Day 14 (D) Day 21. Data are represented as mean \pm SD (n=6) and analysed by one-way ANOVA followed by Tukey's post-hoc test. Asterisk represents a significant difference, *p<0.05, **p<0.01, ***p<0.001. 123

List of Figures

- | | | |
|------------|---|---------|
| 5.1 | Diagrammatic representation of the experimental setup for studying antioxidant activity and histological parameters on the zebrafish model. | 132 |
| 5.2 | Effect of diabetes on the antioxidant enzyme activity in the liver of zebrafish model. Group-I – control; Group-II – diabetic; Group-III – diabetic + EGCG; Group-IV – control + EGCG. (A) SOD (B) CAT. Data are represented as mean \pm SD (n=6) and analysed by one-way ANOVA followed by Tukey's post-hoc test. Asterisk represents a significant difference, *p<0.05, **p<0.01, ***p<0.001. | 145 |
| 5.3 | Effect of diabetes on the antioxidant enzyme activity in the kidney of zebrafish. Group-I – control; Group-II – diabetic; Group-III – diabetic + EGCG; Group-IV – control + EGCG. (A) SOD (B) CAT. Data are represented as mean \pm SD (n=6) and analysed by one-way ANOVA followed by Tukey's post-hoc test. Asterisk represents a significant difference, *p<0.05, **p<0.01, ***p<0.001. | 145-146 |
| 5.4 | Effect of diabetes on the antioxidant enzyme activity in the gills of zebrafish model. Group-I – control; Group-II – diabetic; Group-III – diabetic + EGCG; Group-IV – control + EGCG. (A) SOD (B) CAT. Data are represented as mean \pm SD (n=6) and analysed by one-way ANOVA followed by Tukey's post-hoc test. Asterisk represents a significant difference, *p<0.05, **p<0.01, ***p<0.001. | 146 |
| 5.5 | Histological changes in the liver of test zebrafish. (A) Group-I (B) Group-II (C) Group-III (D) Group-IV. Liver alterations are represented as steatosis (SA), hepatocyte hypertrophy (HP), atrophy (AT), cytoplasmic vacuolation (VA), and necrosis (N).
(Figures captured at 40X magnification) | 147 |
| 5.6 | Histological changes in kidney of test zebrafish. (A) Group-I (B) Group-II (C) Group-III (D) Group-IV. | 148 |

List of Figures

Alterations in the tissue of different groups are represented as vacuole degeneration (VD), mesangial expansion (ME), necrosis (N), tubular degeneration (TD), focal haemorrhage (HR), thickness of the glomerulus (TG), brush border deficit (BD), and dilation of the bowman's space (DC).

(Figures captured at 40X magnification)

- | | | |
|-------------------|--|------------|
| <p>5.7</p> | <p>Histological changes in gills of test zebrafish. (A) Group-I (B-D) Group-II (E) Group-III (F) Group-IV. Alterations in the tissue of different groups are represented as epithelial cell hyperplasia (HL), hypertrophy (HP), lamellar fusion (SL), lifting of the epithelia (EP), edema in lamellae (ED), hemorrhage (HR), lamellar aneurysm (LA), and necrosis (N).</p> <p>(Figures captured at 40X magnification)</p> | <p>149</p> |
| <p>5.8</p> | <p>Histological alteration index (HAI) value of different organs of test zebrafish. Different superscripts denote significant ($p < 0.001$) differences between the exposure groups of the same organs.</p> | <p>150</p> |
| <p>6.1</p> | <p>Diagrammatic representation of the experimental design</p> | <p>161</p> |
| <p>6.2</p> | <p>Effect of diabetes on the GSI of female zebrafish model. Group-I – control; Group-II – diabetic; Group-III – diabetic + EGCG; Group-IV – control + EGCG. (A) Day 1 (B) Day 7 (C) Day 14 (D) Day 21. Data are represented as mean \pm SD ($n=6$) and analysed by one-way ANOVA followed by Tukey's post-hoc test. Asterisk represents a significant difference, *$p < 0.05$, **$p < 0.01$, ***$p < 0.001$.</p> | <p>174</p> |
| <p>6.3</p> | <p>Effect of diabetes on the HSI of female zebrafish model. Group-I – control; Group-II – diabetic; Group-III – diabetic + EGCG; Group-IV – control + EGCG. (A) Day 1 (B) Day 7 (C) Day 14 (D) Day 21. Data are represented as mean \pm SD ($n=6$) and analysed by one-way ANOVA</p> | <p>175</p> |

List of Figures

- followed by Tukey's post-hoc test. Asterisk represents a significant difference, * $p < 0.05$, ** $p < 0.01$, *** $p < 0.001$.
- 6.4** Effect of diabetes on the GSI of male zebrafish model. 176
 Group-I – control; Group-II – diabetic; Group-III – diabetic + EGCG; Group-IV – control + EGCG. (A) Day 1 (B) Day 7 (C) Day 14 (D) Day 21. Data are represented as mean \pm SD (n=6) and analysed by one-way ANOVA followed by Tukey's post-hoc test. Asterisk represents a significant difference, * $p < 0.05$, ** $p < 0.01$, *** $p < 0.001$.
- 6.5** Effect of diabetes on the HSI of male zebrafish model. 177
 Group-I – control; Group-II – diabetic; Group-III – diabetic + EGCG; Group-IV – control + EGCG. (A) Day 1 (B) Day 7 (C) Day 14 (D) Day 21. Data are represented as mean \pm SD (n=6) and analysed by one-way ANOVA followed by Tukey's post-hoc test. Asterisk represents a significant difference, * $p < 0.05$, ** $p < 0.01$, *** $p < 0.001$.
- 6.6** Assessment of reproductive parameters. Group-I – control; Group-II – diabetic; Group-III – diabetic + EGCG; Group-IV – control + EGCG. (A) Average fecundity (B) Percentage fertilization (C) Percentage hatchability (D) Percentage survival. Data are expressed as mean \pm SD (n=6) and analysed by one-way ANOVA followed by Tukey's post-hoc test. Asterisk represents a significant difference, * $p < 0.05$; ** $p < 0.01$; *** $p < 0.001$. 178
- 6.7** Normal embryonic development of the zebrafish. 179
- 6.8** Evaluation of deformity in the F₁ generation. (A) 180-181
 coagulation, blisters, and uneven cleavage pattern (%), (B) lordosis and swollen body (%), (C) edema (%), (D) tail deformity (%). (E) egg coagulation, (F-G) blisters in early cell development, (H-J) uneven cleavage pattern in early cell stages, (K-N) lordosis and swollen body of the

List of Figures

- larvae, (O-R) pericardial and yolk sac edema, (S-X) tail deformity of developing offspring.
(Figures captured at 40X magnification)
- 6.9** Histological changes in the ovary of test zebrafish. (A) 181
Group-I (B) Group-II (C) Group-III (D) Group-IV. The changes in the structure of the ovary are represented as degeneration of oocyte (Od), vacuolation (Va), atria follicle (AF). Follicles at different stages are represented as developing follicles (I and II), transitioning follicles (III), and fully matured follicles (IV).
(Figures captured at 40X magnification)
- 6.10** Histological changes in the testis of test zebrafish. (A) 182
Group-I (B) Group-II (C) Group-III (D) Group-IV. The different structural changes in the testis are represented as degeneration of spermatids (Ds), vacuolation (Va), degeneration of interstitial site (Is), and decrease in spermatozoa (Sp). Follicles at different stages are represented as primary spermatocyte (I), secondary spermatocyte (II), spermatids (III), and Spermatozoa (IV).
(Figures captured at 40X magnification)

Abbreviations

°C	Degree celsius	DNA	Deoxy ribonucleic acid
4-AAP	4-Aminoantiprine	dpf	Days Post Fertilization
AD	Alzheimer disease	DPP	Diabetes prevention programme
ADA	American Diabetes Association	DPPH	2,2 Diphenyl-1-Picrylhydrazyl
Ag₂CO₃	Silver Carbonate	DPX	Dibutylphthalate
Ag₂O	Silver Oxide		Polystyrene Xylene
AGEs	Advanced glycation end products	DR	Diabetic Retinopathy
ALP	Alkaline Phosphatase	EC	Epicatechin
ALT	Alanine Transaminase	ECG	Epigallocatechin
ANOVA	Analysis of Variance	EDTA	Ethylenediaminetetraacetic Acid
ApoB	Apolipoprotein-B	EGCG	Epigallocatechin Gallate
AST	Aspartate Transaminase	EMR	Electronic Medical Record
ATP	Adenosine Triphosphate	F₁	First Filial Generation
BMI	Body Mass Index	GDM	Gestational Diabetes Mellitus
BMP	Bone Morphogenetic Protein	GLUT-2	Glucose transporter 2
BOD	Biological Oxygen Demand	gm	Gram
CAT	Catalase	GPO	Glycerol Phosphate Oxidase
CCl₄	Carbon Tetrachloride	GPT	Glutamic Pyruvic Transaminase
CHE	Cholesterol Esterase	GSH	Glutathione
CHER	Cholesterol Esterase	GSI	Gonadosomatic Index
CHO	Cholesterol Oxidase	HAI	Histopathological Alterations Index
CHOD	Cholesterol Oxidase	HbA1C	Glycated Hemoglobin
CM	Chylomicron	HDL	High Density Lipoprotein
Cm	Centimeter	HDL-C	High Density Lipoprotein-Cholesterol
COD	Chemical Oxygen Demand	HH	Hedgehog
CPCSA	Committee for the Purpose of Control and Supervision of Experiments on Animals	hpf	Hours Post Fertilization
CuO	Copper (II) Oxide	hrs	Hours
CVD	Cardiovascular Diseases	HSI	Hepatosomatic Index
DAP	Dihydroxyacetone Phosphate	IDDM	Insulin Dependent Diabetes Mellitus
DHBS	3,5-dichloro-2-hydroxy benzene sulphonate	IEAC	Institutional Animal Ethics Committee
DKA	Diabetic ketoacidosis	IU	International Units
DM	Diabetes mellitus	KCl	Potassium Chloride

Abbreviations

KU/L	Kilo-unit Per Liter	P	Cuvette Light Path
L	Liter	PD	Parkinson's Disease
LC₅₀	Lethal Concentration	PEGME	Polyethylene Glycol-Methyl Ether
LCD	Liquid Crystal Display	PKC	Protein kinase C
LDH	Lactate Dehydrogenase	POD	Peroxide
LDL	Low Density Lipoprotein	PVS	Polyvinyl Sulfonic Acid
LDL-C	Low Density Lipoprotein-Cholesterol	ROS	Reactive Oxygen Species
LPL	Lipoprotein Lipase	SD	Standard Deviation
MDA	Malondialdehyde	SEM	Standard Error of the Mean
MED	Minimum Tolerable Dose	SOD	Superoxide Dismutase
mg	Milligram	STZ	Streptozotocin
mg/dl	Milligram/Deciliter	T1DM	Type 1 Diabetes mellitus
mM	Milli Molar	T2DM	Type 2 Diabetes mellitus
mmol/L	Milli Moles Per Liter	TC	Total Cholesterol
MRDM	Malnutrition-related diabetes mellitus	TG	Triglycerides
NADH	Nicotinamide Adenine Dinucleotide Hydrogen	TGF-β	Transforming Growth Factor-Beta
NAFLD	Non-Alcoholic Fatty Liver Disease	TiO₂	Titanium Dioxide
NIDDM	Non-Insulin Dependent Diabetes Mellitus	Tricaine	Tricaine Methane Sulphonate
NKHS	Non Ketotic Hyper Osmolar State	MS-222	Unit Per Liter
NLRP	Nod-like Receptor Protein 3	U/L	Ultra Violet
nm	Nanometer	UV	Vascular Endothelial Growth Factor
NRF-2	Nuclear Factor Erythroid 2-Related Factor 2	VEGF	Very Low-Density Lipoprotein
OECD	Organisation for Economic Co-operation and Development	VLDL	World Health Organisation
		μl	Microliter

Chapter 1

General Introduction

Contents

1.1 Diabetes mellitus

1.2 Global burden of diabetes

1.3 Classification of diabetes

1.4 Diabetes and its complications

1.5 Biochemistry of diabetic complications

1.6 Factors affecting diabetic complications

1.7 Epigallocatechin gallate in biomedical research

1.8 Zebrafish in pharmaceutical research

1.9 Scope and objectives of the study

1.1 Diabetes mellitus

Diabetes mellitus (DM) is a metabolic disorder characterized by persistent elevated blood glucose levels coupled with absolute or relative irregularities in insulin secretion or action (Baynes, 2015). It denotes a state in which insulin fails to maintain glucose and lipid metabolism balance, resulting in increased fasting or postprandial blood glucose levels (Alam *et al.*, 2014). Prolonged deviation from normal homeostasis results in hyperglycemia, eventually leading to diabetes (Banday *et al.*, 2020). Individuals with DM exhibit cells incapable of producing or responding adequately to insulin, a hormone crucial for glucose utilization and storage, produced by pancreatic β -cells. This condition manifests through discernible alterations in glucose, lipid, and protein metabolism, encompassing glycolysis, gluconeogenesis, glycogenesis, glycogenolysis, and the Krebs's cycle (Dashty, 2013; Jiang *et al.*, 2020).

1.2 Global burden of diabetes

Once considered a negligible threat to global health, DM has emerged as one of the foremost challenges in the 21st century, ranking among the most prevalent non-communicable diseases worldwide and the fourth to fifth leading cause of death in industrialized nations. As per the report, DM has affected at least 177 million people globally, which may escalate to 642 million by 2040 (Cochran *et al.*, 2022). The projected incidence of DM is highest in the Middle East and North Africa regions, with an estimated 13.9% increase by the year 2045 (Alam *et al.*, 2021). Furthermore, the top ten countries with the highest prevalence of DM have been identified and determined, where India is ranked 2nd (Figure 1.1 [A-B]). Additionally, DM and its related complications have contributed to high medical expenses for individuals and the national economy.

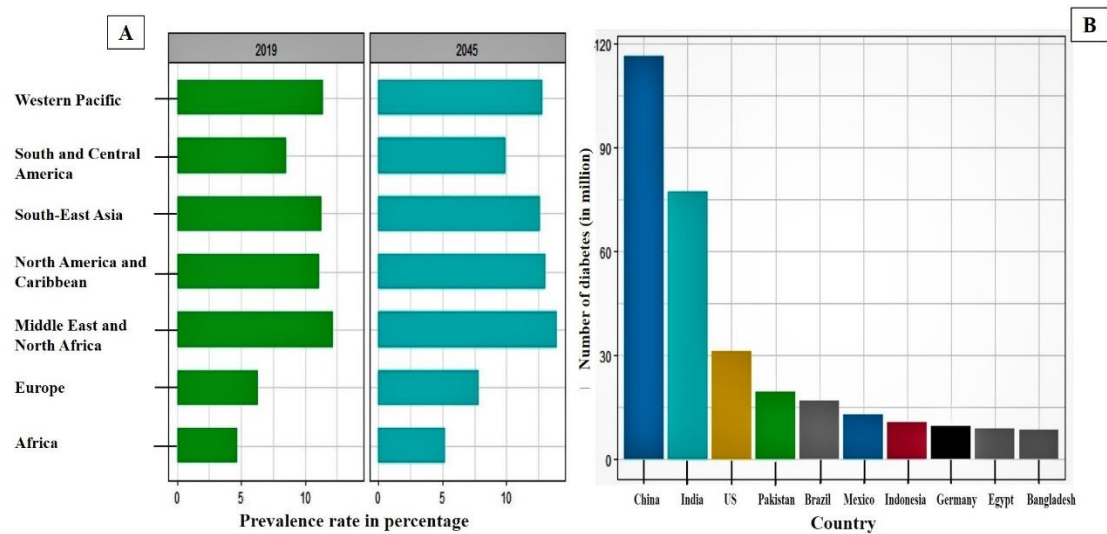


Figure 1.1: (A) Estimated global diabetes prevalence in 2019 and projection for 2045
(B) Countries with a maximum diabetic population.

(Adopted from Alam *et al.*, 2021)

1.3 Classification of diabetes

The WHO established the first widely accepted categorization of DM in 1980, followed by a revised version in 1985 (WHO, 1985). Two basic types of DM have been proposed: (i) insulin-dependent diabetes mellitus (IDDM), or Type 1 diabetes mellitus, and (ii) non-insulin-dependent diabetes mellitus (NIDDM), or Type 2 diabetes mellitus. Further, the 1980 and 1985 reports introduced the terms malnutrition-related diabetes mellitus (MRDM) and gestational diabetes mellitus (GDM) (WHO, 1985).

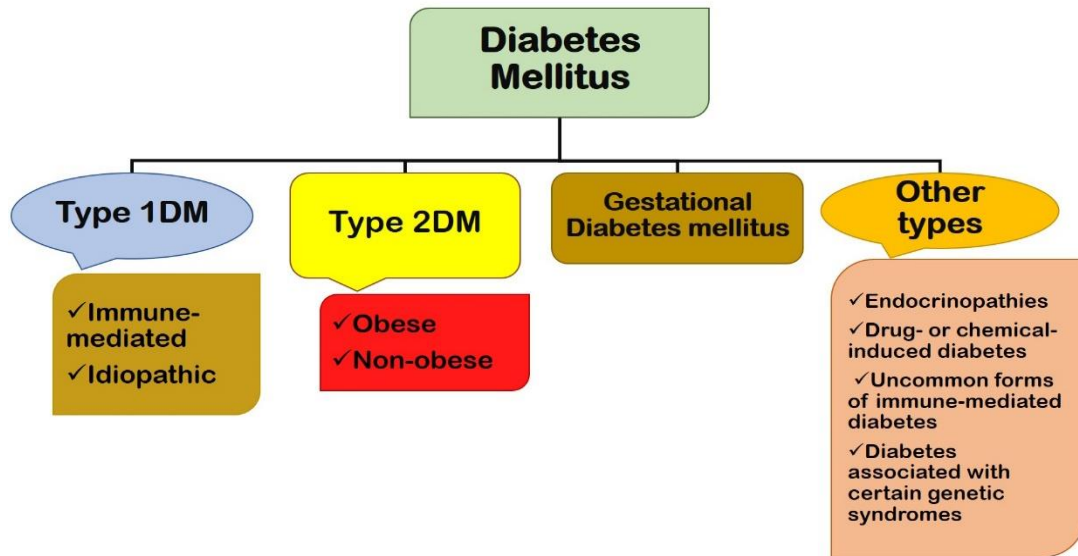


Figure 1.2: Classification of diabetes mellitus

1.3.1 Type 1 Diabetes mellitus (T1DM)

Type 1 diabetes mellitus stems from an unexplained process leading to a decline and eventual cessation of insulin production. This breakdown of pancreatic β -cells results in DM, where insulin is required for sustenance to prevent ketoacidosis and mortality. The loss of the β -cells is indicated by detecting insulin antibodies and anti-glutamic acid decarboxylase, which act against enzymes needed for proper functioning of the pancreas (Tsang *et al.*, 2019; Houeiss *et al.*, 2022). T1DM is a heterogeneous and polygenic condition influenced by various non-HLA (human leukocyte antigen) loci affecting disease susceptibility (Inshaw *et al.*, 2020). It is characterized by insulin insufficiency and extreme hyperglycemia; common symptoms include constant thirst, increased hunger, decreased body weight, polyuria, and episodic ketoacidosis. Individuals with T1DM require exogenous insulin for survival and to avert ketoacidosis (Akil *et al.*, 2021).

1.3.1.1 Causes of T1DM

T1DM is initiated by insulin deficiency due to the death of pancreatic insulin-

producing β -cells. The immune system of the body attacks and eliminates these cells, a process triggered by autoimmune mechanisms. The loss of β -cells may occur over an extended period, and the symptoms of the disease typically manifest rapidly (Roep *et al.*, 2021).

1.3.2 Type-2 diabetes mellitus (T2DM)

T2DM is characterized by dysfunctions in both insulin action and secretion (Reed *et al.*, 2021). This condition occurs when the cells in the body become less responsive to normal insulin levels in the bloodstream. As the condition progresses, there is a decline in the production and secretion of insulin. Various metabolic disturbances arise from this alteration, primarily affecting the liver, muscles, adipose tissue, and kidneys. This impairs glucose elimination, suppresses glucose synthesis, and disrupts lipid breakdown in insulin-sensitive organs (Papachristoforou *et al.*, 2020; Jwad & AL-Fatlawi, 2022). In the initial stages, most individuals with T2DM do not require external insulin but may necessitate it later in life. Although the precise causes are unknown, autoimmune breakdown of β -cells does not occur in T2DM. Individuals with T2DM are more prone to macrovascular and microvascular complications. Altered insulin secretion and insufficient compensation for insulin resistance characterize this condition. Although insulin resistance may improve with weight reduction or pharmaceutical hyperglycemia therapy, it rarely returns to normalcy. Age, obesity, and sedentary lifestyle increase the risk of T2DM (Wondmkun, 2020).

1.3.2.1 Causes of T2DM

The causes of T2DM encompass multiple factors, with a central role played by insulin resistance, where the fat, liver, and muscle of the body inefficiently utilize insulin (Wondmkun, 2020; Ahmed *et al.*, 2021). T2DM symptoms might emerge slowly and be subtle, leading some individuals with T2DM to go untreated for years.

Recent trends indicate an increased occurrence of T2DM in overweight, obese children and adolescents. Genetic susceptibility and environmental factors contribute to the development of T2DM.

1.3.2.1.1 *Obesity and physical inactivity*

T2DM is closely associated with obesity and physical inactivity, which enhance the vulnerability of individuals genetically predisposed to DM (Carbone *et al.*, 2019). An imbalance between calorie consumption and physical exercise contributes to T2DM. Abdominal obesity, characterized by excess belly fat, is a crucial risk indicator not only for insulin resistance and T2DM but also for cardiovascular diseases (CVD) (Cleven *et al.*, 2020). This abdominal fat generates hormones and compounds with long-term adverse effects on vascular health. Lifestyle adjustments, including regular exercise and weight reduction, have been proven to reduce the risk of T2DM (Ross *et al.*, 2023).

1.3.2.1.2 *Genetic susceptibility*

Genetic factors heavily influence the incidence of T2DM, with specific gene variations increasing or decreasing an individual's susceptibility to the condition (Prasad & Groop, 2015). While studies have uncovered many gene variants that increase susceptibility to this type of diabetes, most are undocumented. The identified genes primarily impact insulin production rather than resistance. For instance, variations of the TCF7L2 gene are linked to an increased risk of T2DM (Aboelkhair *et al.*, 2021). Lifestyle modifications have been shown to significantly reduce the risk of T2DM, even in individuals with this genetic variant (Ross *et al.*, 2023).

1.3.2.1.3 *Insulin resistance*

Insulin resistance occurs when fat, muscle, and hepatic cells no longer

respond efficiently to insulin. The pancreas compensates by producing additional insulin, maintaining normal blood glucose levels as long as β -cells produce enough insulin. Glucose levels rise when insulin synthesis is hindered due to β -cell dysfunction, resulting in T2DM (Mathieu *et al.*, 2021).

1.3.2.1.4 Metabolic syndrome

The metabolic syndrome is characterized by individuals who suffer from insulin resistance, such as increased blood sugar level, commonly referred to as insulin resistance disorder (Regufe *et al.*, 2020). Abdominal obesity, elevated blood pressure, and heightened triglyceride and cholesterol levels are common in metabolic syndrome. Lifestyle modifications, including exercise and weight reduction, prove to be effective in correcting metabolic disorders, enhancing insulin response, and reducing the risk of metabolic diseases (Dragano *et al.*, 2020; Colosimo, *et al.*, 2023)

1.3.2.1.5 Abnormal glucose production by the liver

In certain individuals, abnormal glucose production by the liver contributes to increased blood sugar levels. The pancreas usually produces the hormone glucagon in response to low blood insulin and glucose levels, stimulating the liver to release glucose into the bloodstream. Diabetic individuals often exhibit higher glucagon levels, leading to increased glucose production by the liver and elevated blood glucose levels (Jiang *et al.*, 2020; Kumar *et al.*, 2020).

1.3.3 Gestational diabetes mellitus

Gestational Diabetes Mellitus (GDM) is characterized by an underlying pattern of insulin resistance, leading to elevated blood glucose levels in pregnant women. Typically developing around the 24th week of pregnancy (Fu & Retnakaran, 2022). GDM affects approximately 2-5% of pregnancies, with its prevalence

potentially fluctuating postpartum. The condition arises when insulin action is impeded, likely influenced by placental hormones (Palani *et al.*, 2014). Untreated GDM poses risks to both the mother and the offspring, necessitating continuous healthcare monitoring. Infants born from mothers with GDM are at an increased risk of being overweight, and various epigenetic changes in the offspring have been associated with maternal hyperglycemia (Skrypnik *et al.*, 2019). Women with a history of GDM are more prone to recurrence in subsequent pregnancies and are also at an elevated risk of developing T2DM in the later part of life.

1.3.4 Other types of diabetes

Other less common forms of diabetes include endocrinopathies, drug- or chemical-induced diabetes, rare instances of immune-mediated diabetes, and diabetes associated with specific genetic disorders.

1.4 Diabetes and its complications

The management of hyperglycemia is of paramount importance due to its direct and indirect effects on the vascular system, which is a primary cause of morbidity and death in both T1DM and T2DM. Prolonged exposure to persistent hyperglycemia can result in both temporary and permanent complications (Ohiagu *et al.*, 2021). Short-term complications encompass elevated blood sugar levels and diabetic ketoacidosis. At the same time, chronic consequences include avascular disorders like cataracts and vascular disorders such as macrovascular (cardiovascular diseases) and microvascular (retinopathy, nephropathy, and neuropathy) complications (Kumar *et al.*, 2019; Goldstein *et al.*, 2020). Comorbidities are more prevalent in low socioeconomic groups, often associated with poor diabetic and hypertensive control, along with behavioural issues (Goldstein *et al.*, 2020).

1.4.1 Pathogenesis of diabetic complications

As the body progresses from the reversible stage known as pre-diabetes to the diabetic stage, multiple changes occur due to elevated blood glucose levels, resulting in hormone imbalances and weakening of blood vessels and nerves. These changes are driven by metabolic, humoral, and hemodynamic factors (Yehualashet, 2020; Sugahara *et al.*, 2021). When these changes become severe, they can lead to acute or short-term complications and chronic or long-term problems.

1.4.1.1 Acute complications

Acute complications include diabetes ketoacidosis (DKA) and hyperosmolar non-ketotic syndrome (HNS) (Ansari *et al.*, 2022b). DKA arises when insufficient insulin levels result in high blood sugar, increased organic acids, and ketones in the bloodstream, causing acute dehydration and significant alterations in blood chemistry. HNS is characterized by hyperglycemia, severe dehydration, hyper-osmolar plasma, and loss of consciousness (Sesti *et al.*, 2018).

1.4.1.2 Chronic complications

Long-term complications of DM impact multiple organs and are responsible for a large portion of fatality. Chronic conditions are categorized as vascular or avascular. Vascular problems are subdivided into microvascular and macrovascular complications (Jenkins *et al.*, 2019). T1DM increases the risk of microvascular complications while simultaneously elevating the risk of macrovascular complications. Microvascular disorders, including retinopathy (20%), neuropathy (9%), and diabetic nephropathy (up to 10%), are more serious than macrovascular disorders. Avascular effects encompass gastroparesis, sexual dysfunction, skin problems, and cataracts (Kumar *et al.*, 2019).

1.4.1.2.1 Diabetic hepatopathy

Diabetes-associated liver disease is a significant global cause of mortality. The association between DM and hepatic dysfunctions, including liver encephalopathy, portal hypertension, and oesophageal varices bleeding, is well-established in chronic stages (Dewidar *et al.*, 2020). Hyperglycemia is a common symptom of liver damage, and individuals with DM often present the entire spectrum of hepatic impairment, including abnormal levels of hepatic enzymes, non-alcoholic fatty liver disease, cirrhosis, hepatocellular carcinoma, and sudden liver failure. The bidirectional relationship between DM and cirrhosis involves a genetic predisposition for T2DM as a risk factor for chronic liver disease (Arrese *et al.*, 2019; Coman *et al.*, 2021).

1.4.1.2.2 Diabetic nephropathy

Diabetic nephropathy is the most prevalent cause of kidney failure and a significant complication of DM. End-stage renal disease is the progressive deterioration of kidney function, potentially leading to renal failure (Pradeep *et al.*, 2019). Individuals with diabetic nephropathy face an elevated risk of heart disease. The mechanism of diabetic nephropathy, however, is uncertain (Chebotareva *et al.*, 2021). However, structural proteins, including nephrin, podocin, and vascular endothelial growth factor (VEGF), play an important role in developing renal structural defects. Diabetic nephropathy is marked by increased glomerular protein permeability and mesangium extracellular matrix development, eventually leading to glomerulosclerosis and chronic renal failure (Sagoo & Gnudi, 2020; Chen *et al.*, 2020).

1.4.1.2.3 Diabetic wound

Diabetic wounds, affecting approximately 25% of individuals with DM, are serious non-healing conditions, often manifesting as diabetic foot ulcers (Burgess *et al.*, 2021). Typically found in the lower limbs, these wounds pose significant pathological implications, including infection, ulcer development, and various peripheral vascular dysfunctions. Both external wounds, such as burns and cuts, and internal wounds, such as ulcers and ingrown toenails, necessitate prompt medical attention to prevent complications (Dixon & Edmonds, 2021).

1.5 Biochemistry of diabetic complications

DM continues to be a leading cause of mortality and morbidity, with high blood glucose levels implicated in the initiation and progression of microvascular diseases (Alam *et al.*, 2021). Hyperglycemia, particularly detrimental to insulin-independent tissues, contributes to severe conditions such as diabetic retinopathy, liver dysfunction, and nephropathy (Dilworth *et al.*, 2021). Efforts to mitigate these risks have centered on reducing glycemic index levels of glycated haemoglobin (HbA1c), emphasizing the correlation between regulated glucose levels and reduced complication risks. Biochemically, various mechanisms are associated with the onset of these diverse illnesses (Longkumer *et al.*, 2022).

1.6 Factors affecting diabetic complications

Elevated blood sugar levels significantly contribute to chronic diseases, especially in individuals with poorly managed glucose levels (Papachristoforou *et al.*, 2020). Multiple metabolic pathways underpin the development of secondary diabetic complications. Given below are some of the pivotal pathways observed in glucose-induced damage:

1.6.1 Activation of protein kinase-C

Protein kinase C (PKC) activation is a fundamental and universal pathway in regulating hyperglycemia-induced cellular damage and associated biochemical complications (Papachristoforou *et al.*, 2020; Wu *et al.*, 2023). Increased PKC levels produce enhanced growth factor production, including vascular endothelial growth factor, resulting in arterial leakage and angiogenesis (Mesquita *et al.*, 2018).

1.6.2 Non-enzymatic glycation

Non-enzymatic glycation is one of the latest speculations to explain the underlying causes of diabetes complications. It affects the protein structure and could hinder the protein, resulting in structural changes altering the function of the protein (Khalid *et al.*, 2022). Clinical alterations resulting from advanced glycation end products (AGEs) contribute to complications, with AGEs particularly detrimental to kidney cells (Paul *et al.*, 2020).

1.6.3 Polyol pathway

In DM, rapid glucose uptake in tissues independent of insulin occurs, especially in the retina, nerves, and renal glomerulus (Daryabor *et al.*, 2020; Mason *et al.*, 2023). Excess additional glucose is digested in these organs *via* a different route known as the polyol pathway. The polyol pathway, an alternative glucose metabolism route, involves aldose reductase, transforming glucose to sorbitol (Thakur *et al.*, 2021). Accumulated sorbitol induces fluid swelling, altering cell permeability and oxidative stress, contributing to cellular damage and complications like diabetic nephropathy (Bashir, 2019).

1.6.4 Oxidative stress

High blood glucose level generates increased reactive oxygen species (ROS),

leading to decreased antioxidant defence, disruption of cellular processes, and oxidative membrane destruction (Pasupuleti *et al.*, 2020). Oxidative stress, resulting from glucose auto-oxidation, non-enzymatic glycation, and polyol pathway flux, triggers an array of cellular reactions. Dysregulation of crucial regulatory molecules adversely impacts metabolic activities, playing a dual role as both the cause and consequence of diabetic complications (Yadav & Ramana, 2013; Kurutas, 2015; Singh *et al.*, 2022; Saucedo *et al.*, 2023).

1.7 Epigallocatechin gallate in biomedical research

Tea, native to China, is today the most consumed beverage in the world after water. Tea obtained from the leaves of *Camellia sinensis* (L.) Kuntze belongs to the family Theaceae and, to a large extent, is produced in four varieties, i.e., green, oolong, white, and black tea, based on the methods of oxidation and fermentation techniques implemented (Zohora & Arefin, 2022). Green tea is obtained from the non-fermented tea leaves of *C. sinensis* and contains polyphenols and their derivatives. The different polyphenols include epicatechin-3-gallate (ECG), epicatechin (EC), epigallocatechin (EGC), and epigallocatechin gallate (EGCG). Among the different types of polyphenols, EGCG is considered to be the most abundant catechin in green tea infusions (Ratnani & Malik, 2022) and is also the most widely studied catechin. EGCG constitutes approximately 59% of green tea's total catechin content. Out of all catechins, EGCG shows a wide range of beneficial effects against conditions, including anticarcinogenic, antioxidative, antidiabetic, and neurodegenerative effects. Due to the numerous benefits to health and the gaining popularity of tea and its compounds with special reference to EGCG, it is widely marked as a nutraceutical supplement (Ramachandran *et al.*, 2016).

1.7.1 Antidiabetic effect of EGCG

EGCG emerges as a promising therapeutic agent for diabetes and related complications. Experimental studies reveal its role in controlling blood glucose levels, improving insulin secretion, and preventing oxidative stress-related damage (Raposo *et al.*, 2015; Krawczyk *et al.*, 2023). Clinical trials support its potential to improve glycemic control, anthropometric measures, and inflammatory status in T2DM patients (Asbaghi *et al.*, 2021).

1.7.2 Protective effects of EGCG***Anticancer property***

Anticancer properties of EGCG have been a central focus of research. It inhibits tumorigenesis, suppresses angiogenesis, and induces non-apoptotic cell death in various cancers (Shi *et al.*, 2015; Sanati *et al.*, 2023). The effectiveness of EGCG against hypoxia, limiting HIF-1 α and VEGF, adds to its potential in cancer treatment (Fu *et al.*, 2019).

Nervous System Protection

EGCG exhibits protective effects by inhibiting protein fibrillogenesis, reducing oxidative stress, and modulating signaling pathways in neurodegenerative diseases, such as Alzheimer's disease (AD) and Parkinson's disease (PD) (Singh *et al.*, 2016b; Khalatbary & Khademi, 2020). The countering potential of EGCG in neuronal impairment and its implications for PD and AD treatment are notable (Fernandes *et al.*, 2021).

1.7.3 Antioxidative effect of EGCG

EGCG acts as a dietary antioxidant, scavenging ROS and chelating metal ions (Zwolak, 2021). Studies demonstrate its capacity to counteract oxidative stress induced by electromagnetic radiation and showcase its potential therapeutic use in

preventing oxidative stress-related conditions (Ahmed *et al.*, 2017; Pramila & Julius, 2019).

1.8 Zebrafish in pharmaceutical research

1.8.1 Biology of zebrafish

Systemic position of zebrafish

Kingdom	:	Animalia
Phylum	:	Chordata
Class	:	Actinopterygii
Order	:	Cypriniformes
Family	:	Cyprinidae
Genus	:	<i>Danio</i>
Species	:	<i>rerio</i>

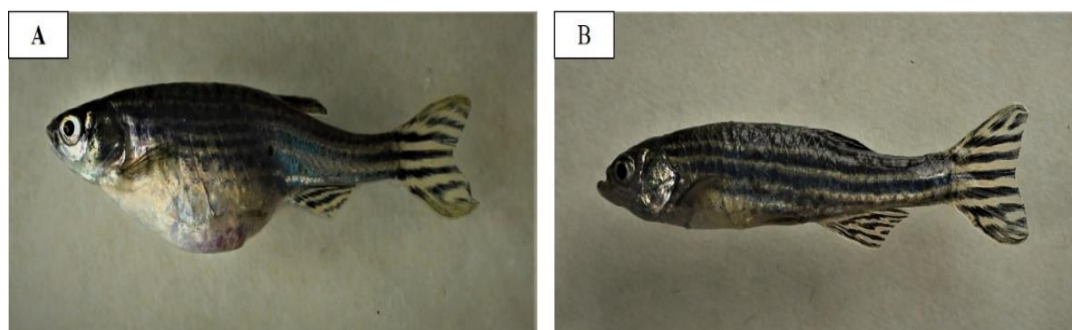


Figure 1.3: Morphology of zebrafish. (A) Female (B) Male

Zebrafish, members of the cyprinidae family, coexisting with barbs, minnows, carps, and other genera, belong to the genus *Danio*, which encompasses over forty closely related species, including the well-known *Danio rerio* (Meyers, 2018; Tan & Armbruster, 2018). Initially documented by Scottish physician Francis Hamilton, these fish are predominantly found in sluggish or still waters in the floodplains of Nepal, India, Bangladesh, and Pakistan (Watts *et al.*, 2012; Arunachalam *et al.*, 2013). Despite thriving in diverse environments, zebrafish prefer

slow-moving, clear, tropical waters with plant life and a muddy bottom. Laboratory zebrafish are typically maintained at 28°C, exhibiting remarkable temperature tolerance levels between 24.6°C and 38.6°C (Sfakianakis *et al.*, 2011; Delomas & Dabrowski, 2018). They feed predominantly on insects, nematodes, and zooplankton, and are prey for larger organisms like needlefish, knifefish, and catfish (Watts *et al.*, 2012). Domesticated zebrafish breed throughout the year, while in natural environments, spawning aligns with the monsoon season (April–August). Reproduction occurs in shallow, overgrown waterways, with experimental breeding often facilitated in shallow plastic containers (Meyers, 2018). Zebrafish initiate reproductive activity at dawn, with circadian rhythms potentially playing a crucial role. The mating behaviour of males and females leads to synchronized egg-laying and fertilization. Gravid females can produce hundreds to thousands of eggs, which adults may devour. Experimental breeding often involves isolating parents from eggs using mesh or marbles (Tsang *et al.*, 2017). Embryonic development at 28°C is rapid, leading to distinguishable features in adult males and females. Zebrafish strains exhibit diverse pigmentation patterns and fin lengths, with variations in lifespan, typically ranging from 3 to 4 years (Kishi *et al.*, 2009; Meyers, 2018).

1.8.2 Zebrafish as an animal model

The zebrafish serves as a valuable model for studying human health conditions and metabolic disorders due to their relevant tissues, including adipose tissue, cardiovascular components, steatosis, and energy balance (Seth *et al.*, 2013; Choi *et al.*, 2021). The pancreas in zebrafish has key cellular architecture and morphogenesis that are similar to the mammalian pancreas, allowing researchers to identify potential treatment targets for pancreatic diseases like DM (Angom & Nakka, 2024). With a 70% physiological and genetic resemblance to humans, zebrafish have

been instrumental in metabolic disease research, particularly diabetes (Gnügge *et al.*, 2004; Benchoula *et al.*, 2019). The zebrafish pancreas regulates glucose metabolism by secreting insulin, somatostatin, and glucagon into the bloodstream. They exhibit glucose metabolism processes similar to humans and mice, responding well to anti-diabetic medications (Ji *et al.*, 2021). Experimental diabetes models involving zebrafish immersed in glucose solutions successfully replicate diabetic conditions and retinopathy seen in humans (Chen & Liu, 2022). They are also utilized to investigate reproductive concerns due to their developmental and physiological advantages. Transparent embryos allow researchers to observe tissues and biological events seamlessly, and the short breeding time facilitates efficient experimentation. The similarities between human and zebrafish development further enhance the utility as a model for in-depth mechanistic studies (MacRae & Peterson, 2023). Zebrafish is an efficient well-accepted biological model with easily interpretable results in various research fields.

1.9 Scope and objectives of the study

Scope of the study

The general scope of this thesis was to explore the novel effect of EGCG in preventing diabetic complications using zebrafish as an animal model. In Chapter 2, acute toxicity was evaluated for EGCG dose in the zebrafish model, wherein the animal's response towards the compound was monitored. Histopathological studies in liver, kidney, and gill tissues were done to understand the acute effect of the compound.

Subsequently, in Chapter 3, the minimum tolerable dose of the compound EGCG was carried out, and further assessment of the general physiology of the model and fin regeneration was done for the control group, diabetic group, diabetic supplemented with EGCG, and control treated with EGCG.

In Chapter 4, the impact of EGCG on lipid profiles and metabolic enzymes in the liver, gills, and kidney tissues was measured for all experimental zebrafish groups.

In Chapter 5, the efficacy of EGCG on antioxidant activities of SOD and CAT within the liver, kidney, and gills was studied. Further histological alterations and the outcome of treatment were recorded.

In Chapter 6, the effect of EGCG on DM-induced reproductive pathology has been observed. Various parameters, such as congenital abnormalities, histopathology of gonads, and measurement of gonadosomatic and hepatosomatic index, were also observed.

Objectives of the study

1. To conduct an acute toxicity study and observe behavioural changes in the zebrafish model under EGCG treatment.
2. To establish a diabetic zebrafish model and determine the minimum effective dose for EGCG.
3. To examine general physiological status and fin regeneration in experimental zebrafish.
4. To evaluate the biochemical as well as histopathological changes in a diabetes-induced zebrafish model and the effects of therapy with EGCG.
5. To assess reproductive performance and developmental deformities in a diabetes-induced zebrafish model treated with EGCG.

Chapter 2

Acute toxicity study and behavioural responses in zebrafish model treated with EGCG

Contents

2.1 Introduction

2.2 Materials and methods

2.3 Results

2.4 Discussion

2.1 Introduction

Paracelsus coined his famous dictum, “All things are poison, and nothing is without poison; only the dose makes a thing, not a poison.” The critical determinant of toxicity of a chemical is the dosage encompassing the quantity and the duration one is subjected to the substance. The expression LC_{50} denotes the potentially hazardous chemical concentration that eliminates 50% of an experimental subject (Faksness *et al.*, 2020). Hazardous substances impact biological organisms across various organizational levels, from molecular to the level of the ecosystem. The understanding that substances initiate biochemical responses at the molecular level before affecting larger organizational structures is widely accepted (Rahmati *et al.*, 2020). Emphasizing the need for in-depth knowledge, elucidating the mode of action and mechanisms of toxic chemicals is crucial. This deeper understanding enhances data interpretation and aids in more effective risk assessment of potentially harmful chemicals for environmental and human safety. While not all hazardous substances are fatal, they can induce health issues, tissue damage, genetic alterations, cancer, and other problems (Sabarwal *et al.*, 2018). The study of toxic action mechanisms evolved to characterise key molecular activities in the cascade leading to toxicity. According to Kuete. (2014) and Patel et al. (2020) some of the most crucial characteristics of toxicity are as follows: (A) Biochemical and molecular toxicology, addressing biochemical and molecular aspects such as xenobiotic-metabolizing enzymes, generation of reactive intermediates, the interaction of xenobiotics with biomolecules, gene expression in metabolism, and toxic signaling pathways. (B) Behavioural toxicology, exploring the influence of toxic substances on human and animal behaviour, represents

Chapter-2 *Acute toxicity study and behavioural responses in zebrafish model treated with EGCG*

the integrated manifestation of the nervous system. (C) Organ toxicity, evaluating impacts on organ function, including neurotoxicity, hepatotoxicity, nephrotoxicity, and more.

Numerous substances, while recognized as harmful, exert indirect effects on organisms. Toxic chemicals in the environment and humans originate from various sources, including synthetic organic molecules, heavy metals, and substances from plants, microorganisms, and animals. Despite recent focus on pesticides, heavy metals, and synthetic substances, there are reports of hazardous effects induced by plant-derived products (Jitäreanu *et al.*, 2022). Plant extracts, prevalent in traditional or folk medicine, have gained popularity due to the perception of their safety. However, like synthetic chemicals, herbal medications can pose potential health hazards due to toxins released during plant metabolism. One such compound under scrutiny is EGCG, a catechin abundant in green tea with recognized antioxidants and anti-inflammatory properties, marketed as a dietary supplement (Cione *et al.*, 2019). While studies in model animals highlight its positive effects, there is limited toxicological evaluation of EGCG. Reports suggest its potential pro-oxidant role, leading to hepatotoxicity and suppression of liver antioxidant enzymes (Wang *et al.*, 2015). Considering the diverse applications of EGCG in biomedical studies, understanding its toxicity is imperative.

Zebrafish is an excellent animal model for toxicity assays due to its cost-effectiveness, short cycle, and ethical advantages over mammalian models. With shared physiological, morphological, and histological characteristics with mammals, zebrafish enable practical assessment of drug targets and safety risks. This model allows for the simultaneous monitoring of multiple organs and studying pharmacokinetic, and

Chapter-2 *Acute toxicity study and behavioural responses in zebrafish model treated with EGCG*

metabolite activities (Choi *et al.*, 2021; Zhang *et al.*, 2022).

Natural products such as EGCG are on the rise, and their application in various biomedical research. Despite findings showcasing the potent nature of EGCG to counteract carcinogenic and mutagenic effects, limited reports on its safe use are available (Alam *et al.*, 2022; Salgado *et al.*, 2022). Therefore, a comprehensive study of the toxicity of EGCG, utilizing acute toxicity bioassays, is essential to ensure the safe application of traditional medicine and promote further research activities. The present chapter aims to examine the acute toxicity in zebrafish models, observe behavioural responses, and assess histological damage in the kidney, liver, and gill tissues under EGCG treatment.

2.2 Materials and methods

2.2.1 Chemicals

Hematoxylin-eosin stain, xylene, and absolute alcohol were procured from Sigma Aldrich. Solutions were meticulously prepared employing deionized water to ensure optimal purity and consistency. Prior to their utilization, glassware and aquariums underwent thorough washing and rinsing with distilled water to prevent any potential contamination.

2.2.2 Characterisation of EGCG

Commercially available purified EGCG (>95%) was procured from Merch. The spectral properties of EGCG fluorescence in distilled water as a solvent were examined using a Fluoromax-4 spectrofluorometer.

2.2.3 Acclimatization of zebrafish

Zebrafish adult wild types of both sexes were procured in bulk from Modern Pet Shop (Government authorised and registered seller) Zoo Road, Sunderpur Guwahati, Assam, India. It was cultured in a zebrafish housing system (Model-NT-ZB-11). The system was standardized to ensure constant temperature ($28 \pm 2^{\circ}\text{C}$), and persistent chemical, biological, and mechanical water filtration, and aeration (7.20 mg/L).

2.2.4 Physico – chemical parameters of fish tanks

Water temperature and pH measurements were conducted using an ISTA LCD Digital aquarium thermometer and a digital LCD pH meter pen, respectively. Additional water parameters were analyzed using the Aqua Merck portable field water analysis kit. The photoperiod was maintained with a multi-circuit digital switch, ensuring a 14-hour light period and a 10-hour dark period.

2.2.5 Assessment of acute toxicity

The 96 hour semi-static acute toxicity test of zebrafish exposed to EGCG was performed according to guideline 203 of the Organisation for Economic Co-operation and Development (OECD, 1992). Adult zebrafish were randomly exposed to (8, 10, 12, 14, 16, 18, 20, 22, 24, 26, 28, and 30) mg of EGCG in 1-liter dechlorinated water. The test performed consisted of ten adult zebrafish. The fresh solution was prepared and changed every 48 hours after the first exposure. The test animals were fed commercially available feed and not fed 24 hours before the experiment. Test animals were observed periodically for four days. Dead animals and faeces were promptly removed from the experimental fish tank to ensure non-interference in the system. Each concentration group was set up with three replicates. A control group was always treated identically, except that they received no treatment with EGCG. The number of dead and live organisms, including the control group, was counted every 24 hours. Dead zebrafish were removed as soon as they were observed. The criterion used to identify the death of the fish was a lack of movement and a lack of reaction to gentle probing. The test was conducted on day four at the same hour the test began.

2.2.6 Behavioural study

Behavioural changes were recorded, such as gulping activity where the zebrafish were observed according to the piping and gasping movement of their opercular at the surface of the experimental solution, hyperactivity like skittering and erratic swimming movements, and hypoactivity such as lethargy, inactivity, weak, quiescent, ceased swimming and immobility were recorded individually in the experimental subjects. In

order to observe the morphological change, the whole-body image of the experimental zebrafish was captured by using a Nikon D3500 digital camera.

2.2.7 Histopathological study

A parallel investigation was conducted to understand morphological alterations, with the lowest (12 mg/L) and highest (30 mg/L) EGCG doses showing moderate and detrimental effects, respectively.

2.2.8 Analysis of histological sections

Histopathological techniques were followed based on the method of Abdelhamid et al. (2020).

2.2.8.1 Fixation: Tissues were fixed in 10% Formaldehyde solution.

2.2.8.2 Washing: Fixed tissues were washed using tap water overnight to remove the fixative.

2.2.8.3 Dehydration: Tissues were dehydrated using an ascending graded series of ethyl alcohols (30%, 50%, 70%, 90%, and 100% or absolute alcohol).

2.2.8.4 Clearing: Xylene was used as a clearing agent to remove ethanol, and tissues were placed in xylene until translucent.

2.2.8.5 Infiltration: Xylene was replaced by paraffin wax, and tissues were embedded in paraffin.

2.2.8.6 Embedding: Following infiltration, the tissues were paraffin-embedded individually. The embedding cassettes were loaded in hot liquid paraffin, and tissues were subsequently placed in the correct position in the cassettes.

Chapter-2 *Acute toxicity study and behavioural responses in zebrafish model treated with EGCG*

2.2.8.7 Sectioning: Semi-automatic microtome Model-RMT: 35 (Radical Scientific Equipment Pvt. Ltd. India) with disposable blades were used for sectioning at 4-5 μ thickness.

2.2.8.8 Staining: The staining was carried out by placing the sections in xylene. After the paraffin wax was removed, the sections were taken through decreasing concentrations of alcohol to hydrate the tissue. The sections were then immersed in distilled water and then stained with haematoxylin, followed by eosin. The sections were immediately washed with running tap water to remove the excess stains. The sections were then dehydrated through a series of increasing concentrations of alcohol, after which it was placed in xylene. The sections after xylene treatment were mounted with Dibutylphthalate Polystyrene Xylene DPX- mountant, and a cover glass (22 x 50 mm, BDH/Merck) was applied. The prepared slides were observed and photographed under a cxi microscope attached to a Sony digital camera (model E31SPM20000KPA; USB 2.0) and analyzed using image J software.

Table 2.1: Tissue block preparation

Sl. No.	Medium	Duration	Change
1.	Absolute alcohol	1 hour	2 Change
2.	Xylene	5 mins	2 Change
Further experiments were carried out at 60°C			
3.	Xylene + Wax (50/50)	40 mins	2 Change
4.	Wax – 1	40 mins	1 Change
5.	Wax – 2	40 mins	1 Change
6.	Wax – 3	40 mins	1 Change

Chapter-2 *Acute toxicity study and behavioural responses in zebrafish model treated with EGCG*

7.	Block preparation	--	-
----	-------------------	----	---

Table 2.2: Haematoxylin and eosin staining

Sl. No.	Medium	Duration	Change
1.	Xylene	10 min	2 Change
2.	100% alcohol	10 min	2 Change
3.	90% alcohol	10 min	2 Change
4.	70 % alcohol	10 min	2 Change
5.	Distill water	10 min	1 Change
6.	Haematoxylin	4 – 6 Sec	-
7.	Eosin	2-4 Sec	-
8.	Wash with running water	10 min	-
9.	70% alcohol	10 min	2 Change
10.	90% alcohol	10 min	2 Change
11.	100% alcohol	10 min	2 Change
12.	Xylene	10 min	2 Change

All reagents except Haematoxylin and Eosin are changed after every 5th run.

2.2.9 Statistical analysis

The recorded mortality data underwent correction for a natural response using Abbott's formula (Abbott, 1925). Subsequently, Probit analysis was applied for LC₅₀ calculation and other statistical parameters at 95% confidence limits, with upper and lower confidence limits determined using IBM SPSS 22.0 software (SPSS Inc., USA). The concentration and corrected % mortality was plotted against the X-Y axis, facilitating the calculation of LC₅₀ for the test substance. Mortality data collected over the 96-hour test period were utilized to determine LC₅₀ values at 24, 48, and 72 hours when sufficient data was

Chapter-2 *Acute toxicity study and behavioural responses in zebrafish model treated with EGCG*

available. The mean number of deaths per 24 hours at each concentration was calculated, plotted on an X-Y scatter plot, and presented using GraphPad Prism Version 5.0. Behavioural response results for adult zebrafish were presented as Mean \pm SD with error bars.

2.3 Results

2.3.1 Characterisation of EGCG

Chemical property

Molecular formula: C₂₂H₁₈O₁₁

Molecular weight: 458.372 gm/mol

Name: Epigallocatechin gallate

Solubility in water: Soluble (5 gm/L)

Solubility: Ethanol, DMSO, dimethyl formamide at about 20 gm/L

Structure:

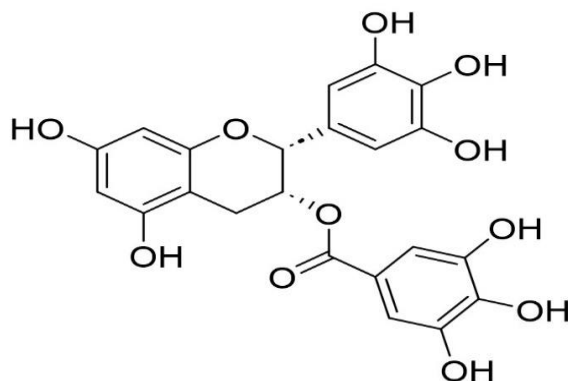


Figure 2.1: Chemical structure of EGCG

2.3.1.1 Spectral property of EGCG fluorescence dissolved in water

EGCG was observed to be a highly fluorescent molecule when excited at approximately 335nm with emission at approximately 399nm as represented in Figure 2.2.

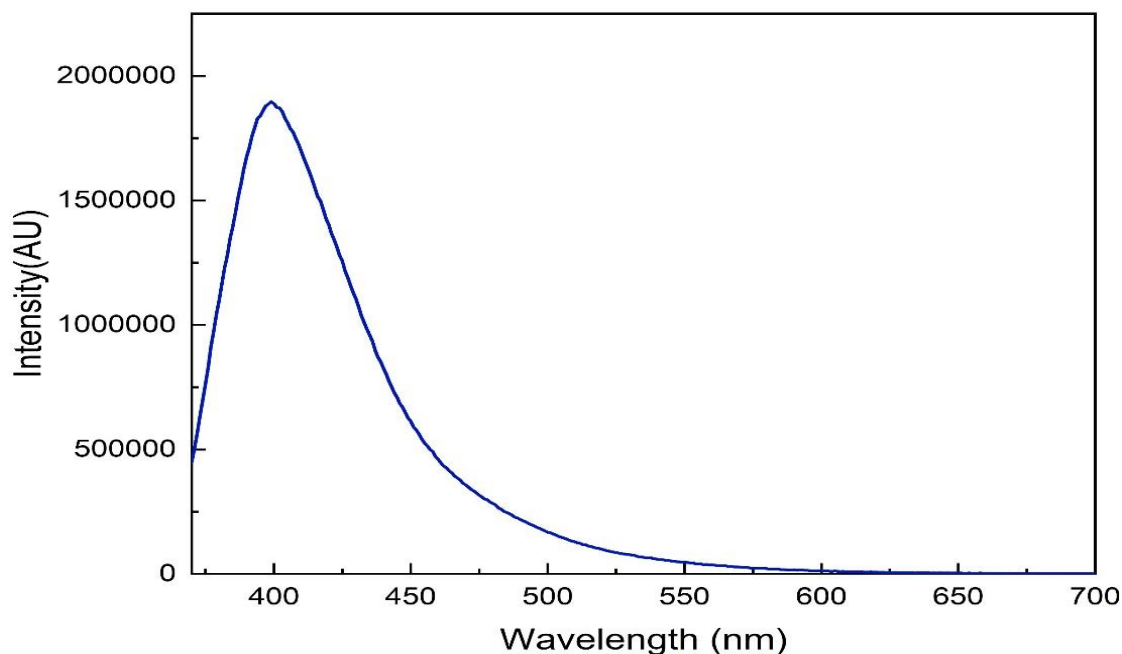


Figure 2.2: Emission spectra of EGCG dissolved in distilled water

2.3.2 Acclimatization of zebrafish

The zebrafish housing is well-equipped and tailored, including a high-density rack and an automated recirculating water system that provides complete water filtering and cleansing. The water filtration system of the aquarium uses chemical, mechanical, and biological filtering, as well as UV radiation, before channeling it into each fish chamber. The animals were housed in a 1-liter separate fish aquarium, with the temperature maintained *via* a submersible heater (300W). Further, the photoperiod was maintained using a multi-circuit digital switch. Figure 2.3 shows the schematic representation of the zebrafish housing system.

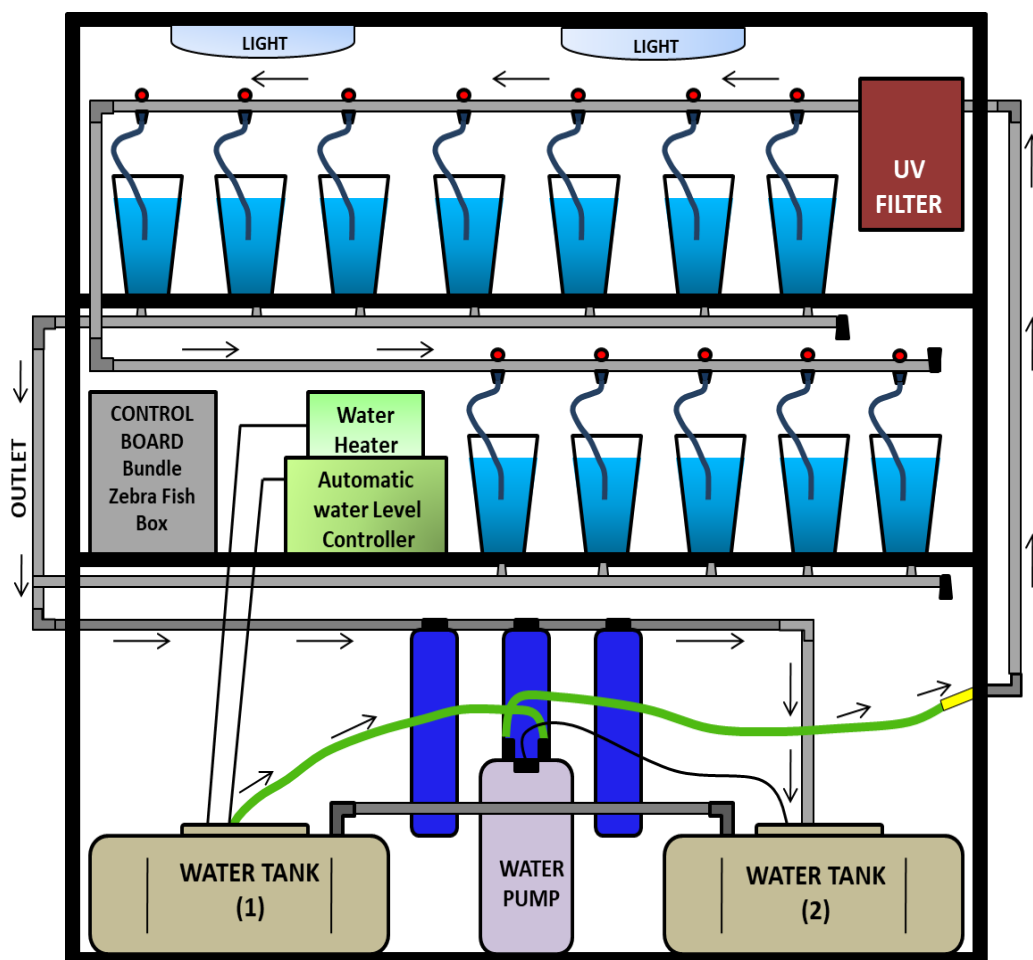


Figure 2.3: Schematic representation of zebrafish housing system.

2.3.3 Physico-chemical parameters of fish tank

The water temperature and pH were maintained at 28°C (25-30°C) and 7.3 (6.5-8.0) respectively. Nitrite, nitrate, and ammonia were all recorded at 0 ppm. The total hardness of the water was maintained between 80-200 mg/L CaCO₃ and conductivity at 1000-200 (μS). The dissolved oxygen concentration was not less than 5 mg/L. The photoperiod was 14 hours of light and 10 hours of darkness. Table 2.3 shows the physico-chemical parameters of water.

Table 2.3: Physico-chemical parameters of the test water.

Environmental parameter	Values
Temperature	28°C
Conductivity	1000-200 (μS)
Photoperiod	14-hr light: 10-hr dark
pH	7.3 (range: 6.5–8.0)
Nitrite	0 (ppm)
Nitrate	0 (ppm)
Ammonia	0 (ppm)
Total hardness	80-200 (mg/L CaCO ₃)

2.3.4 Assessment of acute toxicity

The LC₅₀ was calculated to be 26.91 mg/L, 25.70 mg/L, 23.44 mg/L and 21.37 mg/L for EGCG at 24-hours, 48-hours, 72-hours and 96-hours, respectively, as described in Table 2.4. The linear curve between the mortality of test fish against the different concentrations of EGCG treated for 24 hours, 48 hours, 72 hours and 96 hours showed a highly positive correlation (Figure 2.5[A-D]). The experimental zebrafish displayed dose- and dose-time-

Chapter-2 *Acute toxicity study and behavioural responses in zebrafish model treated with EGCG*

dependent mortality, as shown in Figure 2.4. The mortality was 100% at doses above 30 mg/L in the case of EGCG.

Table 2.4: LC₅₀ of EGCG for various durations (24 hours, 48 hours, 72 hours and 96 hours) in the zebrafish model.

Duration	LC ₅₀ of EGCG (mg/L)
24 hours	26.91
48 hours	25.70
72 hours	23.44
96 hours	21.37

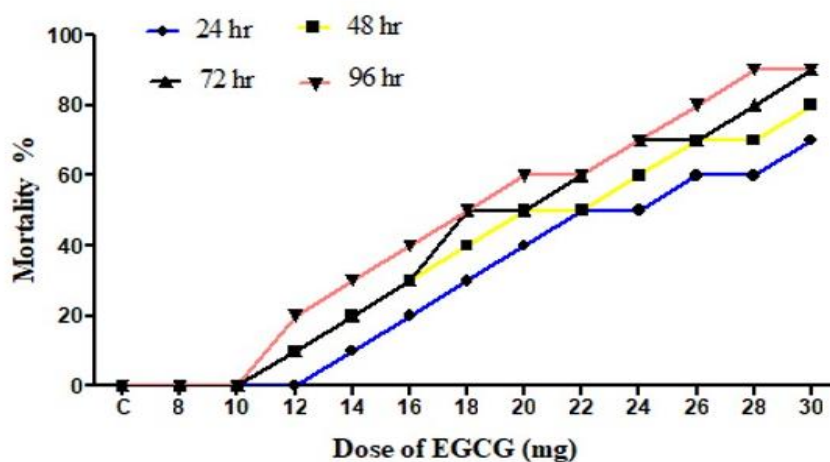


Figure 2.4: Dose-response curve of EGCG (mg/L) after exposure to various periods (24 hours, 48 hours, 72 hours and 96 hours) in the zebrafish model.

Chapter-2 *Acute toxicity study and behavioural responses in zebrafish model treated with EGCG*

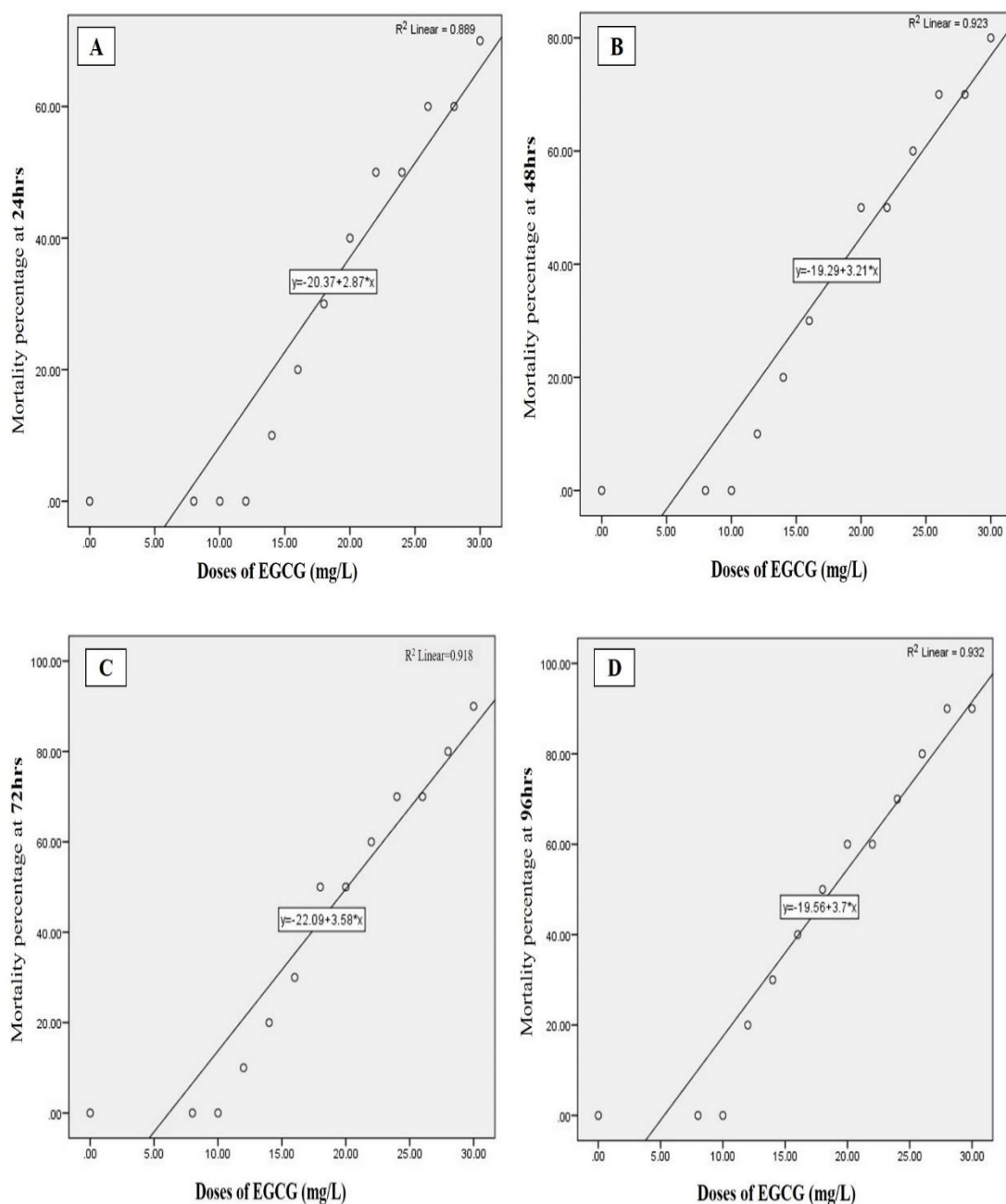


Figure 2.5: Mortality percentage at different durations of EGCG exposure. (A) 24 hours (B) 48 hours (C) 72 hours (D) 96 hours.

2.3.5 Behavioural response

Test animals responded with rapid movement, swimming, swallowing, jumping activity, and immobile behaviour as the concentration of EGCG increased. The behavioural activity of zebrafish under the influence of EGCG is represented in Figure 2.6. At higher doses, fins became harder and stretched. A large amount of mucus was present over the fish's body. The dead zebrafish showed reddish skin coloration in the opercular region due to hemorrhage. There was a decrease in the pigments of the zebrafish body as exposure to time and dose were increased. Severe necrosis and edema were observed in the chest area of the fishes exposed to EGCG (Figure 2.7 [A-D]). The magnitude of damage caused to the organs was found to be a time and dose-dependent factor. Longer duration and higher doses were found to cause more damage.

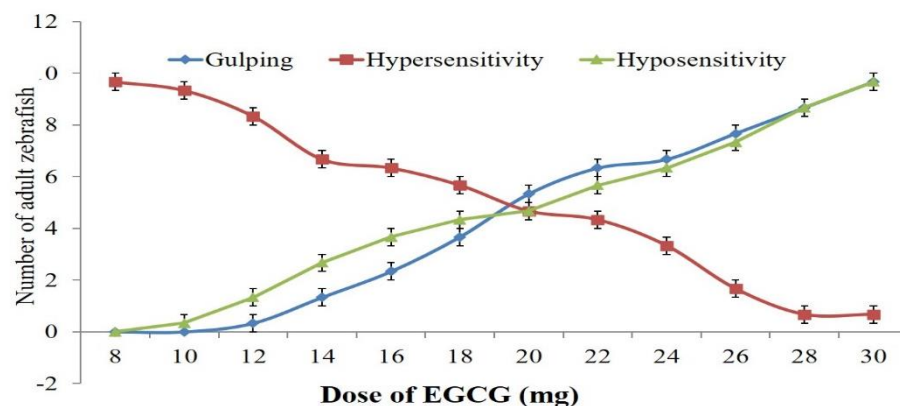


Figure 2.6: Behavioural response in experimental zebrafish under treatment with different doses of EGCG.

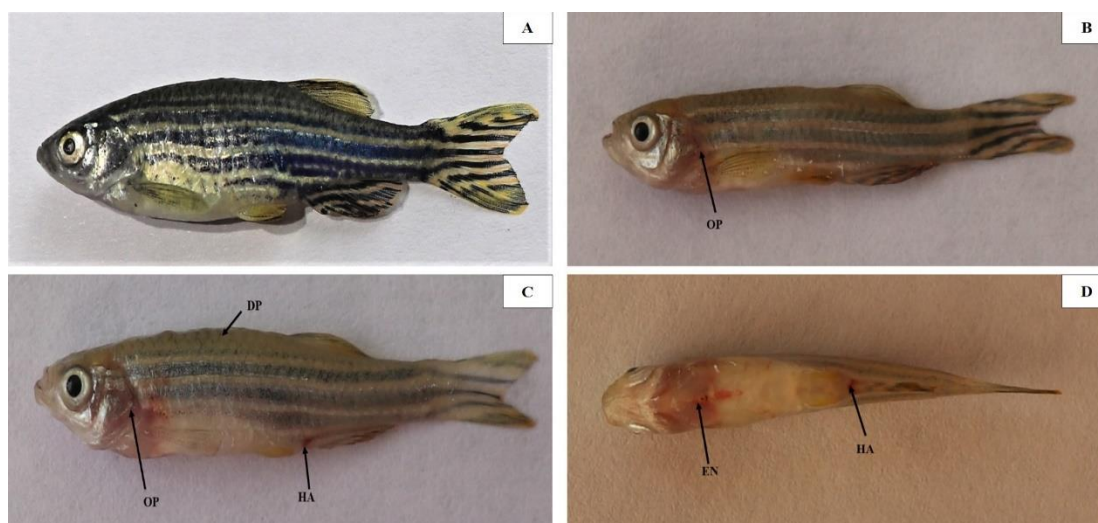


Figure 2.7: Morphological changes in zebrafish model treated with EGCG. (A) Control zebrafish (B) Zebrafish treated with 12 mg/L EGCG exhibiting blood aggregation resulting in red coloration in the opercular area (OP) (C-D) Zebrafish treated with 30 mg/L EGCG exhibited hyperaemia towards the anal fin (HA), increased red coloration in the opercular region (OP), serious edema and necrosis in the thorax area (EN), highly dyspigmentation of the body (DP).

2.3.6 Histopathological study

2.3.6.1 Effects of EGCG on the liver of experimental zebrafish

A comparative study was done to further understand the histopathological changes of the control group, with the minimum dose (12 mg/L of EGCG) where the test animal started showing lethargy and the highest dose (30 mg/L of EGCG) in which the degree of toxicity showed to be harmful, resulting in increased mortality. The test zebrafish showed alterations in the liver tissue compared to the control group, depending on the degree of dose incorporated. Exposure to 12 mg/L of EGCG displayed cell death, necrosis, atrophy, and vacuolar degeneration. In contrast, higher vacuolar degeneration in different areas of the liver, atrophy, necrosis, hypertrophy, and sinusoid space was noticed at 30 mg/L of EGCG. The effect of EGCG on the liver tissue is represented in Figure 2.8[A-C].

2.3.6.2 Effects of EGCG on the kidney of experimental zebrafish

12 mg of EGCG exposure showed histoarchitectural changes in the kidney, such as focal renal tubular degeneration, glomerular shrinkage, and dilation of bowman's space, whereas exposure to 30 mg EGCG showed glomerular shrinkage, acute cellular degeneration, vacuolar degeneration, hemorrhage, and bowman's space dilation. The effect of EGCG on the kidney tissues is represented in Figure 2.9[A-C].

2.3.6.3 Effects of EGCG on gills of experimental zebrafish

In the experimental group, the gills of the zebrafish treated with 30 mg/L of EGCG, exhibited hypertrophy, shortening of secondary lamellae, edema, curling of lamellae, epithelial hyperplasia, epithelial lifting, and lamellar synechiae. Further, a higher dosage of EGCG (30 mg/L) caused mucus secretion and fusion of secondary lamellae, as well as

Chapter-2 *Acute toxicity study and behavioural responses in zebrafish model treated with EGCG*

fusion with the adjacent sides, which can be seen. A lower concentration of EGCG (12 mg/L) showed lesser lamellar fusion and hyperplasia compared to the high dosage. The lamellae's slight epithelial lifting and curling was observed, as described in Figure 2.10[A-D].

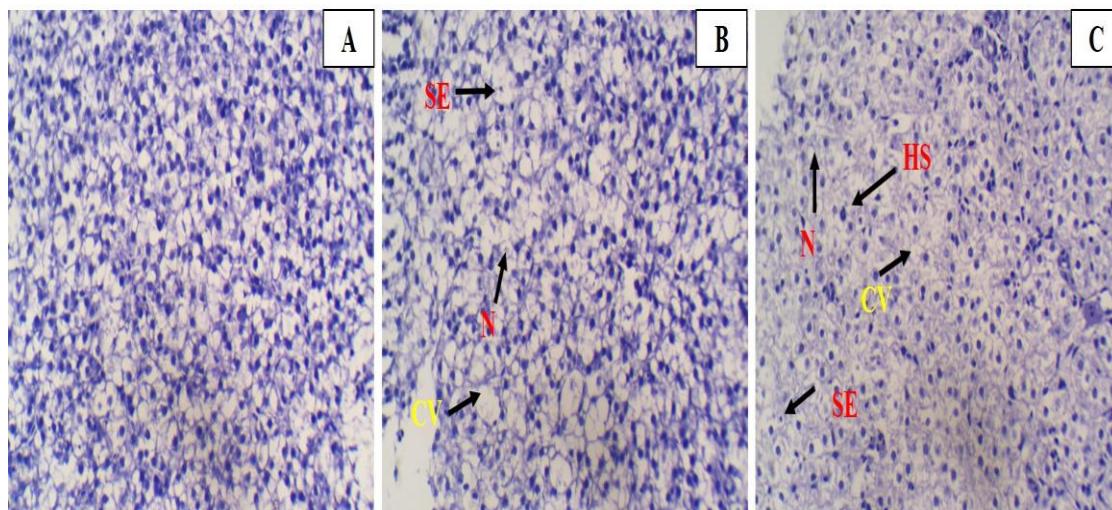


Figure 2.8: Histological changes in zebrafish model treated with EGCG. (A) Control Liver (B) Liver treated with EGCG (12 mg/L) exhibiting atrophy (SE), necrosis (N), vacuolar degeneration (CV) (C) Liver treated with EGCG (30 mg/L) exhibited cell hypertrophy (HS), atrophy (SE), vacuolar degeneration (CV), necrosis (N). (Figures captured at 40X magnification)

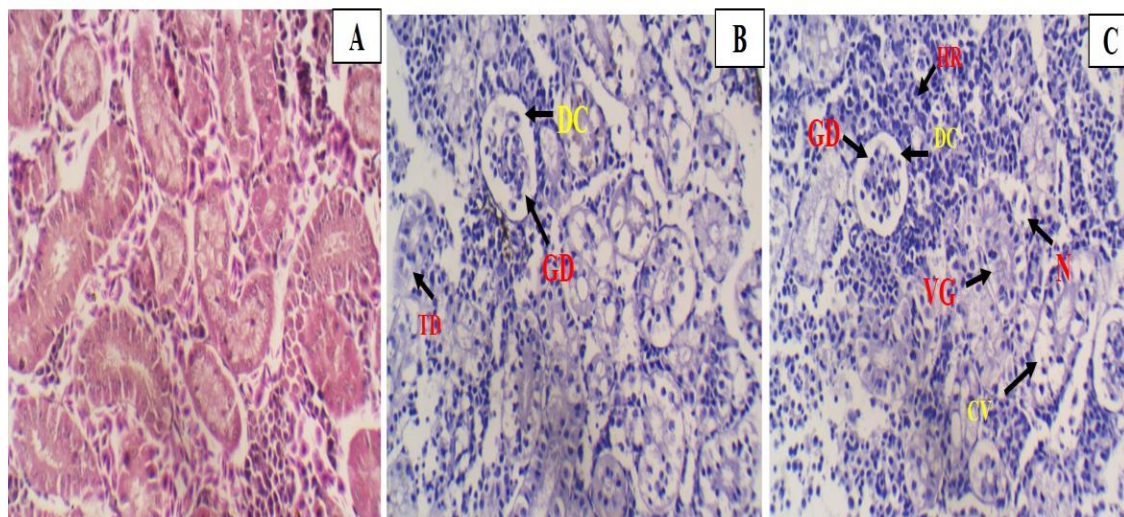


Figure 2.9: Histological changes in zebrafish model treated with EGCG. (A) Control Kidney (B) Kidney treated with EGCG (12 mg/L) exhibiting tubular degeneration (TD), glomerular shrinkage (GD), dilation of bowman's space (DC) (C) Kidney treated with

EGCG (30 mg/L) exhibiting glomerular shrinkage (GD), vacuolation (CV), vacuolar degeneration (VG), hemorrhage (HR), bowman's space dilation (DC), and necrosis (N). (Figures captured at 40X magnification)

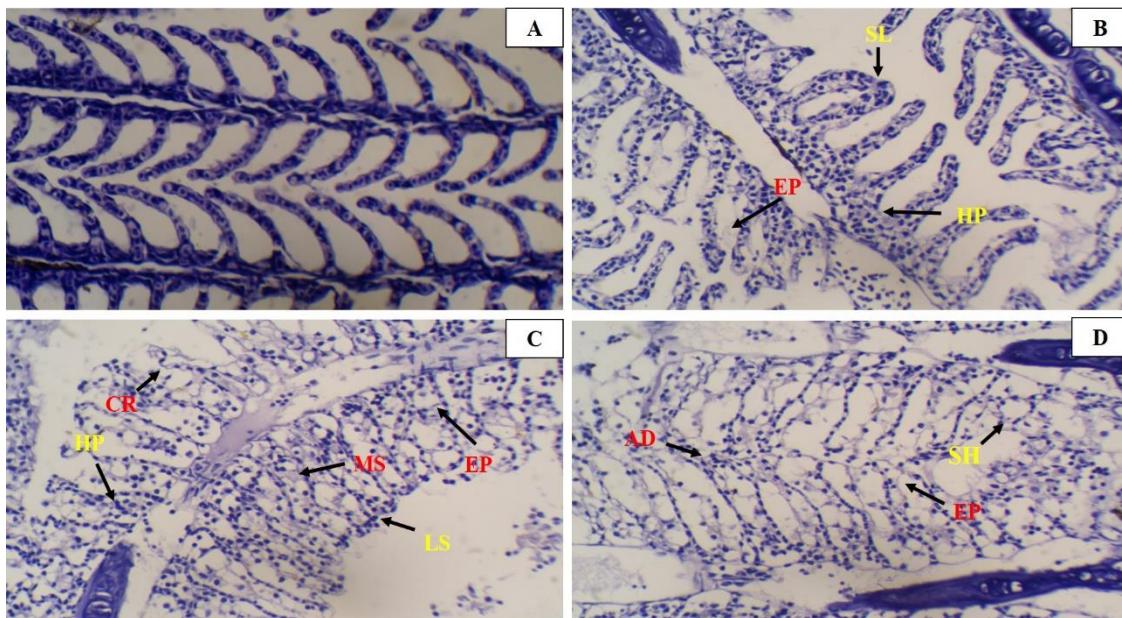


Figure 2.10: Histological changes in zebrafish model treated with EGCG. (A) Control gills (B) Gills treated with EGCG (12 mg/L) exhibiting epithelial lifting (EP), hyperplasia (HP), fusion of secondary lamella (SL) (C-D) Gills treated with EGCG (30 mg/L) exhibiting epithelial lifting (EP), epithelial hyperplasia (HP), curling of lamella (CR), mucus secretion (MS), lamellar synechieae (LS), fusion with secondary and adjacent lamella (AD), and shortening of secondary lamella (SH). (Figures captured at 40X magnification)

2.4 Discussion

In recent years, numerous researches have shown the effects of nutraceuticals on animal models; however, very little research has been done on the determination of LC₅₀ of EGCG in the zebrafish model. The toxicity of test compound was determined by immersing adult zebrafish in the solution of EGCG, observing their behaviour, and undergoing histological changes. Doses above the lethal concentration of EGCG have been found to be harmful to different target organs. A parallel study involving the exposure of adult zebrafish to pyraclostrobin revealed a dosage and time-dependent increase in mortality (Huang *et al.*, 2021).

The assessment of behavioural response is a useful tool for determining the toxicological influence of the test compounds on the test animals (Hong & Zha, 2019). Exposure to chemical compounds in a stressful environment triggered animal defence mechanisms, leading to behavioural alterations such as escape behaviour, settling at the tank bottom, and rapid movement to evade hazardous substances. The treated zebrafish exhibited behavioural changes similar to those observed in other studies, in which zebrafish exposed to “Kandhamal haladi” demonstrated irregular, erratic, and aberrant swimming movements (Satpathy & Parida, 2020). Fin hardening occurs due to muscular stretching, making it difficult for the fish to swim. When zebrafish are exposed to a harmful environment, skin inflammation causes excessive mucus secretion. Mucus establishes a barrier between harmful surroundings and lowers irritation caused by the agents, a common fish’s defence strategy (Leris *et al.*, 2019). The red coloration in the test animal which is considered to be the result of massive hemorrhage was also recorded

when studying the zebrafish response after exposure to propylthiouracil (Schmidt & Braunbeck, 2011). Further, when the toxic substances in the environment are high, the test fishes exhibit hyperemia on various parts of the body. Similar results were seen when treating “Nile Tilapia” with deltamethrin (Yildirim *et al.*, 2006). Disruption of the endocrine gland causes depigmentation, which alters the number of chromatophores in the thoracic area of zebrafish under toxic stress, including necrosis and edema when exposed to the venom of *Bothrops alternatus* (Carvalho *et al.*, 2018).

The liver is the organ that detoxifies fatal chemical enzymes, but it is negatively affected when exposed to a higher toxicity dose. The extent of organ damage was in a time and dose-dependent manner, with longer duration and larger dosages inflicting much more significant harm. Cytoplasmic vacuole and necrosis in the cell in juvenile fish *Colossoma macropomum* were reported when testing the acute toxicity of a hot aqueous extract from *Terminalia catappa* leaves (Meneses *et al.*, 2020). Similarly, cellular hypertrophy, atrophy, cytoplasmic vacuolation, and necrosis were found in common carp subjected to chlorpyrifos (Pal *et al.*, 2012). Cytoplasmic vacuolation and dilation of the sinusoid space were observed in zebrafish when subjected to titanium dioxide (TiO₂) nanoparticles loaded with silver oxide (Ag₂O) and silver carbonate (Ag₂CO₃), as well as pure particles of titanium dioxide (TiO₂) (Mahjoubian *et al.*, 2021). Hypertrophy in the liver tissue results from a biological reaction to stress in the body's environment. Poor hepatocyte metabolism caused by an obstruction of sinusoidal blood flow eventually results in cell atrophy. The creation of vacuoles in the liver cell was thought to signal an early stage of necrosis (Hao *et al.*, 2009; Mai *et al.*, 2019). Hepatocyte necrosis is a

probable cause of lethal compounds invading the cell and building up a toxic material inside the cell over time (Mansouri *et al.*, 2016). The kidney of the zebrafish is found in the ventral section of the vertebral column and has a distinct head and trunk area. It has nephrons with glomeruli, proximal and distal tubules, and a collecting duct, similar to mammalian kidneys. It helps filtrate blood residues and salt and water absorption and maintains tissue homeostasis. The occurrence of degeneration in the tubules, vacuolation of tubules, and change in the glomerulus and the bowman's capsule are considered the most consequent alterations in the kidney due to environmental contamination (Badroo *et al.*, 2020). Aluminum concentrations caused histological changes in the kidney, including cellular degeneration, hemorrhage, and edematous effusion in *Tilapia zillii* (Hadi & Alwan, 2012). Tubular degeneration in adults and zebrafish embryos was reported while investigating the acute toxicity of *Libidibia ferrea*, a traditional anti-inflammatory source (Ferreira *et al.*, 2019). Tubular degeneration, vacuolation, glomerular shrinkage with dilated bowman's space, and necrosis were observed in freshwater fish *Catla Catla* when treated with cypermethrin (Sharma *et al.*, 2021b). The striped catfish *Pangasianodon hypophthalmus* exposed to chromium also caused structural changes such as renal corpuscle shrinkage, bowman's space dilation, and necrosis (Suchana *et al.*, 2021). Tubular alteration in the kidney is thought to be an indirect cause of metabolic failure in zebrafish caused by toxic chemical exposure. These modifications are supposed to lead to necrosis in the long run (Zon & Peterson, 2005)

Fish gills are crucial in determining the impact of toxicants since they are easily impacted by foreign compounds in the water (Luzio *et al.*, 2021). EGCG considerably

impacted the gills of treated groups, causing hypertrophy, hyperplasia, secondary lamellae shortening and fusion, edema, lamellae curling, and epithelial lifting. Tissue-specific toxicity of clothianidin on rainbow trout caused fusion and shortening of the secondary lamellae, hypertrophy of secondary lamellae, and necrosis of secondary lamellae (Dogan *et al.*, 2022). Structural changes, including secondary lamellae curling, epithelial lifting, hyperplasia, and lamella fusing, were reported in *Sparus aurata* subjected to erythromycin and oxytetracycline (Rodrigues *et al.*, 2019). These alterations, serving as defence mechanisms, aimed to minimize blood-environment interaction, protect underlying tissue from toxicants, and increase the number of suitably adapted cells through hyperplasia (Mansouri *et al.*, 2016). Edema and epithelial cell lifting were interpreted as defence mechanisms against environmental xenobiotics (Oliveira *et al.*, 2022). Lamellar synechiae and mucus secretion were observed after short-term exposure to TiO₂ and CuO in the gills of *Cyprinus carpio*. Cell proliferation happens quickly, increasing the size of the epithelial layer and causing fusion between adjacent lamellae, maximizing the oxygen diffusion distance between blood and water (Sharma *et al.*, 2021a). However, fusion of respiratory epithelia reduced the area available for gas exchange, causing hypoxia and stress, ultimately harming fish physiology and leading to death (Lakra *et al.*, 2021).

Chapter 3

Estimation of Minimum effective dose for EGCG, assessment of general physiological status and fin regeneration in experimental zebrafish

Contents

3.1 Introduction

3.2 Materials and methods

3.3 Results

3.4 Discussion

3.1 Introduction

Determining the minimum effective dose (MED) of a therapeutic agent is a pivotal concern within the pharmaceutical domain, essential for optimizing treatment outcomes and minimizing adverse effects. The MED denotes the lowest dose at which a therapeutic effect is observed, offering crucial insights into the dosage regimen required for efficacy. MED determination involves rigorous analysis of responses garnered from placebo-controlled dose-response corresponding-group experimental investigations, wherein multiple levels of dosage of a medication, alongside a control group, are examined for their safety and effectiveness profiles (Thomas & Ting, 2014). Traditional medications dominate global healthcare landscapes, particularly in developing regions, constituting over 80% of therapeutic interventions (Tran *et al.*, 2020). Moreover, plant-based compounds play a significant role in drug discovery, with numerous botanicals and their isolated constituents exhibiting potential therapeutic benefits against conditions like diabetes (Unuofin & Lebelo, 2020; Alam *et al.*, 2022). Establishing the MED with optimal efficacy becomes imperative before leveraging EGCG as anti-diabetic agents, necessitating meticulous dose determination procedures to ensure safety and efficacy.

DM represents a metabolic disorder characterized by persistent hyperglycemia stemming from disruptions in glucose homeostasis within the bloodstream. The ramifications of uncontrolled hyperglycemia encompass a spectrum of complications, including retinopathy, cardiovascular disease, stroke, delayed wound healing, and neuropathy (Artime *et al.*, 2021; Dubey *et al.*, 2022). Among these complications, impaired wound healing stands out as a significant concern, substantially impacting

Chapter-3 *Estimation of the minimum effective dose for EGCG, assessment of general physiological status and fin regeneration in experimental zebrafish*

patients' quality of life (Romanowski & Sen, 2022). The pathophysiology of impaired wound healing in DM is multifaceted, involving chronic inflammation, hyperglycemia-induced tissue damage, hypoxia, sensory neuropathy, and dysregulated neuropeptide signaling (Baltzis *et al.*, 2014; Partoazar *et al.*, 2022). DM-induced alterations in biological mechanisms contribute to delayed wound healing, predisposing patients to secondary complications such as heightened infection risk, impaired angiogenesis, and peripheral vascular insufficiency, often culminating in amputations (Wibowo *et al.*, 2021). Given the escalating prevalence of DM-associated impaired wound healing, there is an urgent surge for effective therapeutic interventions to mitigate its deleterious consequences (Kong *et al.*, 2021).

Zebrafish is a well-established and versatile animal model extensively employed in developmental biology, disease modeling, and tissue regeneration research (Fontana *et al.*, 2022). Unlike in rat studies, where drugs are administered in relatively large quantities, zebrafish metabolic investigations typically necessitate minute amounts of compounds, making them ideal for studying trace chemicals derived from plant extracts. Such small compounds can be conveniently administered by simply adding water in multi-well racks, facilitating absorption by fish through diffusion (Zhong *et al.*, 2019). Notably, zebrafish exhibit a remarkable capacity for regenerative processes, making them invaluable for exploring regenerative biology, particularly organ regeneration (Fan *et al.*, 2022). Among the various tissues amenable to experimental manipulation, the caudal fin of zebrafish stands out as a preferred choice owing to its accessibility, simplistic structure, and rapid regenerative capabilities (Ouyang *et al.*, 2022).

Chapter-3 *Estimation of the minimum effective dose for EGCG, assessment of general physiological status and fin regeneration in experimental zebrafish*

Studies employing streptozotocin (STZ) injection in adult zebrafish have demonstrated sustained hyperglycemia, mimicking key pathological features observed in DM, including elevated blood glucose levels and altered biochemical parameters (Verma *et al.*, 2021). Additionally, zebrafish harbour critical signaling pathways integral to regulatory mechanisms implicated in wound healing processes, notably including the Hedgehog (HH), bone morphogenetic protein (BMP), and Wnt/ β -catenin signaling pathways (Mehta & Singh, 2019).

While synthetic drug therapies remain standard for managing DM-associated wounds, their clinical utility is often hampered by adverse side effects. Consequently, there is a burgeoning interest in alternative therapies with minimal side effects that exhibit promising therapeutic efficacy. Natural extracts, renowned for their potent antioxidant and anti-inflammatory properties, have garnered considerable attention to mitigate DM pathogenesis (Shahwan *et al.*, 2022). EGCG, an extract derived from green tea, has emerged as a notable natural product with high antioxidant and anti-inflammatory attributes (Longkumer *et al.*, 2022). EGCG has been effectively used to treat cancer and cardiovascular diseases and has also emerged as a potent anti-diabetic agent (Beyaz *et al.*, 2022). In an experiment with mice induced with STZ, EGCG reportedly inhibited the high glucose-caused mesangial cell damage by activating the nuclear factor erythroid 2-related factor 2 (NRF-2), which plays a critical role in protection against the oxidative damage and inflammation in diabetic nephropathy (Sun *et al.*, 2017).

Furthermore, EGCG exerts inhibitory effects on adipocyte differentiation and proliferation, thereby enhancing cellular glucose uptake by activating AMP-activated

Chapter-3 *Estimation of the minimum effective dose for EGCG, assessment of general physiological status and fin regeneration in experimental zebrafish*

protein kinase (Asbaghi *et al.*, 2021). Dietary supplementation with EGCG in Goto-Kakizaki rats has been shown to mitigate inflammation in adipose tissue induced by hyperglycemia (Uchiyama *et al.*, 2013). Despite the extensive literature documenting the use of animal models for DM research, there remains a dearth of studies investigating the potential of EGCG in promoting regeneration in the caudal fin of diabetic zebrafish models. Thus, there exists a critical need to elucidate the efficacy of EGCG in facilitating fin regeneration under hyperglycemic conditions in zebrafish. This study holds promise as an initial exploration into the safe and efficacious utilization of EGCG for wound healing and regenerative applications in the hyperglycemic milieu characteristic of diabetic zebrafish models.

3.2 Materials and methods

3.2.1 Chemicals

EGCG ($\geq 95\%$), Streptozotocin, Tricaine MS-222 (Ethyl 3-aminobenzoate methanesulfonate salt), Sodium chloride, Accu Check glucometer, and blood glucose test strips were obtained from Merck and Accu-Chek Active, Mumbai, India, respectively.

3.2.2 Acclimatization of zebrafish

Adult Zebrafish 300-500 mg were procured from Aqua fish & pets, Jorhat Assam, India. Zebrafish were cultured in a zebrafish housing system (Model-NT-ZB-11; Make-Narshi Technologies) to ensure constant temperature ($28 \pm 2^\circ\text{C}$), persistent chemical, biological, and mechanical water filtration and aeration ($7.20 \text{ mg O}_2/\text{L}$). Polycarbonate fish tanks were maintained under a 14h/10hr: day/night photoperiod cycle. Adult zebrafish were fed three times daily with commercially available feed containing protein 28%, crude fat 3%, fiber 4%, and moisture 10%. Detailed acclimatization procedures are provided in Chapter 2.

3.2.3 Induction of diabetes

Induction of DM in the zebrafish was initiated by injecting an STZ dose of 0.35 mg/g of body weight into the peritoneal cavity of the subjects with the aid of a $\frac{1}{2}$ cc syringe equipped with a 27-gauge needle. 2-Phenoxyethanol with a dilution ratio of 1:1000 was used for anesthetizing the subjects. In contrast, normal fish tank water was used as the recovery medium. Anesthetized fish was placed briefly on a paper towel to absorb any excess water, after which the weight of the fish was measured. Zebrafish were placed on a firm surface for injection. After the injection, the fish were transferred to a recovery

Chapter-3 *Estimation of the minimum effective dose for EGCG, assessment of general physiological status and fin regeneration in experimental zebrafish*

water tank and observed for signs of irregular swimming activity, which were absent. This was accomplished by transferring the fish to a standard living tank maintained at a decreased temperature of 22 - 24°C. The zebrafish were injected with 5 STZ injections for prolonged hyperglycemia over three weeks. The six doses were administered in the following way: 3 injections in the first week, followed by booster doses, one each in weeks 1, 3, and 5, on days 11, and 16, respectively (Intine *et al.*, 2013; Longkumer *et al.*, 2020). The induction of DM *via* STZ in the zebrafish model has been represented in Figure 3.1.

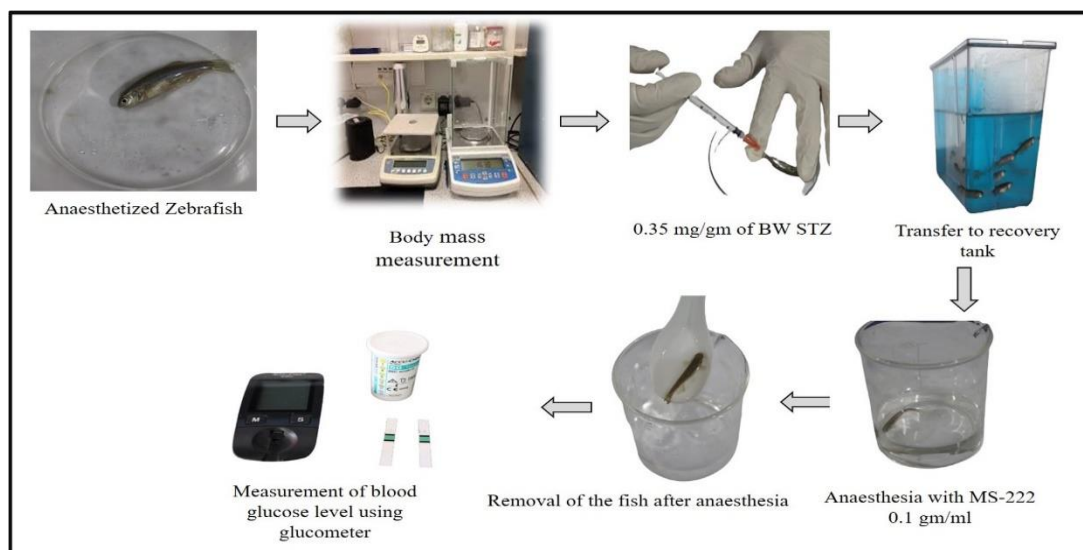


Figure 3.1: Diagrammatic representation of diabetes induction in zebrafish

3.2.4 Minimum effective dose determination

The study involved grouping of animals into 7 groups, weighing between 490-550 mg (n=10). Five different concentrations (1, 2, 4, 6, and 8) mg/L were administered for a duration of 21 days to ascertain the effective dose of EGCG. The dose that yielded no mortality and maintained stable blood glucose levels was selected for subsequent investigations. The MED, denoting the concentration of EGCG at which blood glucose

Chapter-3 *Estimation of the minimum effective dose for EGCG, assessment of general physiological status and fin regeneration in experimental zebrafish*

levels were effectively ameliorated, was determined. The methodology employed in determining the effective dose of EGCG was adopted from the protocol described by Milligan et al. (2013), tailored to the laboratory's experimental setup. The compound EGCG was renewed every 24 hours by replacing it with a freshly prepared solution according to the method described by Edition, 2002. Table 3.1 shows the setup of different experimental groups to determine MED.

Table 3.1: Grouping of experimental models for minimum effective dose determination.

Group I	Control
Group II	Diabetic control
Group IIIa	Diabetic zebrafish treated with 1 mg/L of EGCG for 21 days
Group IIIb	Diabetic zebrafish treated with 2 mg/L of EGCG for 21 days
Group IIIc	Diabetic zebrafish treated with 4 mg/L of EGCG for 21 days
Group IIId	Diabetic zebrafish treated with 6 mg/L of EGCG for 21 days
Group IIIe	Diabetic zebrafish treated with 8 mg/L of EGCG for 21 days

3.2.5 Blood glucose levels determination

Blood glucose levels were assessed in the test animals following a 12-hour fasting period. Zebrafish were then placed in a glucose-free test fish tank for at least 15 minutes to prevent contamination of glucometer strips. Subsequently, the zebrafish were anesthetized in 0.04% Tricaine MS-222 (Tricaine methanesulfonate) solution. Zebrafish were removed from the solution, patted dry with lens cleaning wipes, and placed on a glass surface. The zebrafish blood was obtained by decapitating using a sharp blade behind the eyes, where the heart is located. After this, the blood was collected on a strip directly from the

Chapter-3 *Estimation of the minimum effective dose for EGCG, assessment of general physiological status and fin regeneration in experimental zebrafish*

punctured heart, and the blood glucose levels were read by placing a glucometer test strip (One-Touch Ultra, Accu Check).

3.2.6 Grouping of experimental subjects

The animals (n=6) were divided into four groups weighing 480-590 mg. The experimental groups were observed on day 1 (*i.e.*, after 24 hours of induction of diabetes), day 7, day 14, and day 21. The data were further recorded and analyzed. Table 3.2 and Figure 3.2 shows the grouping of the experimental subjects.

Table 3.2: Grouping of experimental zebrafish

Groups	Treatments
Group I	Control
Group II (Diabetic control)	Treated with a single dose of STZ and booster doses to the experimental subjects
Group III (Diabetic Group treated with EGCG)	Diabetic zebrafish treated with 6 mg/L of EGCG for 21 days
Group IV (Control Group treated with EGCG)	Control zebrafish treated with 6 mg/L of EGCG for 21 days

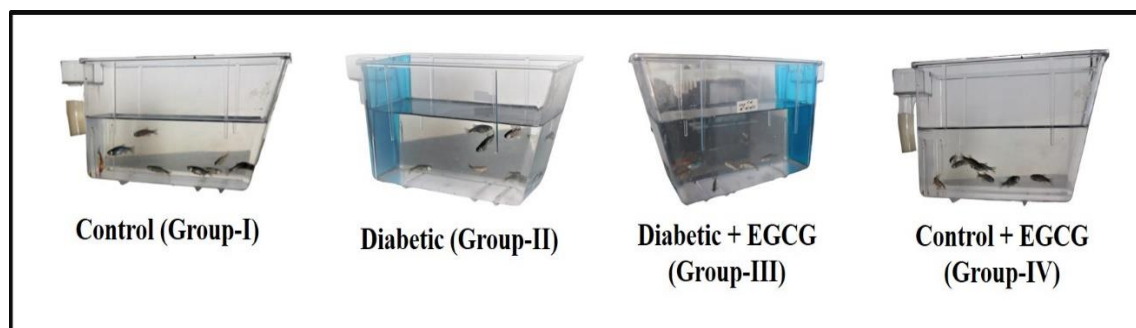


Figure 3.2: Grouping of experimental subjects

3.2.7 EGCG: Dose and period

A concentration of 6 mg of EGCG was dissolved in 6 ml of distilled water before being mixed into a 1-liter fish tank, ensuring uniform distribution. The treatment regimen spanned 21 days to evaluate the effects of EGCG on the experimental zebrafish.

3.2.8 Estimation of body weight

The body weight of the zebrafish was meticulously determined using a high-precision digital weighing machine, Scaletec SAB 200E, which offers an accuracy of 0.01 mg. Each fish was gently placed in a small container containing a known quantity of liquid for a brief period, and the tare function on the weighing machine was utilized to obtain accurate body weight measurements.

3.2.9 Estimation of body length

Following anesthesia induced by exposure to ice-cold water, the length of each zebrafish was measured using digital calipers, specifically the Tresna brand, on a petri dish. Measurements were taken from the tip of the snout to the caudal end of the body, with lengths recorded in centimeter (cm).

3.2.10 Estimation of body mass index

The body mass index (BMI) of the zebrafish subjects (n=6) was calculated by dividing the body weight (in grams) by the square of the body length (in square centimeters). As outlined by Kimmel et al. (2015), this calculation method provides a standardized measure of body composition. Body weight and length measurements were conducted individually on days 1, 7, 14, and 21 of the treatment periods.

3.2.11 Caudal fin regeneration

Zebrafish (n=6) were subjected to anesthesia *via* immersion in an ice water bath for a duration of 1–2 minutes. Once anesthetized, the fish were positioned transversely in a petri dish, and the caudal fin was carefully stretched using a soft brush to facilitate amputation. Fin amputation was precisely executed using a sterile scalpel blade, proximal to the first lepidotrichia branching point, under a dissecting microscope. Subsequently, the fish were transferred to their respective treatment or control water tanks for the regenerative phase. The progress of fin regeneration was monitored and imaged at specified intervals, namely on days 0 (before amputation), 1, 7, 14, and 21. The length of the amputation site along the dorsal-ventral axis was measured and compared across treatment Groups. Imaging was facilitated using an Olympus Stereo Zoom microscope (Model SZX10) equipped with a Sony digital camera model E31SPM20000KPA (USB 2.0), and analysis was conducted using Image J software installed on a high-performance computer. The regeneration percentage was calculated using the formula as described by Sun et al. (2020). Wound healing rate (%) = $(IWA - UWA) / IWA \times 100$, where IWA stands for the initial wound, and UWA stands for the wound made on the first day. Figure 3.3 shows the experimental design for the assessment of fin regeneration in zebrafish.

Chapter-3 *Estimation of the minimum effective dose for EGCG, assessment of general physiological status and fin regeneration in experimental zebrafish*

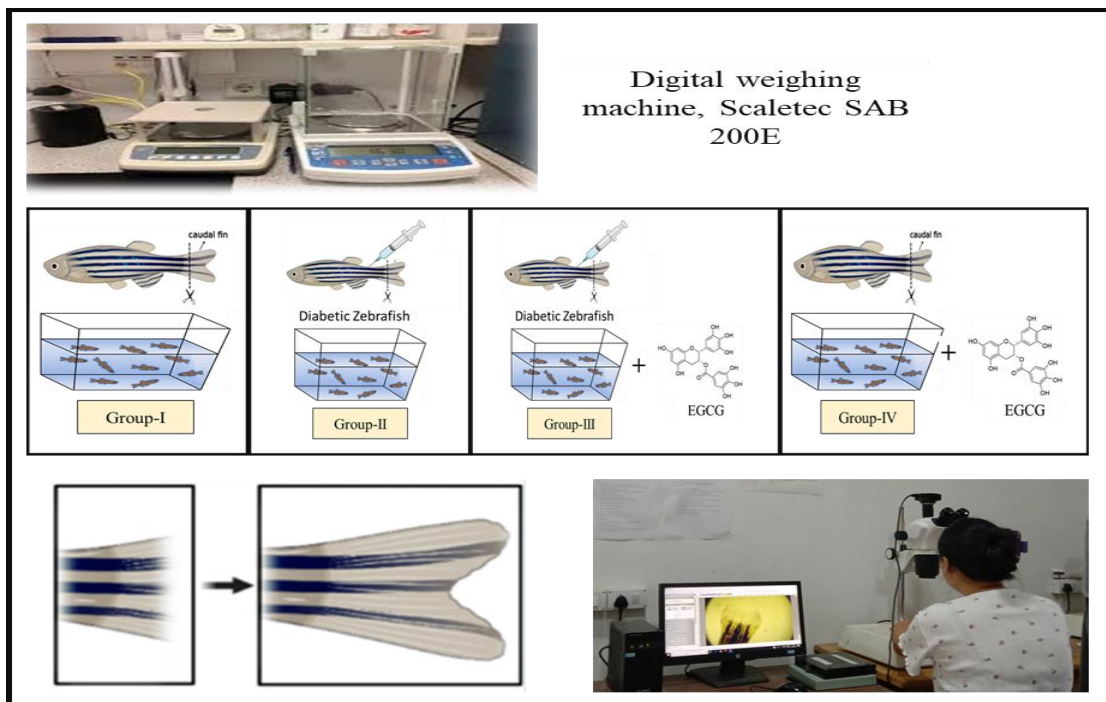


Figure 3.3: Diagrammatic representation of assessment of fin regeneration.

3.2.12 Statistical analysis

Data analysis was performed for blood glucose levels, body weight, body length, BMI and caudal fin regeneration. Values were represented as Mean \pm SD. The glucose levels in the blood and fin growth percentage were performed using GraphPad Prism 5.0 software. One-way analysis of variance (ANOVA) and a post hoc Tukey Honest Significant Difference test was done to determine the significant differences between the treatment groups with an asterisk sign determining the different significant differences * $p < 0.05$; ** $p < 0.01$; *** $p < 0.001$.

3.3 Results

3.3.1 Determination of minimum effective dose

Diabetic zebrafish were subjected to varying doses of EGCG over a 21-days period, with blood glucose levels monitored on days 1, 7, 14, and 21. Notably, administration of EGCG at a concentration of 6 mg/L led to a substantial reduction in blood glucose levels from 299.83 ± 5.1 mg/dl to 99.67 ± 4.7 mg/dl by the end of the treatment period. While all dosages (1, 2, 4, 6, and 8) mg/L exhibited reductions in blood glucose levels compared to the diabetic control from day 7 onwards, the efficacy varied across different dosage groups. Particularly, Group IIIc demonstrated consistent improvement in blood glucose levels compared to other dosage groups. Detailed effects of different EGCG dosages on blood glucose levels are presented in Table 3.3, Figure 3.4 and Figure 3.5.

3.3.2 Body weight

The effect of DM induction on body weight was investigated in this study, revealing significant ($p < 0.05$) values. Group-II zebrafish exhibited a notable reduction in body weight compared to the control group (Group-I) counterparts. Specifically, on day 21 of the experiment, Group-II subjects experienced a substantial decrease in body weight by 37.01%. Interestingly, zebrafish subjects treated with EGCG (Group-III) displayed a remarkable recovery in body weight ($p < 0.01$). By day 21, Group-III exhibited a notable increase in body weight by 29% compared to Group-II counterparts. Conversely, Group-IV, which received EGCG treatment without DM induction, demonstrated negligible changes in body weight compared to Group-I. The body weight of the test groups has been represented in Table 3.4 and Figure 3.6.

3.3.3 Body length

During the course of this investigation, insignificant ($p>0.05$) changes were detected in the body length of the test subjects across the experimental groups. The data pertaining to body length measurements for each experimental group are summarized in Table 3.5 and depicted in Figure 3.7.

3.3.4 Body mass index

In the course of this investigation, significant ($p<0.05$) changes were observed in the body mass index (BMI) of the test subjects. Notably, in Group-II exhibited a lower BMI than those in Group-I, with a progressive decline throughout the experimental period. Specifically, on day 21, Group-II displayed a BMI reduction of 44% relative to the control Group. Conversely, the subjects in Group-III, treated with EGCG, demonstrated a pronounced increase in BMI, amounting to 39% of elevation compared to Group-II. Interestingly, the control Group treated with EGCG exhibited insignificant ($p>0.01$) changes in BMI compared to the control Group. Detailed results of the BMI analysis for each experimental group are presented in Table 3.6 and illustrated in Figure 3.8.

3.3.5 Effect of EGCG on caudal fin regeneration

Caudal fin regeneration was assessed in test zebrafish to investigate the efficacy of EGCG in enhancing fin regeneration. In hyperglycemic conditions, the fins were amputated, and photographs of the fins were captured at various periods, as on day 0, day 1, day 7, day 14, and day 21. Our results revealed notable improvements in caudal fin growth following EGCG treatment in both Group-III and Group-IV. Observation of blastema formation at the wound site was noted in Group-I, III, and IV, while minimal blastema growth was

Chapter-3 *Estimation of the minimum effective dose for EGCG, assessment of general physiological status and fin regeneration in experimental zebrafish*

observed in Group-II. On the 7th day of post-amputation, Group-II exhibited slower caudal fin growth compared to Group I, III, and IV, with fin growth recorded at 6%. However, by the 14th and 21st days, the percentage of fin growth increased to 26% and 41%, respectively, indicating a delayed regenerative response in Group-II. Conversely, zebrafish treated with EGCG (Group III and IV) displayed enhanced fin growth, with percentages reaching 14%, 36%, and 60% on days 7, 14, and 21, respectively, in Group III, and 34%, 55%, and 66%, respectively, in Group IV. In contrast, the control zebrafish exhibited fin growth percentages of 39%, 45%, and 65% on days 7, 14, and 21 of post-amputations, respectively. These findings suggest that while hyperglycemic zebrafish in Group-II exhibited impaired wound healing, treatment with EGCG in Group III and IV resulted in improved caudal fin regeneration compared to the diabetic Group-II. The effect of DM on caudal fin regeneration and the ameliorating effect of EGCG is described in Figure 3.9 and Figure 3.10[A-C].

Chapter-3 *Estimation of the minimum effective dose for EGCG, assessment of general physiological status and fin regeneration in experimental zebrafish*

Table 3.3: Blood glucose levels of different experimental groups. Group-I - Control; Group-II – diabetic; Group-IIIa - diabetic zebrafish treated with 1 mg/L of EGCG; Group-IIIb - diabetic zebrafish treated with 2 mg/L of EGCG; Group-IIIc - diabetic zebrafish treated with 4 mg/L of EGCG; Group-IIId - diabetic zebrafish treated with 6 mg/L of EGCG; Group-IIIE - diabetic zebrafish treated with 8 mg/L of EGCG. Data are represented as mean \pm SD; (n=6).

Exposure Group	Period of exposure (Days)			
	1	7	14	21
Group- I	62.67 \pm 3.5	71.34 \pm 4.5	66.33 \pm 4.1	71.05 \pm 3.4
Group- II	311.66 \pm 4.0	305.66 \pm 3.3	300.16 \pm 4.2	308.05 \pm 3.5
Group- IIIa	298.16 \pm 4.5	242.50 \pm 5.1	178.00 \pm 6.6	143.05 \pm 6.0
Group- IIIb	301.00 \pm 5.8	221.33 \pm 5.7	161.33 \pm 5.0	122.67 \pm 5.3
Group- IIIc	297.67 \pm 5.1	211.33 \pm 7.4	169.83 \pm 5.6	121.34 \pm 4.1
Group-IIId	299.83 \pm 5.1	198.66 \pm 5.7	120.34 \pm 5.4	99.67 \pm 4.7
Group-IIIE	290.34 \pm 6.9	170.83 \pm 4.4	98.83 \pm 4.2	49.33 \pm 5.4

Table 3.4: Effect of diabetes on body weight and its treatment with EGCG in zebrafish model. Group-I – control; Group-II – diabetic; Group-III – diabetic + EGCG; Group-IV – control + EGCG. Data are represented as mean \pm SD; (n=6). Different superscripts denote significant ($p < 0.001$) differences; the same superscripts denote insignificant ($p > 0.05$) results between the columns of the treatment groups.

Treatment Groups	Day 1	Day 7	Day 14	Day 21
Group-I	0.79 \pm 0.01 ^a	0.80 \pm 0.03 ^a	0.84 \pm 0.03 ^a	0.83 \pm 0.03 ^a
Group-II	0.76 \pm 0.03 ^a	0.70 \pm 0.01 ^b	0.67 \pm 0.01 ^b	0.63 \pm 0.02 ^b
Group-III	0.77 \pm 0.02 ^a	0.69 \pm 0.01 ^b	0.70 \pm 0.01 ^b	0.73 \pm 0.02 ^c
Group-IV	0.78 \pm 0.01 ^a	0.79 \pm 0.03 ^a	0.81 \pm 0.06 ^a	0.82 \pm 0.04 ^a

Chapter-3 *Estimation of the minimum effective dose for EGCG, assessment of general physiological status and fin regeneration in experimental zebrafish*

Table 3.5: Effect of diabetes on body length and its treatment with EGCG in zebrafish model. Group-I – control; Group-II – diabetic; Group-III – diabetic + EGCG; Group-IV – control + EGCG. Data are represented as mean \pm SD; (n=6). Different superscripts denote significant ($p < 0.001$) differences; the same superscripts denote insignificant ($p > 0.05$) results between the columns of the treatment groups.

Treatment Groups	Day 1	Day 7	Day 14	Day 21
Group-I	3.74 \pm 0.06 ^a	3.73 \pm 0.11 ^a	3.74 \pm 0.08 ^a	3.75 \pm 0.10 ^a
Group-II	3.72 \pm 0.07 ^a	3.73 \pm 0.10 ^a	3.71 \pm 0.11 ^a	3.72 \pm 0.09 ^a
Group-III	3.73 \pm 0.09 ^a	3.72 \pm 0.10 ^a	3.73 \pm 0.10 ^a	3.74 \pm 0.11 ^a
Group-IV	3.73 \pm 0.09 ^a	3.72 \pm 0.10 ^a	3.75 \pm 0.10 ^a	3.74 \pm 0.10 ^a

Table 3.6: Effect of diabetes on body mass index and its treatment with EGCG in zebrafish model. Group-I – control; Group-II – diabetic; Group-III – diabetic + EGCG; Group-IV – control + EGCG. Data are represented as mean \pm SD; (n=6). Different superscripts denote significant ($p < 0.001$) differences; the same superscripts denote insignificant ($p > 0.05$) results between the columns of the treatment groups.

Treatment Groups	Day 1	Day 7	Day 14	Day 21
Group-I	0.065 \pm 0.021 ^a	0.066 \pm 0.016 ^a	0.068 \pm 0.020 ^a	0.067 \pm 0.017 ^a
Group-II	0.063 \pm 0.017 ^a	0.061 \pm 0.022 ^a	0.058 \pm 0.018 ^b	0.052 \pm 0.010 ^b
Group-III	0.062 \pm 0.017 ^a	0.060 \pm 0.016 ^a	0.062 \pm 0.016 ^{ca}	0.061 \pm 0.014 ^a
Group-IV	0.064 \pm 0.018 ^a	0.064 \pm 0.014 ^a	0.065 \pm 0.021 ^d	0.006 \pm 0.017 ^a

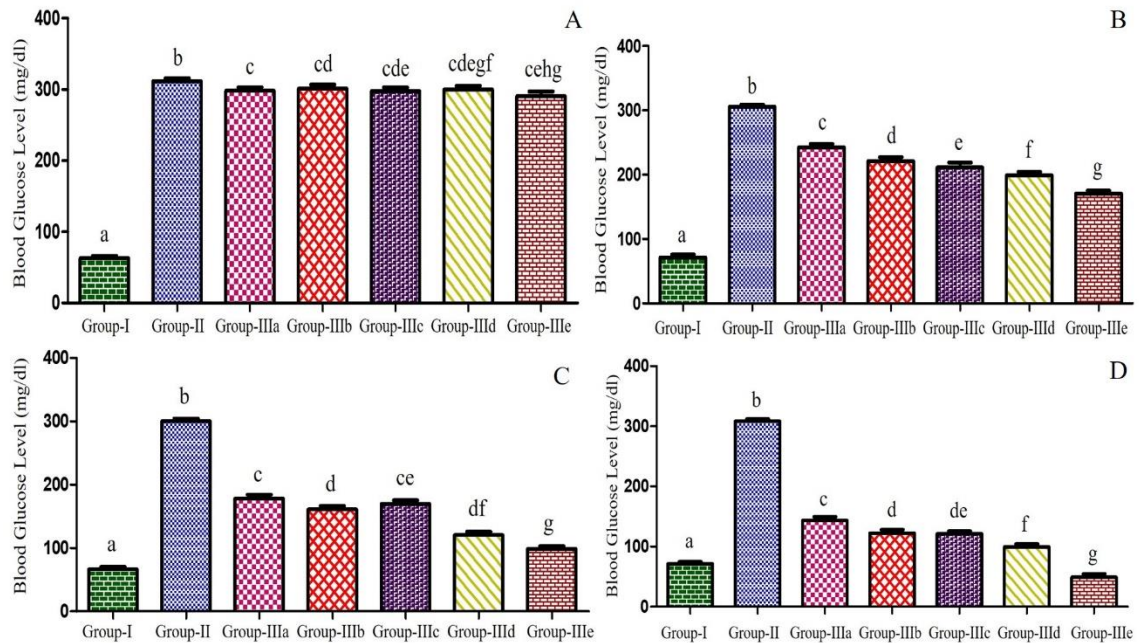


Figure 3.4: Blood glucose levels of different experimental groups. Group-I - Control; Group-II – diabetic; Group-IIIa - diabetic zebrafish treated with 1 mg/L of EGCG; Group-IIIb - diabetic zebrafish treated with 2 mg/L of EGCG; Group-IIIc - diabetic zebrafish treated with 4 mg/L of EGCG; Group-IIId - diabetic zebrafish treated with 6 mg/L of EGCG; Group-IIIE - diabetic zebrafish treated with 8 mg/L of EGCG. (A) Day 1 (B) Day 7 (C) Day 14 (D) Day 21. Data are represented as mean \pm SD; (n=6) and analysed by one-way ANOVA followed by Tukey's post-hoc test. Different superscripts denote significant ($p < 0.001$) differences; the same superscripts denote insignificant ($p > 0.05$) results between the treatment groups.

Chapter-3 *Estimation of the minimum effective dose for EGCG, assessment of general physiological status and fin regeneration in experimental zebrafish*

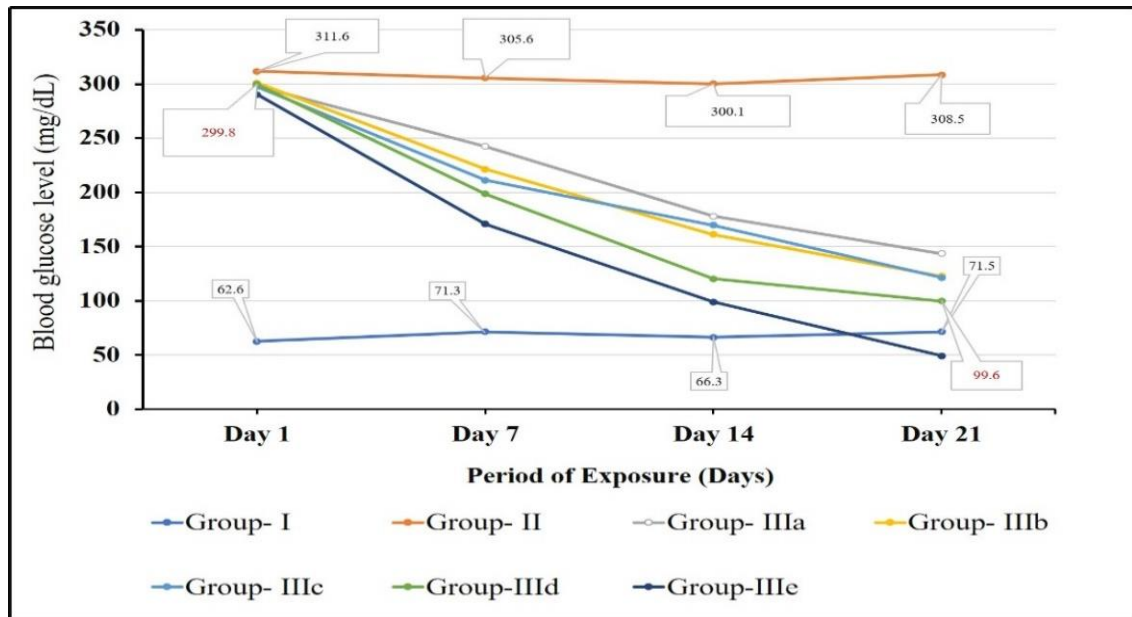


Figure 3.5: Blood glucose levels of different experimental groups. Group-I: control; Group-II: diabetic; Group-IIIa: diabetic zebrafish treated with 1 mg/L of EGCG; Group-IIIb: diabetic zebrafish treated with 2 mg/L of EGCG; Group-IIIc: diabetic zebrafish treated with 4 mg/L of EGCG; Group-IIId: diabetic zebrafish treated with 6 mg/L of EGCG; Group-IIIe: diabetic zebrafish treated with 8 mg/L of EGCG.

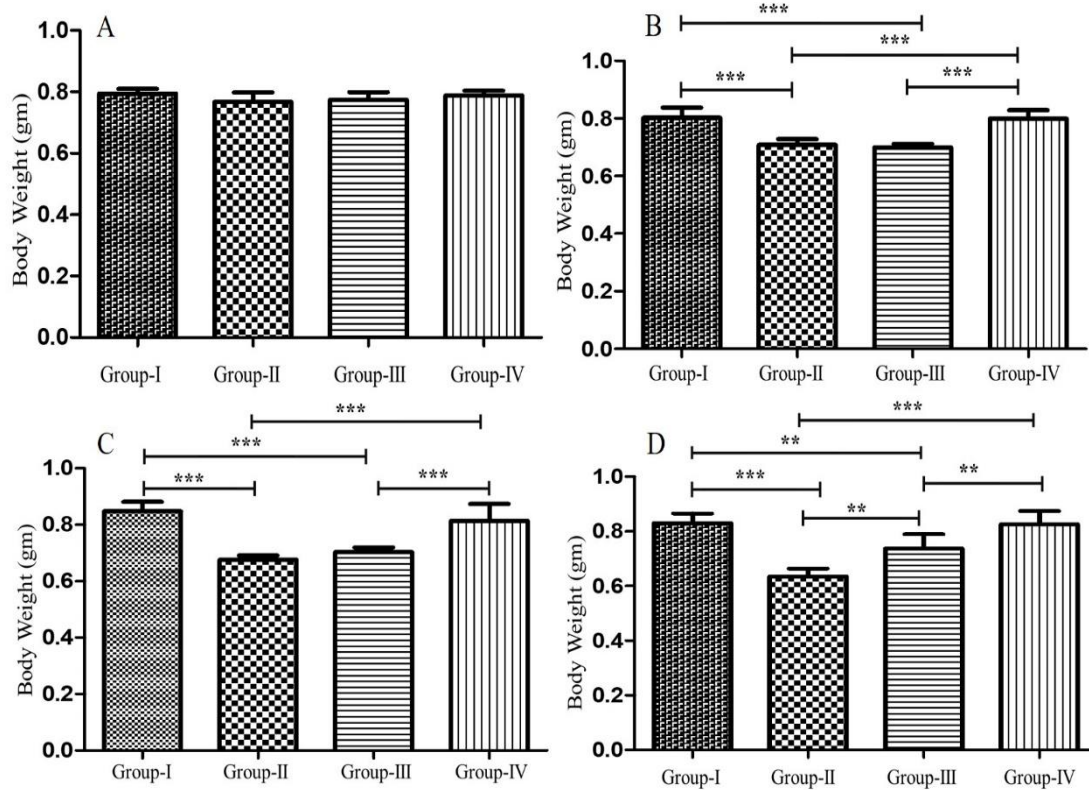


Figure 3.6: Effect of diabetes on body weight and its treatment with EGCG in zebrafish model. Group-I – control; Group-II – diabetic; Group-III – diabetic + EGCG; Group-IV – control + EGCG. (A) Day 1 (B) Day 7 (C) Day 14 (D) Day 21. Data are represented as mean \pm SD; (n=6) and analysed by one-way ANOVA followed by Tukey's post-hoc test. Asterisk represents a significant difference, *p<0.05; **p<0.01; ***p<0.001.

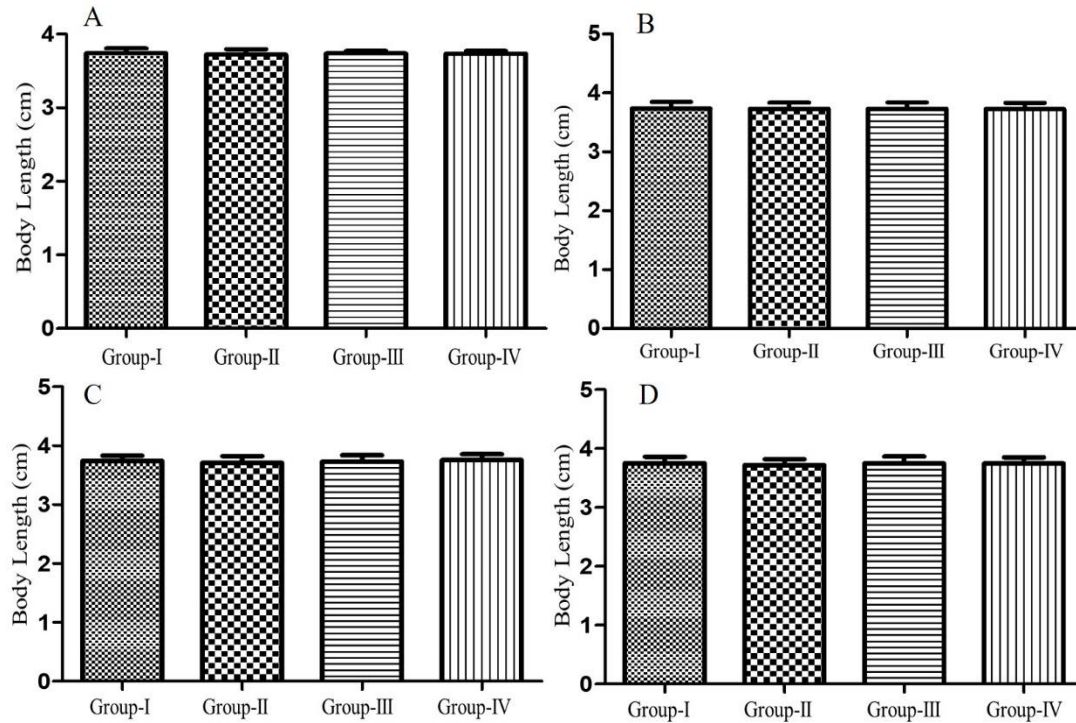


Figure 3.7: Effect of diabetes on body length and its treatment with EGCG in zebrafish model. Group-I – control; Group-II – diabetic; Group-III – diabetic + EGCG; Group-IV – control + EGCG. (A) Day 1 (B) Day 7 (C) Day 14 and (D) Day 21. Data are represented as mean \pm SD; (n=6) and analysed by one-way ANOVA followed by Tukey's post-hoc test. Asterisk represents a significant difference, * $p < 0.05$; ** $p < 0.01$; *** $p < 0.001$.

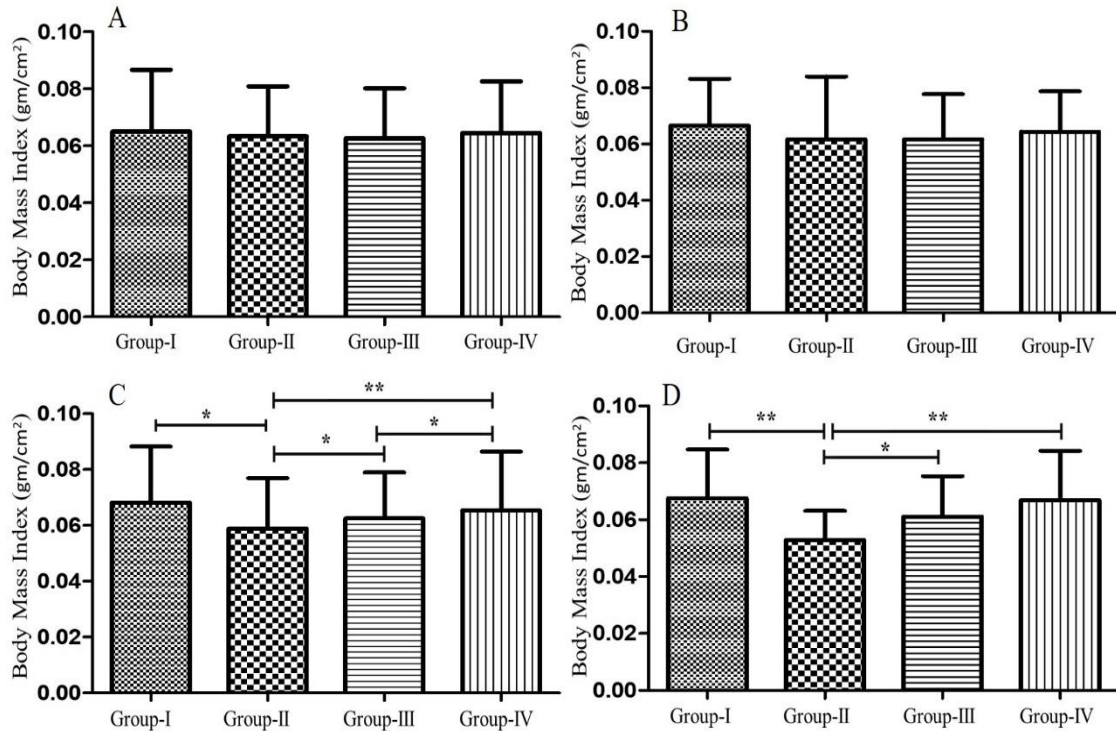


Figure 3.8: Effect of diabetes on body mass index and its treatment with EGCG in zebrafish model. Group-I – control; Group-II – diabetic; Group-III – diabetic + EGCG; Group-IV – control + EGCG. (A) Day 1 (B) Day 7 (C) Day 14 (D) Day 21. Data are represented as mean \pm SD; (n=6) and analysed by one-way ANOVA followed by Tukey's post-hoc test. Asterisk represents a significant difference, * $p < 0.05$; ** $p < 0.01$; *** $p < 0.001$.

Chapter-3 *Estimation of the minimum effective dose for EGCG, assessment of general physiological status and fin regeneration in experimental zebrafish*

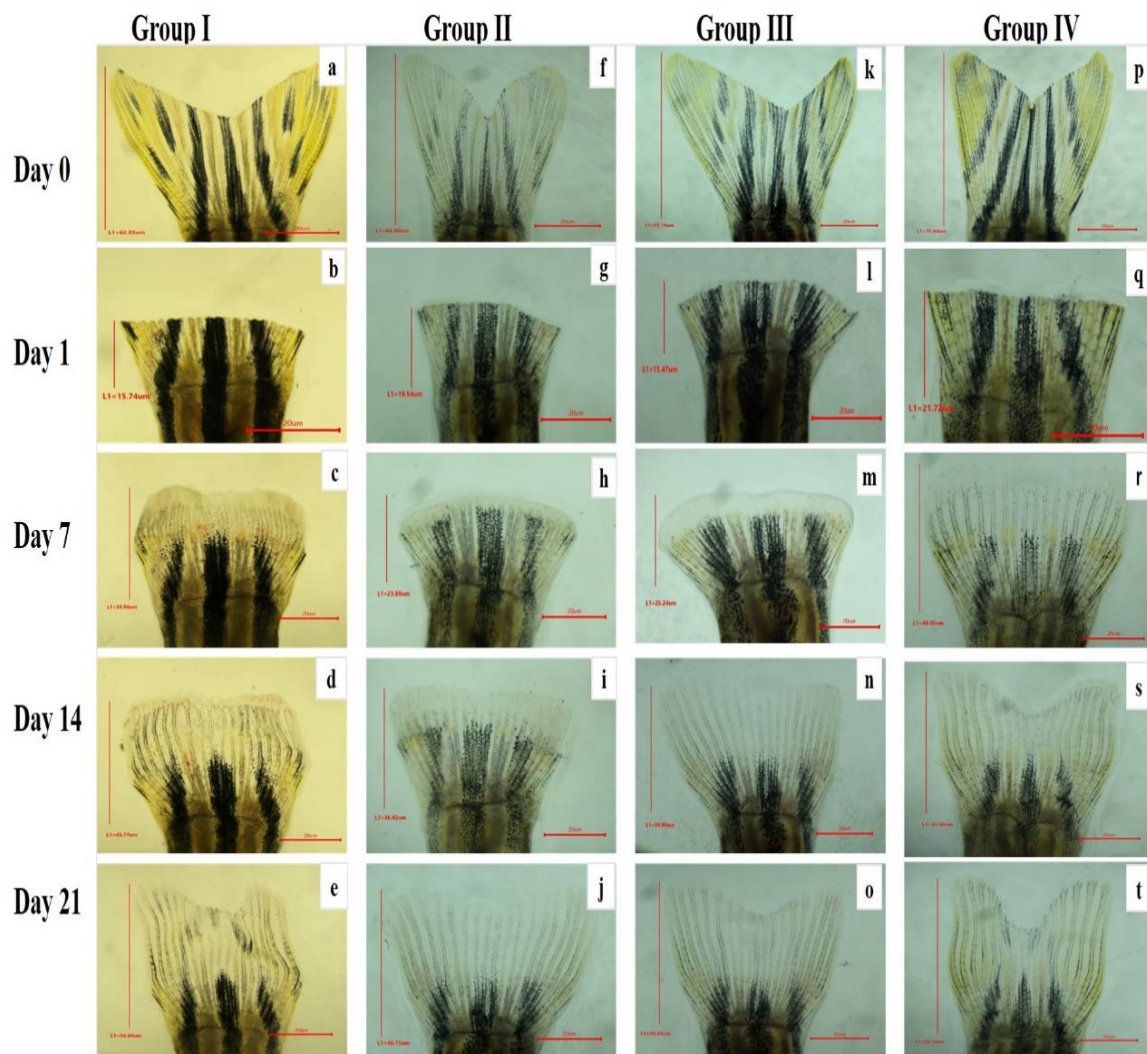


Figure 3.9: Caudal fin regeneration in experimental zebrafish on day 0 (pre amputation), day 1 (initial cut), day 7, day 14 and day 21. (a-e) Control caudal fin, (f-j) Caudal fin of diabetic zebrafish, (k-o) Caudal fin of diabetic zebrafish treated with EGCG, (p-t) Caudal fin of control zebrafish treated with EGCG.

(Image captured at 5X magnification)

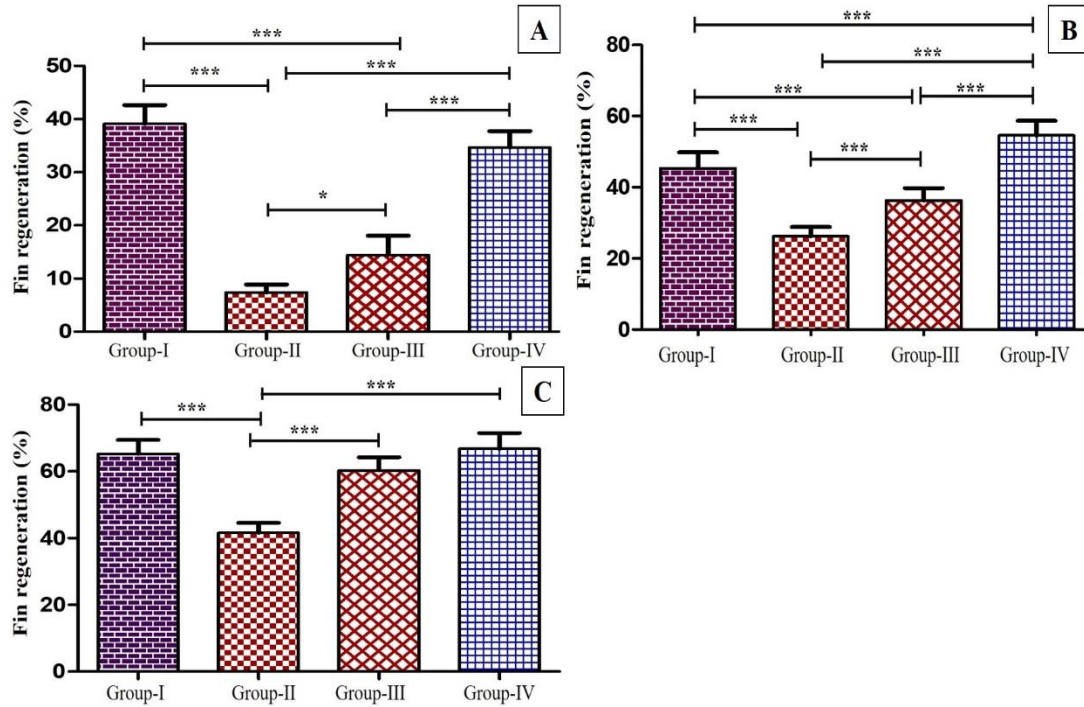


Figure 3.10: Average percentage growth of the caudal fin of zebrafish. Group-I – control; Group-II – diabetic; Group-III – diabetic + EGCG; Group-IV – control + EGCG. (A) Day 7 (B) Day 14 (C) Day 21. Data are represented as mean \pm SD; (n=6) and analysed by one-way ANOVA followed by Tukey's post-hoc test. Asterisk represents a significant difference, * $p < 0.05$; ** $p < 0.01$; *** $p < 0.001$.

3.4 Discussion

Determining the initial dose is a crucial step in drug development. This study assessed the minimum effective dose of EGCG in diabetic zebrafish model. This approach is consistent with similar studies, such as Sabi et al. (2022), who investigated the protective effects of *Ficus benghalensis* in STZ-induced diabetic zebrafish. STZ is commonly used to induce diabetes in animal models due to its selective damage to pancreatic β -cells, leading to increased ROS generation and subsequent DNA strand breaks, ultimately causing diabetes (Sen, 2022). Repeated dosages of EGCG were administered to maximize therapeutic effectiveness while maintaining blood glucose levels within a therapeutic range.

The selection of EGCG doses was based on previous studies in animal models, where EGCG demonstrated protective effects against various conditions. For instance, Wang et al. (2021) reported that 1–2 $\mu\text{mol/L}$ of EGCG enhanced the protective efficacy of the growth and development of zebrafish embryos. Further, Hsieh et al. (2021) used EGCG (94%); 200 mg/kg/day, once/day, between 7 and 17 am, 12 weeks, and recorded that EGCG might prevent neural apoptotic pathways and activate neural survival pathways, providing therapeutic effects on early aged hypertension-induced neural apoptosis. Zhang et al. (2018) also reported that EGCG (0.01-10.0 mg/L) had no adverse effect on zebrafish during an LC_{50} study for 72 hours. Therefore, considering this study, a wide dose range of concentration of EGCG (1, 2, 4, 6, and 8) mg/L was selected for testing the efficacy in the diabetic model.

STZ is well known for its selective pancreatic islet β - cell cytotoxicity and is

Chapter-3 *Estimation of the minimum effective dose for EGCG, assessment of general physiological status and fin regeneration in experimental zebrafish*

extensively used to induce DM (Alavi, *et al.*, 2022). The present study advocates that intra-peritoneal treatment of STZ efficiently produced DM in zebrafish, as evidenced by raised fasting plasma glucose levels. The glucose levels in diabetic zebrafish treated with STZ remained significantly elevated (> 308 mg/dl) on the 21-day of investigation. The diverse concentrations had no mortality or detrimental impact on the experimental animal, but the blood glucose levels exhibited significant variability in the values. The administration of EGCG resulted in a decrease in blood glucose levels, as the concentration of 1-8 mg/L of EGCG induced a significant reduction in plasma glucose levels in diabetic zebrafish. From the 7th day, the blood glucose levels of the diabetic zebrafish were seen to improve, approaching normal control values. A significant drop in blood glucose levels was also found at a dose of 6 mg/L EGCG, where glucose levels reached near normal levels and showed consistent results compared to the other concentrations tested. As a result, the dose of 6 mg/L of EGCG was considered for further trials.

DM induction with STZ is accompanied by the characteristic decrease in body weight, which is related to enhanced muscle wasting due to tissue protein loss (Latha & Daisy, 2011). The drop in protein and albumin levels may be attributed to microproteinuria and albuminuria, both of which are key clinical indicators of diabetic nephropathy or to enhanced protein catabolism (Bellamkonda *et al.*, 2011). The results of this investigation demonstrated a substantial reduction of body weight during the 21-days experimental period, which was consistent with the findings of Lv *et al.* (2022), who observed a decrease in body weight of experimental rats with STZ induction. Additionally,

Chapter-3 *Estimation of the minimum effective dose for EGCG, assessment of general physiological status and fin regeneration in experimental zebrafish*

minimal changes in body length were observed among experimental groups, while BMI levels were considerably lower in diabetic zebrafish. Our study showed that treatment with EGCG attenuated these effects, resulting in weight gain and BMI values closer to normal. EGCG has been shown in studies on DM models to reduce the blood glucose levels and body weight of the experimental model (Ren *et al.*, 2020; Jamir *et al.*, 2023). Diabetic subjects treated with EGCG gained weight when compared to diabetic controls. This can be ascribed to the preventative effect of the extract on muscle wasting and enhancements in insulin secretion and glycogen management. Several researches show that EGCG has many biological effects, such as insulin, suppressing glucose synthesis and PEPCK and glucose-6-phosphatase gene expression (Waltner-Law *et al.*, 2002; Liu *et al.*, 2022). EGCG appears to perform these effects by modulating the redox state of the cell.

Delayed wound healing is considered the main reason behind lower limb amputation in a DM patient. Growth factors, namely insulin-like growth factor, platelet-derived growth factor, fibroblast growth factor, and vascular endothelial growth factor, were recorded to have been altered in DM patients (Dinh *et al.*, 2011). Hyperglycemic conditions are associated with preventing circulating nutrients from reaching wounds and dysfunction of endothelial cells, thus slowing the rate of wound healing. Further, hyperglycemia also interferes with processes necessary for re-epithelialization, such as migration, protein synthesis, and proliferation of keratinocytes and fibroblasts (Hu & Lan, 2016). Another way hyperglycemia impairs wound healing is through free radical damage caused by decreased activity of the antioxidant enzymes glutathione peroxidase and superoxide dismutase (Kant *et al.*, 2022). Hyperglycemia causes reactive oxygen species

Chapter-3 *Estimation of the minimum effective dose for EGCG, assessment of general physiological status and fin regeneration in experimental zebrafish*

(ROS) to be produced *via* the polyol, hexosamine, protein kinase C, and advanced glycation end-product pathways (Ighodaro, 2018). Although ROS are necessary for the initial stages of wound healing, an imbalance in ROS production harms the later stages. Thus, maintaining blood glucose levels in the normal range is the chief priority for any therapy.

The induction of diabetes with STZ resulted in elevated blood glucose levels (>308 mg/dl) throughout the 21-days investigation period. However, treatment with EGCG led to a reduction in blood glucose levels, with 6 mg/L of EGCG demonstrating the most significant reduction, approaching normal control values from the 7th day of the treatment. These findings align with previous studies in STZ-induced animal models, where EGCG administration resulted in decreased blood glucose levels and improved body weight. Mechanisms of action of EGCG in reducing blood glucose levels may involve insulin-like effects, modulation of cell redox states, and suppression of glucose synthesis genes. Moreover, EGCG treatment prevented muscle wasting and enhanced insulin secretion and glycogen management, contributing to improved body weight and blood glucose control.

The present findings showed that the blood glucose levels of the DM-induced zebrafish were improved with the treatment by 6 mg/L of EGCG, reducing the glucose levels to 100 mg/dl. The subjects were considered hyperglycemic when the blood glucose levels were 200-300 mg/dl. Induction of diabetes with STZ was reported to be associated with high blood glucose levels and weight loss (Rad *et al.*, 2022). Further, the control group treated with EGCG showed blood glucose levels similar to fasting blood glucose

Chapter-3 *Estimation of the minimum effective dose for EGCG, assessment of general physiological status and fin regeneration in experimental zebrafish*

levels. Similar results were noted when STZ-induced diabetic mice, when injected with different grades of EGCG (50,100, 200) mg for 17 weeks, significantly decreased their blood glucose levels (Yoon *et al.*, 2014). Study on STZ diabetic mice treated with EGCG showed improvement in serum glucose as well as the body weight of the animal (Roghani & Baluchnejadmojarad, 2010).

Further, insignificant values for the body length of the test subjects across the groups were recorded throughout the experimental period. This observation suggests that the experimental interventions, including DM induction and EGCG treatment, did not exert discernible effects on the body length of the zebrafish subjects. Further analysis and interpretation of these findings may provide insights into the specific physiological responses of zebrafish to the experimental treatments in relation to body size regulation. EGCG is essential in decreasing inflammatory response on the wound site (Li *et al.*, 2016). Studies related to wound tissue of diabetic mice treated with EGCG showed better wound re-epithelialization (Carvalho *et al.*, 2021). The phases of caudal fin regeneration of adult zebrafish involve a series of stereotypic successive steps and take approximately three to four weeks to completely regenerate the amputated fin (Dietrich *et al.*, 2021). In the present study, the wound recovery time was expressed directly by measuring the length of the regenerative fin. During the wound healing period, the blastema of the fish fin and the granulation tissue of the human are similar, as both repair the damaged tissue by providing proliferative blastema cells (Pang *et al.*, 2020). Our results showed that the amputated fin gave positive growth when treated with EGCG in Groups III and IV. The series in which a diabetic wound is healed, and tissues are repaired is vital, and the

Chapter-3 *Estimation of the minimum effective dose for EGCG, assessment of general physiological status and fin regeneration in experimental zebrafish*

underlying action of EGCG on the diabetic regenerative model of zebrafish is still unclear. DM delays the wound healing process as it disturbs the different stages of wound repair: homeostasis, inflammation, proliferation, and remodeling (Patel *et al.*, 2019).

The present study showed that the fin of the hyperglycemic adult zebrafish was severely impaired. It was observed that on days 7th, 14th and 21st, the fin growth was significantly decreased compared to the Group I, III and IV animals. Similarly, when studying the fin regeneration in STZ-induced adult zebrafish, it was recorded that the fin did not show significant growth during 72 hours following amputation. Still, later reductions in the development of the amputated fin were observed in the 2nd and 3rd weeks (Olsen *et al.*, 2010). Works with animal models have described the therapeutic insights of EGCG (Xu *et al.*, 2021). A study with STZ-induced diabetic mice reported that EGCG could improve wound healing before or after the inflammation phase by targeting the Notch signaling pathway (Huang *et al.*, 2019).

The present study comprehensively evaluated the effects of EGCG on blood glucose levels, body weight, body length, BMI, and caudal fin regeneration in a hyperglycemic zebrafish model. The findings highlight the potential of EGCG in mitigating hyperglycemia, improving body weight, and promoting wound healing in diabetic zebrafish. Further research is warranted to elucidate the underlying mechanisms of EGCG action in promoting caudal fin regeneration and its therapeutic implications for diabetic wound healing. Overall, EGCG emerges as a promising candidate for future studies on wound healing, as revealed in DM zebrafish models, offering new insights into potential therapeutic approaches for impaired wound healing associated with diabetes.

Chapter 4

Effect of EGCG on lipid profiles and metabolic enzymes activity in the experimental zebrafish

Contents

4.1 Introduction

4.2 Materials and methods

4.3 Results

4.4 Discussion

4.1 Introduction

Over the past few decades, DM has become a severe metabolic disorder characterized by increased glucose levels in the blood due to disruptions in either insulin secretion or the insulin action mediated by receptors (Mukhtar *et al.*, 2020). DM instigates a cascade of intricate metabolic and biochemical alterations that culminate in structural changes and functional impairments within biomolecular systems (Halim & Halim, 2019). The two debilitating concomitants of DM are hyperglycemia and dyslipidemia, which play a crucial role in developing micro and macrovascular complications (Ghalichi *et al.*, 2022). Notably, discernible symptoms, including excessive thirst (polydipsia), heightened appetite (polyphagia), frequent urination (polyuria), and the loss of muscle mass (sarcopenia) are manifested (Wang *et al.*, 2020). Hyperglycemic conditions amplify glycation processes, yielding AGEs while concurrently generating free radicals and ROS (Paramanya *et al.*, 2023). The prolonged persistence of DM states precipitates complications across diverse organs, prominently affecting the liver and kidneys, thereby contributing to the emergence of diabetic hepatic disorders and nephropathies (Yingrui *et al.*, 2022).

In order to comprehensively examine the complex mechanisms that underlie DM and develop efficacious therapeutic approaches, a wide range of animal models have been utilized, incorporating techniques such as genetic manipulation, surgical interventions, and dietary interventions (Salehpour *et al.*, 2021; Rehman *et al.*, 2023). In this regard, zebrafish has gained importance as a reliable and consistent model in biomedical research, providing the ability to manipulate and replicate experiments. Intraperitoneal administration of STZ in zebrafish specifically destroys pancreatic β -cells, effectively

mimicking the pathogenesis of DM (Rehman *et al.*, 2023), making it an indispensable resource for researching DM (Tanbek & Sandal, 2023).

Diabetic dyslipidemia represents a dysregulated lipid profile prevalent in individuals with DM, encompassing alterations in total cholesterol (TC), triglycerides (TG), low-density very-low-density lipoprotein (VLDL), lipoprotein (LDL) and high-density lipoprotein (HDL) levels (Vekic *et al.*, 2023). Shin et al. (2023) elucidated that glycation processes induced by elevated plasma glucose levels engender modifications in lipoproteins and various proteins, precipitating structural modifications and functional aberrations particularly pronounced in poorly controlled DM states. This glycation-induced perturbation may render proteins vulnerable to oxidative stress, potentially eliciting alterations that render them immunogenic, either through glycation, oxidation, or a combination thereof (Babel & Dandekar, 2021). Such intricate molecular alterations underscore the complex interplay between glycemic control, lipoprotein metabolism, and oxidative stress in the pathogenesis of diabetic dyslipidemia.

Cholesterol, a vital constituent of cellular membranes and a precursor to essential molecules like hormones and bile acids, plays a pivotal role in various physiological processes (Jasim *et al.*, 2022). Cholesterol, which is synthesized primarily in the liver, facilitates cellular growth, vitamin and hormone production, thereby underscoring its indispensability in maintaining overall health and homeostasis. However, perturbations in blood cholesterol levels can inflict substantial harm on the different organs of the body, particularly when low-density lipoprotein cholesterol (LDL-C), often termed "bad cholesterol", becomes elevated, it predisposes individuals to cardiovascular diseases and strokes (Cannon, 2020). In contrast, high-density lipoprotein cholesterol (HDL-C),

regarded as the "good cholesterol," exerts protective effects against cardiovascular ailments by aiding in the removal of excess cholesterol, thereby reducing the risk of atherosclerosis and associated complications (Martagon *et al.*, 2023). In the context of DM patients are often seen to exhibit alterations in both the quantity and functionality of HDL, accentuating their susceptibility to cardiovascular complications (Banerjee *et al.*, 2023). This underscores the interplay between DM and dyslipidemia, with abnormal lipid profiles posing complex clinical implications. Notably, the components of diabetic dyslipidemia, including elevated triglyceride-rich VLDL, are intricately interconnected physiologically (Berberich & Hegele, 2022). Hepatic overproduction of VLDL, laden with TG, constitutes a hallmark feature of diabetic dyslipidemia, with cytosolic TG accumulation serving as a precursor for VLDL-triglyceride synthesis (Packard *et al.*, 2020; Boren *et al.*, 2022). Such insights shed light on the multifaceted mechanisms underpinning dyslipidemia in DM, highlighting the importance of understanding lipid metabolism in diabetes management and cardiovascular risk mitigation.

TG, classified as lipids or fats, are integral components of the bloodstream, serving as essential energy reservoirs in the body. By storing excess calories, TG provides a vital energy source for cellular functions. However, elevated levels often herald additional health complications, particularly predisposing individuals to conditions such as stroke and CVD. These associations are frequently observed with obesity and metabolic syndrome, further characterized by abdominal adiposity, hypertension, dyslipidemia, insulin resistance, hyperglycemia, and abnormal cholesterol profiles (Farnier *et al.*, 2021). The deleterious effects of elevated TG extend to arterial health, contributing to arterial hardening and thickening, known as arteriosclerosis, thereby escalating the risk of adverse

cardiac events, strokes, and heart failure.

Metabolic enzymes, including alanine aminotransferases (ALT), aspartate aminotransferases (AST), and alkaline phosphatase (ALP), orchestrate the intricate interconversion of amino acids, fulfilling augmented energy demands (Samanta *et al.*, 2014). These enzymes serve as pivotal indicators of non-alcoholic fatty liver disease (NAFLD), a condition intimately linked to elevated insulin levels and heightened susceptibility to DM. Of particular note, ALP is critical in facilitating transphosphorylation mechanisms crucial for aquatic organisms' mineralization and membrane transport processes (Amjad *et al.*, 2018). Perturbations in the activities of these enzymatic markers signify underlying cellular metabolic changes, furnishing diagnostic insights into the health status and organ damage precipitated by the metabolic stresses associated with DM.

Given the constraints and adverse effects associated with conventional antidiabetic therapies, contemporary research endeavors are increasingly directed toward exploring alternative therapeutic modalities for managing DM. This pursuit underscores the imperative to unravel novel treatment avenues that offer enhanced efficacy and improved safety profiles, thereby ameliorating the burden of this pervasive metabolic disorder. The expansive array of plant-derived compounds, rich in diverse phytochemicals, has emerged as a focal point in the quest for effective management strategies for DM (Anand *et al.*, 2019). Utilized in traditional medicinal practices, a myriad of plant species including *Acacia arabica*, *Azadirachta indica*, *Allium cepa*, *Aloe vera*, *Berberis vulgaris*, *Capsicum frutescens*, *Camellia sinensis*, *Cinnamomum zeylanicum*, *Eugenia jambolana*, and *Helicteres isora*, are revered for their purported anti-

diabetic properties (Ansari *et al.*, 2022a). The therapeutic efficacy of these medicinal plants in managing DM is attributed to a spectrum of mechanisms, encompassing augmentation of insulin secretion from pancreatic β -cells, enhancement of insulin receptor binding, attenuation of insulin resistance, and improvement in glucose tolerance (Tran *et al.*, 2020).

Empirical investigations have underscored the favorable outcomes of EGCG supplementation in managing DM, as evidenced by clinical trials conducted in both human subjects and experimental animals (Wan *et al.*, 2022; Jamir *et al.*, 2023). Furthermore, EGCG intake correlates with enhanced glucose tolerance and augmented insulin responsiveness (Wan *et al.*, 2022). Beyond glycemic control, green tea and its bioactive constituents have demonstrated anti-obesity effects (Rawat *et al.*, 2021) and conferred hepatorenal protection in diabetic rodent models (Soussi *et al.*, 2020). Mechanistically, EGCG exerts renoprotective effects by attenuating oxidative stress-induced apoptosis in diabetic nephropathy, modulating the expression of proapoptotic and anti-apoptotic proteins such as Bax and Bcl-2 (Mohan *et al.*, 2017). Similarly, EGCG ameliorates liver damage induced by agents like carbon tetrachloride (CCl₄) by enhancing liver function and reducing oxidative stress markers such as malondialdehyde (MDA) while augmenting glutathione (GSH) levels (Mostafa-Hedeab *et al.*, 2022). Moreover, pretreatment with EGCG has been shown to mitigate liver damage induced by methotrexate, as evidenced by improvements in hepatic cytosolic enzyme levels and prevention of hepatic toxicity (Pradhan *et al.*, 2023).

Despite the burgeoning evidence elucidating the therapeutic potential of EGCG in various facets of DM pathology, more knowledge is still needed concerning its effect

on lipid metabolism and metabolic enzyme activities in DM-induced zebrafish models. Thus, this study explores the intricate interplay between EGCG supplementation and lipid profiles and metabolic enzyme activities, specifically ALT, AST, and ALP in the liver, kidney, and gills of zebrafish afflicted with STZ-induced diabetes. By elucidating the dynamic changes ensuing from EGCG treatment, this investigation aims to unravel the therapeutic potential of EGCG in ameliorating the disruptions caused by DM.

4.2 Materials and methods**4.2.1 Chemicals**

EGCG was sourced from Merck, while lipid profile kits and metabolic enzymes kits were procured from ERBA Chemicals (Erba Diagnostics, Mannheim GmbH, Germany). Enzyme activity assays were conducted using the Benesphera C61 clinical semi-automatic biochemical analyzer.

4.2.2 Experimental design

The experimental protocol involved categorizing the zebrafish (n=6) into distinct groups as follows: Group-I: control, Group-II: diabetic, Group-III: diabetic + EGCG, Group-IV: control + EGCG. Experimental Groups III and IV were subjected to EGCG supplementation at a dose of 6 mg/L of water throughout the experimental duration.

4.2.3 Blood collection for lipid profile

Before blood collection, experimental fish from each group (n=6) underwent a 24-hour fasting period. For blood collection, fish were anesthetized and disinfected with 70% ethanol, and their tails were amputated. Subsequently, the fish body was immersed in a 1.5 mL tube containing 120 µL of citrate EDTA buffer, allowing blood to flow while centrifuging at low speed (50 rpm). Post-centrifugation, the fish body was discarded, and the supernatant was further centrifuged at 8000 rpm for 10 minutes to obtain plasma samples (pools of 5 fish). Commercial assay kits from ERBA Diagnostics (Mannheim GmbH, Germany) were employed to quantify TC, HDL-C, TG, and LDL-C. The Benesphera clinical chemistry Analyzer C61 facilitated all analyses. Figure 4.1 shows the experimental blood collection setup and studying the lipid profiles of zebrafish model.

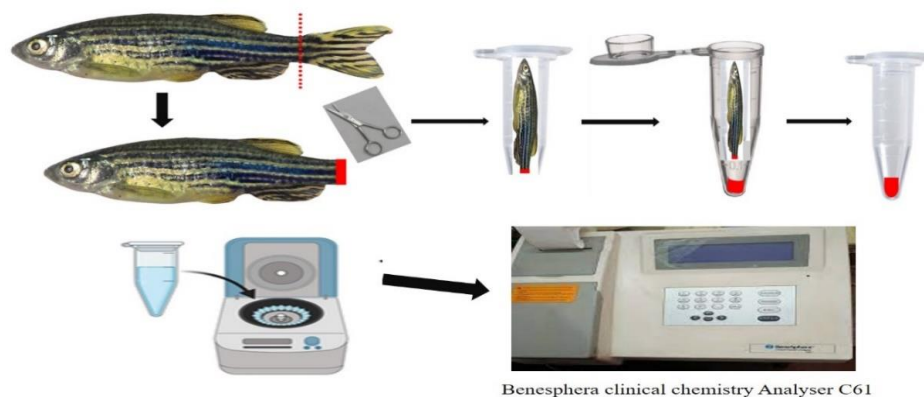


Figure 4.1: Diagrammatic representation of blood collection for lipid profile in zebrafish model.

4.2.4 Tissue preparation

The hepatic, gill, and renal tissues were meticulously dissected, finely minced, and homogenized at a concentration of 2.5% w/v utilizing ice-cold 0.15% KCl-0.1M phosphate buffer (pH 7.4) in a glass homogenizer. Subsequently, the resulting homogenate underwent centrifugation at 2000 rpm for 15 minutes at 4°C, facilitating the separation of cellular debris. The supernatant containing the soluble fraction of cellular components was collected for subsequent biochemical analyses. Figure 4.2 shows the experimental design for the tissue collection and processing of metabolic enzyme activities.

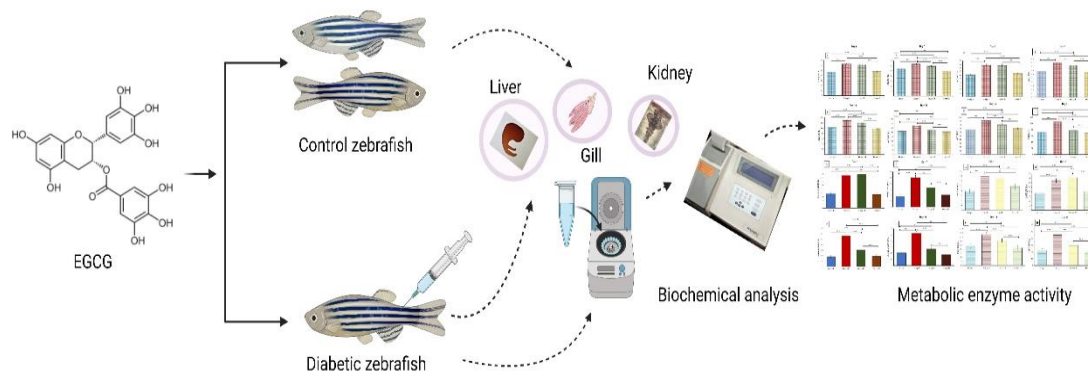
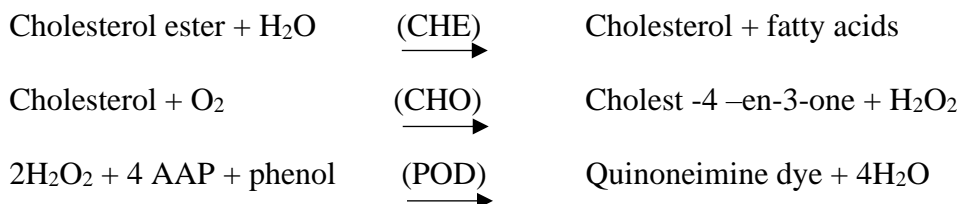


Figure 4.2: Experimental design for tissue collection and studying metabolic enzymes activities.

4.2.5 Biochemical analysis

The activity levels of alanine aminotransferase (ALT), aspartate aminotransferase (AST), and alkaline phosphatase (ALP) were determined using commercially available ERBA kits, following the established protocol as outlined by Hajam et al. (2022). This method entails colorimetric assays to quantify enzyme activity, providing insights into the metabolic status and organ function of the experimental subjects.

4.2.6 Total cholesterol (TC)**Principle**

Absorbance of Quinoneimine so formed is directly proportional to cholesterol concentration at 505 nm.

Reagent composition

Buffer (pH – 6.4)	100 mmol/L
Cholesterol oxidase	> 100 U/L
Cholesterol esterase	>200 U/L
Peroxidase	>3000 U/L
4 – Amino antipryine	0.3 mmol/L
Phenol	5 mmol/L
Cholesterol standard	200 mg/dl

Assay parameters

Mode	End point
Wavelength 1 (nm)	505
Wavelength 2 (nm)	670
Sample volume (μl)	5
Working reagent (μl)	500
Incubation time (min)	10
Incubation temperature (°C)	37
Normal low (mg/dl)	0
Normal high (mg/dl)	200
Linearity low (mg/dl)	0
Linearity high (mg/dl)	1000
Concentration of standard (mg/dl)	200
Absorbance limit	0.4
Blank with	Reagent
Units	mg/dl

Assay procedure

Pipette into tubes	Blank	Standard	Test
Working reagent	500 μl	500 μl	500 μl
Distilled water	5 μl	-	-
Standard	-	5 μl	-
Sample	-	-	5 μl

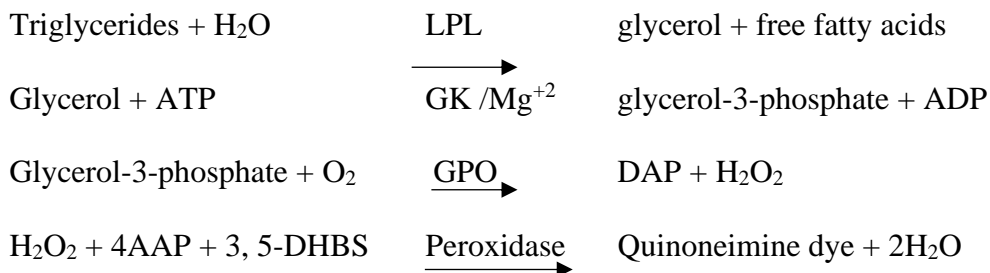
The reagents were mixed well and incubated for 10 minutes at 37°C. Finally, the absorbance of the test and standard was read against the reagent blank.

Calculation

$$\text{Cholesterol (mg/dl)} = \frac{\text{Abs of Test}}{\text{Abs of Standard}} \times \text{Concentration of Std. (mg/dl)}$$

4.2.7 Triglycerides (TG)

GPO – Trinder method

Principle

The intensity of Chromogen (Quinoneimine) formed is proportional to the triglycerides concentration in the sample when measured at 505 nm (500-540nm).

Reagent 1: Triglycerides reagent

Active Ingredient	Concentration
ATP	2.5 mmol/L
Mg ²⁺	2.5 mmol/L
4-Aminoantipyrine	0.8 mmol/L
3-5 DHBS	1 mmol/L
Peroxidase	>2000 U/L
Glycerol kinase	>550 U/L
GPO	>8000 U/L
Lipoprotein lipase	>3500 U/L
Buffer (pH 7.0 ± 0.1 at 20°C)	53 mmol/L
Triglycerides standard	200 mg/dl (2.3 mmol/L)

Reagents reconstitution procedure

Before reconstitution, the reagent bottle and Aqua-4 were equilibrated to room temperature (15-30°C). Subsequently, 20 ml of Aqua-4 was added to each vial containing the reagents. The mixture was gently swirled to facilitate dissolution and allowed to stand

undisturbed for 10 minutes at room temperature, allowing complete reconstitution. Following this incubation period, the reconstituted solution was deemed ready for use in the experimental procedures. This reconstitution protocol ensures optimal solubility and stability of the reagents, enhancing the reliability and accuracy of subsequent analytical measurements.

Assay parameters

Mode	End Point
Wavelength 1 (nm)	505
Wavelength 2 (nm)	670
Sample volume (μl)	5
Reagent volume (μl)	500
Incubation time (min)	10
Incubation temperature (°C)	37
Normal low (mg/dl)	25
Normal high (mg/dl)	160
Linearity low (mg/dl)	0
Linearity high (mg/dl)	1000
Concentration of standard (mg/dl)	1000
Blank with	Reagent
Absorbance limit	0.5
Units	mg/dl

Assay procedure

Pipette into tubes marked	Blank	Standard	Test
Working reagent	500 μl	500 μl	500 μl
Distilled water	5 μl	-	-
Standard		5 μl	-
Test	-	-	5 μl

The reagents were mixed and incubated at 37°C for 10 minutes. After incubation, the absorbance of the standard and each test was read at 505 nm (500-540 nm) on bichromatic analysers against reagent blank.

Calculations

$$\text{Triglycerides (mg/dl)} = \frac{\text{Absorbance of test}}{\text{Absorbance of standard}} \times \text{Concentration of standard (mg/dl)}.$$

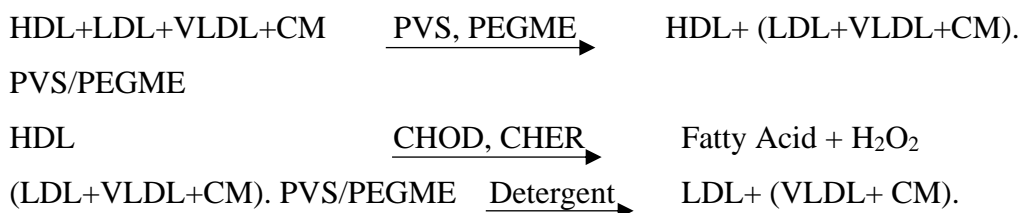
4.2.8 Very low-density lipoprotein (VLDL)

VLDL concentration was calculated using the formula (VLDL-cholesterol = triglycerides/5) as describe by Mashi, (2017).

4.2.9 Low-density lipoprotein (LDL)

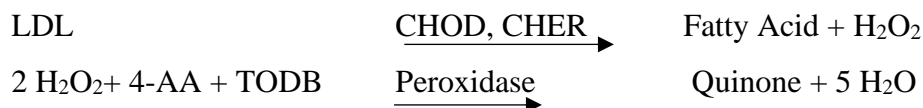
Principle

The LDL assay employs a modified precipitation method utilizing polyvinyl sulfonic acid (PVS) and polyethylene-glycol methyl ether (PEGME), incorporating optimized quantities of these components and selected detergents. LDL, VLDL, and chylomicrons (CM) react with PVS and PEGME, forming complexes that render LDL, VLDL, and CM inaccessible to cholesterol oxidase (CHOD) and cholesterol esterase (CHER). In contrast, high-density lipoprotein (HDL) selectively reacts with the enzymes. Adding reagent R2 containing a specific detergent releases LDL from the PVS/PEGME complex. The released LDL subsequently reacts with the enzymes, resulting in the production of hydrogen peroxide (H₂O₂), which is quantified using the Trinder reaction.



Chapter-4***Effect of EGCG on lipid profiles and metabolic enzymes activity in the experimental zebrafish***

PVS/PEGME.

**Reagent composition: R1**

MES buffer (pH 6.5)	50 mmol/L
Polyvinyl sulfonic acid	50 mg/L
Polyethylene glycolmethylester	30 ml/L
4-aminoantipyrine	0.9 g/L
Cholesterol esterase	5 kU/L
Cholesterol oxidase	20 KU/L
Peroxidase	5 KU/L

Reagent composition: R2

MES buffer (pH 6.5)	50 mmol/L
Detergent	
TODB N,N-Bis (4-sulfobutyl)-3-methylanine	3 mmol/L

Reagent preparation

The calibrator is reconstituted with 1 ml of deionized water at 20-25°C and mixed gently to avoid foaming. Following reconstitution, it is allowed to stand for a minimum of 30 minutes until complete dissolution before use. The reconstituted calibrator is stored at 2-8°C to maintain stability.

Assay parameters

Mode	1-Point End
Wavelength 1 (nm)	600
Wavelength 2 (nm)	700
Sample volume (μl)	3

Chapter-4***Effect of EGCG on lipid profiles and metabolic enzymes activity in the experimental zebrafish***

Reagent 1 volume (μL)	375
Reagent 2 volume (μL)	125
Incubation time (min).	5
Incubation temperature (°C)	37
Normal low (mg/dl)	0
Normal high (mg/dl)	130
Linearity low (mg/dl)	2.6
Linearity high (mg/dl)	263
Blank with	Reagent
Absorbance limit (Max.)	0.3
Units	mg/dl

Assay procedure

Pipette in Tube	Reagent Blank	Sample/Calibrator
Reagent 1	375 μl	375 μl
Distilled water	3 μl	-
Sample/calibrator	-	3μl
Mix and incubate at 37°C		
125 μl	125 μl	-
Mix and incubate at 37°C for 5 min.		

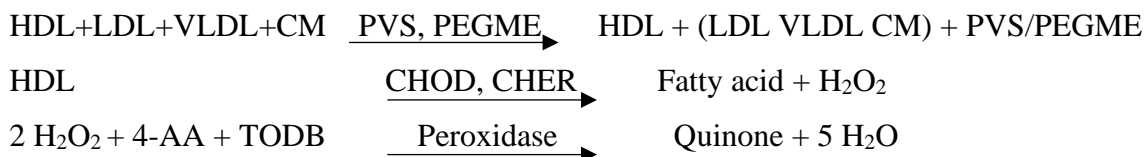
The final absorbance was read at the wavelength of 600nm against the reagent blank.

Calculation

$$\text{LDL C} = \frac{\text{Absorbance of Sample} - \text{Absorbance of Blank}}{\text{Absorbance of Calibrator} - \text{absorbance of Blank}} \times \text{Concentration of Calibrator.}$$

4.2.10 High-density lipoprotein (HDL)**Principle**

Similar to the LDL assay, the HDL assay utilizes a modified precipitation method employing polyvinyl sulfonic acid (PVS) and polyethylene glycol-methyl ether (PEGME) along with optimized quantities of these components and selected detergents. LDL, VLDL, and chylomicrons (CM) interact with PVS and PEGME, leading to their precipitation and rendering them inaccessible to cholesterol oxidase (CHOD) and cholesterol esterase (CHER). Conversely, HDL selectively interacts with the enzymes, generating a detectable signal through the Trinder reaction.

**Reagent composition: R1**

MES buffer (pH 6.5)	6.5 mmol/L
TODB N, N-Bis (4-sulfobutyl) – 3 – methylaniline	3 mmol/L
Polyvinyl sulfonic acid	50 mg/L
Polyethylene-glycol-methyl ester	30 ml/L
MgCl ₂	2 mmol/L

Reagent composition: R2

MES buffer (pH 6.5)	50 mmol/L
Cholesterol esterase	5 kU/L
Cholesterol oxidase	20 KU/L
Peroxidase	5 kU/L
4- aminoantipyrine	0.9 g/L

Chapter-4***Effect of EGCG on lipid profiles and metabolic enzymes activity in the experimental zebrafish***

Detergent	0.5 %
-----------	-------

Reagent preparation

Reagents R1 and R2 are in liquid form and ready to use. The calibrator is reconstituted with 1 ml of deionized water at 20-25°C and mixed gently. After reconstitution, it can stand for at least 30 minutes before use.

Assay parameter

Mode	1-Point End
Wavelength 1 (nm)	600
Wavelength 2 (nm)	700
Sample volume (µL)	3
Reagent 1 volume (µL)	375
Reagent 2 volume (µL)	125
Incubation time (min.)	5
Incubation temperature (°C)	37
Normal low (mg/dl)	42
Normal high (mg/dl)	79.5
Linearity low (mg/dl)	1.9
Linearity high (mg/dl)	193
Blank with	Reagent
Absorbance limit (Max.)	0.3
Units	mg/dl

Assay procedure

Pipette in Tube	Reagent Blank	Sample/Calibrator
Reagent 1	375 µl	375 µl
Distilled water	3 µl	-
Sample/calibrator	-	3µl
Mix and incubate at 37°C		

Chapter-4***Effect of EGCG on lipid profiles and metabolic enzymes activity in the experimental zebrafish***

125 µl	125 µl	-
Mix and incubate at 37°C for 5 min.		

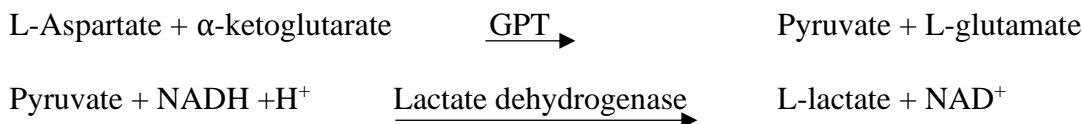
The final absorbance was read at the wavelength 600nm against the reagent blank.

Calculation:

$$\text{HDL-C} = \frac{\text{Absorbance of sample} - \text{Absorbance of sample blank}}{\text{Absorbance of calibrator} - \text{Absorbance of calibrator blank}} \times \text{Concentration of calibrator}$$

4.2.11 Alanine aminotransferase (ALT) activity

Approximately 50 µL of tissue sample fluid was added to 500 µL of ALT working reagent and homogenized. Absorbance was measured at 340 nm.

Principle

The decrease in absorbance rate due to oxidation of NADH to NAD is proportional to GPT/ALT activity.

Kit contents**Reagent 1: Buffer**

Tris buffer	110 mM, pH 7.5
L-Alanine	550 mM

Reagent 2: Enzymes

LDH	≥ 1200 U/L
NADH	0.2 mM
α-Ketoglutarate	16mM

Preparation of working reagent

Reconstitute reagents as per instructions on individual bottle labels to prepare working

reagents.

Test procedure

The working reagent 1.0 ml and 100 µl of the sample was pipette into the test tube. Mixed and after 1 minute of incubation, the change in absorbance was measured ($\Delta OD/min$) for 3 minutes. The mean absorbance change per minute was determined as ($\Delta OD/min$).

Assay parameters

Input Parameters	Values
Type of reaction	Kinetic
Slope of reaction	Decreasing
Wavelength	340 nm
Factor	1746
Incubation time	60 sec.
Interval time	60 sec.
Interval no.	3
Flow cell temperature	37°C
Molar extinction coefficient	6.3
$\Delta OD/min$. limit	0.200
Units	IU/L
Upper normal value	49 IU/L
Lower normal value	0.0 IU/L
Linearity	350 IU/L
Working reagent volume	1.0 mL
Sample volume	100 µl

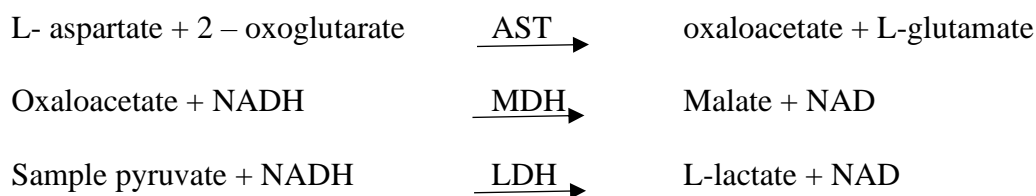
Calculations

$$\text{ALT Activity (IU/L)} = \frac{\Delta OD}{\text{min}} \times 1746$$

4.2.12 Aspartate aminotransferase (AST) activity

About 50 µL of tissue sample fluid was mixed with 500 µL of AST working reagent and homogenized. Absorbance was measured at 340 nm.

Principle:

**Reagent composition: R1**

2-Oxyglutarate	12 mmol/L
L-Aspartate	200 mmol/L
MDH	≥545 U/L
LDH	≥909 U/L
NADH (Yeast)	≥0.18 mmol/L
Tris Buffer (pH = 7.8 ±0.1 at 25°C)	80 mmol/L
EDTA	5.0 mmol/L

Reagent reconstitution

Initially, the reagent bottle and Aqua-4 were allowed to attain room temperature (15-30°C). 20 ml of AQUA-4 was added to each of the vials. The mixture was made to dissolve slowly and allowed to stand for 10 minutes at room temperature, after which it was ready to be used.

Assay parameters

Mode	Kinetic
Wavelength	340
Sample volume (µl)	50

Chapter-4***Effect of EGCG on lipid profiles and metabolic enzymes activity in the experimental zebrafish***

Reagent volume (µl)	500
Lag time (Sec.)	60
Kinetic interval (Sec.)	60
No. of readings	3
Kinetic factor	1768
Reaction temperature (°C)	37°C
Reaction direction	Decreasing
Normal low (IU/L)	0
Normal high (IU/L)	35
Linearity low (IU/L)	0
Linearity high (IU/L)	450
Absorbance limit (Min.)	0.8
Blank with	Water
Units	IU/L

Assay procedure

Pipette	Volume
Working	1000 µl
Test	100 µl

Calculations

The general formula for converting absorbance change into international units (IU) of activity is:

$$\text{IU/L} = \frac{\left(\Delta \frac{A}{\text{min}}\right) \times T.V. \times 10^3}{S.V. \times \text{Absorptivity} \times P};$$

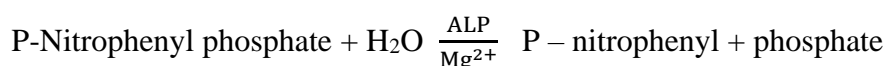
Where;

Absorptivity = mill molar absorptivity of NADH at 340 nm = 6.22

Activity of AST = $\Delta \text{ Abs/min} \times 1768$

4.2.13 Alkaline phosphatase (ALP) activity

Approximately 20 µL of serum was added to 1000 µL of ALP reagent (p-Nitrophenyl Phosphate, Mg^{2+}) and homogenized. Absorbance was measured at 405 nm.

Principle**Reagent composition: R1**

p-nitrophenyl phosphate	16 mmol/L
Mg^{2+}	4 mmol/L
Tris/carbonate buffer (pH 10.2 ± 0.2 at 25°C)	-

Reagent constitution

Initially, the reagent bottle and Aqua-4 were allowed to attain room temperature ($15-30^\circ\text{C}$). 20 ml of AQUA-4 was added to each of the vials. The mixture was made to dissolve slowly and allowed to stand for 10 minutes at room temperature, after which it was ready to be used.

Assay parameters

Mode	Kinetic
Wavelength (nm)	405
Sample volume (µl)	10/20
Reagent volume	500
Lag time (Sec.)	60
Kinetic interval (Sec.)	60
No. of readings	3

Chapter-4***Effect of EGCG on lipid profiles and metabolic enzymes activity in the experimental zebrafish***

Kinetic factor	2713
Reaction temperature (°C)	37
Reaction direction	Increasing
Normal low (IU/L)	42
Normal high (IU/L)	128
Linearity low (IU/L)	0
Linearity high (IU/L)	1000
Absorbance limit (Max.)	0.800
Blank with	Distilled Water
Units	IU/L

Assay procedure

Pipette	Volumes
Working reagent	1000 µL
Test	20 µL

Calculations

The general formula for converting absorbance change into International Units (IU) of activity is:

$$U/L = \frac{(\Delta A/\text{min}) \times T.V. \times 10^3}{S.V. \times \text{Absorptivity} \times P}$$

Absorptivity = millimolar absorptivity of p-nitrophenyl phosphate at 405 nm = 18.8

Activity of ALP at 37°C (IU/L) = ($\Delta A_{405}/\text{min}$) x factor (2713)

4.2.14 Statistical analysis

Data analysis was conducted using GraphPad Prism 5.0 software and presented as mean \pm SD. Intergroup comparisons were performed using one-way analysis of variance (ANOVA) followed by Tukey's post hoc test. Asterisk represents a significant difference, * $p < 0.05$, ** $p < 0.01$, and *** $p < 0.001$.

4.3 Results

4.3.1 Total cholesterol (TC)

The baseline TC levels for Group-I were 285.84 ± 5.6 mg/dL on day 1, slightly increasing to 287.84 ± 6.9 mg/dL by day 21. Group-II exhibited significantly elevated TC levels, recording a mean level of 354.84 ± 5.4 mg/dL on day 21. Conversely, Group-III showed notable improvement in TC levels, with a mean of 290.67 ± 6.7 mg/dL on day 21. Compared to Group-I, Group-II demonstrated a substantial increase in TC levels by 23.27 % after 21 days of treatment. In contrast, Group-III showed a reduction in TC levels by 18.07 % on day 21. Group-IV exhibited marginal changes in TC levels compared to Group-I throughout the study period. Detailed data on TC levels across the experimental groups are meticulously presented in Table 4.1 and Figure 4.3.

4.3.2 Triglycerides (TG)

The baseline TG levels for Group-I were 248.67 ± 7.0 mg/dL on day 1, increasing slightly to 254.34 ± 7.4 mg/dL by day 21. Group-II displayed elevated TG levels, recording a mean of 336 ± 6.7 mg/dL on day 21, while Group-III showed an improvement in TG levels, with a mean of 270.84 ± 6.8 mg/dL. Compared to Group-I, Group-II exhibited a significant increase in TG levels by 32.28 % after 21 days of treatment. However, Group-III demonstrated a reduction in TG levels by 19.64 % on day 21. Additionally, insignificant results were observed between Group-IV and Group-I. Detailed data about TG levels across the experimental groups are meticulously presented in Table 4.2 and Figure 4.4.

4.3.3 Very low-density lipoprotein (VLDL)

VLDL plays a crucial role in lipid metabolism, particularly in transporting triglycerides synthesized in the liver to peripheral tissues. VLDL levels in each experimental group to

assess lipid dynamics and treatment effects were evaluated. On day 21 of the experiment, the mean VLDL level in Group-I was recorded as 50.84 ± 6.0 mg/dL. Group-II exhibited markedly elevated VLDL levels, with a mean of 76.83 ± 5.3 mg/dL. At the same time, Group-III showed an encouraging improvement in VLDL levels, displaying a mean level of 55.34 ± 6.1 mg/dL. Comparing these findings with the baseline level in Group-I, it becomes apparent that Group-II experienced a significant increase in VLDL levels by 43.39 % over the 21-day treatment period. Conversely, Group-III demonstrated a notable reduction in VLDL levels by 27.63 % on day 21, indicating a positive response to the treatment regimen. Furthermore, Group-IV displayed insignificant ($p > 0.05$) values of VLDL that deviated from those of Group-I throughout the study duration. Detailed data pertaining to VLDL levels across the experimental groups are presented in Table 4.3 and visually depicted in Figure 4.5.

4.3.4 Low-density lipoprotein (LDL)

The mean LDL level for Group-I on day 21 was 179 ± 7.0 mg/dL, slightly higher than the baseline of 174 ± 7.7 mg/dL on day 1. Group-II exhibited markedly elevated LDL levels, that recorded 229.84 ± 6.9 mg/dL on day 21. Conversely, Group-III improved LDL levels, were recorded as 183.50 ± 7.0 mg/dL. Compared to Group-I, Group-II demonstrated a significant ($p < 0.001$) increase in LDL levels by 28.15 % after 21 days of treatment. In contrast, Group-III showed a reduction in LDL levels by 20.08% on day 21. Group-IV exhibited insignificant change in LDL levels compared to Group-I throughout the study period. Detailed LDL results across the experimental period of 21 days are presented in Table 4.4 and Figure 4.6.

4.3.5 High-density lipoprotein (HDL)

High-density lipoprotein (HDL) is widely recognized as a protective factor against CVD, exerting its beneficial effects through the reverse cholesterol transport pathway. Given its importance, HDL levels across the experimental groups were recorded to elucidate the effect of the treatment regimen on lipid metabolism. At the onset of the study, Group-I zebrafish exhibited the HDL level of 74.16 ± 6.5 mg/dL. However, Group-II subjects displayed a significant ($p < 0.001$) decrement in HDL levels, and was recorded as 43.50 ± 6.3 mg/dL on day 21, highlighting the dyslipidemic state induced by diabetes. In contrast, Group-III demonstrated a remarkable improvement in HDL levels, reaching an average of 68.17 ± 5.5 mg/dL on day 21, signifying a positive treatment response.

Comparing the percentage change in HDL levels between Group-I and Group-II reveals a substantial decline of 41.89 % in the latter, underscoring the detrimental effect of diabetes on lipid metabolism. Conversely, Group-III exhibited a notable enhancement in HDL levels, registering a remarkable 58.13 % increase on day 21 compared to Group-II, indicative of the therapeutic efficacy of the intervention. While Group-IV exhibited a slight reduction in HDL levels, statistical analysis showed insignificant value compared to Group-I. The HDL levels across experimental groups are summarized in Table 4.5 and visually depicted in Figure 4.7.

4.3.6 Hepatic tissue alanine aminotransferase (ALT) activity

ALT, an enzyme predominantly found in hepatocytes, is a sensitive biomarker for assessing liver function and integrity. Elevations in ALT levels often signify hepatocellular injury or dysfunction, making it a pivotal parameter in evaluating the hepatic effect of diabetes and therapeutic interventions. The study evaluated the hepatic

tissue ALT activity across different experimental groups to discern the effects of diabetes induction and treatment intervention on liver health.

In Group-I, the baseline ALT activity on day 1 was recorded as 93.67 ± 2.16 , with subsequent measurements showing modest fluctuations over the 21 days. Conversely, Group-II, comprising diabetic zebrafish, exhibited a pronounced increase in ALT activity, with a significant elevation of 25.34 %, 26.83 %, 28.85 %, and 30.67 % observed on days 1, 7, 14, and 21, respectively, compared to Group-I. Remarkably, Group-III, subjected to the treatment regimen, displayed a gradual decline in ALT activity throughout the 21 days, indicative of a therapeutic response. The ALT values in Group-III were recorded as 122.50 ± 2.73 , 118.84 ± 2.48 , 119.67 ± 2.73 , and 110.68 ± 2.16 on days 1, 7, 14, and 21, respectively, demonstrating a notable amelioration compared to Group-II.

Moreover, statistical analysis revealed insignificant differences between Group-I and Group-IV, suggesting that the treatment intervention effectively mitigated diabetes-induced hepatic injury. The detailed dataset on hepatic ALT activity is meticulously presented in Table 4.6, complemented by visual representations in Figure 4.8.

4.3.7 Gill tissue alanine aminotransferase (ALT) activity

The investigation into gill tissue ALT activity in diabetic zebrafish unveiled significant alterations compared to the control group, providing valuable insights into the systemic effects of diabetes beyond hepatic tissues. Diabetic zebrafish showed a significant ($p < 0.001$) rise in ALT activity in the gill tissues on 21 days of the experiment compared to the control. In Group-I, the ALT activity of gill measured 110.84 ± 2.85 on day 1, 109.84 ± 2.31 on day 7, 118.84 ± 3.18 on day 14, and 117.66 ± 2.65 on day 21. Group-II demonstrated a substantial increase in ALT activity, with increments of 31.35 %, 35.67

%, 37.84 %, and 39.67 % estimated on days 1, 7, 14, and 21, respectively, in contrast to Group-I. Interestingly, Group-III exhibited a consistent decrease in ALT activity throughout the 21-day treatment period, displaying values of 132.17 ± 2.48 on day 1, 130.84 ± 2.48 on day 7, 127.17 ± 2.85 on day 14, and 125.00 ± 3.68 on day 21. The statistical analysis revealed insignificant differences ($p > 0.05$) between the ALT activity of Group-IV and Group-I. The comprehensive data on gill tissue ALT activity is meticulously depicted in Table 4.7 and Figure 4.9.

4.3.8 Renal tissue alanine aminotransferase (ALT) activity

Renal tissue ALT activity is a pivotal indicator of metabolic dysregulation and cellular injury within the kidneys, warranting comprehensive evaluation in diabetic conditions. The meticulous examination of renal tissue ALT activity in diabetic zebrafish revealed significant alterations compared to the control group, shedding light on the renal manifestations of diabetes. Inducing diabetes in zebrafish led to a significant ($p < 0.001$) increase in ALT activity within renal tissues compared to the control group in 21 days. In Group-I, ALT activity in the kidney tissue was measured as 60.83 ± 3.18 on day 1, 67.50 ± 3.27 on day 7, 67.17 ± 2.78 on day 14, and 72.17 ± 2.78 on day 21. Notably, Group-II exhibited a considerable rise in kidney ALT activity, with an increase of 11.66 %, 9.83 %, 7.83 %, and 5.34 % observed on days 1, 7, 14, and 21, respectively, compared to Group I. Impressively, Group-III demonstrated a consistent decreasing trend in kidney ALT activity throughout the 21-day treatment period, presenting values of 87.67 ± 3.01 on day 1, 83.16 ± 3.95 on day 7, 80.84 ± 2.13 on day 14, and 77.34 ± 2.16 on day 21. Statistical analysis underscored the significant ($p < 0.001$) differences between Group-II and Group-III, affirming the therapeutic efficacy in mitigating renal tissue injury associated with

diabetes. The effect of DM on the ALT activity in the kidney tissue of the experimental zebrafish on different days is represented in Table 4.8 and Figure 4.10.

4.3.9 Hepatic tissue aspartate aminotransferase (AST) activity

Hepatic tissue AST activity, a key parameter reflective of hepatic health and function, was meticulously evaluated to discern the hepatic manifestations of diabetes and assess the therapeutic efficacy of the intervention. The investigation into hepatic tissue AST activity in diabetic zebrafish showed alterations in the tissue compared to the control group, highlighting the systemic effect of diabetes on hepatic function.

Diabetes induction in zebrafish resulted in a significant ($p<0.001$) increase in AST activity in liver tissues compared to Group-I. In Group-I, the AST activity was measured as 20.50 ± 1.87 , 21.84 ± 2.63 , 23.17 ± 2.31 , and 24.67 ± 2.73 on days 1, 7, 14, and 21, respectively. The liver AST activity in Group-II displayed a substantial increase, presenting a 59.33 % elevation on day 21 compared to Group-I. Notably, Group-III manifested a significant ($p<0.001$) decrease in AST activity over the 21-day treatment period, with values measured as 31.34 ± 2.65 , 34.35 ± 3.38 , 29.84 ± 2.48 , and 28.83 ± 2.63 on days 1, 7, 14, and 21, respectively. Statistical analysis revealed insignificant differences ($p>0.05$) between the liver AST activity of Group I and Group IV. The detailed dataset on hepatic tissue AST activity, meticulously presented in Table 4.9 and Figure 4.11.

4.3.10 Gills tissue aspartate aminotransferase (AST) activity

Aspartate aminotransferase (AST) activity is a crucial indicator of cellular integrity and metabolic processes, reflecting tissue damage or physiological changes. In this section, the AST activity within the gill tissues of diabetic zebrafish over a 21-day experimental period was evaluated, aiming to elucidate potential alterations and therapeutic responses.

Diabetic zebrafish exhibited a significant ($p < 0.001$) rise in AST activity within gill tissues compared to the control group throughout the duration of the experiment. Specifically, in Group-I the baseline AST activity on day 1 was measured as 20.34 ± 2.87 , with marginal fluctuations observed in subsequent measurements. Conversely, Group-II, comprising diabetic zebrafish, demonstrated a substantial increase in gill AST activity, with a remarkable elevation of 54.66 % noted on day 21 compared to Group-I. Impressively, Group-III, subjected to the treatment regimen, displayed a consistent reduction in gill AST activity over the 21 days, indicative of a therapeutic response. Notably, AST values in Group-III were recorded as 31.50 ± 2.42 , 31.34 ± 2.58 , 30.67 ± 2.80 , and 28.17 ± 2.92 on days 1, 7, 14, and 21, respectively. Statistical analysis revealed insignificant ($p > 0.05$) differences between the AST gill activity of Group-I and Group-IV. The comprehensive dataset on gill tissue AST activity is meticulously summarized in Table 4.10, complemented by visual representations in Figure 4.12.

4.3.11 Renal tissue aspartate aminotransferase (AST) activity

Renal tissues play a pivotal role in metabolic homeostasis and waste excretion, making them susceptible to pathological alterations in conditions such as diabetes. In this section, we meticulously evaluated the dynamics of AST activity within the renal tissues of diabetic zebrafish to discern potential alterations and therapeutic responses.

Induction of diabetes in zebrafish resulted in a significant ($p < 0.001$) rise in AST activity within renal tissues compared to the control group over the 21-day experimental period. Specifically, in Group-I, the baseline AST activity on day 1 was measured as 18.84 ± 2.48 , with modest fluctuations observed in subsequent measurements. Conversely, Group-II, exhibited a notable elevation in renal AST activity, with significant increments of 58.83

% and 54.83 % noted on days 14 and 21, respectively, compared to Group-I. Remarkably, Group-III, subjected to the treatment regimen, manifested a significant ($p < 0.001$) reduction in renal AST activity over the 21 days, reaching reductions of 69.33 % and 71.83 % on days 14 and 21, respectively, compared to Group-II.

Statistical analysis revealed insignificant ($p > 0.05$) differences between the renal AST activity of Group-I and Group-IV. The detailed dataset on renal tissue AST activity is meticulously presented in Table 4.11, complemented by visual representations in Figure 4.13.

4.3.12 Hepatic tissue alkaline phosphatase (ALP) activity

Alkaline phosphatase (ALP) activity indicates liver health and biliary function, reflecting alterations in hepatobiliary physiology. ALP activity within hepatic tissues of diabetic zebrafish over a 21-day experimental period was measured to elucidate potential alterations and therapeutic responses.

Group-I, representing the control, the baseline ALP activity on day 1 was measured as 19.03 ± 1.89 , with minor fluctuations observed in subsequent measurements. Conversely, Group-II, comprising diabetic zebrafish, exhibited a marked elevation in hepatic ALP activity, with substantial increase ranging from 56.83 %, 49.84 %, 47.33 %, and 43.33 % noted across the experimental timeline compared to Group-I. Impressively, Group-III, subjected to the treatment regimen, displayed a considerable reduction in hepatic ALP activity over the 21 days, with values reaching 72.84 % lower on day 21 than Group-II. Statistical analysis revealed insignificant ($p > 0.05$) differences between the hepatic ALP activity of Group-I and Group-IV, underscoring the potential efficacy of the treatment regimen in mitigating liver tissue injury associated with diabetes. The detailed dataset on

hepatic tissue ALP activity is meticulously presented in Table 4.12, complemented by visual representations in Figure 4.14.

4.3.13 Renal tissue alkaline phosphatase (ALP) activity

The renal tissue of diabetic zebrafish exhibited a noteworthy increase in ALP activity compared to the control group, signifying renal involvement in the diabetic condition. In Group-I, the ALP activity was measured as 11.84 ± 2.85 , 10.34 ± 2.16 , 11.17 ± 2.78 , and 13.34 ± 2.68 on days 1, 7, 14, and 21, respectively. Notably, Group-II displayed a substantial elevation in ALP activity, indicating a 72.16 % increase on day 21 compared to Group-I, suggesting renal dysfunction associated with diabetes progression. Remarkably, Group-III exhibited a significant ($p < 0.001$) reduction in kidney ALP activity over the 21-day treatment period, demonstrating an 84.16 % decrease on day 21 compared to Group-II. This reduction suggests a potential ameliorative effect of the treatment intervention on renal ALP activity. Furthermore, statistical analysis revealed insignificant differences ($p > 0.05$) in ALP activities between Group-I and Group-IV test zebrafish, indicating that the treatment alone did not significantly affect renal ALP activity compared to the control.

The alterations in renal ALP activity observed in diabetic zebrafish underscore the complex interplay between diabetes and renal function. The effect of ALP activity in the renal tissue of the test zebrafish across different time points is represented in Table 4.13 and Figure 4.15.

Table 4.1: Effect of diabetes on the cholesterol level in zebrafish model. Group-I – control; Group-II – diabetic; Group-III – diabetic + EGCG; Group-IV – control + EGCG. Data are expressed as mean \pm SD (n=6). Different superscripts denote significant ($p < 0.001$) differences; the same superscripts denote insignificant ($p > 0.05$) results between the columns of the exposure groups.

Groups	Treatment period	
	Day 1	Day 21
Group-I	285.84 \pm 5.6 ^a	287.84 \pm 6.9 ^a
Group-II	301.67 \pm 6.0 ^b	354.84 \pm 5.4 ^b
Group-III	300.17 \pm 5.0 ^b	290.67 \pm 6.7 ^c
Group-IV	286.34 \pm 6.4 ^a	286.34 \pm 6.5 ^a

Table 4.2: Effect of diabetes on the triglyceride level in zebrafish model. Group-I – control; Group-II – diabetic; Group-III – diabetic + EGCG; Group-IV – control + EGCG. Data are expressed as mean \pm SD (n=6). Different superscripts denote significant ($p < 0.001$) differences; the same superscripts denote insignificant ($p > 0.05$) results between the columns of the exposure groups.

Groups	Treatment period	
	Day 1	Day 21
Group-I	248.67 \pm 7.0 ^a	254.34 \pm 7.4 ^a
Group-II	313.34 \pm 6.5 ^b	336.50 \pm 6.7 ^b
Group-III	311.34 \pm 6.8 ^b	270.84 \pm 6.8 ^c
Group-IV	249.67 \pm 6.7 ^a	253.50 \pm 5.0 ^a

Table 4.3: Effect of diabetes on the very low-density lipoprotein in zebrafish model. Group-I – control; Group-II – diabetic; Group-III – diabetic + EGCG; Group-IV – control + EGCG. Data are expressed as mean \pm SD (n=6). Different superscripts denote significant ($p < 0.001$) differences; the same superscripts denote insignificant ($p > 0.05$) results between the columns of the exposure groups.

Groups	Treatment period	
	Day 1	Day 21
Group-I	50.84 \pm 6.0 ^a	53.5 \pm 5.5 ^a
Group-II	62.33 \pm 6.9 ^b	76.83 \pm 5.3 ^b
Group-III	63.16 \pm 6.0 ^b	55.34 \pm 6.1 ^c
Group-IV	49.17 \pm 5.9 ^a	53.84 \pm 7.1 ^a

Table 4.4: Effect of diabetes on the low-density lipoprotein in zebrafish model. Group-I – control; Group-II – diabetic; Group-III – diabetic + EGCG; Group-IV – control + EGCG. Data are expressed as mean \pm SD (n=6). Different superscripts denote significant ($p < 0.001$) differences; the same superscripts denote insignificant ($p > 0.05$) results between the columns of the exposure groups.

Groups	Treatment period	
	Day 1	Day 21
Group-I	174.16 \pm 7.7 ^a	179.34 \pm 7.0 ^a
Group-II	192.34 \pm 7.5 ^b	229.84 \pm 6.9 ^b
Group-III	193.83 \pm 7.0 ^b	183.50 \pm 7.0 ^c
Group-IV	173.83 \pm 6.7 ^a	176.67 \pm 6.8 ^a

Table 4.5: Effect of diabetes on the high-density lipoprotein in zebrafish model. Group-I – control; Group-II – diabetic; Group-III – diabetic + EGCG; Group-IV – control + EGCG. Data are expressed as mean \pm SD (n=6). Different superscripts denote significant ($p<0.001$) differences; the same superscripts denote insignificant ($p>0.05$) results between the columns of the exposure groups.

Groups	Treatment period	
	Day 1	Day 21
Group-I	70.16 \pm 6.2 ^a	74.16 \pm 6.5 ^a
Group-II	58.33 \pm 6.8 ^b	43.50 \pm 6.3 ^b
Group-III	59.34 \pm 6.9 ^b	68.17 \pm 5.5 ^c
Group-IV	71.5 \pm 6.6 ^a	72.50 \pm 7.6 ^a

Table 4.6: Effect of diabetes on the hepatic ALT activity and its treatment with EGCG in zebrafish model. Group-I – control; Group-II – diabetic; Group-III – diabetic + EGCG; Group-IV – control + EGCG. Data are expressed as mean \pm SD (n=6). Different superscripts denote significant ($p<0.001$) differences; the same superscripts denote insignificant ($p>0.05$) results between the columns of the exposure groups.

Groups	Treatment period			
	Day 1	Day 7	Day 14	Day 21
Group-I	93.67 \pm 2.16 ^a	107.67 \pm 3.32 ^a	101.17 \pm 2.78 ^a	105.17 \pm 2.48 ^a
Group-II	125.34 \pm 2.16 ^b	126.83 \pm 2.63 ^b	128.85 \pm 2.31 ^b	130.67 \pm 3.65 ^b
Group-III	122.50 \pm 2.73 ^b	118.84 \pm 2.48 ^c	119.67 \pm 2.73 ^c	110.68 \pm 2.16 ^c
Group-IV	95.17 \pm 2.78 ^a	98.84 \pm 3.43 ^a	98.84 \pm 3.06 ^a	102.33 \pm 2.59 ^a

Table 4.7: Effect of diabetes on the gills ALT activity and its treatment with EGCG in zebrafish model. Group-I – control; Group-II – diabetic; Group-III – diabetic + EGCG; Group-IV – control + EGCG. Data are expressed as mean \pm SD (n=6). Different superscripts denote significant ($p < 0.001$) differences; the same superscripts denote insignificant ($p > 0.05$) results between the columns of the exposure groups.

Groups	Treatment period			
	Day 1	Day 7	Day 14	Day 21
Group-I	93.67 \pm 2.16 ^a	107.67 \pm 3.32 ^a	101.17 \pm 2.78 ^a	105.17 \pm 2.48 ^a
Group-II	125.34 \pm 2.16 ^b	126.83 \pm 2.63 ^b	128.85 \pm 2.31 ^b	130.67 \pm 3.65 ^b
Group-III	122.50 \pm 2.73 ^b	118.84 \pm 2.48 ^c	119.67 \pm 2.73 ^c	110.68 \pm 2.16 ^c
Group-IV	95.17 \pm 2.78 ^a	98.84 \pm 3.43 ^a	98.84 \pm 3.06 ^a	102.33 \pm 2.59 ^a

Table 4.8: Effect of diabetes on the renal ALT activity and its treatment with EGCG in zebrafish model. Group-I – control; Group-II – diabetic; Group-III – diabetic + EGCG; Group-IV – control + EGCG. Data are expressed as mean \pm SD (n=6). Different superscripts denote significant ($p < 0.001$) differences; the same superscripts denote insignificant ($p > 0.05$) results between the columns of the exposure groups.

Groups	Treatment period			
	Day 1	Day 7	Day 14	Day 21
Group-I	60.83 \pm 3.18 ^a	67.50 \pm 3.27 ^a	67.17 \pm 2.78 ^a	72.17 \pm 2.78 ^a
Group-II	88.34 \pm 2.58 ^b	90.17 \pm 2.71 ^b	92.17 \pm 2.78 ^b	105.34 \pm 2.16 ^b
Group-III	87.67 \pm 3.01 ^b	83.16 \pm 3.95 ^c	80.84 \pm 2.13 ^c	77.34 \pm 2.16 ^c
Group-IV	64.67 \pm 2.80 ^a	65.67 \pm 2.80 ^a	70.84 \pm 2.48 ^a	68.66 \pm 2.73 ^a

Table 4.9: Effect of diabetes on the hepatic AST activity and its treatment with EGCG in zebrafish model. Group-I – control; Group-II – diabetic; Group-III – diabetic + EGCG; Group-IV – control + EGCG. Data are expressed as mean \pm SD (n=6). Different superscripts denote significant ($p<0.001$) differences; the same superscripts denote insignificant ($p>0.05$) results between the columns of the exposure groups.

Groups	Treatment period			
	Day 1	Day 7	Day 14	Day 21
Group-I	20.50 \pm 1.87 ^a	21.84 \pm 2.63 ^a	23.17 \pm 2.31 ^a	24.67 \pm 2.73 ^a
Group-II	30.67 \pm 2.16 ^b	31.84 \pm 3.86 ^b	38.84 \pm 3.55 ^b	40.67 \pm 3.51 ^b
Group-III	33.17 \pm 2.78 ^b	34.35 \pm 3.38 ^b	29.84 \pm 2.48 ^c	28.83 \pm 2.63 ^c
Group-IV	17.67 \pm 2.58 ^a	23.67 \pm 2.33 ^a	24.67 \pm 2.33 ^a	21.67 \pm 3.20 ^a

Table 4.10: Effect of diabetes on the gills AST activity and its treatment with EGCG in zebrafish model. Group-I – control; Group-II – diabetic; Group-III – diabetic + EGCG; Group-IV – control + EGCG. Data are expressed as mean \pm SD (n=6). Different superscripts denote significant ($p<0.001$) differences; the same superscripts denote insignificant ($p>0.05$) results between the columns of the exposure groups.

Groups	Treatment period			
	Day 1	Day 7	Day 14	Day 21
Group-I	22.50 \pm 2.73 ^a	20.34 \pm 2.58 ^a	22.35 \pm 2.50 ^a	21.84 \pm 2.48 ^a
Group-II	32.00 \pm 2.60 ^b	31.34 \pm 2.58 ^b	46.16 \pm 3.32 ^b	45.34 \pm 2.50 ^b
Group-III	35.16 \pm 3.31 ^b	32.34 \pm 2.58 ^c	33.84 \pm 3.06 ^c	28.17 \pm 2.92 ^c
Group-IV	24.67 \pm 2.94 ^a	17.16 \pm 2.40 ^a	21.84 \pm 2.48 ^a	19.83 \pm 2.31 ^a

Table 4.11: Effect of diabetes on the renal AST level and its treatment with EGCG in zebrafish model. Group-I – control; Group-II – diabetic; Group-III – diabetic + EGCG; Group-IV – control + EGCG. Data are expressed as mean \pm SD (n=6). Different superscripts denote significant ($p < 0.001$) differences; the same superscripts denote insignificant ($p > 0.05$) results between the columns of the exposure groups.

Groups	Treatment period			
	Day 1	Day 7	Day 14	Day 21
Group-I	19.67 \pm 2.16 ^a	18.67 \pm 2.16 ^a	24.16 \pm 2.96 ^a	22.16 \pm 2.31 ^a
Group-II	34.35 \pm 2.58 ^b	32.17 \pm 2.31 ^b	38.16 \pm 2.16 ^b	45.17 \pm 3.43 ^b
Group-III	32.67 \pm 2.58 ^b	35.50 \pm 2.42 ^c	30.67 \pm 2.16 ^c	28.17 \pm 2.78 ^c
Group-IV	24.17 \pm 2.78 ^a	20.34 \pm 2.73 ^a	21.67 \pm 2.80 ^a	19.84 \pm 3.06 ^a

Table 4.12: Effect of diabetes on the hepatic ALP level and its treatment with EGCG in zebrafish model. Group-I – control; Group-II – diabetic; Group-III – diabetic + EGCG; Group-IV – control + EGCG. Data are expressed as mean \pm SD (n=6). Different superscripts denote significant ($p < 0.001$) differences; the same superscripts denote insignificant ($p > 0.05$) results between the columns of the exposure groups.

Groups	Treatment period			
	Day 1	Day 7	Day 14	Day 21
Group-I	19.03 \pm 1.89 ^a	18.16 \pm 3.06 ^a	17.85 \pm 2.31 ^a	20.83 \pm 2.23 ^a
Group-II	43.17 \pm 2.82 ^b	50.16 \pm 3.92 ^b	56.16 \pm 3.18 ^b	52.34 \pm 3.26 ^b
Group-III	44.16 \pm 2.48 ^b	33.34 \pm 2.16 ^c	30.67 \pm 2.58 ^c	27.16 \pm 2.78 ^c
Group-IV	17.83 \pm 2.63 ^a	20.83 \pm 2.31 ^a	19.00 \pm 2.60 ^a	18.34 \pm 3.78 ^a

Table 4.13: Effect of diabetes on the renal ALP level and its treatment with EGCG in zebrafish model. Group-I – control; Group-II – diabetic; Group-III – diabetic + EGCG; Group-IV – control + EGCG. Data are expressed as mean \pm SD (n=6). Different superscripts denote significant ($p < 0.001$) differences; the same superscripts denote insignificant ($p > 0.05$) results between the columns of the exposure groups.

Groups	Treatment period			
	Day 1	Day 7	Day 14	Day 21
Group-I	11.84 \pm 2.85 ^a	10.34 \pm 2.16 ^a	13.17 \pm 2.78 ^a	12.34 \pm 2.73 ^a
Group-II	18.17 \pm 3.48 ^b	16.84 \pm 3.18 ^b	21.17 \pm 3.65 ^b	25.50 \pm 3.83 ^b
Group-III	17.67 \pm 2.58 ^b	20.17 \pm 2.31 ^c	15.34 \pm 2.58 ^a	16.67 \pm 2.80 ^a
Group-IV	10.67 \pm 2.16 ^a	7.67 \pm 2.17 ^a	11.17 \pm 2.70 ^a	12.16 \pm 2.31 ^a

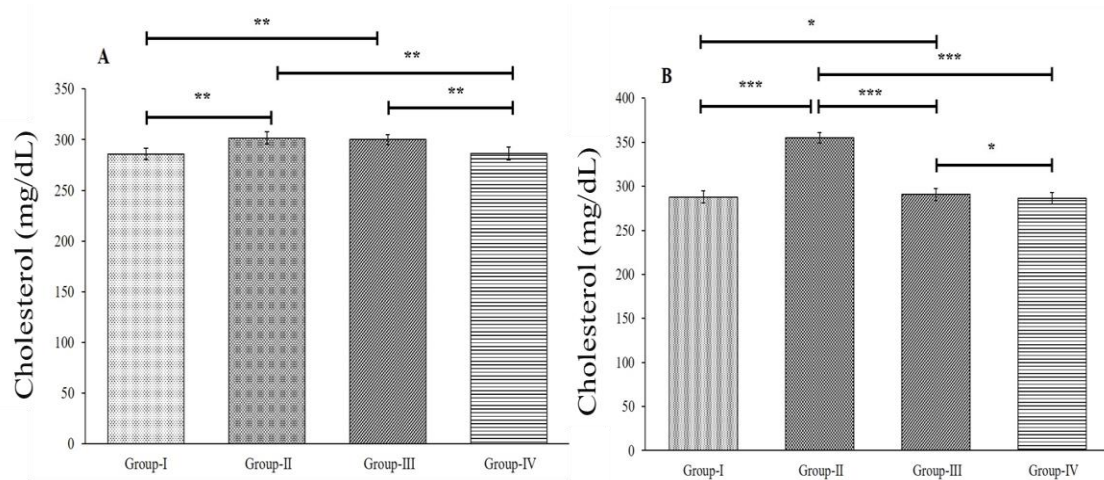


Figure 4.3: Effect of diabetes on the cholesterol level in zebrafish model. Group-I – control; Group-II – diabetic; Group-III – diabetic + EGCG; Group-IV – control + EGCG. (A) Day 1 (B) Day 21. Data are represented as mean \pm SD (n=6) and analysed by one-way ANOVA followed by Tukey's post-hoc test. Asterisk represents a significant difference, *p<0.05, **p<0.01, ***p<0.001.

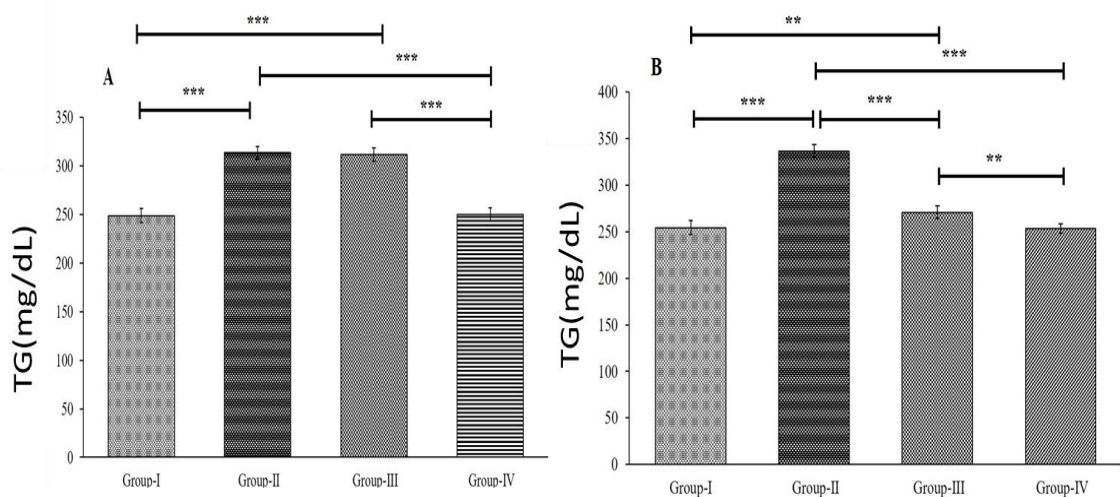


Figure 4.4: Effect of diabetes on the triglyceride level in zebrafish model. Group-I – control; Group-II – diabetic; Group-III – diabetic + EGCG; Group-IV – control + EGCG. (A) Day 1 (B) Day 21. Data are represented as mean \pm SD (n=6) and analysed by one-way ANOVA followed by Tukey's post-hoc test. Asterisk represents a significant difference, *p<0.05, **p<0.01, ***p<0.001.

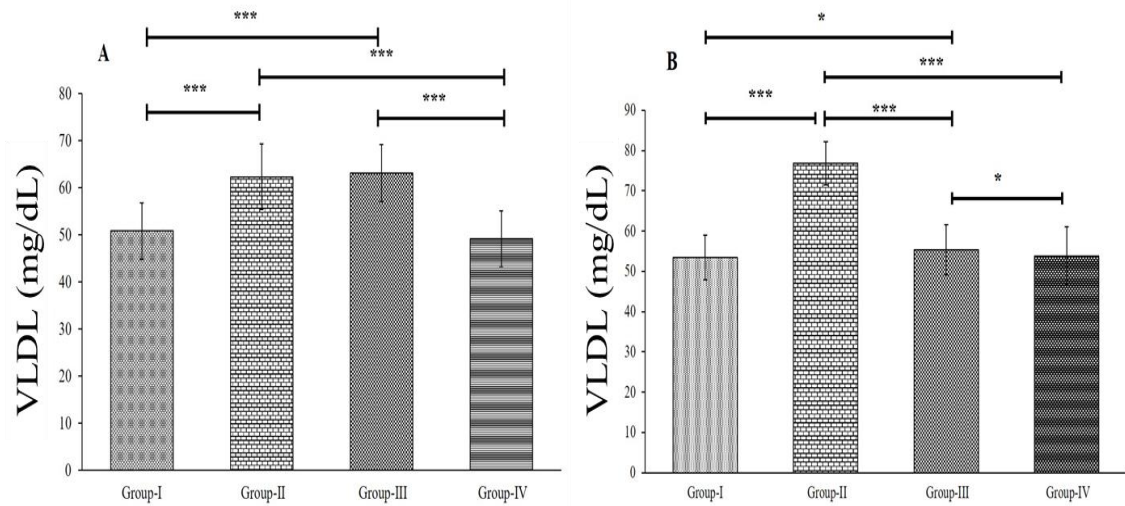


Figure 4.5: Effect of diabetes on the very low-density lipoprote in zebrafish model. Group-I – control; Group-II – diabetic; Group-III – diabetic + EGCG; Group-IV – control + EGCG. (A) Day 1 (B) Day 21. Data are represented as mean \pm SD (n=6) and analysed by one-way ANOVA followed by Tukey's post-hoc test. Asterisk represents a significant difference, *p<0.05, **p<0.01, ***p<0.001.

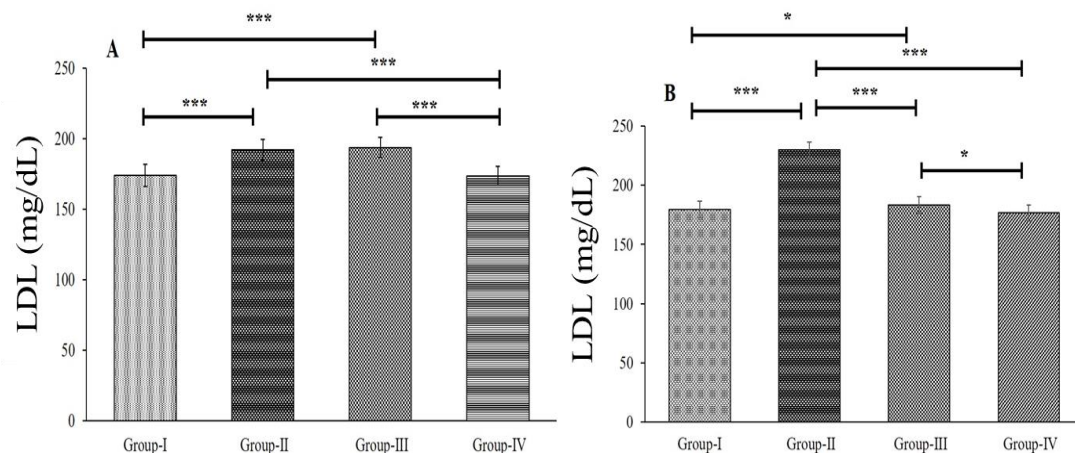


Figure 4.6: Effect of diabetes on the low-density lipoprotein in zebrafish model. Group-I – control; Group-II – diabetic; Group-III – diabetic + EGCG; Group-IV – control + EGCG. (A) Day 1 (B) Day 21. Data are represented as mean \pm SD (n=6) and analysed by one-way ANOVA followed by Tukey's post-hoc test. Asterisk represents a significant difference, *p<0.05, **p<0.01, ***p<0.001.

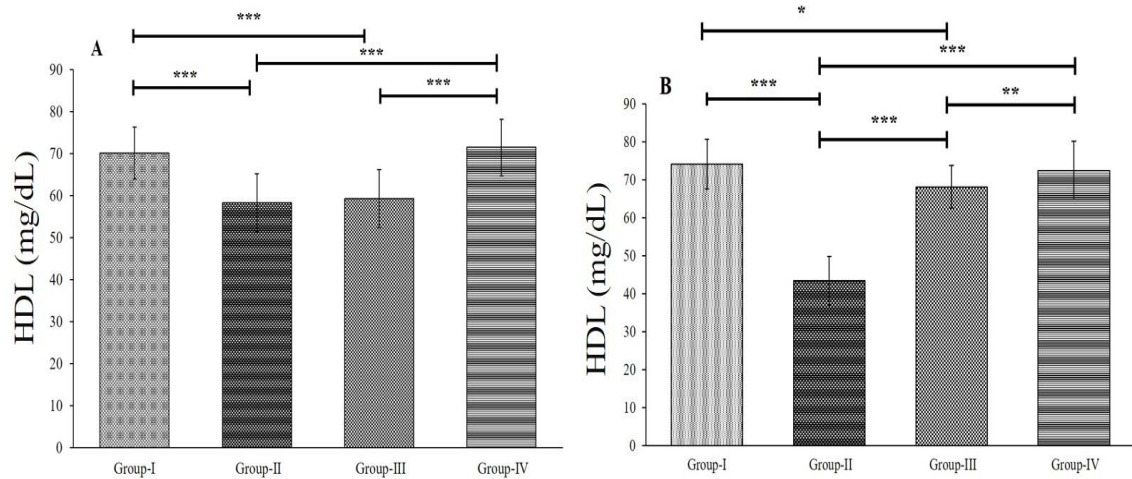


Figure 4.7: Effect of diabetes on the high-density lipoprotein in zebrafish model. Group-I – control; Group-II – diabetic; Group-III – diabetic + EGCG; Group-IV – control + EGCG. (A) Day 1 (B) Day 21. Data are represented as mean \pm SD (n=6) and analysed by one-way ANOVA followed by Tukey's post-hoc test. Asterisk represents a significant difference, *p<0.05, **p<0.01, ***p<0.001.

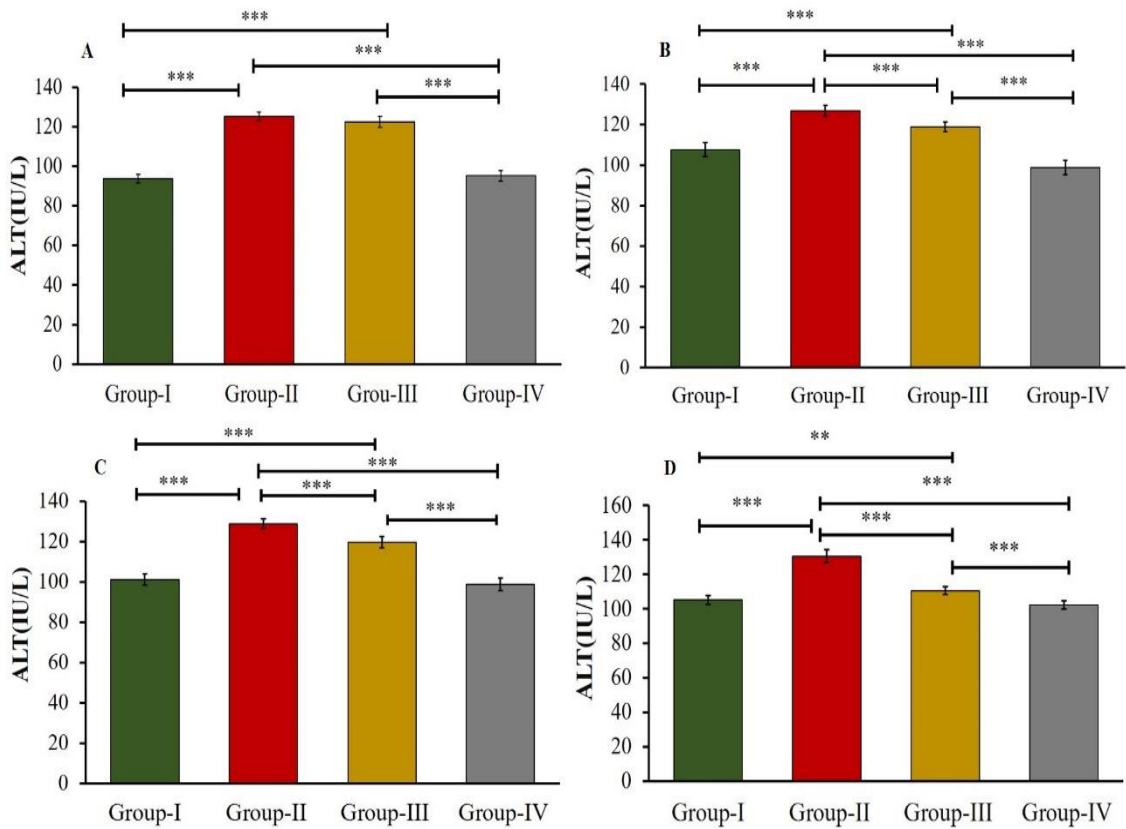


Figure 4.8: Effect of diabetes on the hepatic ALT activity and its treatment with EGCG in zebrafish model. Group-I - control; Group-II - diabetic; Group-III - diabetic + EGCG; Group-IV - control + EGCG. (A) Day 1 (B) Day 7 (C) Day 14 (D) Day 21. Data are represented as mean \pm SD (n=6) and analysed by one-way ANOVA followed by Tukey's post-hoc test. Asterisk represents a significant difference, * $p < 0.05$, ** $p < 0.01$, *** $p < 0.001$.

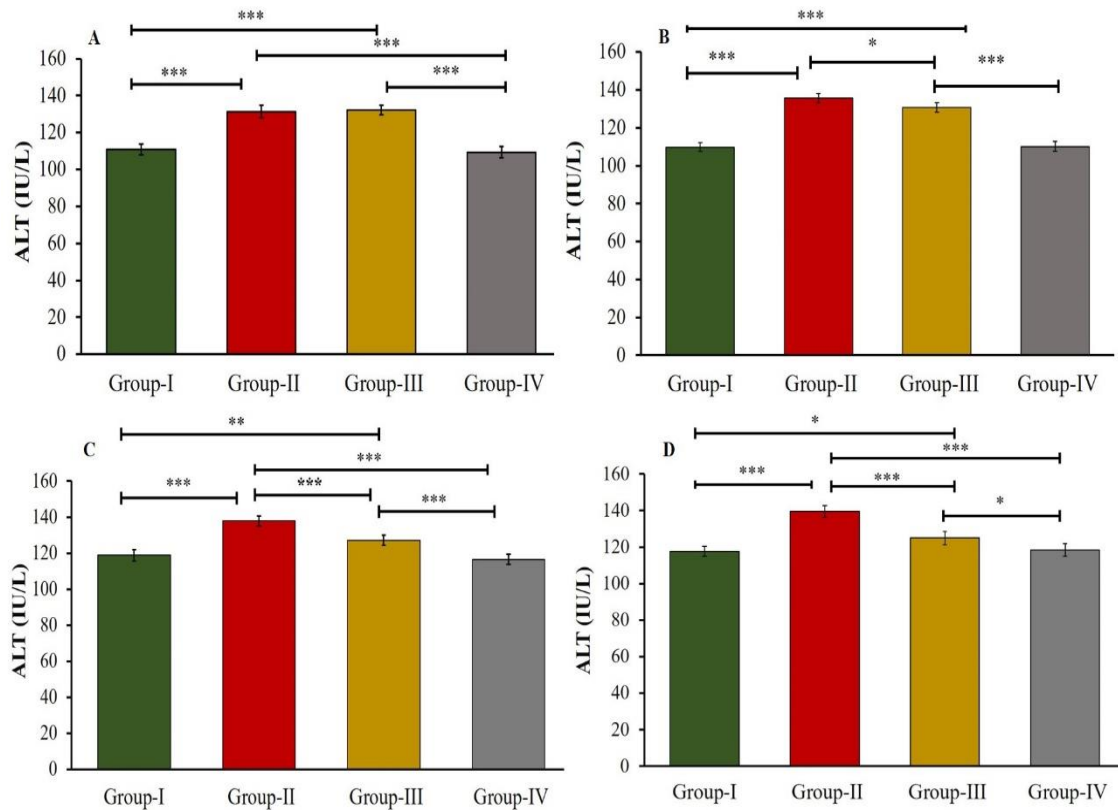


Figure 4.9: Effect of diabetes on the gills ALT activity and its treatment with EGCG in zebrafish model. Group-I - control; Group-II - diabetic; Group-III - diabetic + EGCG; Group-IV - control + EGCG. (A) Day 1 (B) Day 7 (C) Day 14 (D) Day 21. Data are represented as mean \pm SD (n=6) and analysed by one-way ANOVA followed by Tukey's post-hoc test. Asterisk represents a significant difference, *p<0.05, **p<0.01, ***p<0.001.

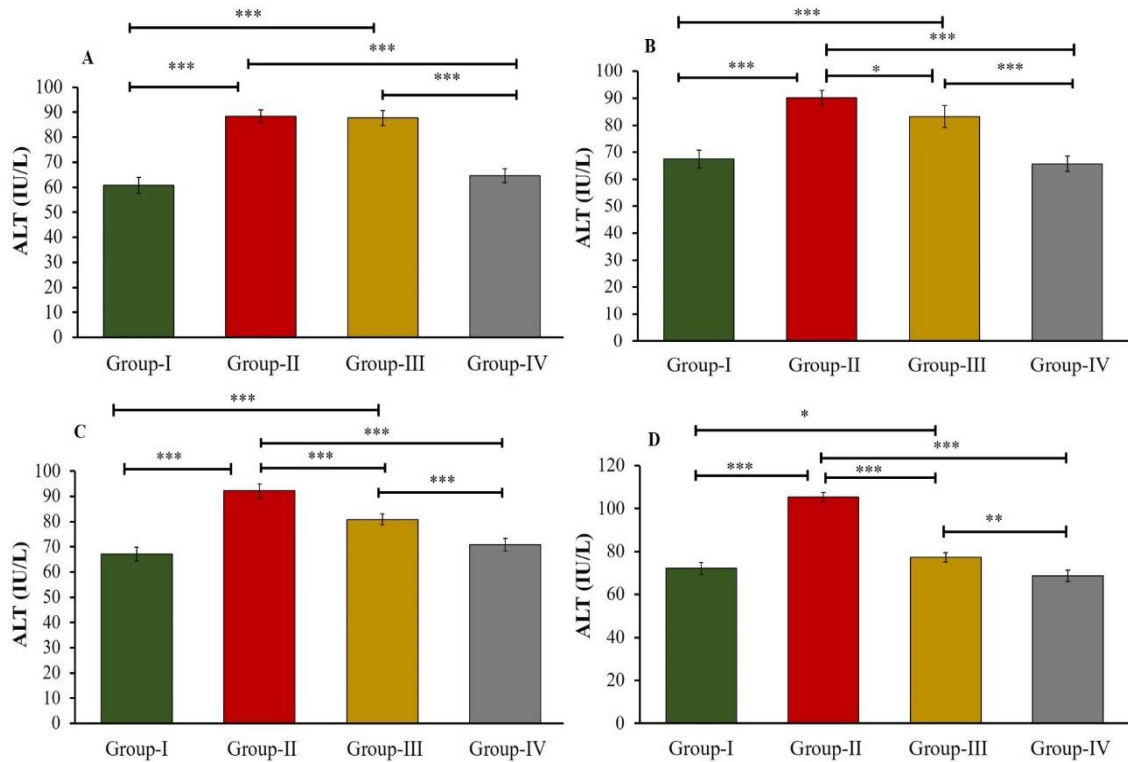


Figure 4.10: Effect of diabetes on the renal ALT activity and its treatment with EGCG in zebrafish model. Group-I - control; Group-II - diabetic; Group-III - diabetic + EGCG; Group-IV - control + EGCG. (A) Day 1 (B) Day 7 (C) Day 14 (D) Day 21. Data are represented as mean \pm SD (n=6) and analysed by one-way ANOVA followed by Tukey's post-hoc test. Asterisk represents a significant difference, * $p < 0.05$, ** $p < 0.01$, *** $p < 0.001$.

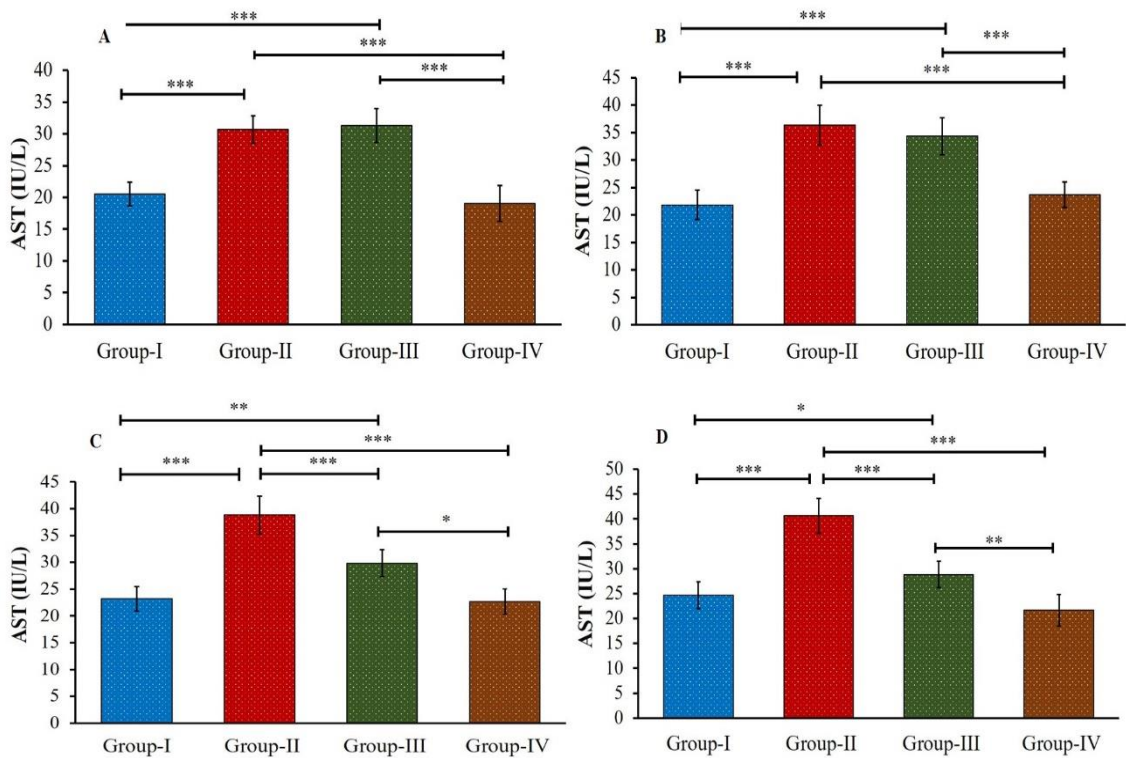


Figure 4.11: Effect of diabetes on the hepatic AST activity and its treatment with EGCG in zebrafish model. Group-I - control; Group-II - diabetic; Group-III - diabetic + EGCG; Group-IV - control + EGCG. (A) Day 1 (B) Day 7 (C) Day 14 (D) Day 21. Data are represented as mean \pm SD (n=6) and analysed by one-way ANOVA followed by Tukey's post-hoc test. Asterisk represents a significant difference, * $p < 0.05$, ** $p < 0.01$, *** $p < 0.001$.

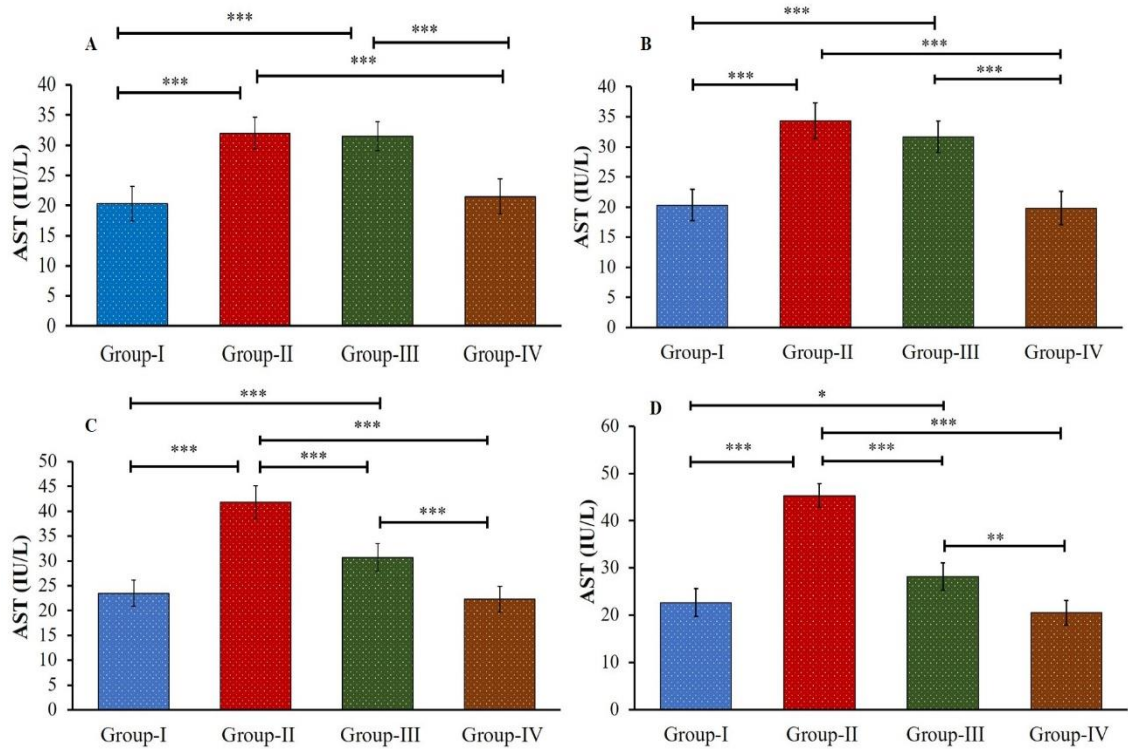


Figure 4.12: Effect of diabetes on the gills AST activity and its treatment with EGCG in zebrafish model. Group-I - control; Group-II - diabetic; Group-III - diabetic + EGCG; Group-IV - control + EGCG. (A) Day 1 (B) Day 7 (C) Day 14 (D) Day 21. Data are represented as mean \pm SD (n=6) and analysed by one-way ANOVA followed by Tukey's post-hoc test. Asterisk represents a significant difference, * $p < 0.05$, ** $p < 0.01$, *** $p < 0.001$.

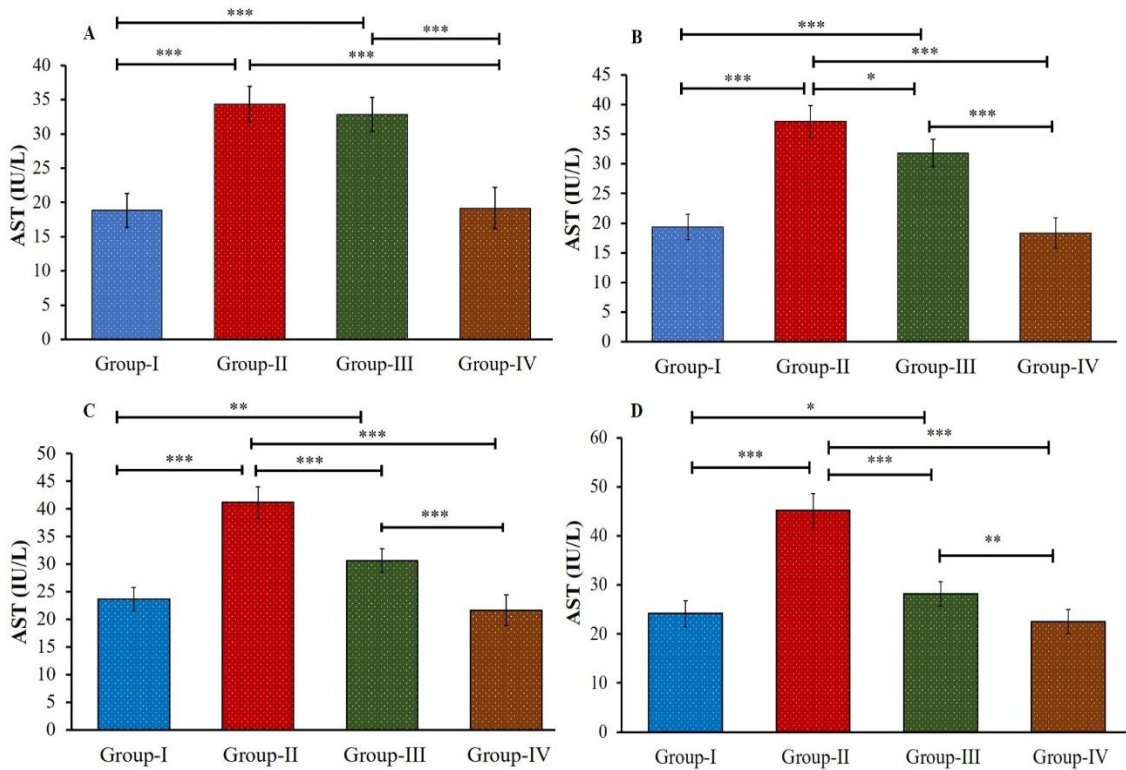


Figure 4.13: Effect of diabetes on the renal AST level and its treatment with EGCG in zebrafish model. Group-I - control; Group-II - diabetic; Group-III - diabetic + EGCG; Group-IV - control + EGCG. (A) Day 1 (B) Day 7 (C) Day 14 (D) Day 21. Data are represented as mean \pm SD (n=6) and analysed by one-way ANOVA followed by Tukey's post-hoc test. Asterisk represents a significant difference, * $p < 0.05$, ** $p < 0.01$, *** $p < 0.001$.

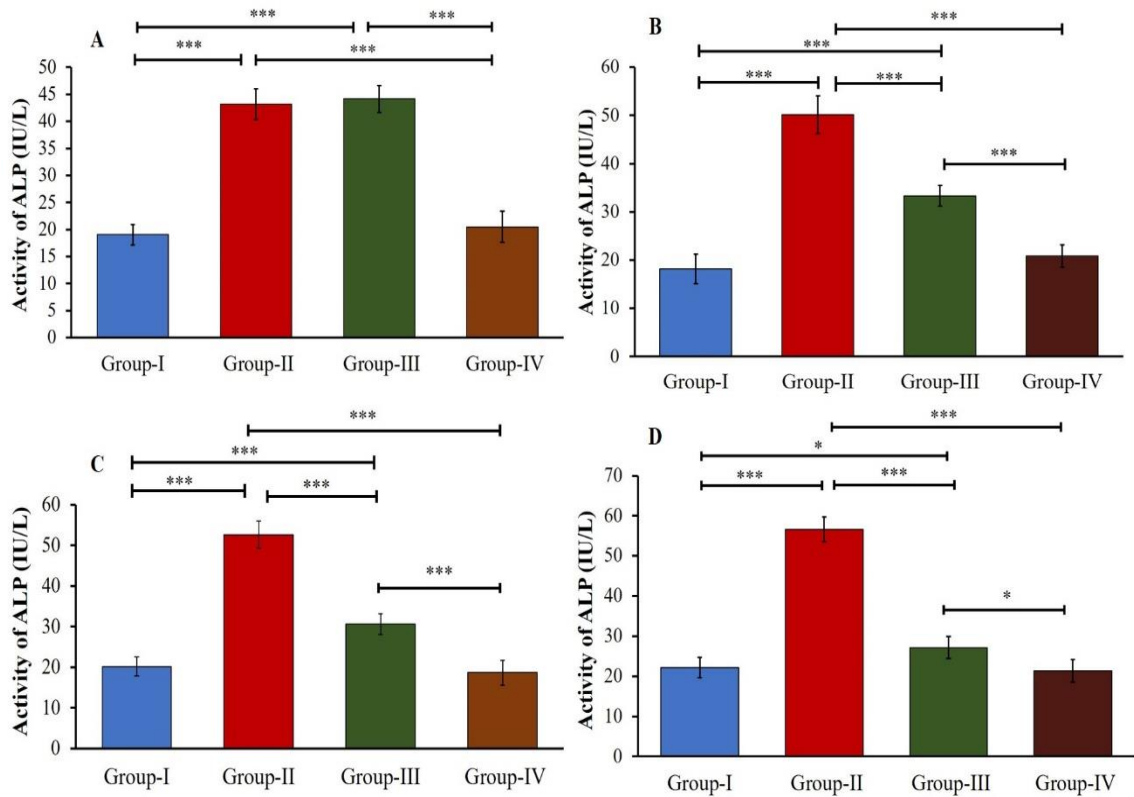


Figure 4.14: Effect of diabetes on the hepatic ALP level and its treatment with EGCG in zebrafish model. Group-I - control; Group-II - diabetic; Group-III - diabetic + EGCG; Group-IV - control + EGCG. (A) Day 1 (B) Day 7 (C) Day 14 (D) Day 21. Data are represented as mean \pm SD (n=6) and analysed by one-way ANOVA followed by Tukey's post-hoc test. Asterisk represents a significant difference, *p<0.05, **p<0.01, ***p<0.001.

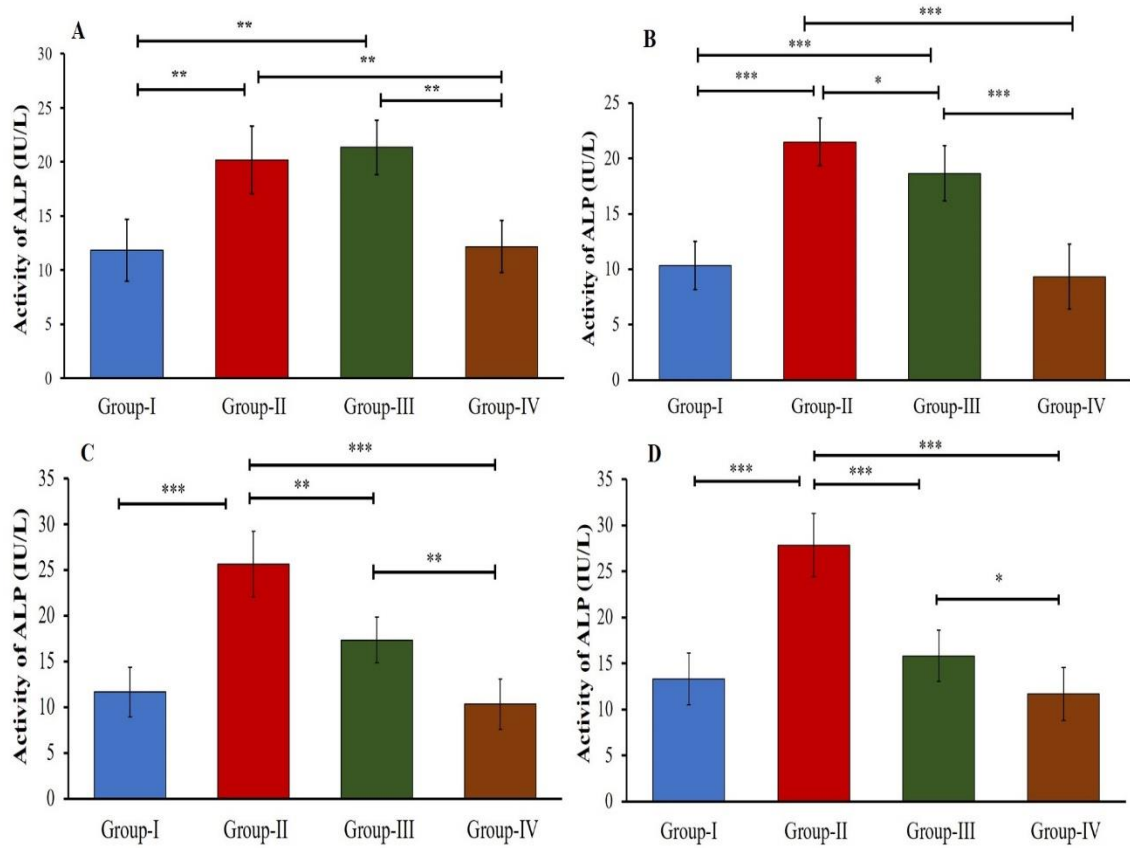


Figure 4.15: Effect of diabetes on the renal ALP level and its treatment with EGCG in zebrafish model. Group-I - control; Group-II - diabetic; Group-III - diabetic + EGCG; Group-IV - control + EGCG. (A) Day 1 (B) Day 7 (C) Day 14 (D) Day 21. Data are represented as mean \pm SD (n=6) and analysed by one-way ANOVA followed by Tukey's post-hoc test. Asterisk represents a significant difference, * $p < 0.05$, ** $p < 0.01$, *** $p < 0.001$.

4.4 Discussion

Diabetes mellitus is a multifaceted medical condition characterized by the gradual deterioration of metabolic function and the dysregulation of blood sugar levels, often resulting in structural changes across various organs (Song *et al.*, 2022). STZ administration is a common approach in establishing diabetic animal models, particularly due to its selective targeting of pancreatic β -cells, thus disrupting cellular metabolic and oxidative processes (Amirkhosravi *et al.*, 2023). The utilization of zebrafish as a diabetic model holds promise due to its rapid detection of diabetic symptoms within a 24-hour timeframe, presenting a suitable platform for research (Mathur *et al.*, 2011). Longkumer *et al.* (2020) successfully induced DM in adult zebrafish through intraperitoneal administration of STZ, leading to a significant increase in glucose levels within a 24-hour period, mimicking the effects observed in humans.

The selection of zebrafish as an experimental model is further justified by its physiological similarities to humans, particularly in terms of pancreatic structure, lipid metabolism, glucose regulation, and adipose tissue biology. Plant-based supplements, such as Epigallocatechin gallate (EGCG), are often favoured for their potentially fewer side effects compared to synthetic drugs. EGCG, known for its water-soluble antioxidant properties, has been proposed to inhibit oxidative stress and mitigate immunotoxicity induced by toxins (Zhang *et al.*, 2013). Alterations in lipoproteins and lipid concentrations, frequently observed in individuals with diabetes, involve the participation of enzymes such as alanine aminotransferase (ALT) and aspartate aminotransferase (AST), present ubiquitously in tissues like the liver, kidney, heart, and fish gills, serving as reliable indicators of overall organ health. These enzymes play vital roles in amino acid

synthesis and deamination processes, crucial during periods of heightened energy demand (Samim & Vaseem, 2023).

During the 21-days of experiment, diabetic zebrafish showed poor glycemic control, with higher TC, TG, VLDL, and LDL levels and lower HDL levels than the control group. Risk factors associated with diabetes, such as hypertension and dyslipidemia, play an essential role in the development of cardiovascular disease. Studies on the diabetic rat model have shown similar dyslipidemia trends, indicating that insulin shortage and oxidative stress are responsible for impaired lipid metabolism (Rao *et al.*, 2021). One of the most noticeable aspects of diabetes dyslipidemia is an increase in LDL particles from either LDL-P or apolipoprotein-B (ApoB) (Neels *et al.*, 2023). There is also an increased risk of nephropathy because LDL particles are more atherogenic (Vekic *et al.*, 2022). Insulin resistance is the primary cause of dyslipidemia in diabetics.

The release of free fatty acids from adipose tissue escalates in cases of peripheral insulin resistance, subsequently intercepted by the liver, culminating in heightened triglyceride (TG) production by hepatic cells (Alves-Bezerra & Cohen, 2017). High quantities of triglycerides and LDL cholesterol contribute to the development of atherosclerosis by oxidizing or glycation these lipid particles, resulting in artery blockage and narrowing (Lee *et al.*, 2021). The hepatic stimulation generated by triglyceride production increases ApoB release and the synthesis of triglyceride-rich VLDL. The VLDL's high triglyceride content enriches HDL and LDL, increasing their cholesterol levels through the action of cholesterol ester transfer protein (Ben-Aicha *et al.*, 2020).

Triglyceride-rich LDL molecules contribute to the development of tiny dense LDL, which is then digested by lipoprotein lipase or hepatic lipase (Zhang *et al.*, 2022).

LDL particles have been shown to buildup in the endothelium of blood arteries in DM, producing thickening and restriction of blood flow (Khatana *et al.*, 2020). According to studies, LDL cholesterol plays an important role in the development of atherosclerosis because of its small size, which allows it to pass through the endothelium barrier (Jin *et al.*, 2022). The underlying pathophysiology of dyslipidemia raises the likelihood of CVD. Indeed, the lipid abnormalities reported in the diabetic group of the present study support the preceding findings.

EGCG has been shown to improve dyslipidemia by considerably lowering triglycerides and LDL cholesterol levels (Wen *et al.*, 2023). Similarly, the improved lipid profile of the treated groups supports the previously documented capability of EGCG to improve lipid metabolism in DM. These findings imply that using EGCG may be helpful in preventing cardiovascular problems caused by lipid metabolism disruptions that are common in DM.

The results also demonstrated a notable elevation in the activity of ALT and AST in the hepatic tissue of diabetic zebrafish. This outcome can be attributed to the impairment of biochemical processes within the Krebs cycle, leading to tissue damage and subsequent leakage of enzymes into the circulatory system (Bhattacharjee *et al.*, 2020). The findings align with the results reported in a study conducted by Amirkhosravi *et al.* (2023) wherein elevated levels of serum ALT and AST were observed in diabetic rats. A correlation between pesticide exposure and increased activity of ALT and AST has also been reported in fishes by Bojarski & Witeska, (2020). Increased levels of ALT and AST, commonly used markers for liver function, have been identified as contributing factors in the progression of DM (Yazdi *et al.*, 2019; Jarhahzadeh *et al.*, 2021). Further, elevated

levels of ALT and AST activity in the gill and kidney tissues were observed in the diabetic zebrafish. These observations indicate mitochondrial dysfunction caused by reactive oxygen species and increased permeability of harmful substances in cell membranes (Ugbomeh *et al.*, 2019; Wang *et al.*, 2022). The current observations hint at active transamination, a pivotal process in energy metabolism (Jestadi *et al.*, 2014).

Furthermore, the diabetic cohort exhibited heightened ALP activity in hepatic and renal tissues, recognized as a marker for genotoxic and cytotoxic effects. This aligns with the previous result by Jestadi *et al.* (2014), Hosseini *et al.* (2017), and Nazir *et al.* (2020), where the ALP activities in the diabetic animal increased drastically throughout their study. The administration of EGCG resulted in a significant restoration of enzyme activities in test subjects, suggesting a potential protective effect against organ damage. The hepatoprotective properties of EGCG have been evident against various toxins (Parasuraman *et al.*, 2021). In diabetic rats, EGCG showed promising results in reducing the renal inflammation caused by the disease (Yang *et al.*, 2022). The results of the present study confirm the feasibility of the lipid profiles and enzyme shifts as early diabetes indicators in zebrafish models. Furthermore, EGCG emerges as a potential contender for alleviating diabetic complications. This study contributes significantly to the growing diabetes pathophysiology knowledge and presents a promising direction for developing innovative therapeutic approaches.

Chapter 5

Evaluation of therapeutic efficacy of EGCG on oxidative stress and histopathological changes in zebrafish model

Contents

5.1 Introduction

5.2 Materials and methods

5.3 Results

5.4 Discussion

5.1. Introduction

DM presents a substantial global health challenge characterized by hyperglycemia arising from disruptions in insulin secretion, insulin action, or both. DM poses significant risks, contributing to a spectrum of severe health complications that impair quality of life and escalate mortality rates (Jwad & AL-Fatlawi, 2022). Patients with DM exhibit increased generation of free radicals and decreased antioxidant status, leading to oxidative damage to cellular components such as lipids, nucleic acids, and proteins (Black, 2022). Chronic DM instigates a cascade of pathological processes that culminate in organ dysfunction and failure, impacting vital organs such as the kidney and liver.

STZ stands as a widely utilized diabetogenic agent, instrumental in triggering DM *via* the destruction of pancreatic β -cells, mirroring the pathology seen in human subjects (Yang *et al.*, 2023). Its mechanism involves the alkylation of DNA upon entering pancreatic β -cells through the glucose transporter GLUT2, leading to cellular damage. STZ-induced diabetic animal models closely mimic human symptoms, exhibiting polyuria, polydipsia, and weight loss (Rashmi *et al.*, 2023). The pathophysiology of DM underscores the role of oxidative stress, characterized by an imbalance between ROS production and antioxidant defence mechanisms (Khalid *et al.*, 2022). Enhanced ROS levels and compromised antioxidant defence contribute to cellular damage, fostering diabetic complications. Oxidative stress, coupled with non-enzymatic glycosylation, exacerbates the severity of chronic hyperglycemia complications (Cavati *et al.*, 2023).

The therapeutic effects of EGCG extend to diabetic nephropathy prevention by modulating key pathways involved in oxidative stress and inflammation. Studies have elucidated its protective effects against STZ-induced diabetic nephropathy in mice,

Chapter-5 *Evaluation of therapeutic efficacy of EGCG on oxidative stress and histopathological changes in zebrafish model*

showcasing its potential to ameliorate renal damage (Soussi *et al.*, 2020; Kanlaya & Thongboonkerd, 2019). Furthermore, EGCG exhibits hepatoprotective properties, shielding liver cells from inflammatory insults and oxidative damage (Yoon *et al.*, 2014). EGCG holds promise as a potent therapeutic agent in managing DM and its associated complications. Its multifaceted benefits encompass glycemic control, organ protection, and oxidative stress mitigation. Understanding the mechanistic underpinnings of the actions of EGCG is imperative for harnessing its full therapeutic potential in combating the global burden of DM.

Zebrafish (*Danio rerio*) is a well-established and widely used model organism for studying metabolic diseases. Its versatility spans larval and adult stages, rendering it invaluable for compound screening and toxicological assessments. Notably, zebrafish share analogous metabolic organs with humans, including the kidney and liver, underscoring their relevance in disease modeling (Lei *et al.*, 2023). Studies have leveraged this similarity to successfully recapitulate human pathologies, including DM, within zebrafish models (Geba *et al.*, 2024).

Considering the multifaceted relationship between diabetes, inflammation, and oxidative stress, there exists a pressing need to develop safe and effective treatment therapies capable of improving DM-related complications. Despite the recognized role of oxidative stress in DM pathogenesis, the influence of antioxidants on insulin activity still needs to be explored, leaving a discernible gap in understanding the potential of compounds such as EGCG in DM management. EGCG administration has effectively prevented high-fat diet-induced insulin resistance in murine models (Liu *et al.*, 2022). The present study endeavors to evaluate the impact of EGCG on the enzymatic antioxidant activities of superoxide dismutase (SOD) and catalase (CAT) within the liver,

Chapter-5 *Evaluation of therapeutic efficacy of EGCG on oxidative stress and histopathological changes in zebrafish model*

kidney, and gills of zebrafish. Additionally, it seeks to elucidate the potential of EGCG in ameliorating histopathological alterations in the selected organs of the zebrafish model induced with DM. The outcomes derived from the present study hold substantial promise for advancing therapeutic strategies targeting DM and its associated complications. By unraveling the antioxidative potential of EGCG and its ability to mitigate histological aberrations in zebrafish organs, the present study contributes valuable insights into developing novel therapeutics to alleviate the burden of DM-related morbidities.

5.2. Materials and methods

5.2.1 Chemicals

EGCG (>95%), hematoxylin-eosin stain, xylene, and absolute alcohol were procured from Merck. All other chemicals used were of reagent grade. Solutions were prepared employing deionized water to ensure optimal purity and consistency.

5.2.2 Acclimatization of zebrafish

The zebrafish were carefully housed in a specialized housing system (Model-NT-ZB-11; Make-Narshi Technologies), providing a controlled environment with a constant temperature of $28\pm 2^{\circ}\text{C}$. The system ensured continuous chemical, biological, and mechanical water filtration and aeration, maintaining dissolved oxygen. Polycarbonate fish tanks adhered to a 14-hour light and 10-hour dark photoperiod cycle. Detailed acclimatization procedures are provided in Chapter 2.

5.2.3 Experimental design

Adult zebrafish of both genders, demonstrating robust health, were randomly assigned to four experimental Groups, namely Group-I (control), Group-II (diabetic), Group-III (diabetic + EGCG), and Group-IV (control + EGCG). Experimental Groups III and IV were subjected to treatment with 6 mg/L of EGCG for a duration of 21 days. On the 21st day, the animals were euthanized, and vital organs such as the liver, kidney, and gills were promptly excised and prepared for subsequent antioxidant parameter measurement and histological examinations. The detailed representation of the experimental setup is described in Figure 5.1.

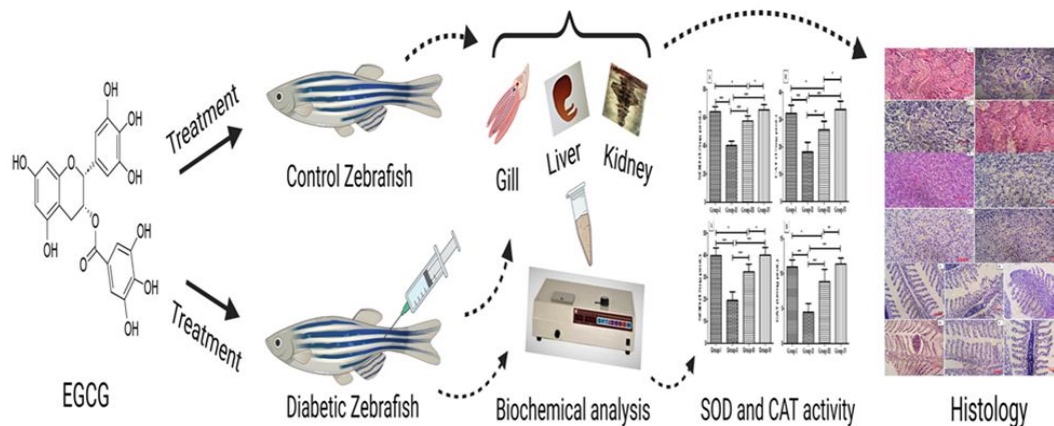


Figure 5.1: Diagrammatic representation of the experimental setup for studying antioxidant activity and histological parameters on the zebrafish model.

5.2.4 Induction of diabetes mellitus

DM was induced in zebrafish specimens *via* intraperitoneal injection of STZ. The diabetic groups received booster doses of STZ over 21 days to ensure the persistence of hyperglycemia, which was in line with established protocols (Longkumer *et al.*, 2020). A detailed induction of DM in the zebrafish model is provided in Chapter 3.

5.2.5 Tissue preparation

Four zebrafish from each group were euthanized on ice on day 21 of the experiment. Subsequently, the kidney, liver, and gill tissues were dissected, minced, and homogenized at a concentration of 2.5% w/v in ice-cold 0.15% KCl-0.1M phosphate buffer (pH 7.4) utilizing a glass homogenizer. Following homogenization, the resultant mixture underwent centrifugation at 2000 rpm for 15 minutes at 4°C, with the resulting supernatant collected for subsequent biochemical parameter analyses.

5.2.6 Biochemical assay

5.2.6.1 Superoxide dismutase (SOD) (EC 1.15.1.1)

SOD activity was measured using the method described by Misra & Fridovich (1972), which is based on the oxidation of epinephrine to adrenochrome by the enzyme. The ensuing reaction was quantified spectrophotometrically at 480 nm.

Reagents

1. EDTA
2. Carbonate Buffer:0.05M, pH 10.2
3. Epinephrine: 3mM

Procedure

A 0.5 ml aliquot of tissue homogenate underwent dilution with 0.5 ml of distilled water, followed by adding 0.25 ml of ethanol and 0.15 ml of chloroform. The resultant mixture was vigorously shaken for 1 minute and subsequently subjected to centrifugation at 2000 rpm.

The enzymatic activity in the supernatant was determined by adding 1.5 ml of buffer to 0.5 ml of the supernatant. Adding 0.4 ml epinephrine initiated the reaction, and the ensuing change in optical density per minute was measured spectrophotometrically. The activity was quantified and expressed as Units/mg/protein.

5.2.6.2 Catalase assay (CAT) (E.C. 1.11.1.6)

CAT activity was determined using the method described by Sinha (1972). This method relies on reducing dichromate in acetic acid to chromic acid in the presence of hydrogen peroxide, with the transient formation of perchromic acid as an intermediate. The ensuing reaction was monitored spectrophotometrically at 610 nm.

Reagents

1. Phosphate buffer: 0.01M, pH 7
2. Dichromate acetic acid reagent: Prepared using 5% potassium dichromate diluted in acetic acid
3. Hydrogen peroxide: 0.2M
4. Diluted acetic acid: Prepared at a ratio of 1:3 v/v in distilled water

Procedure

Each of the four test tubes was added with 1 ml of phosphate buffer, followed by the addition of 0.1 ml of aliquoted tissue homogenate. Subsequently, 1 ml of hydrogen peroxide was introduced into each test tube to initiate the reaction. The reaction was arrested at predetermined intervals (15, 30, 45, and 60 seconds) by adding 2 ml of dichromate acetic acid reagent. The tubes were then boiled for 10 minutes, followed by cooling and subsequent measurement at 610 nm.

Simultaneously, a zero-time control was executed by introducing the dichromate-acetic acid reagent prior to the addition of hydrogen peroxide. Standard hydrogen peroxide solutions spanning a concentration range of 4-20 μM were subjected to identical treatment for calibration purposes. Catalase activity was quantified and expressed as units/mg/protein, providing valuable insights into the antioxidative capacity of the zebrafish tissue samples under investigation.

5.2.7 Histopathology

On day 21, liver, kidney, and gill tissues were meticulously harvested, weighed, and cleansed in physiological saline solution to eliminate extraneous debris or blood residues. Subsequently, the tissues were fixed in 10% buffered formalin for a period of 24 hours to facilitate preservation. Histopathological evaluation of the liver, kidney, and gills was

Chapter-5 *Evaluation of therapeutic efficacy of EGCG on oxidative stress and histopathological changes in zebrafish model*

conducted employing a well-established protocol as described by Abdelhamid et al. (2020). Following fixation, the tissues underwent thorough washing in running tap water overnight to remove residual fixative. Subsequent dehydration was accomplished *via* a graded series of alcohol solutions. The tissues were then sectioned at a 4-5 µm thickness utilizing a semi-automatic rotary microtome (model: RMT-35) to facilitate histological examination. Staining was performed using Harris-hematoxylin for nuclei and eosin as a counterstain. Following dehydration and clearing, the sections were mounted in DPX to ensure optimal visualization. Prepared slides were meticulously observed and documented under a CX1 microscope equipped with a Sony digital camera (model E31SPM20000KPA; USB 2.0). Image analysis was performed utilizing Image J software, as detailed in Chapter 2.

5.2.8 Determination of histological alteration index (HAI) in liver, kidney, and gills

The Histological Alteration Index (HAI), which is based on the severity of the damages, was adopted to quantify the presence of histological abnormalities semi-quantitatively (Flores-Lopes & Thomaz, 2011; Pal *et al.*, 2012). Minor alterations (I) refer to changes that do not affect the normal function of the tissues and can be reversed with improved environmental conditions. Moderate alterations (II) are more severe and can cause significant damage to normal function. Severe alterations (III) result in irreparable damage with little possibility of recovery, even with improved water quality.

The HAI for each specimen was computed using the formula: $HAI = (1 \times SI) + (10 \times SII) + (100 \times SIII)$, where SI, SII, and SIII denote the number of alterations graded as 1, 2, and 3, respectively. The resulting HAI scores were interpreted as follows: scores between 0 and 10 indicating normal organ function, 11-20 suggesting minor damage, 21-50 reflecting substantial alterations, 50-100 representing severe damage, and scores above

Chapter-5 *Evaluation of therapeutic efficacy of EGCG on oxidative stress and histopathological changes in zebrafish model*

100 indicative of irreversible tissue damage.

Table 5.1: Stages of histological alteration in liver, kidney, and gills.

Stage	Histological alterations		
	Liver	Kidney	Gills
I	Nuclear hypertrophy	Dilation of glomerular capillaries	Hypertrophy and hyperplasia of gill epithelium
	Irregularly shaped nucleus	Hypertrophy of the cell nucleus	Lamellar epithelial lifting and edema
	Cellular hypertrophy	Cytoplasmic vacuolation	Lamellar Fusion Club shaping of lamellae
	Cytoplasmic vacuolation	Tubular regeneration	Marginal canal dilation
	Cellular atrophy	Hypertrophy of tubular epithelial cell	Lamellae shortening
II	Nuclear vacuolation	Reduction of Bowman's space	Mucus cell hyperplasia
	Cytoplasmic degeneration	Obstruction of Bowman's space	Chloride cells hyperplasia
	Cellular rupture	Blood congestion in glomeruli capillaries	Leukocyte infiltration
	Blood congestion	Tubular degeneration	Hemorrhage
	Hemorrhage	Decrease of the tubular lumen caliber	----
	Nuclear degeneration	Hemorrhage	----
	Bile stagnation	leukocytes infiltration	----
III	Focal necrosis	Necrosis	Lamellar aneurysm
	---	---	Necrosis and cell degeneration

Adopted from (Flores-Lopes & Thomaz, 2011; Pal *et al.*, 2012).

5.2.9 Statistical analysis

Statistical analysis was performed using GraphPad Prism 5.0 software, and the results were presented as mean \pm SD. One-way analysis of variance (ANOVA) with Tukey's post hoc test was used for comparisons between groups, with * $p < 0.05$, ** $p < 0.01$, and *** $p < 0.001$ considered statistically significant.

5.3 Results

5.3.1 SOD and CAT activity in the liver

The hepatic activities of SOD and CAT were recorded in different experimental groups of zebrafish. In Group-I, Group-II, Group-III, and Group-IV, the antioxidant activity of SOD in the liver was assessed. Group-II exhibited a significant ($p < 0.001$) reduction in SOD activity, measuring 47.0 ± 2.5 U/mg prot, compared to Group-I, which displayed an activity of 79.0 ± 4.3 U/mg prot in the liver. However, Group-III demonstrated a notable increase in SOD activity at 71.0 ± 3.5 U/mg prot compared to Group-II. Group-IV exhibited statistically insignificant differences ($p > 0.05$) compared to Group-I. The SOD activity of liver in the experimental zebrafish on day 21 is depicted in Table 5.2 and Figure 5.2(A).

Likewise, the CAT activity in the hepatic tissue was evaluated in Group-I, Group-II, Group-III, and Group-IV. Group-I displayed a CAT activity of 26.0 ± 2.6 , whereas Group-II showed a significantly ($p < 0.001$) reduced CAT activity at 10.2 ± 1.9 U/mg prot. In contrast, Group-III exhibited a substantial increase in CAT activity compared to Group-II, suggesting the therapeutic effect of EGCG. Group-IV showed insignificant ($p > 0.05$) CAT activity compared to Group-I. The CAT activity in the liver of the test zebrafish on day 21 is depicted in Table 5.2 and Figure 5.2(B).

5.3.2 SOD and CAT activity in the kidney

The SOD and CAT activities in the renal activities were assessed in zebrafish from Group-I, Group-II, Group-III, and Group-IV on day 21. In Group-I, the SOD activity in the kidney was measured at 64.0 ± 3.5 U/mg prot. Group-II exhibited a significant ($p < 0.001$) reduction in SOD activity, recording 40.2 ± 3.1 U/mg prot compared to Group-I. Conversely, Group-III displayed a substantial increase in SOD activity compared to

Chapter-5 *Evaluation of therapeutic efficacy of EGCG on oxidative stress and histopathological changes in zebrafish model*

Group-II, with a recorded value of 57.4 ± 3.6 U/mg prot. and this increase was highly statistically significant ($p < 0.001$). Group-IV, on the other hand, showed insignificant change ($p > 0.05$) compared to Group-I, with a SOD activity value of 65.5 ± 3.7 U/mg prot. Table 5.3 and Figure 5.3(A) illustrates the SOD activity in the kidney of the various experimental groups on day 21.

The CAT activity in the kidney, Group-I exhibited the highest value, measuring 32.2 ± 3.0 U/mg prot. Group-II showed a significant ($p < 0.001$) reduction in CAT activity compared to Group-I, with a value of 18.1 ± 3.6 U/mg prot. However, Group-III, which received EGCG treatment, displayed an increase in CAT activity (26.3 ± 3.1 U/mg prot.), indicating the therapeutic effect of EGCG. Importantly, Group-IV demonstrated insignificant ($p > 0.05$) result compared to Group-I, with a CAT activity value of 30.5 ± 3.2 U/mg prot. The CAT activity in the kidney of the test zebrafish on day 21 is presented in Table 5.3 and Figure 5.3(B).

5.3.3 SOD and CAT activity in the gills

In the gills, the SOD activity was significantly ($p < 0.001$) higher in Group-I compared to Group-II; the value was recorded to be 39.7 ± 3.4 U/mg prot and 19.4 ± 3.8 U/mg prot, respectively. A significant ($p < 0.001$) increase in CAT activity was recorded in Group-III, with the value of 32.4 ± 3.4 U/mg prot showing the ameliorating effect of EGCG. Insignificant ($p > 0.05$) results were obtained between Group-IV and Group-I test zebrafish. The SOD activity in the gills of the experimental zebrafish on day 21 is represented in Table 5.4 and Figure 5.4(A).

A similar trend was observed for CAT activity in the gills of test zebrafish. The Group-II zebrafish gills showed lower CAT values than the Group-I, with values of 4.4 ± 1.2 U/mg prot and 10.9 ± 1.0 U/mg prot, respectively, which was highly significant ($p < 0.001$).

Chapter-5 *Evaluation of therapeutic efficacy of EGCG on oxidative stress and histopathological changes in zebrafish model*

Treatment with EGCG in Group-III resulted in a significantly ($p<0.001$) higher CAT activity value of 8.8 ± 1.7 U/mg prot, indicating the potential healing effect of EGCG. Further insignificant ($p>0.05$) value was measured compared to Group-IV and Group-I. The CAT activity in the gills of different groups on day 21 is represented in Table 5.4 and Figure 5.4(B).

5.3.4 Histology of liver

Histological analysis of the liver, a vital metabolic organ, was examined on day 21 to elucidate the effects of EGCG administration on hepatic morphology and integrity. Administration of EGCG in the experimental Group-III exhibited a protective effect on the organs. The liver of Group-I displayed a normal hepatic lobule architecture, with hepatocytes forming branched cords and separated by blood sinusoids. The cells had a polyhedral appearance, basophilic granules, and rounded vesicular central nuclei. Portal areas showed normal connective tissue cells with minimal inflammatory infiltration. In Group-II, the histopathological damage was more severe, with a significantly ($p<0.001$) higher HAI value of 114.3 ± 6.5 compared to Group-I. Histological alterations such as steatosis, hepatocyte hypertrophy, atrophy, cytoplasmic vacuolation, and necrosis were observed in the liver tissue of Group-II. In Group-III, these alterations were less pronounced, and the HAI value was significantly ($p<0.001$) lower, with a value of 24.1 ± 5.6 , indicating a mitigating effect. The liver structure of Group-IV appeared normal but exhibited some hypertrophy and atrophy, although insignificant ($p>0.05$) when compared to Group-I. The histological changes in the liver of test zebrafish, represented in Figure 5.5(A-D), correspond to the HAI values of the liver in different experimental groups, as represented in Figure 5.8.

5.3.5 Histology of kidney

The kidney of the zebrafish consists of pinwheel-shaped nephron configurations, and the Group-I exhibited a normal renal histological structure. The brush border, proximal tubule, and distal tubule were orderly arranged. In contrast, the kidney of Group-II showed severe histological alterations, including vacuole degeneration, mesangial expansion, necrosis, tubular degeneration, focal hemorrhage, thickened glomerulus, brush border deficit, and dilation of Bowman's space. The HAI was significantly ($p<0.001$) higher with a value of 133.5 ± 5.5 in Group-II. These kidney tissue alterations were observed to be improved in the Group-III. A reduced HAI value of 32.3 ± 4.7 was revealed in Group-III, which is significantly ($p<0.001$) lower when compared to Group-II. The Group-IV showed a similar histological structure to Group-I, with minimal tubular alterations that were insignificant ($p>0.05$) when compared to Group-I. The histological changes in the kidney of test zebrafish, depicted in Figure 5.6(A-D), are paralleled by the HAI values of the kidney in the various experimental groups, as illustrated in Figure 5.8.

5.3.6 Histology of gills

The gill histological sections of Group-I exhibited a normal structure, with primary lamellae organized in two rows and alternating secondary lamellae projecting over the lateral side. In contrast, the Group-II showed severe histopathological alterations in the gills, including epithelial cell hyperplasia, hypertrophy, lamellar fusion, lifting of the epithelia, edema in lamellae, hemorrhage, lamellar aneurysm, and necrosis. The HAI values were significantly ($p<0.001$) higher in Group-II with value (237 ± 5.6) compared to Group-I, Group-III, and Group-IV, with HAI values of 96.0 ± 3.2 for Group-III, and 4.0 ± 2.3 in Group-IV, respectively. In the present study, Group-III gill structure showed less severe damage than Group-II, indicating a healing effect of EGCG. The treatment

Chapter-5 *Evaluation of therapeutic efficacy of EGCG on oxidative stress and histopathological changes in zebrafish model*

Group-IV exhibited slight epithelial lifting and hypertrophy in the lamella, but these changes were insignificant ($p>0.05$) compared to Group-I. The histological changes in the gills of test zebrafish, as shown in Figure 5.7(A-F), are accompanied by the presentation of HAI values for the kidney in the diverse experimental groups, detailed in Figure 5.8.

Table 5.2: Effect of diabetes on the antioxidant enzyme activity in the liver of zebrafish model. Group-I – control; Group-II – diabetic; Group-III – diabetic + EGCG; Group-IV – control + EGCG. Data are expressed as mean \pm SD (n=6). Different superscripts denote significant ($p < 0.001$) differences; the same superscripts denote insignificant ($p > 0.05$) results between the columns of the exposure groups on day 21.

Groups	Parameters	
	SOD (U/mg/prot.)	CAT (U/mg/prot.)
Group- I	79.0 \pm 4.3 ^a	26.0 \pm 2.6 ^a
Group- II	47.0 \pm 2.5 ^b	10.2 \pm 1.9 ^b
Group- III	71.0 \pm 3.5 ^c	21.2 \pm 3.2 ^c
Group-IV	80.1 \pm 4.1 ^a	26.5 \pm 2.5 ^a

Table 5.3: Effect of diabetes on the antioxidant enzyme activity in the kidney of zebrafish model. Group-I – control; Group-II – diabetic; Group-III – diabetic + EGCG; Group-IV – control + EGCG. Data are expressed as mean \pm SD (n=6). Different superscripts denote significant ($p < 0.001$) differences; the same superscripts denote insignificant ($p > 0.05$) results between the columns of the exposure groups on day 21.

Groups	Parameters	
	SOD (U/mg/prot.)	CAT (U/mg/prot.)
Group- I	64.0 \pm 3.5 ^a	32.2 \pm 3.0 ^a
Group- II	40.2 \pm 3.1 ^b	18.1 \pm 3.6 ^b
Group- III	57.4 \pm 3.6 ^c	26.3 \pm 3.1 ^c
Group-IV	65.5 \pm 3.7 ^a	33.7 \pm 2.9 ^a

Chapter-5 *Evaluation of therapeutic efficacy of EGCG on oxidative stress and histopathological changes in zebrafish model*

Table 5.4: Effect of diabetes on the antioxidant enzyme activity in the gills of zebrafish model. Group-I – control; Group-II – diabetic; Group-III – diabetic + EGCG; Group-IV – control + EGCG. Data are expressed as mean \pm SD (n=6). Different superscripts denote significant ($p < 0.001$) differences; the same superscripts denote insignificant ($p > 0.05$) results between the columns of the exposure groups on day 21.

Groups	Parameters	
	SOD (U/mg/prot.)	CAT (U/mg/prot.)
Group- I	39.7 \pm 3.4 ^a	10.9 \pm 1.0 ^a
Group- II	19.4 \pm 3.8 ^b	4.4 \pm 1.2 ^b
Group- III	32.4 \pm 3.4 ^c	8.8 \pm 1.7 ^c
Group-IV	40.0 \pm 3.4 ^a	11.3 \pm 0.8 ^a

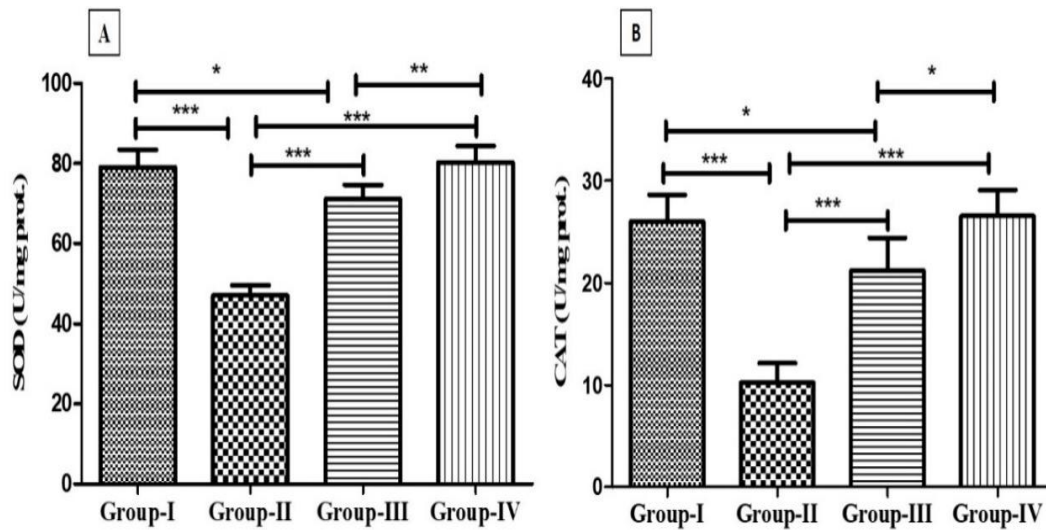


Figure 5.2: Effect of diabetes on the antioxidant enzyme activity in the liver of zebrafish model. Group-I – control; Group-II – diabetic; Group-III – diabetic + EGCG; Group-IV – control + EGCG. (A) SOD (B) CAT. Data are represented as mean \pm SD (n=6) and analysed by one-way ANOVA followed by Tukey's post-hoc test. Asterisk represents a significant difference, *p<0.05, **p<0.01, ***p<0.001.

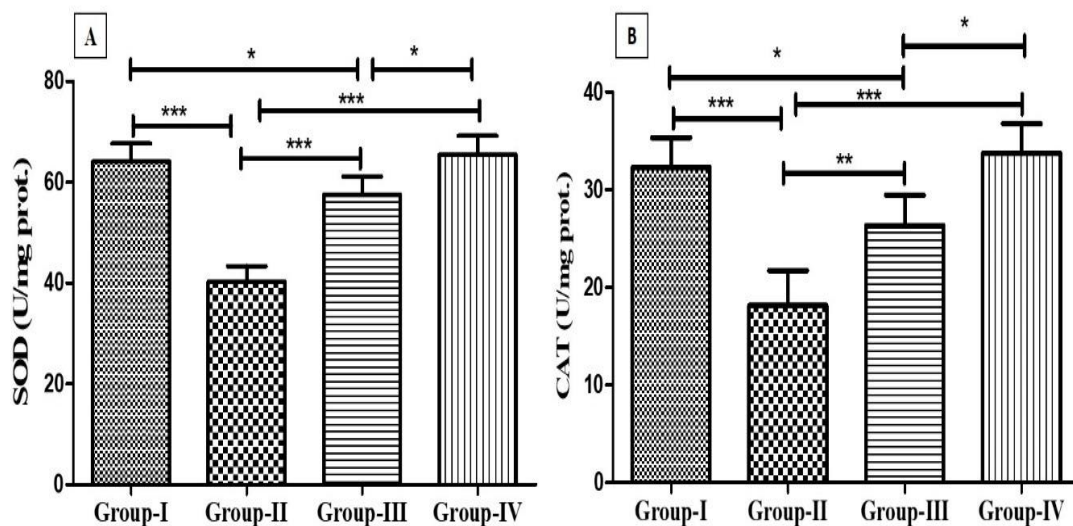


Figure 5.3: Effect of diabetes on the antioxidant enzyme activity in the kidney of zebrafish. Group-I – control; Group-II – diabetic; Group-III – diabetic + EGCG; Group-IV – control + EGCG. (A) SOD (B) CAT. Data are represented as mean \pm SD (n=6) and analysed by one-way ANOVA followed by Tukey's post-hoc test. Asterisk represents a

significant difference, * $p < 0.05$, ** $p < 0.01$, *** $p < 0.001$.

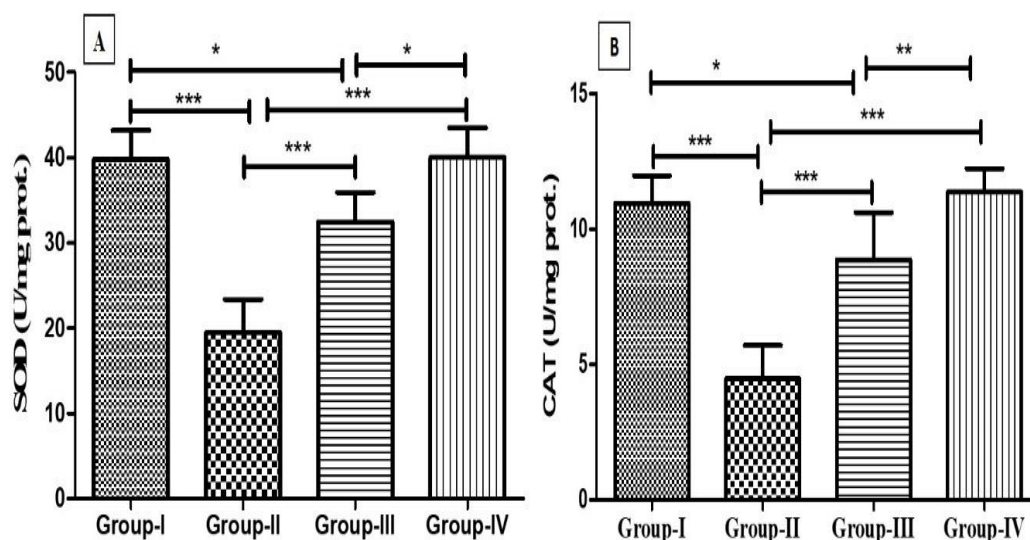


Figure 5.4: Effect of diabetes on the antioxidant enzyme activity in the gills of zebrafish model. Group-I – control; Group-II – diabetic; Group-III – diabetic + EGCG; Group-IV – control + EGCG. (A) SOD (B) CAT. Data are represented as mean \pm SD (n=6) and analysed by one-way ANOVA followed by Tukey's post-hoc test. Asterisk represents a significant difference, * $p < 0.05$, ** $p < 0.01$, *** $p < 0.001$.

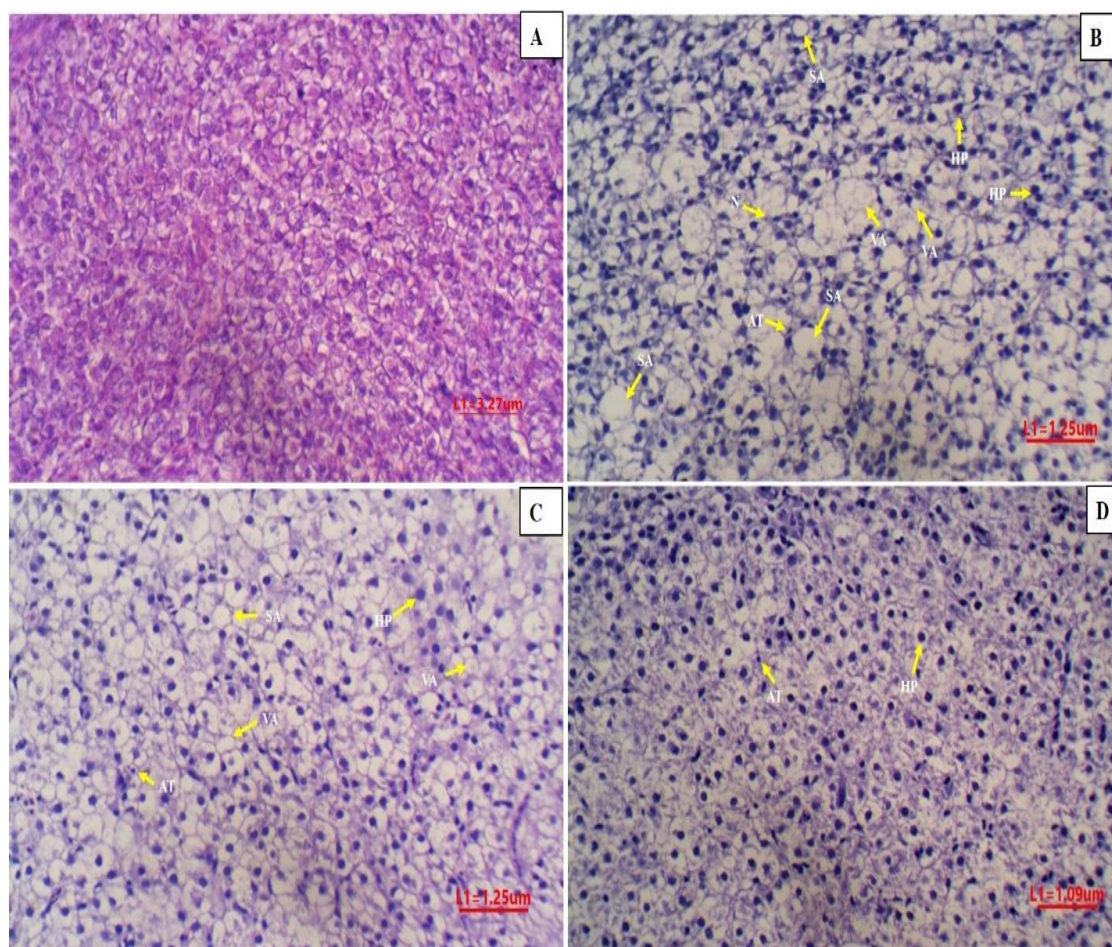


Figure 5.5: Histological changes in the liver of test zebrafish. (A) Group-I (B) Group-II (C) Group-III (D) Group-IV. Liver alterations are represented as steatosis (SA), hepatocyte hypertrophy (HP), atrophy (AT), cytoplasmic vacuolation (VA), and necrosis (N).

(Figures captured at 40X magnification)

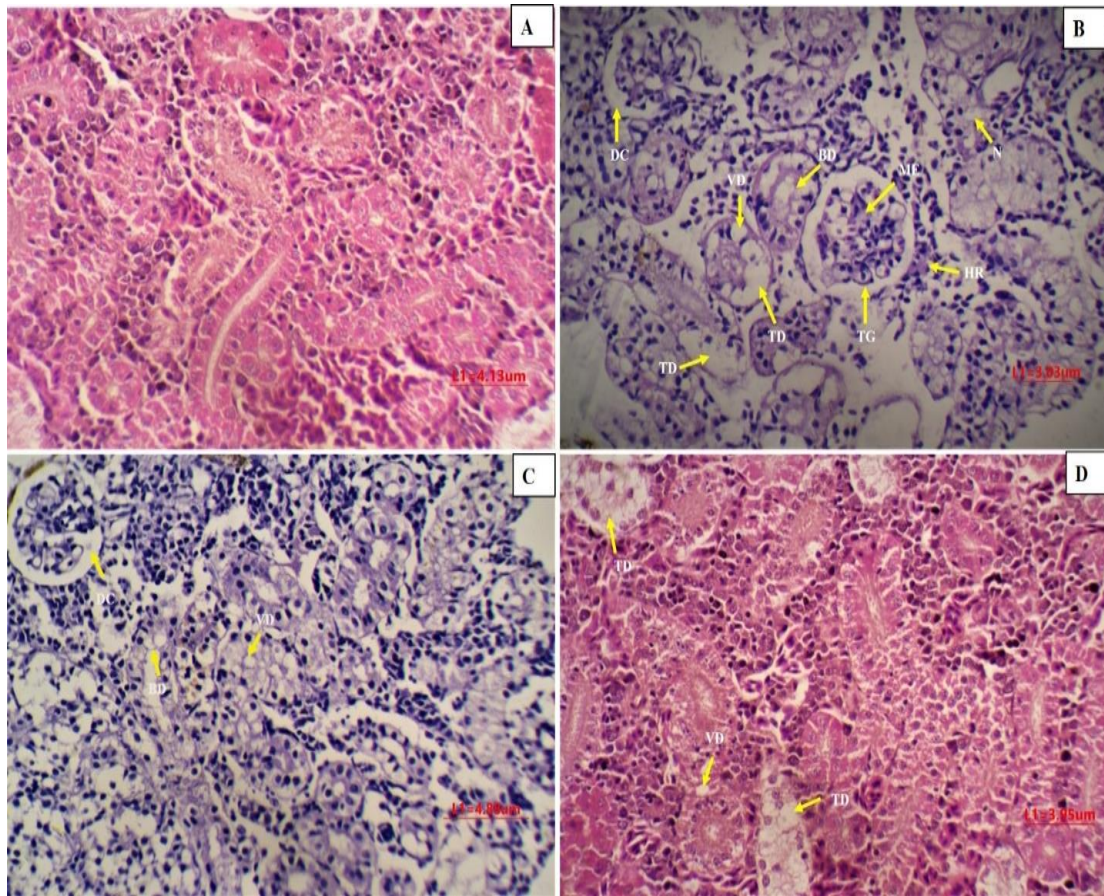


Figure 5.6: Histological changes in kidney of test zebrafish. (A) Group-I (B) Group-II (C) Group-III (D) Group-IV. Alterations in the tissue of different groups are represented as vacuole degeneration (VD), mesangial expansion (ME), necrosis (N), tubular degeneration (TD), focal haemorrhage (HR), thickness of the glomerulus (TG), brush border deficit (BD), and dilation of the bowman's space (DC). (Figures captured at 40X magnification)

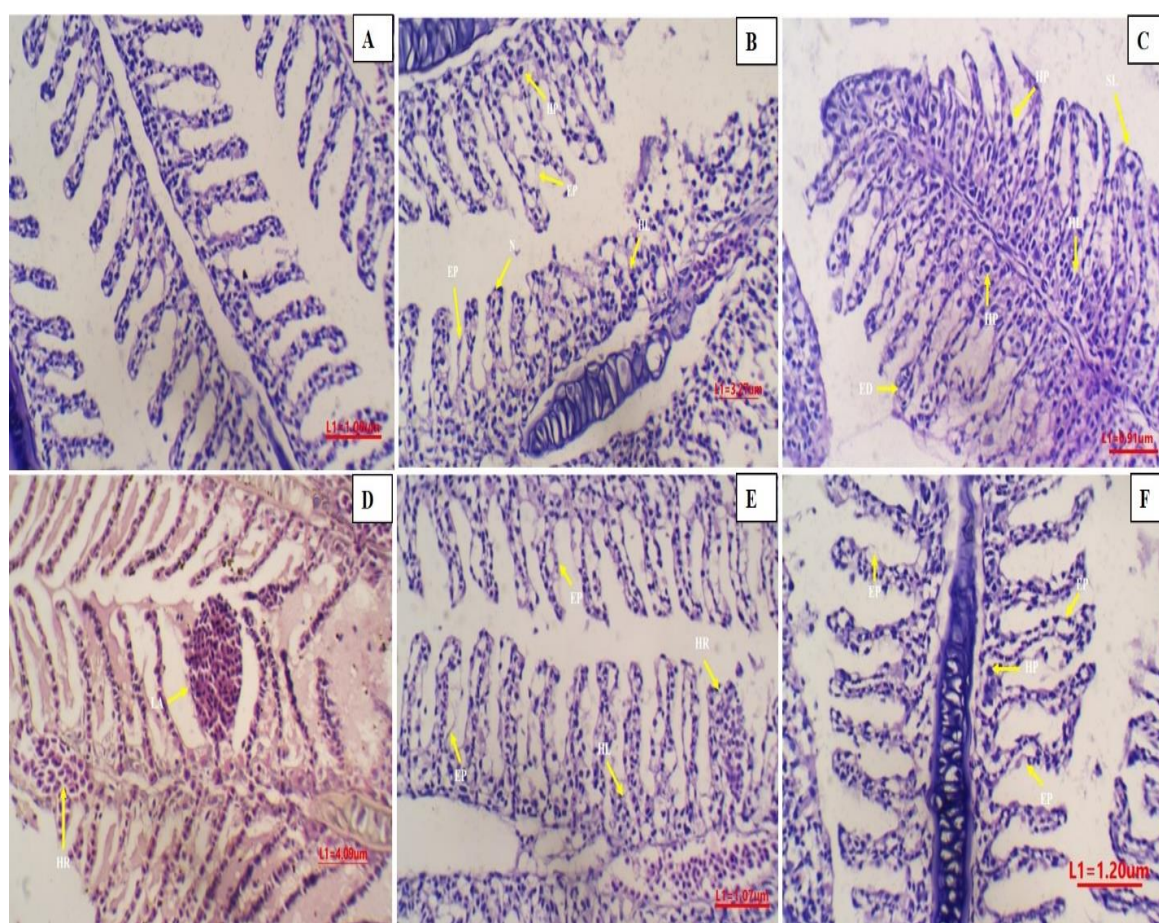


Figure 5.7: Histological changes in gills of test zebrafish. (A) Group-I (B-D) Group-II (E) Group-III (F) Group-IV. Alterations in the tissue of different groups are represented as epithelial cell hyperplasia (HL), hypertrophy (HP), lamellar fusion (SL), lifting of the epithelia (EP), edema in lamellae (ED), hemorrhage (HR), lamellar aneurysm (LA), and necrosis (N).

(Figures captured at 40X magnification)

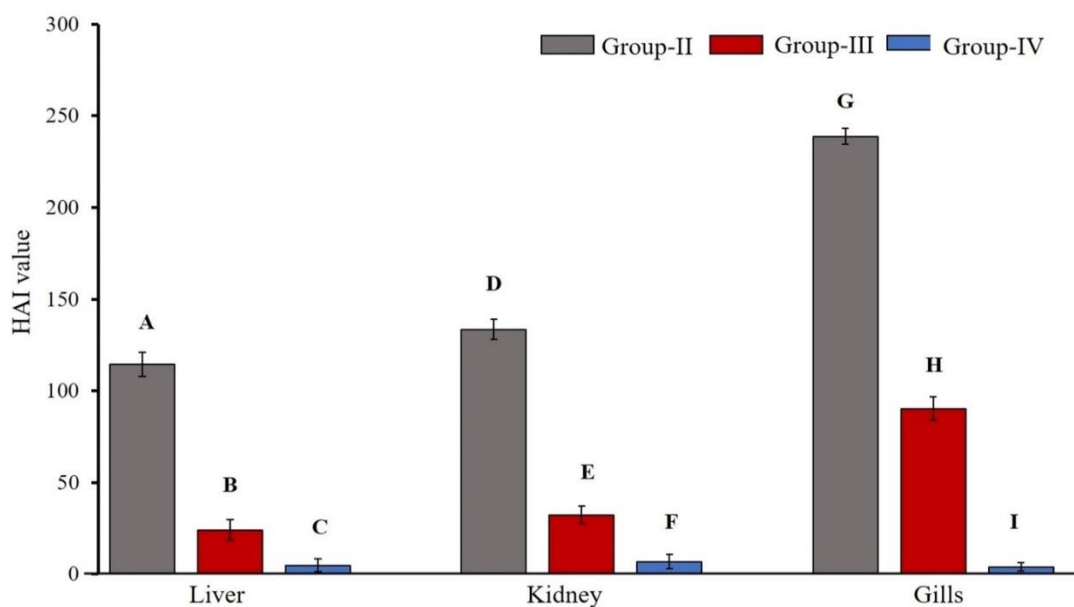


Figure 5.8: Histological alteration index (HAI) value of different organs of test zebrafish. Different superscripts denote significant ($p < 0.001$) differences between the exposure groups of the same organs.

5.4 Discussion

DM is a formidable global health challenge, and its treatment avenues frequently fall short of addressing its complicated character (Kerry *et al.*, 2022). In this context, polyphenols such as EGCG, a prominent component of green tea, have garnered attention for their antioxidant properties and potential in combating the oxidative stress implicated in chronic degenerative ailments (Truong & Jeong, 2021). Oxidative stress, a hallmark of DM progression and pathogenesis, stems from prolonged hyperglycemia, which triggers an overproduction of ROS and subsequent cellular damage (Mandal *et al.*, 2022; Zhang *et al.*, 2023). Zebrafish, a widely recognized model organism, can counter increased oxidative stress through enzymes like SOD and CAT (Guru *et al.*, 2022).

SOD is a critical component of the scavenger pathway responsible for neutralizing ROS, while CAT and glutathione peroxidase enzymes break down hydrogen peroxide produced by SOD (Cheng *et al.*, 2022). The results of the present study are consistent with recent research by Al-Sowayan & AL-Sallali, (2023), where a considerable reduction in SOD and CAT activity in STZ-induced diabetic rat models was documented. This decline in antioxidant enzymes predisposes various organs to oxidative damage due to the accumulation of harmful radicals, potentially exacerbating DM complications (Firdous & Singh, 2016). The observed decrease in CAT activity in diabetic conditions is attributed to heightened superoxide anion production, as evidenced in rodent and zebrafish models (Pérez Gutiérrez *et al.*, 2022). Further, the reduced CAT and SOD levels in the gills may be linked to elevated oxidative stress associated with DM, further elevating the risk of harm from free radicals (Correia *et al.*, 2023). Prolonged DM may lead to tissue lipid peroxidation and direct ROS attacks on proteins, contributing to the loss of tissue antioxidant capabilities. Treatment with EGCG demonstrated a

Chapter-5 *Evaluation of therapeutic efficacy of EGCG on oxidative stress and histopathological changes in zebrafish model*

notable improvement in tissue antioxidant levels, indicating its effectiveness in mitigating oxidative stress within the liver, kidney, and gills of diabetic zebrafish. In various studies, EGCG has garnered recognition as a potent antioxidant agent (Singh *et al.*, 2011; Bartosikova & Necas, 2018). Flavonoids in green tea, particularly EGCG, have been documented for their antioxidant and iron-chelating properties, countering the detrimental effects of oxygen-depleted free radicals associated with chronic diseases (Hutachok *et al.*, 2023).

The present findings resonate with contemporary research, showcasing the capacity of EGCG to activate SOD and CAT, thereby replenishing antioxidant enzyme levels (Soussi *et al.*, 2022). Notably, EGCG administration has shown efficacy in decreasing lipid peroxidation and nitrite content while boosting SOD activity in diabetic rats (Baluchnejadmojarad & Roghani, 2012; Akpoveso *et al.*, 2023). Moreover, it is envisaged that EGCG has the role of suppressing hepatic gluconeogenesis and enhancing insulin signaling pathways, underscoring its multifaceted therapeutic benefits in DM management.

The pivotal role of the liver in glucose homeostasis and insulin action underscores its significance in metabolic regulation. This present investigation into STZ-induced diabetic zebrafish revealed notable histological alterations in the liver, mirroring findings observed in STZ-induced rat models. These alterations encompass vacuolation, hepatocyte hypertrophy, atrophy, steatosis, and necrosis, reflecting a spectrum of pathological changes consistent with diabetic liver pathology documented in prior research (El-Megharbel *et al.*, 2022; Ghalwas *et al.*, 2022).

Histologically, atrophy and hypertrophy denote adaptive responses in shifting metabolic demands, whereas vacuolation signals metabolic disruption and cellular injury

Chapter-5 *Evaluation of therapeutic efficacy of EGCG on oxidative stress and histopathological changes in zebrafish model*

(Shreenidhi & Bose, 2022). The observed increase in apoptosis aligns with its role in tissue homeostasis and dysregulation in diabetic states (Sharma *et al.*, 2021c). STZ-induced diabetes triggers a cascade of events, including oxidative stress, inflammation, and dysregulated apoptotic pathways, culminating in cellular demise and diabetes-related complications (Farid *et al.*, 2022). The necrotic changes in the liver cells of the present experimental DM groups can likely be attributed to increased oxidative stress. Notably, EGCG is known for its antioxidant properties and has shown ameliorating results in insulin resistance, maintaining glucose homeostasis, and suppressing liver inflammation (Legeay *et al.*, 2015; Wan *et al.*, 2022). Multiple studies have showcased the favourable impact of EGCG on liver histopathology, including the alleviation of fatty changes, necrosis, and inflammation (Zhou *et al.*, 2017; Soussi *et al.*, 2022; Mostafa-Hedeab *et al.*, 2022). Throughout the study, EGCG treatment demonstrated the potential to mitigate oxidative stress and restore normal liver histological features in diabetic zebrafish. The antioxidant and anti-inflammatory properties of EGCG and its role in regulating glucose homeostasis collectively contribute to its therapeutic efficacy. These observations align harmoniously with research conducted in diabetic animal models and instances of liver toxicity (Legeay *et al.*, 2015; Sampath *et al.*, 2017; Mostafa-Hedeab *et al.*, 2022).

In zebrafish, the kidney is an essential organ for toxin excretion, providing valuable insights into environmental influences and the progression of disease states such as diabetes. Meticulous examination of DM-induced diabetic zebrafish uncovered a spectrum of histological irregularities within renal tissues, echoing findings observed in analogous diabetic animal models. These renal anomalies comprised vacuole degeneration, mesangial expansion, necrosis, tubular degeneration, focal hemorrhage, glomerular thickening, and dilation of Bowman's space, mirroring the structural kidney

Chapter-5 *Evaluation of therapeutic efficacy of EGCG on oxidative stress and histopathological changes in zebrafish model*

aberrations documented in DM-induced animal models. These findings correspond to earlier studies conducted in animals induced with STZ, which reported analogous structural kidney irregularities like vacuole degeneration, glomerular thickening, and dilation of Bowman's space (Omara *et al.*, 2012; Duman *et al.*, 2022).

Glomerular hypertrophy, stemming from heightened plasma flow and glomerular capillary hydrostatic pressure, represents an incipient stage of glomerular impairment in diabetic pathology (Thomas & Ford Versypt, 2022). Renal glomerular hypertrophy is attributed to increased plasma flow and glomerular capillary hydrostatic pressure (Deng *et al.*, 2023). Elevated glucose levels can induce excessive apoptosis in mesangial cells, resulting in Bowman's capsule expansion and widening Bowman's space due to glycogen accumulation (Zhang *et al.*, 2015). Furthermore, proximal tubule necrosis, characterized by deficits in the brush border and epithelial cell alterations, underscores the intricate and multifaceted nature of diabetic renal pathology (Alipin *et al.*, 2019). A comparable loss of brush border and necrosis in the kidney tissues has been reported in DM-induced mice *via* STZ (Fareed *et al.*, 2023). Cell vacuolization in kidney tubules can indicate cellular adaptation or destruction depending on the specific cellular context. Glycogen deposition is associated with cell vacuolization, and it is worth noting that anti-inflammatory drugs have been shown to improve vacuolar alterations (Zhou *et al.*, 2017).

Following treatment with EGCG, a striking restoration of the observed histological kidney alterations was evident in diabetic zebrafish. Notably, the kidney structure of zebrafish treated with EGCG resembles that of healthy counterparts. This observed efficacy of EGCG can be attributed to its potent antioxidant and anti-inflammatory properties, which play pivotal roles in mitigating the deleterious effects inflicted by ROS on kidney tissues. The mechanism of EGCG action involves direct

Chapter-5 *Evaluation of therapeutic efficacy of EGCG on oxidative stress and histopathological changes in zebrafish model*

scavenging of ROS and indirect suppression of ROS-producing enzymes, along with binding to pro-oxidizing metal ions. Notably, its antioxidant properties are underscored by its capability to neutralize the DPPH radical, demonstrating its robust antioxidative potential (Thangapandiyan & Miltonprabu, 2014). Zebrafish treated with EGCG exhibited kidney structures with nearly normal glomerular and tubular cell architecture, minimal inflammation, tubular expansion, and congestion compared to untreated diabetic fish. This echoes the findings from studies conducted in rats and mice, demonstrating the ameliorative effects of EGCG on diabetic nephropathy (Yoon *et al.*, 2014). Furthermore, EGCG has exhibited anti-inflammatory properties, suppressing endoplasmic reticulum stress responses and inhibiting apoptosis in renal tissues (Yang *et al.*, 2022).

While indispensable for respiration and maintaining physiological equilibrium, fish gills are exceptionally vulnerable to environmental pollutants due to their thin and exposed structure. Like other freshwater teleosts, the gill architecture in zebrafish comprises branchial arches housing primary filaments and secondary lamellae, facilitating efficient gas exchange (Macirella & Brunelli, 2017). Beyond their primary role in oxygen exchange, fish gills serve essential functions such as osmotic regulation, nitrogenous compound excretion, and acid-base balance maintenance in adult fish (Giaretta *et al.*, 2023). However, the delicate nature of gill membranes, which enables efficient oxygen exchange, also makes them vulnerable to various environmental pollutants, even at low concentrations in the water (Haque *et al.*, 2022). Fish possess remarkable sensitivity to alterations in their chemical and physical surroundings, and their physiological changes can indicate the impact of changing environmental conditions (Haque *et al.*, 2022).

Histological aberrations observed in the gills of zebrafish, including epithelial

Chapter-5 *Evaluation of therapeutic efficacy of EGCG on oxidative stress and histopathological changes in zebrafish model*

cell hyperplasia and hypertrophy, lamellar fusion, epithelial lifting, and lamellar edema, are commonly construed as defence mechanisms elicited in response to exposure to environmental irritants (Ortiz-Delgado *et al.*, 2021). These alterations, induced by toxins or pathogenic agents, range from first-degree gill changes such as hypertrophy, hyperplasia, epithelial lifting, and fusion of secondary lamellae to more severe damage, including hemorrhage, lamellar aneurysm, and necrosis. Such histopathological variations align with those documented in fish gills exposed to diverse pollutants and are generally considered nonspecific responses (Azadbakht *et al.*, 2019). Similar first-degree lesions have been observed in the gills of *Clarias gariepinus*, signifying the potential of gill tissues as indicators of xenobiotic exposure and the effects of pharmaceutical particles, even at low concentrations (Trombini *et al.*, 2022). Additionally, histopathological changes like hyperplasia, epithelial lifting, lamellar fusion, necrosis, and hemorrhage have been reported in *Osteobrama belangeri* following exposure to unionized ammonia (Mangang & Pandey, 2021).

Hyperplasia, characterized by increased cell numbers, can significantly reduce the interlamellar space in fish gills, ultimately resulting in lamellar fusion, compromising efficient gas exchange, and detrimentally impacting overall fish health (Nimet *et al.*, 2019). Gill lamellae lifting is typically associated with the penetration of environmental contaminants through the gill epithelium and basement membrane, effectively lengthening the distance for diffusion (Kirthi *et al.*, 2022). Lamellar cell hypertrophy further reduces the lamellar space and has the potential to induce secondary lamellar fusion and capillary hemorrhage. These responses collectively suggest that epithelial thickening, through cell multiplication, is a defence mechanism to impede further entry of pollutants.

Chapter-5 *Evaluation of therapeutic efficacy of EGCG on oxidative stress and histopathological changes in zebrafish model*

The manifestation of gill filament curling is often associated with the collapse of the vascular skeleton within fish gills, possibly due to low hydrostatic pressure within the pillar cell system (Pal *et al.*, 2012). Aneurysms, indicative of severe structural changes in the gills, arise from disruptions in blood flow within the gill structure. Morphological alterations in pillar cells can adversely affect blood circulation in lamellar capillaries, triggering downstream effects (Neelima *et al.*, 2015; Badroo *et al.*, 2020). In extreme environmental stress, impaired or collapsed pillar cells can induce increased blood flow, resulting in congestion and aneurysms. While these responses protect against toxicants, they may impede gill respiration, potentially outweighing their protective effects against toxin uptake.

The findings of this study demonstrate the therapeutic potential of EGCG in mitigating oxidative stress and histopathological changes in a zebrafish model. The antioxidant properties of EGCG, coupled with its ability to enhance endogenous antioxidant defences and promote tissue repair, highlight its promise as a natural therapeutic agent for managing oxidative stress-related diseases.

Chapter 6

Effect of EGCG on diabetes-induced reproductive performance and developmental deformities in zebrafish model

Contents

6.1 Introduction

6.2 Materials and methods

6.3 Results

6.4 Discussion

6.1 Introduction

The global reduction in birth rates, particularly evident in industrialized nations, has ignited substantial discourse. It is predominantly concerned with discerning the relative influence of sociocultural and biological factors, especially with DM, on reproductive well-being. Exposure to toxins such as endocrine disruptors is a major biological cause of concern for decreased fertility. In addition, the increasing prevalence of DM may also play a crucial role in the alarming decline in birth rates (Molina *et al.*, 2021). DM is known to cause vascularization and endothelial dysfunctions, leading to reproductive impairment in both men and women (Devi *et al.*, 2015). DM can result in congenital malformations, increasing perinatal morbidity and mortality among pregnant women. The pathophysiology of pregnancy complications in diabetic women is not entirely understood. However, it is believed to be related to the pro-inflammatory and pro-oxidative intrauterine environment due to metabolic abnormalities (Sharma *et al.*, 2022). DM can also lead to male reproductive dysfunctions, hindering spermatogenesis and reducing the quality and quantity of sperm produced, with accompanying dysfunctions of the hypothalamic-pituitary-testicular axis, which results in decreased levels of hormones like luteinizing hormone, follicle-stimulating hormone, and testosterone. Chronic hyperglycemia can also result in loss of *libido* and erectile dysfunction, leading to male infertility (Singh *et al.*, 2016a).

Natural compounds of herbal origin have gained popularity as epigenetic modulators and are used as alternative therapies for treating various metabolic diseases (He *et al.*, 2022). EGCG, a catechin abundant in green tea, is known for its potent antioxidant and anti-inflammatory properties. It has also been reported to regulate

disease-specific targets and improve metabolic functions (Jamir *et al.*, 2023). EGCG has shown efficacy in enhancing glucose tolerance, increasing glucose secretion, and preserving the pathological changes in islet structure in db/db mice (Blahova *et al.*, 2021).

The utilization of zebrafish as a model organism for studying metabolic disorders has surged owing to their genetic similarity and shared organ systems with humans. Zebrafish are frequently employed in embryonic toxicity studies and drug screening due to their transparent embryos and rapid development. Furthermore, they are cost-effective, easy to maintain, and provide highly reproducible statistical data (Li & Ge, 2020). Adult zebrafish can develop a long-term diabetic condition similar to humans and can be used to investigate DM-related pathologies. The glucose metabolism in zebrafish works similarly to humans as it is regulated by the direct release of insulin and glucagon into the bloodstream (Lee & Yang, 2021).

However, the effect of EGCG on DM-induced zebrafish remains largely unexplored. Thus, the objective of this study was to induce diabetes in adult zebrafish *via* STZ treatment and to evaluate the associated reproductive parameters in the first filial generation (F₁) for 14 days post-fertilization (dpf). Additionally, this study aimed to investigate the potential benefits of EGCG treatment in improving reproductive performance and restoring histoarchitectures of the reproductive organs in the DM-induced zebrafish model, thereby highlighting the significance of EGCG in combating diabetic embryopathy. To the best of our knowledge, there are no existing reports detailing the effects of EGCG on developmental abnormalities, hepato-somatic index (HSI), and gonado-somatic index (GSI) in a diabetic zebrafish model.

6.2 Materials and methods

6.2.1 Chemicals

EGCG (>95%) and STZ were obtained from Merck. Before usage, all glassware and aquariums underwent thorough cleaning procedures and were subsequently rinsed with distilled water to ensure study accuracy. Additionally, xylene, hematoxylin-eosin solution, and absolute alcohol were employed in the study.

6.2.2 Induction of diabetes

DM was induced in adult zebrafish by administering STZ following the protocols described (Longkumer *et al.*, 2020). Post-injection, the zebrafish were closely monitored for abnormal behaviour and then transferred to a normal water tank for recovery. The detailed induction process of diabetes in zebrafish is described in Chapter 3.

6.2.3 Acclimatization of zebrafish

Adult zebrafish were obtained from Aqua Fish & pets, Jorhat Assam, India, and housed in a zebrafish housing system (Model-NT-ZB-11; Make-Narshi Technologies) with constant temperature, biological and mechanical water filtration, and aeration. The zebrafish were maintained under a 14h/10hr: day/night photoperiod cycle and were fed commercially available Optimum Super NovaTM fish feed containing protein 28%, crude fat 3%, fibre 4%, and moisture 10%. The detailed acclimatization of the zebrafish is described in Chapter 2.

6.2.4 Experimental design

Zebrafish of approximately 500-600 mg in weight for females and 390-420 mg for males were selected from the stock. The zebrafish were divided into groups: Group-I - control, Group-II - diabetic, Group-III - diabetic + EGCG, and Group-IV - control +

Chapter-6 *Effect of EGCG on diabetes-induced reproductive performance and developmental deformities in zebrafish model*

EGCG. An effective dose of 6 mg/L of EGCG was used for the study. The treatment with EGCG was maintained throughout the experiment. Figure 6.1 describes the experimental design of the study.

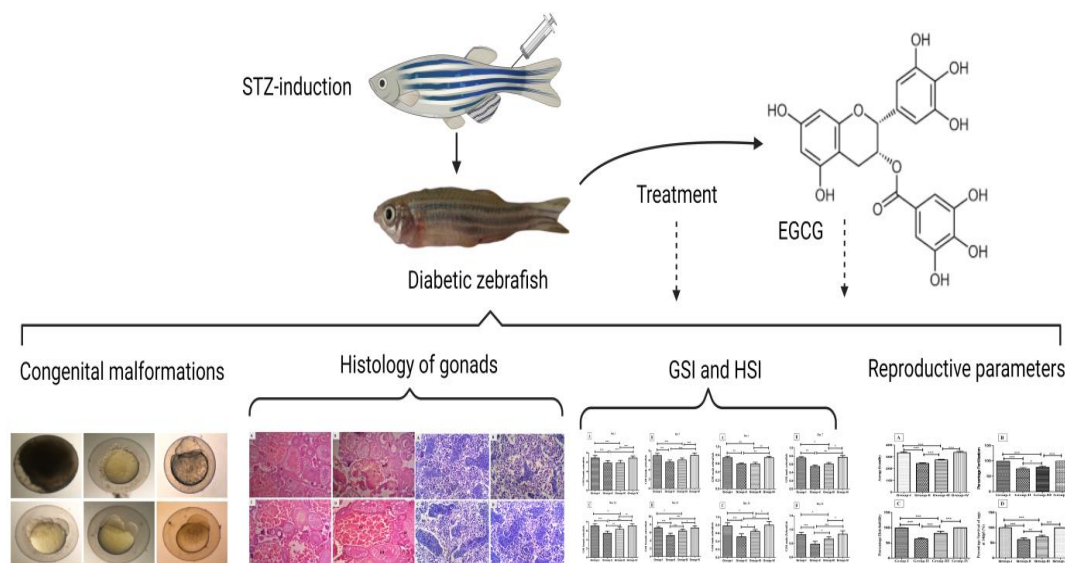


Figure 6.1: Diagrammatic representation of the experimental setup for reproductive performance and developmental deformities in the zebrafish model.

6.2.5 Larval rearing

Zebrafish larvae were reared by collecting eggs in a clean Petri dish filled with deionized water to prevent contamination. Initially, larvae obtained nutrients from their yolk sac until a few days after hatching. Afterward, they were fed a combination of zooplankton paramecium and crushed dry fish pellets (approximately 100 microns in size). After 14 days, they were transferred to a 1-liter aquarium, and their nutritional provision was adjusted systematically to accommodate their advancing age.

6.2.6 Determination of gonadosomatic (GSI) and hepatosomatic index (HSI)

On days 1, 7, 14, and 21, the gonadosomatic index (GSI) and hepatosomatic index (HSI) were quantified for each sexually mature male and female zebrafish under study. By the end of day 21, a histological examination was conducted on the gonadal tissues.

The computation of GSI and HSI values was calculated using the formulas: [gonad weight in (g) / total weight in (g)] x 100, and [liver weight in (g) / total weight in (g)] x 100 respectively as described by Jan & Jan. (2017).

6.2.7 Assessment of reproductive parameters

Male and female zebrafish were introduced into a breeding chamber in a 2:1 male-to-female ratio to investigate reproductive parameters. The eggs from the F₁ generation of the designated groups were gathered and subjected to a comprehensive 14-day analysis within a petri dish containing distilled water. Various parameters such as: average fecundity, percentage fertilization, percentage hatching, and percentage survival. Average fecundity represented the total number of eggs laid, both viable and non-viable, during the spawning activity. The determination of the percentage of fertilization was done once the zebrafish eggs reached the 4-8 celled developmental stage. Subsequently, the percentage hatching and percentage survival for the experimental groups were calculated using the formula described by Adebayo et al. (2006).

Percentage fertilization = (Number of viable eggs/Total number of eggs laid per spawning activity) × 100

Percentage hatching = (Total number of eggs hatched/Total number of eggs laid per spawning activity) × 100

Percentage survival = (Total number of eggs survived up to larva stage/Total number of eggs hatched) × 100

6.2.8 Deformity assessment

A deformity assessment of embryos was conducted for the test groups to evaluate malformations from zero-hour post-fertilization (0 hpf) to 14 dpf. Deformities such as

early cell stage anomalies, lordosis, edema, and tail deformities were recorded. The percentage of embryo deformity was calculated using the formula described by (Adebayo *et al.*, 2006)

$$\text{Percentage deformity} = (\text{Total number of deformed embryos} / \text{Total number of embryos}) \times 100$$

6.2.9 Histopathological study

After 21-days of the treatment period, gonads were dissected out, washed in physiological saline solution, and preserved in 10% buffer formalin. Following fixation, tissues underwent dehydration, embedding in paraffin blocks, and sectioning at 4-5 μ thickness. Harris-hematoxylin stain was applied, followed by eosin counterstaining. The detailed procedure of the histological study is described in Chapter 2.

6.2.10 Image pre-processing and processing

The collected eggs were first examined under an Olympus Stereo zoom microscope (Model SZX10) to remove debris. Images of the eggs at different developmental stages and the histological slides of the ovary and testis were captured using a labomed cxi binocular microscope, equipped with magnifications ranging from 4X to 100X. The microscope was connected to a Sony digital camera model E31SPM20000KPA (USB 2.0). Images were processed using ImageJ software.

6.2.11 Statistical analysis

Statistical analysis was conducted using GraphPad Prism 5.0 software and presented as mean \pm SD. One-way analysis of variance (ANOVA) with Tukey's post hoc test was used for comparisons between groups, with $p < 0.05$, $p < 0.01$, and $p < 0.001$ indicating statistical significant.

6.3 Results

6.3.1 GSI and HSI in female subjects

GSI and HSI assessments are crucial for evaluating the reproductive health and liver condition of test fish. This study observed changes in GSI and HSI values in female zebrafish under different experimental durations. Group-I showed a slight increasing trend in GSI values over the 21-day experimental period, but the changes were insignificant ($p>0.05$). Conversely, Group-II had significantly ($p<0.001$) lower GSI values compared to Group-I, indicating the detrimental impact of diabetes on the reproductive organs of test zebrafish. However, Group-III led to a significant ($p<0.001$) improvement in GSI values, suggesting potential therapeutic effects in restoring reproductive health in diabetic subjects. The changes in the values of GSI of the female experimental subjects are described in Table 6.1 and Figure 6.2[A-D].

The HSI values of Group-I showed a similar trend as that of GSI, with a slightly increasing value over the experimental duration, but it was insignificant ($p>0.05$). In contrast, Group-II had significantly ($p<0.001$) higher HSI values than Group-I, indicating liver damage. Further, Group-III showed a significant ($p<0.001$) decrease in the HSI values over the course of the study compared to Group-II. The changes in the HSI value of the different experimental groups are depicted in Table 6.1 and Figure 6.3[A-D].

6.3.2 GSI and HSI in male subjects

The change in the value of GSI and HSI of the male experimental zebrafish was examined and recorded. The Group-I subject recorded a similar increasing trend of GSI and HSI values as that of female subjects. In contrast, the Group-II subjects had a significantly ($p<0.001$) lower GSI value and significantly ($p<0.001$) higher HSI value

than the Group-I, indicating the detrimental impact of diabetes on male reproductive organs. However, Group-III subjects over the period of 21 days showed a significant ($p < 0.001$) improvement in GSI and HSI values, suggesting the potential therapeutic effects of EGCG in restoring reproductive health in diabetic conditions. Additionally, Group-IV showed insignificant ($p > 0.05$) values of GSI and HSI compared to Group-I. Table 6.2, Figure 6.4[A-D], and Figure 6.5[A-D] depicts the change in the GSI and HSI of the experimental zebrafish.

6.3.3 Assessment of reproductive parameters

6.3.3.1 Normal development of zebrafish embryo

The normal development of the zebrafish embryo was studied, and represented in Table 6.3. The eggs are telolecithal, and the pattern of cleavage is discoidal and meroblastic. The embryogenesis of the zebrafish from fertilization to hatching took 96- hours to complete.

Zygote stage

The zygote stage of the zebrafish embryo occurs early on, where the cytoplasm accumulates at the animal pole. One cell stage of the embryo is represented in Figure 6.7.

Cleavage stage

The cleavage of the embryo occurs at the animal pole from 0.45 minutes to 1-hour post-fertilization. The embryo at this stage undergoes cell division from the 2-cell blastomere stage to the 16-cell blastomeres stage, as represented in Figure 6.7, which is followed by the blastula stage.

Blastula stage

The blastula stage occurs from 2 hours post fertilization to 4 hours post fertilization.

During the blastula stage, the blastomere increases in number, and the interface between the yolk and the blastoderm appears to be flat, as represented in Figure 6.7.

Gastrula stage

The blastula stage is followed by a series of changes in the embryo known as the gastrula stage, where the cell spreads over to the vegetal pole, replacing the margin of the blastoderm and starting gastrulation. During the gastrula stage, 50% epiboly and 75% epiboly are seen covering nearly half of the yolk, as represented in Figure 6.7.

Segmentation stage

The Gastrula stage is followed by segmentation, which starts at 10 hours and 30 minutes post-fertilization, and the formation of the first somites is observed. The somites begin to develop. Further, the mesoderm of the early trunk develops, and segmentation in the tail occurs, as represented in Figure 6.7.

Hatching

The embryo hatched from 48 hours post-fertilization to 96 hours post-fertilization. The twisting movement of the unhatched larvae inside the egg was visible before the hatching time. Figure 6.7 represents the hatched larvae at 48 hours.

120 hours old hatched larvae

The larvae feed on the yolk sac and the yolk sac until they are slowly replaced by a developing alimentary canal, as depicted in Figure 6.7.

14-day old larvae

The 14-day-old larvae had a clear pigmented body, and further, the yolk sac was replaced by an alimentary canal. The fins were beginning to develop, as depicted in Figure 6.7.

6.3.3.2 Average fecundity

The change in the average fecundity of the test zebrafish under different experimental conditions has been represented in Table 6.4 and Figure 6.6(A). Group-I exhibited the value of average fecundity as 334 ± 7.9 , while Group-II had a significantly ($p < 0.001$) lower value (244 ± 4.7), indicating the detrimental impact of diabetes on reproductive performance. However, treatment of diabetic zebrafish with EGCG improved the fecundity value, as seen in Group-III which depicted higher fecundity values than Group-II, as evident in Figure 6.6(A). Although the fecundity of Group-III was still significantly ($p < 0.05$) lower than the control group, these results suggest a potential beneficial effect of EGCG in restoring reproductive health in diabetic conditions. Furthermore, Group-IV had slightly higher average fecundity than the control group, though statistically insignificant ($p > 0.01$), indicating the potential benefits of EGCG treatment in the fecundity of healthy subjects.

6.3.3.3 Percentage fertilization

Fertilization is a crucial aspect of reproduction, and the percentage of fertilized eggs is a measure of reproductive success. Results showed that the percentage of fertilized eggs was significantly lower in Group-II (74.8 ± 3.0) compared to Group-I (98.9 ± 0.3), indicating a harmful effect of diabetes on egg fertilization. However, treatment with EGCG showed a potential impact on the fertilization percentage of the experimental group. The Group-III showed an improved fertilization percentage with a value of (79.0 ± 3.0) which is higher than Group-II, suggesting that EGCG treatment may improve fertilization in diabetic conditions. Moreover, the fertilization percentage of Group-IV was slightly higher than that of Group-I, although this difference was insignificant ($p > 0.05$). These results suggest that EGCG treatment may potentially

affect fertilization and pathological conditions in the subjects. The effect of diabetes on the average fertilization of the zebrafish embryo is depicted in Table 6.4 and Figure 6.6(B).

6.3.3.4 Percentage hatchability

The eggs of the control zebrafish showed a higher hatchability percentage which was 99.4 ± 0.3 . Group-I showed nearly complete hatchability of eggs. In contrast, Group-II had a significantly ($p < 0.001$) lower hatchability percentage of (62.9 ± 4.2), indicating potential detrimental effects on zebrafish egg hatchability. However, Group-III demonstrated a significantly ($p < 0.001$) higher hatchability percentage (81.5 ± 6.6) than Group-II, suggesting potential beneficial effects in mitigating diabetes-related hatchability issues. Interestingly, insignificant ($p > 0.05$) difference in hatchability percentage was observed when compared between Group-I and Group-IV, implying that the EGCG treatment in Group-IV did not affect zebrafish egg hatchability, the percentage hatchability of the different groups is depicted in Table 6.4 and Figure 6.6(C).

6.3.3.5 Percentage survival

Results of the present study showed that Group-I and Group-IV had the best survival values, with survival percentages of 99.7 ± 0.5 and 99.5 ± 0.2 , respectively. The finding suggests that these groups had a high survival rate, indicating that the conditions for the eggs were optimal. On the other hand, the Group-II zebrafish showed a significantly ($p < 0.001$) lower survival percentage (60.6 ± 5.1) indicating that diabetes may have detrimental effects on the survival of zebrafish eggs. However, the study reveals that Group-III had a significantly ($p < 0.001$) better survival percentage of 70.8 ± 4.4 compared to Group-II adding to the protective effect of EGCG. The result of

the different groups are depicted in Table 6.4 and Figure 6.6(D).

6.3.3.6 Deformity assessment

The deformity assessment of zebrafish larvae revealed the highest malformations in Group-II, while Group-I and Group-IV exhibited the least malformations. It has been recorded that Group-III had lower malformations than Group-II, as shown in Table 6.5. Malformations were categorized into the coagulation of egg, blisters, uneven cleavage, lordosis, swollen body, edema, and tail deformities, which are represented in Figure 6.8[E-X]. Group-II had the highest malformations compared to the Group-I, but treatment with EGCG in Group-III showed notable reductions as described in Figure 6.8[A-D]. In the case of tail deformities, Group-II had higher deformities compared to Group-I, but Group-III demonstrated a remarkable reduction in tail malformations.

6.3.4 Histopathological study

6.3.4.1 Histopathology of the ovary

The histological analysis showed that Group-II had marked alterations in the ovarian structure compared to Group-I, including oocyte degeneration, vacuolation, atria follicles, and a reduced number of matured oocytes. These findings indicate that DM adversely affects the ovarian structure of test zebrafish, which can lead to impaired reproduction. Interestingly, treatment with EGCG, as in Group III, improved the ovarian structure of diabetic zebrafish, as evidenced by a decrease in oocyte degeneration as well as a decrease in atria follicles and an increase in the number of matured follicles. These results suggest that EGCG may have a potential therapeutic effect on diabetic-associated ovarian dysfunction. Furthermore, the histological analysis of Group IV showed an ovarian structure similar to that of Group I. This finding indicates that EGCG treatment did not adversely affect the ovarian structure of

control subjects. The histological analysis of the different groups is represented in Figure 6.9[A-D].

6.3.4.2 Histopathology of the testis

The Group-I result showed a normal testis histology containing different stages of spermatogenesis. In contrast, Group-II showed several histological lesions, including degeneration of spermatids, vacuolation, degeneration of the interstitial site, and decreased number of spermatozoa. These results suggest that diabetes significantly impacted the testicular tissue of zebrafish. However, Group-III improved the histological structure of the testis. Although few alterations, such as vacuolation and degeneration of spermatozoa, were still observed, their incidence was lower than that of Group-II. Furthermore, the histological sections of Group IV and Group I showed normal histoarchitecture without any lesions and alterations. Figure 6.10[A-D] depicts the histological sections of the testis under different experimental conditions.

Table 6.1: Changes in GSI and HSI of female experimental zebrafish model. Group-I – control; Group-II – diabetic; Group-III – diabetic + EGCG; Group IV – control + EGCG. Data are expressed as mean \pm SD (n=6). Different superscripts denote significant ($p<0.001$) differences; the same superscripts denote insignificant ($p>0.05$) results between the columns of the exposure groups.

Parameter	Groups	Exposure (Days)			
		Day1	Day 7	Day 14	Day 21
GSI	Group-I	6.91 \pm 0.49 ^a	7.01 \pm 0.45 ^a	7.10 \pm 0.42 ^a	7.14 \pm 0.34 ^a
	Group-II	5.80 \pm 0.55 ^b	5.61 \pm 0.43 ^b	5.48 \pm 0.47 ^b	5.30 \pm 0.57 ^b
	Group-III	5.82 \pm 0.56 ^b	6.05 \pm 0.41 ^b	6.33 \pm 0.45 ^c	6.42 \pm 0.38 ^c
	Group-IV	6.98 \pm 0.44 ^a	7.03 \pm 0.51 ^a	7.11 \pm 0.44 ^a	7.16 \pm 0.50 ^a
HSI	Group-I	0.70 \pm 0.10 ^a	0.75 \pm 0.06 ^a	0.76 \pm 0.08 ^a	0.79 \pm 0.09 ^a
	Group-II	1.28 \pm 0.11 ^b	1.30 \pm 0.12 ^b	1.36 \pm 0.18 ^b	1.54 \pm 0.12 ^b
	Group-III	1.29 \pm 0.15 ^b	1.15 \pm 0.14 ^b	1.07 \pm 0.16 ^c	0.99 \pm 0.09 ^c
	Group-IV	0.70 \pm 0.12 ^a	0.73 \pm 0.12 ^a	0.75 \pm 0.12 ^a	0.77 \pm 0.11 ^a

Table 6.2: Changes in GSI and HSI of male experimental zebrafish model. Group-I – control; Group-II – diabetic; Group-III – diabetic + EGCG; Group IV – control + EGCG. Data are expressed as mean \pm SD (n=6). Different superscripts denote significant ($p<0.001$) differences; the same superscripts denote insignificant ($p>0.05$) results between the columns of the exposure groups.

Parameter	Groups	Exposure (Days)			
		Day 1	Day 7	Day 14	Day 21
GSI	Group-I	0.73 \pm 0.09 ^a	0.75 \pm 0.07 ^a	0.78 \pm 0.07 ^a	0.82 \pm 0.07 ^a
	Group-II	0.58 \pm 0.05 ^b	0.54 \pm 0.08 ^b	0.51 \pm 0.06 ^b	0.48 \pm 0.09 ^b
	Group-III	0.59 \pm 0.08 ^b	0.60 \pm 0.09 ^b	0.63 \pm 0.04 ^c	0.66 \pm 0.07 ^c
	Group-IV	0.73 \pm 0.07 ^a	0.77 \pm 0.09 ^a	0.79 \pm 0.08 ^a	0.83 \pm 0.12 ^a
HSI	Group-I	0.70 \pm 0.10 ^a	0.75 \pm 0.06 ^a	0.76 \pm 0.08 ^a	0.79 \pm 0.09 ^a
	Group-II	1.28 \pm 0.11 ^b	1.30 \pm 0.12 ^b	1.36 \pm 0.17 ^b	1.54 \pm 0.12 ^b

Chapter-6 *Effect of EGCG on diabetes-induced reproductive performance and developmental deformities in zebrafish model*

	Group-III	1.29±0.07 ^b	1.15±0.14 ^b	1.07±0.16 ^c	0.99±0.09 ^c
	Group-IV	0.70±0.12 ^a	0.73±0.12 ^a	0.75±0.12 ^a	0.77±0.11 ^a

Table 6.3: Normal development of zebrafish embryo

Stages	Characterization	Time (hours)
Fertilization	Zygote	0 hour
Zygote stage	Accumulation of cytoplasm at the animal pole. One cell stage	0 hour
Cleavage stage	2 cell stage -16 cell stage division	0.45 minutes -1 hour:30 minutes
Blastula stage	Increase in the number of blastomers. The interface between the yolk and blastoderm is flat	2 hours - 4 hours
Gastrula stage	Epibolic movements start; blastoderm becomes thin and curve	5 hours-10 hours
Segmentation stage	Somites start to develop; undifferentiated mesodermal components of the early tail and tail segments are visible; muscular twitches and an extended tail are observed	10:30 hours- 20 hours
Pharyngula stage	Movement of the tail is spontaneous; the tail detached from the yolk, body pigmentations, retina pigmentation and heart beat is observed	24 hours-36 hours
Hatching	Normal heart beat, yolk extension begins to taper, pigmentation is well defined, and foregut starts to develop	48 hours-96 hours

Table 6.4: Average fecundity, % fertilization, % hatchability and % survival of the F₁ generation. Group-I – control; Group-II – diabetic; Group-III – diabetic + EGCG; Group IV – control + EGCG. Data are expressed as mean \pm SD (n=6). Different superscripts denote significant (p<0.001) differences; the same superscripts denote insignificant (p>0.05) results between the columns of the exposure groups.

Group	Average fecundity	Fertilization (%)	Hatchability (%)	Survival (%)
Group-I	334 \pm 7.9 ^a	98.9 \pm 0.3 ^a	99.4 \pm 0.3 ^a	99.7 \pm 0.5 ^a
Group-II	244 \pm 4.7 ^b	74.8 \pm 3.0 ^b	62.9 \pm 4.2 ^b	60.6 \pm 5.1 ^b
Group-III	274 \pm 5.0 ^c	79.0 \pm 3.0 ^c	81.5 \pm 6.6 ^c	70.8 \pm 4.4 ^c
Group-IV	338 \pm 7.8 ^a	99.1 \pm 0.3 ^a	99.6 \pm 0.2 ^a	99.5 \pm 0.2 ^a

Table 6.5: Percentage deformities of the F₁ generation. Groups: (I) – control; (II) – diabetic; (III) – diabetic + EGCG; (IV) – control + EGCG. Data are expressed as mean \pm SD (n=6). Different superscripts denote significant (p<0.001) differences; the same superscripts denote insignificant (p>0.05) results between the columns of the exposure groups.

Groups	Percentage Deformity						
	24 hpf	48 hpf	72 hpf	120 hpf	168 hpf	10 dpf	14 dpf
I	2.9 \pm 0.1 ^a	1.8 \pm 0.2 ^a	0.0 ^a	0.0 ^a	0.0 ^a	0.0 ^a	0.0 ^a
II	24.4 \pm 1.5 ^b	29.1 \pm 3.7 ^b	20.8 \pm 1.7 ^b	17.3 \pm 2.7 ^b	10.0 \pm 1.6 ^b	5.1 \pm 1.6 ^b	3.9 \pm 1.4 ^b
III	13 \pm 1.7 ^c	19.8 \pm 2.6 ^c	6.2 \pm 1.5 ^c	5.9 \pm 1.9 ^c	5.3 \pm 2.8 ^c	2.2 \pm 0.9 ^c	0.0 ^c
IV	3.0 \pm 0.2 ^a	1.4 \pm 0.2 ^a	0.0 ^a	0.0 ^a	0.0 ^a	0.0 ^a	0.0 ^a

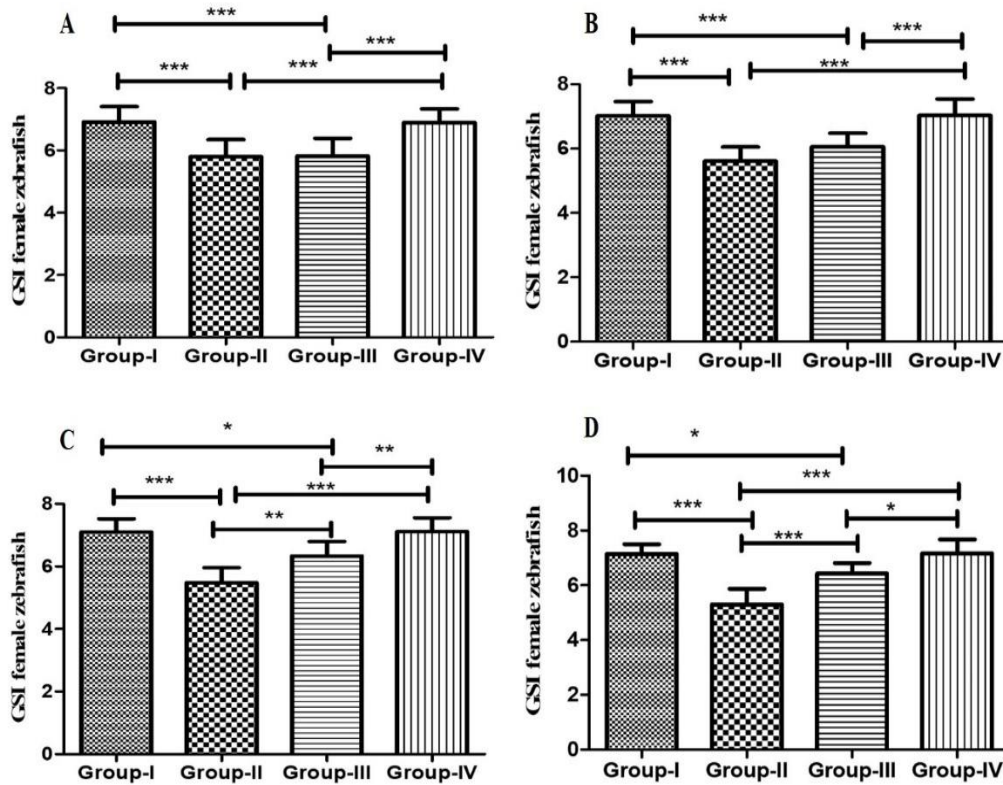


Figure 6.2: Effect of diabetes on the GSI of female zebrafish model. Group-I – control; Group-II – diabetic; Group-III – diabetic + EGCG; Group-IV – control + EGCG. (A) Day 1 (B) Day 7 (C) Day 14 (D) Day 21. Data are represented as mean \pm SD (n=6) and analysed by one-way ANOVA followed by Tukey's post-hoc test. Asterisk represents a significant difference, * $p < 0.05$, ** $p < 0.01$, *** $p < 0.001$.

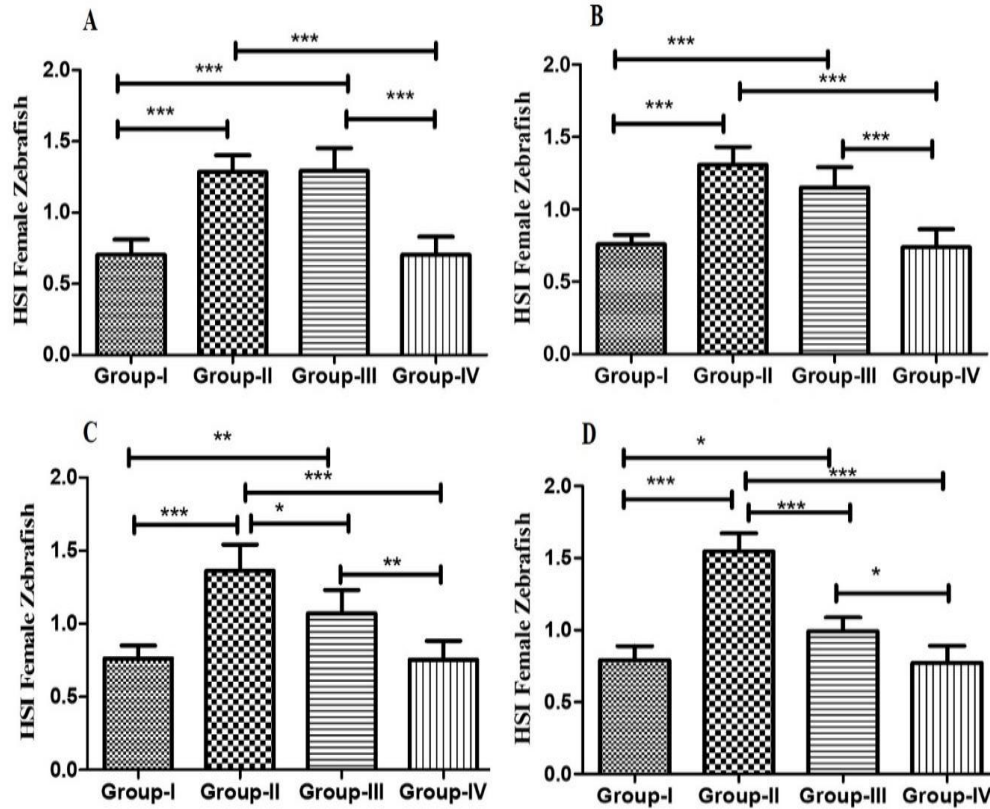


Figure 6.3: Effect of diabetes on the HSI of female zebrafish model. Group-I – control; Group-II – diabetic; Group-III – diabetic + EGCG; Group-IV – control + EGCG. (A) Day 1 (B) Day 7 (C) Day 14 (D) Day 21. Data are represented as mean \pm SD (n=6) and analysed by one-way ANOVA followed by Tukey's post-hoc test. Asterisk represents a significant difference, * $p < 0.05$, ** $p < 0.01$, *** $p < 0.001$.

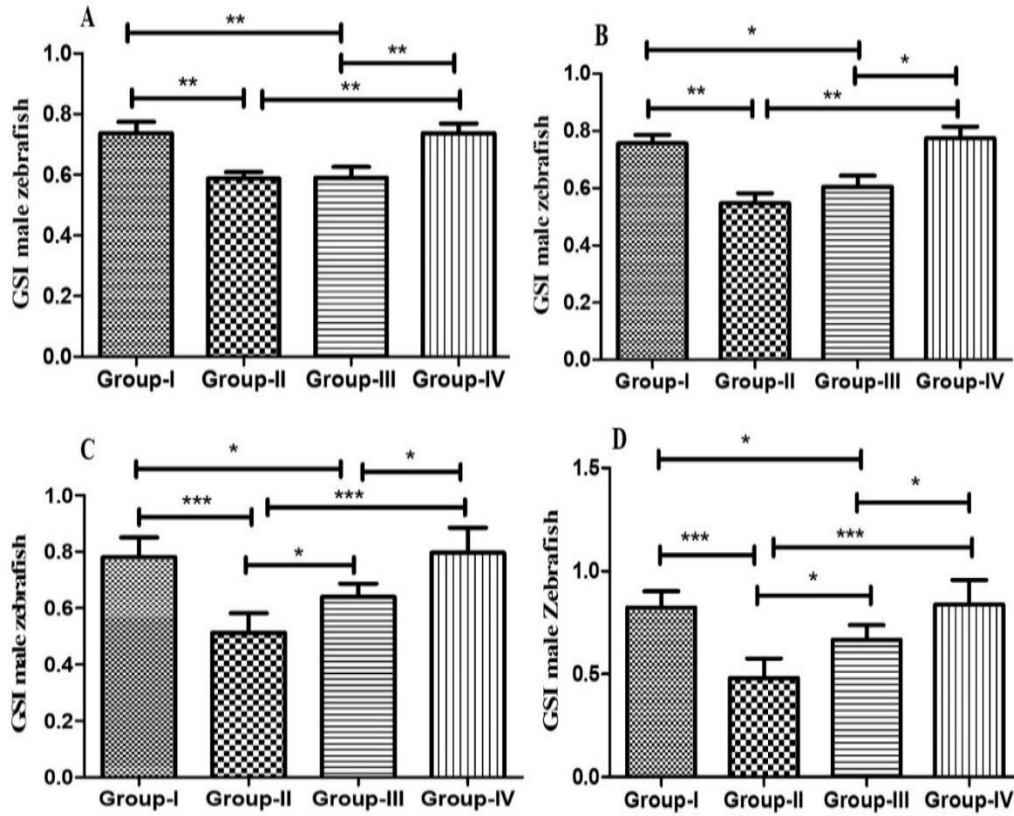


Figure 6.4: Effect of diabetes on the GSI of male zebrafish model. Group-I – control; Group-II – diabetic; Group-III – diabetic + EGCG; Group-IV – control + EGCG. (A) Day 1 (B) Day 7 (C) Day 14 (D) Day 21. Data are represented as mean \pm SD (n=6) and analysed by one-way ANOVA followed by Tukey's post-hoc test. Asterisk represents a significant difference, *p<0.05, **p<0.01, ***p<0.001.

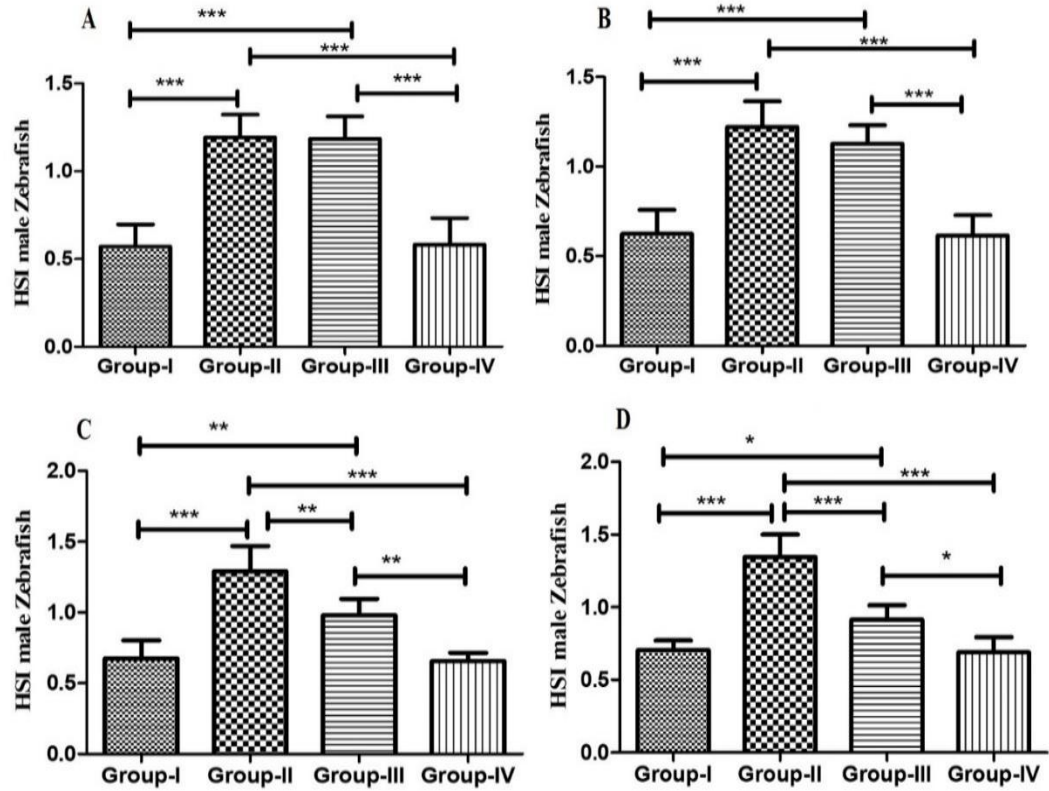


Figure 6.5: Effect of diabetes on the HSI of male zebrafish model. Group-I – control; Group-II – diabetic; Group-III – diabetic + EGCG; Group-IV – control + EGCG. (A) Day 1 (B) Day 7 (C) Day 14 (D) Day 21. Data are represented as mean \pm SD (n=6) and analysed by one-way ANOVA followed by Tukey's post-hoc test. Asterisk represents a significant difference, * $p < 0.05$, ** $p < 0.01$, *** $p < 0.001$.

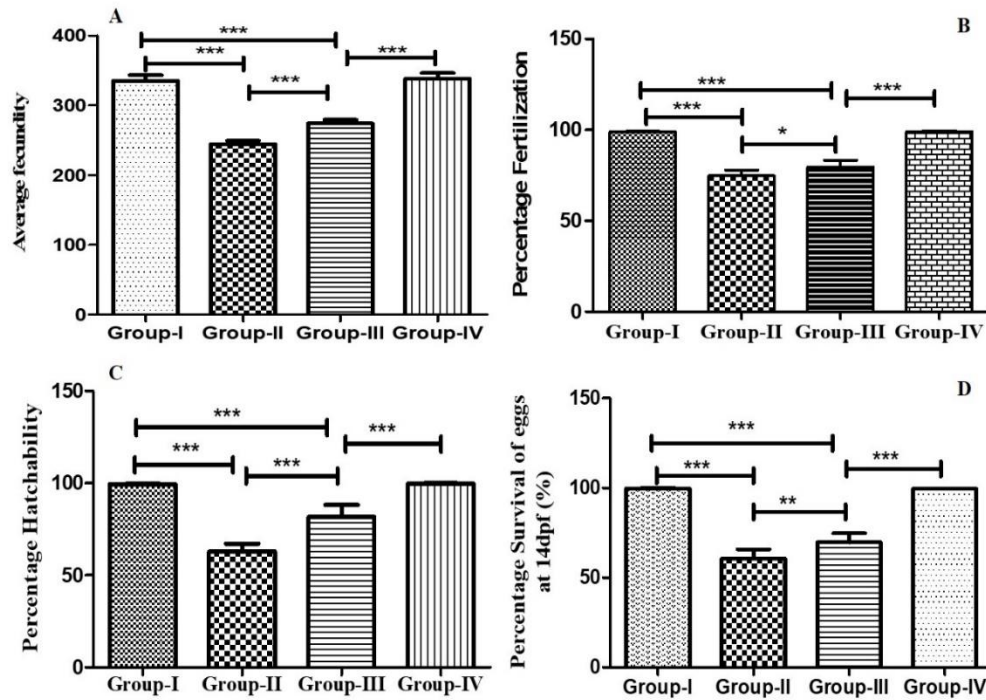


Figure 6.6: Assessment of reproductive parameters. Group-I – control; Group-II – diabetic; Group-III – diabetic + EGCG; Group-IV – control + EGCG. (A) Average fecundity (B) Percentage fertilization (C) Percentage hatchability (D) Percentage survival. Data are expressed as mean \pm SD (n=6) and analysed by one-way ANOVA followed by Tukey's post-hoc test. Asterisk represents a significant difference, *p<0.05; **p<0.01; ***p<0.001.



Figure 6.7: Normal embryonic development of the zebrafish.

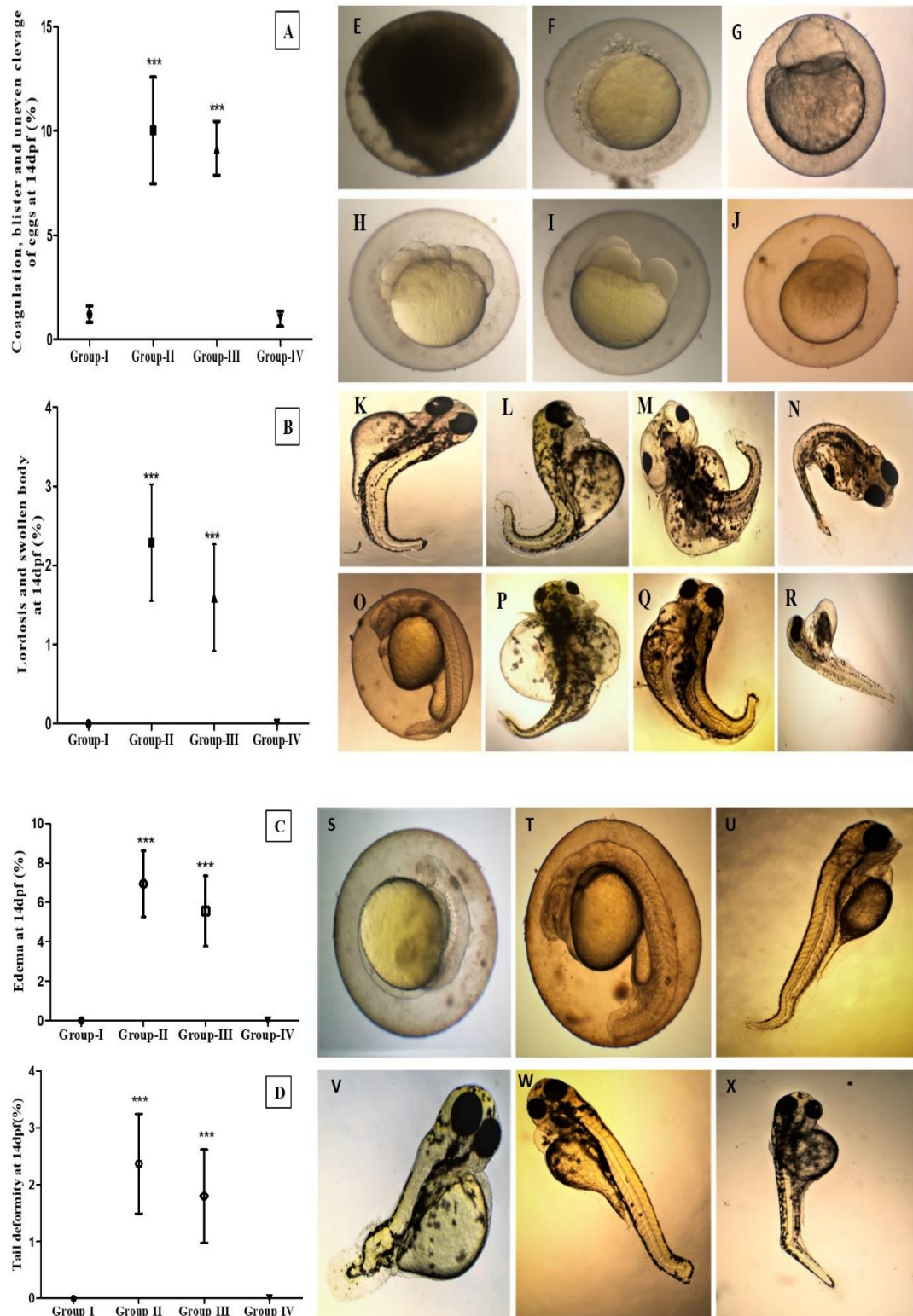


Figure 6.8: Evaluation of deformity in the F₁ generation. (A) coagulation, blisters, and uneven cleavage pattern (%), (B) lordosis and swollen body (%), (C) edema (%), (D) tail deformity (%). (E) egg coagulation, (F-G) blisters in early cell development, (H-J)

uneven cleavage pattern in early cell stages, (K-N) lordosis and swollen body of the larvae, (O-R) pericardial and yolk sac edema, (S-X) tail deformity of developing offspring.

(Figures captured at 40X magnification)

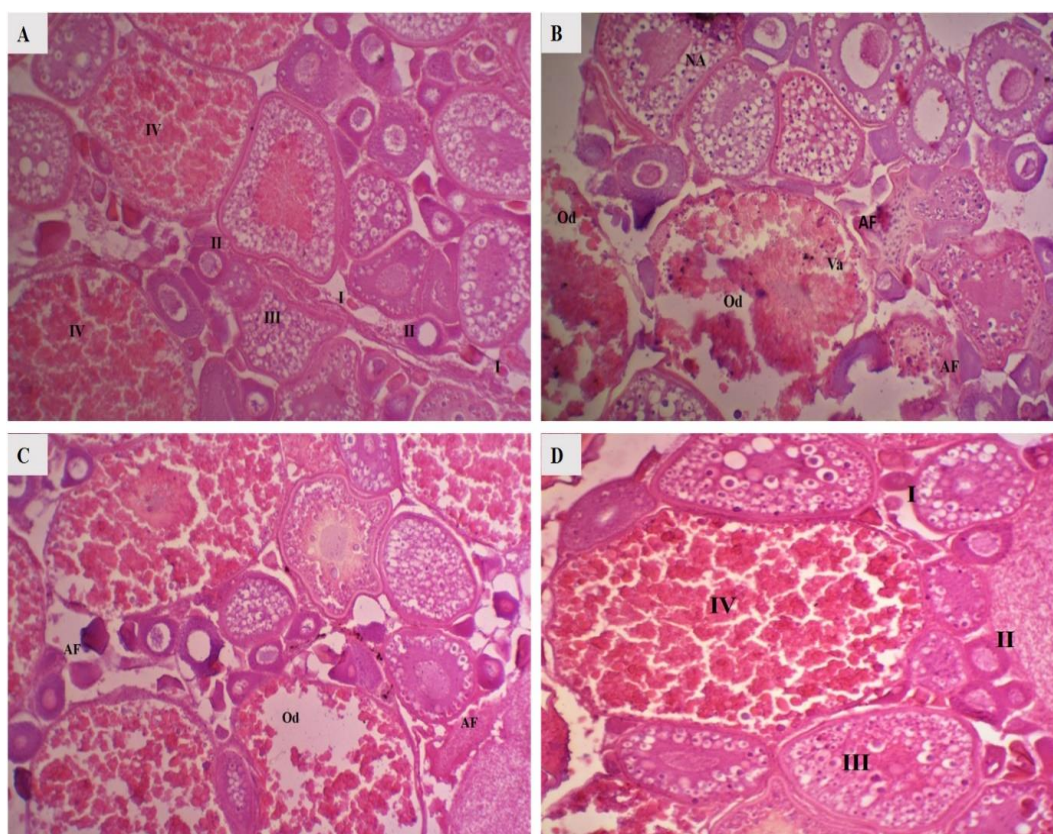


Figure 6.9: Histological changes in the ovary of test zebrafish. (A) Group-I (B) Group-II (C) Group-III (D) Group-IV. The changes in the structure of the ovary are represented as degeneration of oocyte (Od), vacuolation (Va), atretic follicle (AF). Follicles at different stages are represented as developing follicles (I and II), transitioning follicles (III), and fully matured follicles (IV).

(Figures captured at 40X magnification)

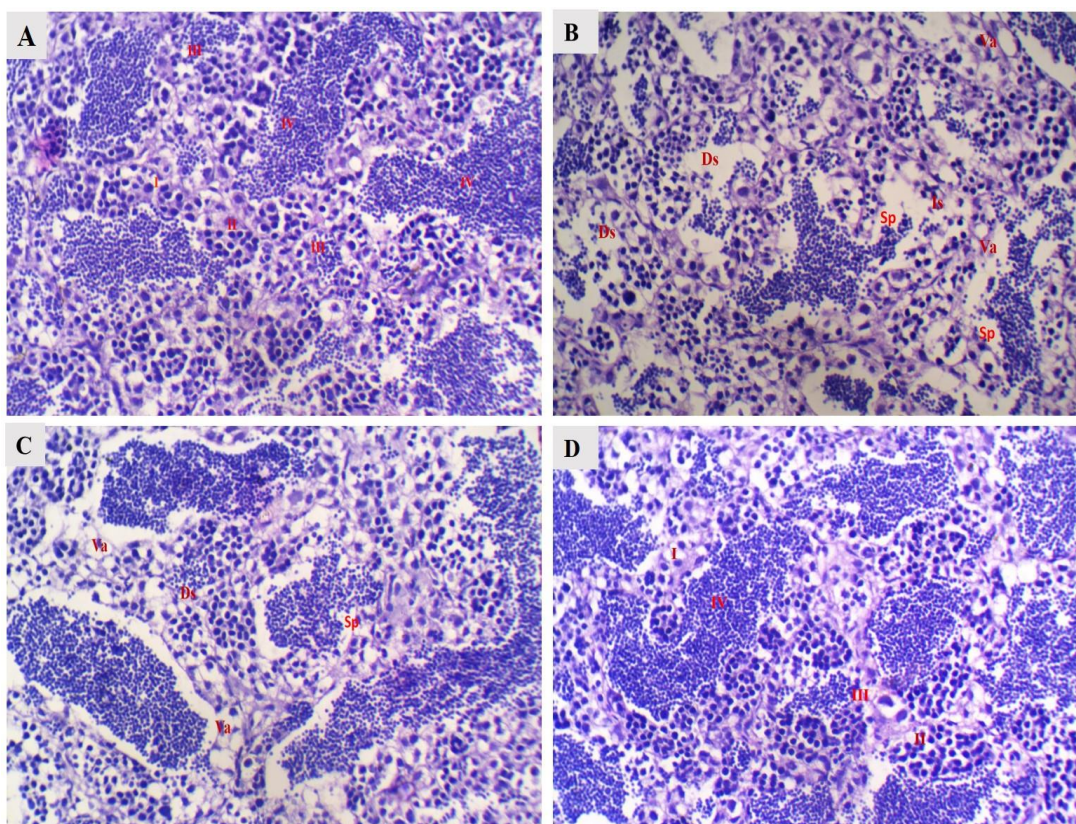


Figure 6.10: Histological changes in the testis of test zebrafish. (A) Group-I (B) Group-II (C) Group-III (D) Group-IV. The different structural changes in the testis are represented as degeneration of spermatids (Ds), vacuolation (Va), degeneration of interstitial site (Is), and decrease in spermatozoa (Sp). Follicles at different stages are represented as primary spermatocyte (I), secondary spermatocyte (II), spermatids (III), and Spermatozoa (IV).

(Figures captured at 40X magnification)

6.4 Discussion

This study delves into the intricate interplay between metabolic disorders, particularly diabetes, and their impact on reproductive function in zebrafish, offering insights into fundamental biology and potential therapeutic avenues. The observed effects of diabetes, such as systemic pathological changes leading to severe complications and impaired reproductive function due to elevated blood glucose levels, underscore the importance of understanding these dynamics in both basic research and potential therapeutic interventions (Molina *et al.*, 2021). The remarkable antioxidant properties of EGCG and its possible role in enhancing gamete quality and fertility are of significant relevance in reproductive health. Its mechanisms, including inhibition of lipid absorption and antioxidative actions, provide a promising avenue for therapeutic intervention (Zhang *et al.*, 2021; Jamir *et al.*, 2023).

The findings, specifically the decrease in gonadal size indicated by GSI and the increase in liver size indicated by HSI in STZ-induced diabetic zebrafish, shed light on the repercussions of diabetes on gonadal development. These changes are likely linked to energy demands during gonadal development and disruptions in the gonadotropin-releasing hormone axis (Ye & Chen, 2020). The rise in HSI could be attributed to fatty acid accumulation and liver enlargement due to diabetes-induced metabolic shifts (Goessling & Sadler, 2015). The beneficial effects of EGCG supplementation on GSI and HSI, especially in Group-III, highlight its potential to counteract the DM-induced disruptions. However, during this study, the response recorded in Group IV further underscores the positive effect of EGCG treatment in the untreated subjects.

The normal embryo was monitored to understand the growth of zebrafish

eggs over time. According to Salis et al. (2021), zebrafish eggs are telolecithal, and their cleavage pattern is discoidal and meroblastic, resembling the vast majority of teleost fish. The exploration of the embryonic stage in zebrafish has witnessed an astonishing rise in prominence. It is a unique approach that permits researchers to investigate the early phases of the full and well-characterized embryonic stage in a vertebrate embryo in a rapid and simple culture system. The embryonic development was observed to be rapid at 28°C, the chorion was seen to be dragged away from the egg after fertilization, and the clear cytoplasm advanced toward the animal pole within the embryo, detaching the blastodisc from the more substantial underlying yolk layer.

The blastodisc exhibited meroblastic cleavage 45 minutes after fertilization. The yolk remained intact. With the advancement of the cleavage stage, a clump of cells on the animal pole was produced called the blastula (Marlow, 2020). Further, in the mid-blastula stage, the cell division was observed to lengthen and become asynchronous; cells initiate transcription of their respective genome instead of depending on maternally supplied mRNA, and cell motility is visible (Kane & Kimmel, 1993; Liu *et al.*, 2021). Around the same time, the marginal cells that still have attachments with the yolk disintegrate, guiding their nuclei and cytoplasmic contents to enter the yolk and establishing a multi-nucleated yolk fluid-filled layer (Bruce, 2016). Subsequently, a couple of other phases, epiboly, or the structured reducing and broadening of the blastula that entirely surrounds the yolk, begins at nearly four hpf, governed by myosin motors within the yolk syncytial layer (Bruce & Heisenberg, 2020). The fraction of the yolk encapsulated by enclosing cells determines the stages during epiboly. At 50% epiboly, cells on the embryo's eventual dorsal side begin involuting, developing the embryonic barrier, and cells continually involute and stretch

backward in the direction of the animal pole as epiboly progresses towards the vegetal pole (Pathak & Barresi, 2020). Epiboly is complete at about 10 hpf, characterized by the tailbud emerging close to the original vegetal pole while the head develops towards the former animal pole. The trunk mesoderm is eventually segmented into somites, arranged from anterior to posterior, typically the initial somites developing around 20 minutes and later somites growing every 30 minutes. At the same duration, nerve impulses start, with the ectodermal layer folding into the nervous system (Bruce, 2016; Diaz-Cuadros *et al.*, 2021). Development and differentiation persist, with nearly all primary organ systems formed by 36 hpf.

The larvae hatch within 48-72 hpf, marking the completion of the embryonic stage. During days 3 and 4, the swim bladder increases, enabling upward swimming within the water column, and then the larvae fish commence to consume food (Robertson *et al.*, 2007). Though the progression of embryonic phases has been standardized to promote growth at 28.5°C, embryos can be nurtured at a higher or lower temperature to accelerate or delay growth. Following the embryonic stage, the zebrafish live the next four weeks as a larva. Development within the larval phase dramatically depends on humidity, temperature, and individual traits, making standardization of larval stages more complex, with size representing an ideal criterion for larval staging (Singleman & Holtzman, 2014). As the fish attain 4 weeks, they are referred to as juveniles, as they will become sexually developed 10 to 12 weeks after fertilization. The sexual identification processes in zebrafish remain intricate and not entirely understood, yet it does not rely on sex chromosomal inheritance. Instead, environmental influences or polygenic sex determination systems could have a role (Liew *et al.*, 2012). Males gradually have a leaner abdomen, whereas gravid females

obtain a broader, rounder abdomen. The usual duration of zebrafish varies depending on strain and rearing; however, zebrafish may survive for 3 to 4 years before exhibiting signs of aging at approximately 2 years.

The impact of parental diabetes on embryonic development, driven by nutrient transfer and epigenetic modifications, is an emerging interest. Maternal hyperglycemia's influence on DNA methylation and acetylation during oocyte formation aligns with its role as a teratogen in diabetic pregnancy (Das & Maitra, 2021). The developmental alterations in diabetic zebrafish offspring underscore the intricate cascade of events stemming from maternal hyperglycemia-induced ROS increases, ultimately leading to congenital disabilities. The subjects treated with EGCG had a positive effect on embryonic development, resulting in increased fecundity, fertilization, hatchability, and offspring survival. In addition, the subjects treated with EGCG had fewer deformities compared to the diabetic group. Similarly, Zhong et al. (2016) observed decreased neural tube abnormalities in diabetic mice treated with EGCG; additionally, it prevented the maternal DM-induced DNA methyltransferase expression and activity, which contributed to an inhibition of DNA hypermethylation.

The reduced mature follicles in the ovary, fibrosis, and vacuolation resonate with the adverse effects of prolonged hyperglycemia and oxidative stress (Paula *et al.*, 2023). The impact of diabetes on ovarian structure and follicular development parallels observations in related studies, emphasizing the role of oxidative stress imbalance in these alterations.

The ability of EGCG to improve follicular development, indicated by decreased atresia and increased follicle counts, holds promise for future therapeutic applications. Similarly, in the male reproductive system, the reduction in

spermatogonia and histological changes align with the findings, underlining the vulnerability of spermatogenic cells to diabetes-induced stress (Zhang *et al.*, 2020; Huang *et al.*, 2020).

The protection of EGCG against germ cell apoptosis and histopathological alterations is consistent with its antioxidative potential and role in maintaining cellular homeostasis. However, the balance between the positive and negative effects of EGCG on fertility highlights the need for tailored interventions (Jiang *et al.*, 2022). The study reveals that EGCG counteracts diabetes-related reproductive issues by safeguarding ovaries and testes, improving follicle and sperm quality, and enhancing reproductive capacity.

Chapter 7

Summary and conclusion

The diabetes state induced by STZ in zebrafish causes discernible alterations to the overall tissues, having a significant impact on the hepatic, renal, and gill tissues with cascading effects on the overall test subject's vitality. Adopting zebrafish as an experimental model is prudent, leveraging their physiological similarity to human systems and making them an effective platform for understanding the complexities of metabolic diseases.

The acute toxicity study and behavioural responses in the zebrafish model treated with EGCG represent a comprehensive investigation into the safety and potential therapeutic effects of EGCG in aquatic environments. EGCG, a bioactive compound found in green tea, has garnered significant attention for its diverse health benefits in humans, ranging from antioxidant properties to potential therapeutic applications in various diseases. However, its effects on organisms, particularly zebrafish, remain relatively unexplored.

This study aimed to fill this gap by assessing the acute toxicity of EGCG in zebrafish and evaluating its impact on various behavioural parameters, including swimming behaviour, overall physiological status, and histological damage in the liver, kidney, and gill tissues.

The findings of this study provide valuable insights into the safety profile and potential therapeutic effects of EGCG in the zebrafish model. Furthermore, the study demonstrated that the zebrafish model was extremely sensitive to EGCG, as indicated by their behavioural reactions, confirming the usefulness of zebrafish as a model for studying the effects of EGCG. A high concentration of EGCG was explicitly proven to be toxic, inflicting severe damage to the gills, kidneys, and liver, interfering with the experimental normal physiological functions of the zebrafish model.

The investigation into estimating the minimum effective dose for EGCG and

its effects on the general physiological status and fin regeneration in experimental zebrafish offers valuable insights into the potential therapeutic applications of EGCG. Despite the extensive literature documenting the use of animal models for DM research, there remains a dearth of studies investigating the potential of EGCG in promoting regeneration in the caudal fin of diabetic zebrafish model. This study holds promise as an initial exploration into the safe and efficacious utilization of EGCG for wound healing and regenerative applications in the hyperglycemic milieu characteristic of the diabetic zebrafish model.

In the present study, the results showed that EGCG had a significant effect on blood glucose levels, body weight, body mass index, and caudal fin regrowth in the hyperglycemic zebrafish model, indicating its role in facilitating tissue repair and regeneration processes. Furthermore, understanding the mechanism of EGCG in enhancing caudal fin regeneration in DM-induced zebrafish may have larger implications. The results suggested that EGCG could be used as a powerful adjuvant along with a known potent drug to treat poor wound healing in the zebrafish model.

Further, the investigation into the effect of EGCG on lipid profiles and metabolic enzyme activity in experimental zebrafish provides valuable insights into the potential therapeutic applications of EGCG in managing metabolic disorders and associated complications. The study aimed to elucidate the impact of EGCG on lipid metabolism and the activity of key metabolic enzymes in zebrafish, which serve as important indicators of overall metabolic health and disease status.

The study also revealed that EGCG treatment resulted in significant improvements in lipid profiles in zebrafish with dyslipidemia, including reduced levels of total cholesterol (TC), triglycerides (TG), low-density lipoprotein (LDL), and very-low-density lipoprotein (VLDL), as well as increased levels of high-density lipoprotein

(HDL) and cholesterol. These findings suggest that EGCG may exert beneficial effects on lipid metabolism, potentially mitigating the risk of cardiovascular disease and other metabolic complications associated with dyslipidemia.

Furthermore, the study demonstrated that EGCG treatment modulated the activity of key metabolic enzymes, including alanine aminotransferase (ALT), aspartate aminotransferase (AST), and alkaline phosphatase (ALP) in zebrafish tissues. EGCG treatment resulted in a notable reduction in ALT and AST activity in the hepatic tissue, indicating improved liver function and reduced hepatic damage. Further, the study recorded the ameliorating effect of ALT and AST in the renal and gills tissue, suggesting a potential protective effect against organ damage and overall health of the subject. Additionally, EGCG treatment led to a decrease in ALP activity in hepatic and renal tissues, suggesting a potential protective effect against genotoxic and cytotoxic effects. The discernible increase in the lipid profile and enzymes following diabetic induction, combined with their subsequent restoration following EGCG administration, emphasizes the critical role these parameters play as sensitive markers heralding diabetes progression and, thus, potential targets for therapeutic interventions.

The study further demonstrates EGCG as a promising therapeutic agent against diabetes-related complications, demonstrating efficacy in mitigating oxidative stress, ameliorating histopathological lesions, and preserving organ integrity in diabetic zebrafish. Oxidative stress is a crucial factor in the pathogenesis of various diseases, including metabolic disorders, neurodegenerative diseases, and cardiovascular diseases. The therapeutic potential of EGCG was assessed in a zebrafish model, which offers unique advantages for studying oxidative stress and histopathological changes due to its genetic tractability, rapid development, and physiological similarities to humans.

The findings of this study underscore the therapeutic potential of EGCG in mitigating oxidative stress and histopathological changes in a zebrafish model. EGCG treatment enhanced the activity of antioxidant enzymes such as superoxide dismutase (SOD) and catalase (CAT), which play critical roles in neutralizing ROS and protecting cells from oxidative damage. Moreover, EGCG treatment demonstrated remarkable efficacy in mitigating histopathological changes associated with oxidative stress, including tissue damage, inflammation, and cellular apoptosis. Histological analysis in the liver, kidney, and gills tissue revealed a significant reduction in tissue damage and inflammatory cell infiltration in EGCG-treated zebrafish compared to untreated controls. Furthermore, EGCG treatment promoted tissue regeneration and restoration of normal histological features, indicating its potential for tissue repair and recovery.

This study also contributes valuable insights into the intersection of metabolic disorders and reproductive health. DM is a complex metabolic disorder characterized by chronic hyperglycemia and systemic complications affecting various organ systems, including the reproductive system. Reproductive dysfunction and developmental abnormalities are common complications of diabetes, giving rise to deleterious challenges to affected individuals.

The findings of the study revealed that EGCG had an ameliorating effect on the reproductive parameters in DM-induced zebrafish. EGCG improves the GSI and HSI of diabetic zebrafish. EGCG administration further improves the hatchability, fertility, and survival of the offspring of the first filial generation to diabetic parent zebrafish. Furthermore, EGCG treatment demonstrated significant efficacy in preventing developmental deformities in zebrafish embryos exposed to maternal diabetes. Zebrafish embryos from diabetic mothers treated with EGCG exhibited reduced incidence and severity of developmental abnormalities compared to untreated

controls. EGCG-treated embryos showed improved embryonic development, reduced oxidative stress, and enhanced cellular viability, indicating its protective effects against diabetes-induced teratogenicity.

Additionally, EGCG treatment effectively mitigated diabetes-induced reproductive dysfunction in zebrafish, as evidenced by improvements in testicular morphology, follicle development, and sperm quality. EGCG-treated zebrafish exhibited increased follicle counts, reduced atresia, and enhanced sperm quality compared to untreated diabetic controls. These findings suggest that EGCG can potentially restore reproductive function and improve fertility in diabetic individuals. The findings of this study highlight the potential therapeutic benefits of EGCG in mitigating diabetes-induced reproductive dysfunction and developmental deformities in a zebrafish model. The antioxidant and anti-inflammatory properties of EGCG, coupled with its ability to regulate glucose metabolism and improve cellular function, make it a promising candidate for managing diabetic complications affecting reproductive health and embryonic development.

Further research is warranted to elucidate the underlying mechanisms of the protective effects of EGCG and optimize its clinical applications in preventing and treating diabetic reproductive complications. This finding significantly enhances our understanding of the mechanisms at play, offering new perspectives for managing reproductive health in metabolic disorders. In the ever-advancing field of diabetes research, the present study highlights the intricate ensemble of metabolic abnormalities and the possibility of EGCG to realign the disrupted system.

Recommendations and future perspective

The ability of EGCG to alleviate diabetes symptoms ignites a growing hope for developing novel therapy regimens. However, this research commends for further

investigations into the inner workings of the defensive arsenal of EGCG. The complicated arrangement of molecular events that provide EGCG with its exceptional efficiency warrants rigorous dissection, providing a broader explication of its mechanism of action. Furthermore, the precise mechanism underscoring the protective attributes of EGCG necessitates further scrutiny, warranting a comprehensive exploration to unveil its latent potential for translation into clinical applications for diabetes management. Some recommendations for future studies are laid below.

1. Conduct in-depth research on how EGCG affects zebrafish behaviour and neurodevelopment over the long run.
2. Exploring of potential interactions between EGCG and other environmental stressors to assess combined toxicity effects.
3. Investigation of the molecular mechanisms underlying the effects of EGCG on fin regeneration to elucidate its regenerative potential.
4. Optimising dosage regimens when combined with other therapeutic drugs to ascertain the most efficient and long-lasting treatment plans for fin regeneration.
5. Exploration of the influence of EGCG on other physiological parameters, such as immune function and reproductive health.
6. Examination of the long-term effects of EGCG treatment on lipid metabolism and metabolic enzyme activity in zebrafish.
7. Elucidation of the molecular pathways involved in EGCG-mediated protection
8. against oxidative stress and tissue damage.
9. Investigation of the potential synergistic effects of EGCG with other antioxidants or therapeutic agents for enhancing repair and regeneration in the affected organs.

10. Examination of the underlying mechanisms by which EGCG improves reproductive function and prevents developmental abnormalities in diabetic zebrafish.
11. Investigation of the optimal timing and duration of EGCG treatment during critical developmental stages to maximize the therapeutic benefits.

Additionally, EGCG has varied impacts on different cell types, both in *vitro* and in *vivo*. Although the qualities of EGCG have been steadily defined, specific issues still remain. In terms of use, combining EGCG with other anti-diabetic medications can have a synergistic and beneficial impact. Nevertheless, EGCG still faces numerous hurdles for therapeutic implementation. EGCG has limited bioavailability, whether administered orally or *via* venous injection, and concentration, derivatives, and other circumstances easily influence its effects. Solutions are still needed on how to transport EGCG to the desired sites effectively.

References

- Abbott, W. S. (1925). A method of computing the effectiveness of an insecticide. *Journal of Economic Entomology*, 18(2), 265-267.
- Abdelhamid, F. M., Mahgoub, H. A., & Ateya, A. I. (2020). Ameliorative effect of curcumin against lead acetate-induced hemato-biochemical alterations, hepatotoxicity, and testicular oxidative damage in rats. *Environmental Science and Pollution Research*, 27(10), 10950-10965.
- Aboelkhair, N. T., Kasem, H. E., Abdelmoaty, A. A., & El-Edel, R. H. (2021). TCF7L2 gene polymorphism as a risk for type 2 diabetes mellitus and diabetic microvascular complications. *Molecular Biology Reports*, 48(6), 5283-5290.
- Adebayo, O. T. (2006). Reproductive performance of african clariid catfish *Clarias gariepinus* broodstocks on varying maternal stress. *Journal of Fisheries International*, 1(1-2):17-20.
- Ahmed, B., Sultana, R., & Greene, M. W. (2021). Adipose tissue and insulin resistance in obese. *Biomedicine & pharmacotherapy*, 137, 111315. <https://doi.org/10.1016/j.biopha.2021.111315>
- Ahmed, N. A., Radwan, N. M., Aboul Ezz, H. S., & Salama, N. A. (2017). The antioxidant effect of Green Tea Mega EGCG against electromagnetic radiation-induced oxidative stress in the hippocampus and striatum of rats. *Electromagnetic biology and medicine*, 36(1), 63–73.
- Akil, A. A., Yassin, E., Al-Maraghi, A., Aliyev, E., Al-Malki, K., & Fakhro, K. A. (2021). Diagnosis and treatment of type 1 diabetes at the dawn of the personalized medicine era. *Journal of translational medicine*, 19(1), 137. <https://doi.org/10.1186/s12967-021-02778-6>
- Akpoveso, O. P., Ubah, E. E., & Obasanmi, G. (2023). Antioxidant Phytochemicals as Potential Therapy for Diabetic Complications. *Antioxidants (Basel, Switzerland)*, 12(1), 123. <https://doi.org/10.3390/antiox12010123>
- Alam, M., Ali, S., Ashraf, G. M., Bilgrami, A. L., Yadav, D. K., & Hassan, M. I. (2022). Epigallocatechin 3-gallate: From green tea to cancer therapeutics. *Food chemistry*, 15;379:132135. <https://doi.org/10.1016/j.foodchem.2022.132135>
- Alam, S., Hasan, M. K., Neaz, S., Hussain, N., Hossain, M. F., & Rahman, T. (2021). Diabetes Mellitus: insights from epidemiology, biochemistry, risk factors, diagnosis, complications and comprehensive management. *Diabetology*,

References

2(2), 36-50.

- Alam, U., Asghar, O., Azmi, S., & Malik, R. A. (2014). General aspects of diabetes mellitus. *Handbook of clinical neurology*, 126, 211–222.
<https://doi.org/10.1016/B978-0-444-53480-4.00015-1>
- Alavi, M. S., Fanoudi, S., Hosseini, M., & Sadeghnia, H. R. (2022). Beneficial effects of levetiracetam in streptozotocin-induced rat model of Alzheimer's disease. *Metabolic Brain Disease*, 37(3), 689-700.
- Alipin, K., Istiqamah, N., & Maryani, A. Madihah. (2019). The potential of combined *curcuma xanthorrhiza* rhizome and *averrhoa blimbi* fruit extract on decreasing blood glucose levels, insulinitis degree and liver structure repair of diabetic male wistar rats streptozotocin induced. *Journal of Diabetes and Metabolism*, 10:835. doi: 10.35248/2155-6156.19.10.835
- Al-Sowayan, N. S., & AL-Sallali, R. M. (2023). The effect of aloin in blood glucose and antioxidants in male albino rats with Streptozotocin-induced diabetic. *Journal of King Saud University-Science*, 35(4), 102589.
<https://doi.org/10.1016/j.jksus.2023.102589>
- Alves-Bezerra, M., & Cohen, D. E. (2017). Triglyceride metabolism in the liver. *Comprehensive Physiology*, 8(1), 1–8.
- Amirkhosravi, L., Kordestani, Z., Nikooei, R., Safi, Z., Yeganeh-Hajahmadi, M., & Mirtajaddini-Goki, M. (2023). Exercise-related alterations in MCT1 and GLUT4 expressions in the liver and pancreas of rats with STZ-induced diabetes. *Journal of diabetes and metabolic disorders*, 22(2), 1355–1363.
- Amjad, S., Sharma, A. K., & Serajuddin, M. (2018). Toxicity assessment of cypermethrin nanoparticles in *Channa punctatus*: Behavioural response, micronuclei induction and enzyme alteration. *Regulatory toxicology and pharmacology: RTP*, 100, 127–133.
- Anand, U., Jacobo-Herrera, N., Altemimi, A., & Lakhssassi, N. (2019). A comprehensive review on medicinal plants as antimicrobial therapeutics: potential avenues of biocompatible drug discovery. *Metabolites*, 9(11), 258.
<https://doi.org/10.3390/metabo9110258>
- Angom, R. S., & Nakka, N. M. R. (2024). Zebrafish as a model for cardiovascular and metabolic disease: The future of precision medicine. *Biomedicines*, 12(3), 693. <https://doi.org/10.3390/biomedicines12030693>

References

- Ansari, P., Akther, S., Hannan, J. M. A., Seidel, V., Nujat, N. J., & Abdel-Wahab, Y. H. A. (2022a). Pharmacologically active phytomolecules isolated from traditional antidiabetic plants and their therapeutic role for the management of diabetes mellitus. *Molecules*, 27(13), 4278.
<https://doi.org/10.3390/molecules27134278>
- Ansari, U., Hanif, M. K., Paracha, A. I., Quratulain, Tariq, A., & Haneef, S. (2022b). Comparing the effect of chronic hyperglycemia on intra ocular pressure in diabetic patients. *Pakistan Journal of Pathology*, 33(4), 119-123.
- Arrese, M., Barrera, F., Triantafilo, N., & Arab, J. P. (2019). Concurrent nonalcoholic fatty liver disease and type 2 diabetes: diagnostic and therapeutic considerations. *Expert review of gastroenterology & hepatology*, 13(9), 849–866.
- Artime, E., Romera, I., Díaz-Cerezo, S., & Delgado, E. (2021). Epidemiology and economic burden of cardiovascular disease in patients with type 2 diabetes mellitus in Spain: A systematic review. *Diabetes therapy: research, treatment and education of diabetes and related disorders*, 12(6), 1631–1659.
- Arunachalam, M., Raja, M., Vijayakumar, C., Malaïammal, P., & Mayden, R. L. (2013). Natural history of zebrafish (*Danio rerio*) in India. *Zebrafish*, 10(1), 1–14.
- Asbaghi, O., Fouladvand, F., Gonzalez, M. J., Ashtary-Larky, D., Choghakhori, R., & Abbasnezhad, A. (2021). Effect of green tea on glycemic control in patients with type 2 diabetes mellitus: A systematic review and meta-analysis. *Diabetes & metabolic syndrome*, 15(1), 23–31.
- Azadbakht, F., Shirali, S., Ronagh, M. T., & Zamani, I. (2019). Assessment of Gill Pathological Responses in Yellowfin Sea Bream (*Acanthopagrus Latus*) Under Aeromonas Hydrophila Exposure. *Archives of Razi Institute*, 74(1), 83–89.
- Babel, R. A., & Dandekar, M. P. (2021). A review on cellular and molecular mechanisms linked to the development of diabetes complications. *Current diabetes reviews*, 17(4), 457-473.
- Badroo, I. A., Nandurkar, H. P., & Khanday, A. H. (2020). Toxicological impacts of herbicide paraquat dichloride on histological profile (gills, liver, and kidney)

References

- of freshwater fish *Channa punctatus* (Bloch). *Environmental science and pollution research international*, 27(31), 39054–39067.
- Baltzis, D., Eleftheriadou, I., & Veves, A. (2014). Pathogenesis and treatment of impaired wound healing in diabetes mellitus: new insights. *Advances in therapy*, 31(8), 817–836.
- Baluchnejadmojarad, T., & Roghani, M. (2012). Chronic oral epigallocatechin-gallate alleviates streptozotocin-induced diabetic neuropathic hyperalgesia in rat: involvement of oxidative stress. *Iranian journal of pharmaceutical research*, 11(4), 1243–1253.
- Banday, M. Z., Sameer, A. S., & Nissar, S. (2020). Pathophysiology of diabetes: An overview. *Avicenna journal of medicine*, 10(4), 174–188.
- Banerjee, Y., Patti, A. M., Giglio, R. V., Ciaccio, M., Vichithran, S., Faisal, S., Stoian, A. P., Rizvi, A. A., & Rizzo, M. (2023). The role of atherogenic lipoproteins in diabetes: Molecular aspects and clinical significance. *Journal of diabetes and its complications*, 37(8), 108517.
<https://doi.org/10.1016/j.jdiacomp.2023.108517>
- Bartosikova, L., & Necas, J. (2018). Epigallocatechin gallate: A review. *Veterinárni medicína*, 63(10), 443–467.
- Bashir, S. O. (2019). Concomitant administration of resveratrol and insulin protects against diabetes mellitus type-1-induced renal damage and impaired function via an antioxidant-mediated mechanism and up-regulation of Na⁺/K⁺-ATPase. *Archives of physiology and biochemistry*, 125(2), 104–113.
- Baynes, H. W. (2015). Classification, pathophysiology, diagnosis and management of diabetes mellitus. *Journal of diabetes and metabolism*, 6: 541.
[doi:10.4172/2155-6156.1000541](https://doi.org/10.4172/2155-6156.1000541)
- Bellamkonda, R., Rasineni, K., Singareddy, S. R., Kasetti, R. B., Pasurla, R., Chippada, A. R., & Desireddy, S. (2011). Antihyperglycemic and antioxidant activities of alcoholic extract of *Commiphora mukul* gum resin in streptozotocin induced diabetic rats. *Pathophysiology*, 18(4), 255–261.
- Ben-Aicha, S., Badimon, L., & Vilahur, G. (2020). Advances in HDL: Much More than Lipid Transporters. *International journal of molecular sciences*, 21(3), 732. <https://doi.org/10.3390/ijms21030732>

References

- Benchoula, K., Khatib, A., Jaffar, A., Ahmed, Q. U., Sulaiman, W. M. A. W., Abd Wahab, R., & El-Seedi, H. R. (2019). The promise of zebrafish as a model of metabolic syndrome. *Experimental animals*, 68(4), 407-416.
- Berberich, A. J., & Hegele, R. A. (2022). A modern approach to dyslipidemia. *Endocrine Reviews*, 43(4), 611-653.
- Beyaz, S., Özlem, G. Ö. K., & Aslan, A. (2022). The therapeutic effects and antioxidant properties of epigallocatechin-3 gallate: A new review. *International Journal of Secondary Metabolite*, 9(2), 125-136.
- Bhattacharjee, B., Pal, P. K., Chattopadhyay, A., & Bandyopadhyay, D. (2020). Oleic acid protects against cadmium induced cardiac and hepatic tissue injury in male Wistar rats: A mechanistic study. *Life sciences*, 244, 117324. <https://doi.org/10.1016/j.lfs.2020.117324>
- Black, H. S. (2022). A synopsis of the associations of oxidative stress, ROS, and antioxidants with diabetes mellites. *Antioxidants*, 11(10), 2003. <https://doi.org/10.3390/antiox1110200>
- Blahova, J., Martiniakova, M., Babikova, M., Kovacova, V., Mondockova, V., & Omelka, R. (2021). Pharmaceutical drugs and natural therapeutic products for the treatment of type 2 diabetes mellitus. *Pharmaceuticals (Basel, Switzerland)*, 14(8), 806. <https://doi.org/10.3390/ph14080806>
- Bojarski, B., & Witeska, M. (2020). Blood biomarkers of herbicide, insecticide, and fungicide toxicity to fish-a review. *Environmental science and pollution research international*, 27(16), 19236–19250.
- Boren, J., Taskinen, M. R., Björnson, E., & Packard, C. J. (2022). Metabolism of triglyceride-rich lipoproteins in health and dyslipidaemia. *Nature Reviews Cardiology*, 19(9), 577-592.
- Bruce, A. E. (2016). Zebrafish epiboly: Spreading thin over the yolk. *Developmental Dynamics*, 245(3), 244-258.
- Bruce, A. E., & Heisenberg, C. P. (2020). Mechanisms of zebrafish epiboly: A current view. *Current topics in developmental biology*, 136, 319-341.
- Burgess, J. L., Wyant, W. A., Abdo Abujamra, B., Kirsner, R. S., & Jozic, I. (2021). Diabetic Wound-Healing Science. *Medicina (Kaunas, Lithuania)*, 57(10), 1072. <https://doi.org/10.3390/medicina57101072>

References

- Cannon, C. P. (2020). Low-density lipoprotein cholesterol: lower is totally better. *Journal of the American College of Cardiology*, 75(17), 2119-2121.
- Carbone, S., Del Buono, M. G., Ozemek, C., & Lavie, C. J. (2019). Obesity, risk of diabetes and role of physical activity, exercise training and cardiorespiratory fitness. *Progress in cardiovascular diseases*, 62(4), 327-333.
- Carvalho, J. C. T., Keita, H., Santana, G. R., de Souza, G. C., Dos Santos, I. V. F., Amado, J. R. R., Kourouma, A., Prada, A. L., Carvalho, H. O., & Silva, M. L. (2018). Effects of *Bothrops alternatus* venom in zebrafish: a histopathological study. *Inflammopharmacology*, 26, 273-284.
- Carvalho, M. T. B., Araújo-Filho, H. G., Barreto, A. S., Quintans-Júnior, L. J., Quintans, J. S. S., & Barreto, R. S. S. (2021). Wound healing properties of flavonoids: A systematic review highlighting the mechanisms of action. *Phytomedicine: international journal of phytotherapy and phytopharmacology*, 90, 153636.
<https://doi.org/10.1016/j.phymed.2021.153636>
- Cavati, G., Pirrotta, F., Merlotti, D., Ceccarelli, E., Calabrese, M., Gennari, L., & Mingiano, C. (2023). Role of advanced glycation end-products and oxidative stress in type-2-diabetes-induced bone fragility and implications on fracture risk stratification. *Antioxidants (Basel, Switzerland)*, 12(4), 928.
<https://doi.org/10.3390/antiox12040928>
- Chebotareva, N., Bobkova, I., Lysenko, L., & Moiseev, S. (2021). Urinary markers of podocyte dysfunction in chronic glomerulonephritis. *Advances in experimental medicine and biology*, 1306, 81–99.
- Chen, C., & Liu, D. (2022). Establishment of zebrafish models for diabetes mellitus and its microvascular complications. *Journal of Vascular Research*, 59(4), 251-260.
- Chen, Y., Lee, K., Ni, Z., & He, J. C. (2020). Diabetic kidney disease: challenges, advances, and opportunities. *Kidney diseases*, 6(4), 215-225.
- Cheng, X. M., Hu, Y. Y., Yang, T., Wu, N., & Wang, X. N. (2022). Reactive oxygen species and oxidative stress in vascular-related diseases. *Oxidative medicine and cellular longevity*, 2022, 7906091.
<https://doi.org/10.1155/2022/7906091>

References

- Choi, T. Y., Choi, T. I., Lee, Y. R., Choe, S. K., & Kim, C. H. (2021). Zebrafish as an animal model for biomedical research. *Experimental & Molecular Medicine*, 53(3), 310-317.
- Cione, E., La Torre, C., Cannataro, R., Caroleo, M. C., Plastina, P., & Gallelli, L. (2019). Quercetin, epigallocatechin gallate, curcumin, and resveratrol: From dietary sources to human microRNA modulation. *Molecules (Basel, Switzerland)*, 25(1), 63. <https://doi.org/10.3390/molecules25010063>
- Cleven, L., Krell-Roesch, J., Nigg, C. R., & Woll, A. (2020). The association between physical activity with incident obesity, coronary heart disease, diabetes and hypertension in adults: a systematic review of longitudinal studies published after 2012. *BMC public health*, 20(1), 726. <https://doi.org/10.1186/s12889-020-08715-4>
- Cochran, B. J., Manandhar, B., & Rye, K. A. (2022). HDL and diabetes. *Advances in experimental medicine and biology*, 1377, 119–127.
- Colosimo, S., Mitra, S. K., Chaudhury, T., & Marchesini, G. (2023). Insulin resistance and metabolic flexibility as drivers of liver and cardiac disease in T2DM. *Diabetes research and clinical practice*, 206, 111016. <https://doi.org/10.1016/j.diabres.2023.111016>
- Coman, L. I., Coman, O. A., Bădăraș, I. A., Păunescu, H., & Ciocîrlan, M. (2021). Association between liver cirrhosis and diabetes mellitus: A review on hepatic outcomes. *Journal of clinical medicine*, 10(2), 262. <https://doi.org/10.3390/jcm10020262>
- Correia, A. S., Cardoso, A., & Vale, N. (2023). Oxidative stress in depression: The link with the stress response, neuroinflammation, serotonin, neurogenesis and synaptic plasticity. *Antioxidants (Basel, Switzerland)*, 12(2), 470. <https://doi.org/10.3390/antiox12020470>
- Daryabor, G., Atashzar, M. R., Kabelitz, D., Meri, S., & Kalantar, K. (2020). The effects of type 2 diabetes mellitus on organ metabolism and the immune system. *Frontiers in immunology*, 11, 1582. <https://doi.org/10.3389/fimmu.2020.01582>
- Das, J., & Maitra, A. (2021). Maternal DNA methylation during pregnancy: A review. *Reproductive sciences*, 28(10), 2758–2769.

References

- Dashty M. (2013). A quick look at biochemistry: carbohydrate metabolism. *Clinical biochemistry*, 46(15), 1339–1352.
- Delomas, T. A., & Dabrowski, K. (2018). Larval rearing of zebrafish at suboptimal temperatures. *Journal of thermal biology*, 74, 170-173.
- Deng, B., Song, A., & Zhang, C. (2023). Cell-cycle dysregulation in the pathogenesis of diabetic kidney disease: An update. *International journal of molecular sciences*, 24(3), 2133. <https://doi.org/10.3390/ijms24032133>
- Devi, S., Singh, K., & Pankaj, P. P. (2015). Female sexual dysfunctions in diabetes mellitus: Prevalence risk factor and diagnosis. *Bulletin of Pure & Applied Sciences-Zoology*, 34(1 & 2), 17-23.
- Dewidar, B., Kahl, S., Pafili, K., & Roden, M. (2020). Metabolic liver disease in diabetes - From mechanisms to clinical trials. *Metabolism: clinical and experimental*, 111S, 154299. <https://doi.org/10.1016/j.metabol.2020.154299>
- Diaz-Cuadros, M., Pourquié, O., & El-Sherif, E. (2021). Patterning with clocks and genetic cascades: Segmentation and regionalization of vertebrate versus insect body plans. *PLoS genetics*, 17(10), e1009812. <https://doi.org/10.1371/journal.pgen.1009812>
- Dietrich, K., Fiedler, I. A., Kurzyukova, A., López-Delgado, A. C., McGowan, L. M., Geurtzen, K., Hammond, C. L., Busse, B., & Knopf, F. (2021). Skeletal biology and disease modeling in zebrafish. *Journal of Bone and Mineral Research*, 36(3), 436-458.
- Dilworth, L., Facey, A., & Omoruyi, F. (2021). Diabetes Mellitus and Its Metabolic Complications: The Role of Adipose Tissues. *International journal of molecular sciences*, 22(14), 7644. <https://doi.org/10.3390/ijms22147644>
- Dinh, T., Elder, S., & Veves, A. (2011). Delayed wound healing in diabetes: Considering future treatments. *Diabetes Management*, 1(5), 509-519.
- Dixon, D., & Edmonds, M. (2021). Managing Diabetic Foot Ulcers: Pharmacotherapy for Wound Healing. *Drugs*, 81(1), 29–56.
- Dogan, D., Nur, G., & Deveci, H. A. (2022). Tissue-specific toxicity of clothianidin on rainbow trout (*Oncorhynchus mykiss*). *Drug and chemical toxicology*, 45(4), 1851–1861.

References

- Dragano, N. R., Fernø, J., Diéguez, C., López, M., & Milbank, E. (2020). Recent updates on obesity treatments: available drugs and future directions. *Neuroscience*, 437, 215-239.
- Dubey, R., Prabhakar, P. K., & Gupta, J. (2022). Epigenetics: Key to improve delayed wound healing in type 2 diabetes. *Molecular and cellular biochemistry*, 477(2), 371-383.
- Duman, K. E., Dogan, A., & Kaptaner, B. (2022). Ameliorative role of *Cyanus depressus* (M.Bieb.) Soják plant extract against diabetes-associated oxidative-stress-induced liver, kidney, and pancreas damage in rats. *Journal of food biochemistry*, 46(10), e14314. <https://doi.org/10.1111/jfbc.14314>
- Edition, F. (2002). Methods for measuring the acute toxicity of effluents and receiving waters to freshwater and marine organisms, 5th ed.; *US Environmental Protection Agency US EPA*: Washington, DC, USA, Volume 232, p. 266.
- El-Megharbel, S. M., Al-Thubaiti, E. H., Qahl, S. H., Al-Eisa, R. A., & Hamza, R. Z. (2022). Synthesis and spectroscopic characterization of dapagliflozin/Zn (II), Cr (III) and Se (IV) novel complexes that ameliorate hepatic damage, hyperglycemia and oxidative injury induced by streptozotocin-induced diabetic male rats and their antibacterial activity. *Crystals*, 12(3), 304. <https://doi.org/10.3390/cryst12030304>
- Faksness, L. G., Altin, D., Størseth, T. R., Nordtug, T., & Hansen, B. H. (2020). Comparison of artificially weathered Macondo oil with field samples and evidence that weathering does not increase environmental acute toxicity. *Marine environmental research*, 157, 104928. <https://doi.org/10.1016/j.marenvres.2020.104928>
- Fan, C., Ouyang, Y., Yuan, X., & Wang, J. (2022). An enhancer trap zebrafish line for lateral line development and regulation of six2b expression. *Gene expression patterns*, 43, 119231. <https://doi.org/10.1016/j.gep.2022.119231>
- Fareed, S. A., Yousef, E. M., & Abd El-Moneam, S. M. (2023). Assessment of effects of rosemary essential oil on the kidney pathology of diabetic adult male albino rats. *Cureus*, 15(3), e35736. <https://doi.org/10.7759/cureus.35736>
- Farid, M. M., Aboul Naser, A. F., Salem, M. M., Ahmed, Y. R., Emam, M., & Hamed, M. A. (2022). Chemical compositions of *Commiphora opobalsamum* stem

References

- bark to alleviate liver complications in streptozotocin-induced diabetes in rats: Role of oxidative stress and DNA damage. *Biomarkers*, 27(7), 671-683.
- Farnier, M., Zeller, M., Masson, D., & Cottin, Y. (2021). Triglycerides and risk of atherosclerotic cardiovascular disease: An update. *Archives of cardiovascular diseases*, 114(2), 132–139.
- Fernandes, L., Cardim-Pires, T. R., Foguel, D., & Palhano, F. L. (2021). Green tea polyphenol epigallocatechin-gallate in amyloid aggregation and neurodegenerative diseases. *Frontiers in neuroscience*, 15, 718188. <https://doi.org/10.3389/fnins.2021.718188>
- Ferreira, D. Q., Ferraz, T. O., Araújo, R. S., Cruz, R. A. S., Fernandes, C. P., Souza, G. C., Ortiz, B. L. S., Sarquis, R. S. F. R., Miranda, J. C. M. M., Garrett, R., Carvalho, J. C. T., & Oliveira, A. E. M. F. M. (2019). *Libidibia ferrea* (jucá), a Traditional Anti-Inflammatory: A study of acute toxicity in adult and embryos zebrafish (*Danio rerio*). *Pharmaceuticals*, 12(4), 175. <https://doi.org/10.3390/ph12040175>
- Firdous, S. M., & Singh, A. (2016). Effect of *Ipomoea staphylina* leaves on streptozotocin-nicotinamide induced type-II diabetes in wistar rats. *Asian pacific journal of health sciences*, 3(3), 30-44.
- Flores-Lopes, F., & Thomaz, A. T. (2011). Histopathologic alterations observed in fish gills as a tool in environmental monitoring. *Brazilian Journal of Biology*, 71(1), 179-188.
- Fontana, B. D., Norton, W. H. J., & Parker, M. O. (2022). Modelling ADHD-like phenotypes in zebrafish. *Current topics in behavioral neurosciences*, 57, 395–414.
- Fu, J. D., Yao, J. J., Wang, H., Cui, W. G., Leng, J., Dong, L. Y., & Fan, K. Y. (2019). Effects of EGCG on proliferation and apoptosis of gastric cancer SGC7901 cells via down-regulation of HIF-1 α and VEGF under a hypoxic state. *European Review for Medical and Pharmacological Sciences*, 23(1), 155-161.
- Fu, J., & Retnakaran, R. (2022). The life course perspective of gestational diabetes: An opportunity for the prevention of diabetes and heart disease in women. *EClinicalMedicine*, 45, 101294. <https://doi.org/10.1016/j.eclinm.2022.101294>

References

- Geba, K. M., Khallaf, A.G., Atyah, A. H., Mousa, D. B., Abousaada, E. A. M., Shaltout, R. A. A., El-Torgoman, A. M. A. K., Abdel-Bary, H. M., & El Sayed, I. E. T. (2024). Simplified protocol for production of persistent hyperglycemic zebrafish model for type ii diabetes mellitus studying. *Egyptian Journal of Aquatic Biology and Fisheries*, 28(2), 963-976.
- Ghalichi, F., Ostadrahimi, A., & Saghaei-Asl, M. (2022). Vanadium and diabetic dyslipidemia: A systematic review of animal studies. *Journal of trace elements in medicine and biology: organ of the Society for Minerals and Trace Elements*, 71, 126955. <https://doi.org/10.1016/j.jtemb.2022.126955>
- Ghalwash, A. A., Baalash, A. A., Gaafar, N. K., Wasfy, R. E., & Noeman, S. E. D. A. (2022). The interplay between oat beta glucan, gut microbiota and gut-liver axis in treatment of obesity associated non-alcoholic steatohepatitis and Type II diabetes mellitus. *Indian Journal of Biochemistry and Biophysics*, 59(1), 14-22.
- Giaretta, E. P., Hauser-Davis, R. A., Abilhoa, V., & Wosnick, N. (2023). Carbonic anhydrase in elasmobranchs and current climate change scenario implications. *Comparative biochemistry and physiology. Part A, Molecular & integrative physiology*, 281, 111435. <https://doi.org/10.1016/j.cbpa.2023.111435>
- Gnügge, L., Meyer, D., & Driever, W. (2004). Pancreas development in zebrafish. *Methods in cell biology*, 76, 531–551.
- Goessling, W., & Sadler, K. C. (2015). Zebrafish: an important tool for liver disease research. *Gastroenterology*, 149(6), 1361-1377.
- Goldstein, A. S., Janson, B. J., Skeie, J. M., Ling, J. J., & Greiner, M. A. (2020). The effects of diabetes mellitus on the corneal endothelium: A review. *Survey of ophthalmology*, 65(4), 438-450.
- Guru, A., Velayutham, M., & Arockiaraj, J. (2022). Lipid-lowering and antioxidant activity of RF13 peptide from vacuolar protein sorting-associated protein 26B (VPS26B) by modulating lipid metabolism and oxidative stress in HFD induced obesity in zebrafish larvae. *International Journal of Peptide Research and Therapeutics*, 28(2), 74. <https://doi.org/10.1007/s10989-022-10376-3>

References

- Hadi, A. A., & Alwan, S. F. (2012). Histopathological changes in gills, liver and kidney of fresh water fish, *Tilapia zillii*, exposed to aluminum. *International Journal of Pharmacy & Life Sciences*, 3(11), 2071-2081.
- Hajam, Y. A., Kumar, R., Reshi, M. S., Rawat, D. S., AlAsmari, A. F., Ali, N., Mohamed Ali, Y.S., & Ishtikhar, M. (2022). Administration of *Costus igneus* Nak leaf extract improves diabetic-induced impairment in hepatorenal functions in male albino rats. *Journal of King Saud University-Science*, 34(4), 101911. <https://doi.org/10.1016/j.jksus.2022.101911>
- Halim, M., & Halim, A. (2019). The effects of inflammation, aging and oxidative stress on the pathogenesis of diabetes mellitus (type 2 diabetes). *Diabetes & metabolic syndrome*, 13(2), 1165–1172.
- Hao, L., Wang, Z., & Xing, B. (2009). Effect of sub-acute exposure to TiO₂ nanoparticles on oxidative stress and histopathological changes in Juvenile Carp (*Cyprinus carpio*). *Journal of environmental sciences*, 21(10), 1459–1466.
- Haque, M. F., Shawon, M. M. H., Alam, M. J., Chaity, A. S., Mohanta, M. K., Saha, A. K., & Nasrin, T. (2022). Reduction of toxic effects of textile dye, basic red-18 on tilapia fish by bioremediation with a novel bacterium, *mangrovibacter yixingensis* strain AKS2 isolated from textile wastewater. *Annual Research & Review in Biology*, 37(11), 12-29.
- He, C., Wang, D., Wang, R., Huang, Y., Huang, X., Shen, S., Lv, J., & Wu, M. (2022). Epigallocatechin gallate induces the demethylation of actinin alpha 4 to inhibit diabetic nephropathy renal fibrosis via the NF-KB signaling pathway in vitro. *Dose-response: a publication of International Hormesis Society*, 20(2), 15593258221105704. <https://doi.org/10.1177/15593258221105704>
- Hong, X., & Zha, J. (2019). Fish behavior: A promising model for aquatic toxicology research. *The Science of the total environment*, 686, 311–321.
- Hosseini, A., Mollazadeh, H., Amiri, M. S., Sadeghnia, H. R., & Ghorbani, A. (2017). Effects of a standardized extract of *Rheum turkestanicum* Janischew root on diabetic changes in the kidney, liver and heart of streptozotocin-induced diabetic rats. *Biomedicine & pharmacotherapy*, 86, 605–611.

References

- Houeiss, P., Luce, S., & Boitard, C. (2022). Environmental triggering of type 1 diabetes autoimmunity. *Frontiers in endocrinology*, 13, 933965. <https://doi.org/10.3389/fendo.2022.933965>
- Hsieh, M. H., Cui, Z. Y., Yang, A. L., Nhu, N. T., Ting, S. Y., Yu, S. H., Cheng, Y. J., Lin, Y. Y., Wu, X. B., & Lee, S. D. (2021). Cerebral cortex apoptosis in early aged hypertension: Effects of epigallocatechin-3-gallate. *Frontiers in aging neuroscience*, 13, 705304. <https://doi.org/10.3389/fnagi.2021.705304>
- Hu, S. C., & Lan, C. E. (2016). High-glucose environment disturbs the physiologic functions of keratinocytes: Focusing on diabetic wound healing. *Journal of dermatological science*, 84(2), 121–127.
- Huang, X., Yang, S., Li, B., Wang, A., Li, H., Li, X., Luo, J., Liu, F., & Mu, W. (2021). Comparative toxicity of multiple exposure routes of pyraclostrobin in adult zebrafish (*Danio rerio*). *The Science of the total environment*, 777, 145957. <https://doi.org/10.1016/j.scitotenv.2021.145957>
- Huang, Y. J., Wang, K. L., Chen, H. Y., Chiang, Y. F., & Hsia, S. M. (2020). Protective effects of epigallocatechin gallate (EGCG) on endometrial, breast, and ovarian cancers. *Biomolecules*, 10(11), 1481. <https://doi.org/10.3390/biom10111481>
- Huang, Y. W., Zhu, Q. Q., Yang, X. Y., Xu, H. H., Sun, B., Wang, X. J., & Sheng, J. (2019). Wound healing can be improved by (-)-epigallocatechin gallate through targeting Notch in streptozotocin-induced diabetic mice. *Federation of American Societies for Experimental Biology*, 33(1), 953–964.
- Hutachok, N., Koonyosying, P., Paradee, N., Samakradhamrongthai, R. S., Utama-Ang, N., & Srichairatanakool, S. (2023). Testing the feasibility and dietary impact of macaroni fortified with green tea and turmeric curcumin extract in diabetic rats. *Foods*, 12(3), 534. <https://doi.org/10.3390/foods12030534>
- Ighodaro O. M. (2018). Molecular pathways associated with oxidative stress in diabetes mellitus. *Biomedicine & pharmacotherapy*, 108, 656–662.
- Inshaw, J. R. J., Cutler, A. J., Crouch, D. J. M., Wicker, L. S., & Todd, J. A. (2020). Genetic variants predisposing most strongly to type 1 diabetes diagnosed under age 7 years lie near candidate genes that function in the immune system and in pancreatic β -cells. *Diabetes Care*, 43(1), 169–177.

References

- Intine, R. V., Olsen, A. S., & Sarras, M. P., Jr (2013). A zebrafish model of diabetes mellitus and metabolic memory. *Journal of visualized experiments*, (72), e50232. <https://doi.org/10.3791/50232>
- Jamir, A., Longkumer, S., & Pankaj, P. P. (2023). Epigallocatechin gallate improves caudal fin regeneration in the streptozotocin-induced diabetic zebrafish model. *Journal of Pharmaceutical Negative Results*, 14(3), 1264-1270.
- Jan, M., & Jan, N. (2017). Studies on the fecundity (F), gonadosomatic index (GSI) and hepatosomatic index (HSI) of *Salmo trutta fario* (Brown trout) at Kokernag trout fish farm, Anantnag, Jammu and Kashmir. *International Journal of Fisheries and Aquatic Studies*, 5(6), 170-173.
- Jarhahzadeh, M., Alavinejad, P., Farsi, F., Husain, D., & Rezazadeh, A. (2021). The effect of turmeric on lipid profile, malondialdehyde, liver echogenicity and enzymes among patients with nonalcoholic fatty liver disease: a randomized double blind clinical trial. *Diabetology & metabolic syndrome*, 13(1), 112. <https://doi.org/10.1186/s13098-021-00731-7>
- Jasim, O. H., Mahmood, M. M., & Ad'hiah, A. H. (2022). Significance of lipid profile parameters in predicting pre-diabetes. *Archives of Razi Institute*, 77(1), 277–284. <https://doi.org/10.22092/ARI.2021.356465.1846>
- Jenkins, A. J., Scott, E., Fulcher, J., Kilov, G., & Januszewski, A. S. (2019). Management of diabetes mellitus. *Comprehensive Cardiovascular Medicine in the Primary Care Setting*, 113-177. doi.org/10.1007/978-3-319-97622-8_7
- Jestadi, D. B., Phaniendra, A., Babji, U., Srinu, T., Shanmuganathan, B., & Periyasamy, L. (2014). Effects of short term exposure of atrazine on the liver and kidney of normal and diabetic rats. *Journal of toxicology*, 536759. <https://doi.org/10.1155/2014/536759>
- Ji, W., Zhang, C., Song, C., & Ji, H. (2021). Three DPP-IV inhibitory peptides from Antarctic krill protein hydrolysate improve glucose levels in the zebrafish model of diabetes. *Food Science and Technology*, 42, e58920. <http://dx.doi.org/10.1590/fst.58920>
- Jiang, S., Huang, C., Zheng, G., Yi, W., Wu, B., Tang, J., Liu, X., Huang, B., Wu, D., Yan, T., Li, M., Wan, C., & Cai, Y. (2022). EGCG inhibits proliferation and

References

- induces apoptosis through downregulation of SIRT1 in nasopharyngeal carcinoma cells. *Frontiers in nutrition*, 9, 851972.
<https://doi.org/10.3389/fnut.2022.851972>
- Jiang, S., Young, J. L., Wang, K., Qian, Y., & Cai, L. (2020). Diabetic-induced alterations in hepatic glucose and lipid metabolism: The role of type 1 and type 2 diabetes mellitus. *Molecular medicine reports*, 22(2), 603–611.
- Jin, X., Yang, S., Lu, J., & Wu, M. (2022). Small, dense low-density lipoprotein-cholesterol and atherosclerosis: Relationship and therapeutic strategies. *Frontiers in cardiovascular medicine*, 8, 804214.
<https://doi.org/10.3389/fcvm.2021.804214>
- Jităreanu, A., Trifan, A., Vieriu, M., Caba, I. C., Mârțu, I., & Agoroaei, L. (2022). Current trends in toxicity assessment of herbal medicines: A narrative review. *Processes*, 11(1), 83. <https://doi.org/10.3390/pr11010083>
- Jwad, S. M., & AL-Fatlawi, H. Y. (2022). Types of diabetes and their effect on the immune system. *Journal of advances in pharmacy practices* 4(1), 21-30.
- Kane, D. A., & Kimmel, C. B. (1993). The zebrafish midblastula transition. *Development (Cambridge, England)*, 119(2), 447–456.
- Kanlaya, R., & Thongboonkerd, V. (2019). Molecular mechanisms of epigallocatechin-3-gallate for prevention of chronic kidney disease and renal fibrosis: preclinical evidence. *Current developments in nutrition*, 3(9), nzz101. <https://doi.org/10.1093/cdn/nzz101>
- Kant, V., Sharma, M., Jangir, B. L., & Kumar, V. (2022). Acceleration of wound healing by quercetin in diabetic rats requires mitigation of oxidative stress and stimulation of the proliferative phase. *Biotechnic & histochemistry*, 97(6), 461–472.
- Kerry, R. G., Das, G., Golla, U., Del Pilar Rodriguez-Torres, M., Shin, H. S., & Patra, J. K. (2022). engineered probiotic and prebiotic nutraceutical supplementations in combating non-communicable disorders: A review. *Current pharmaceutical biotechnology*, 23(1), 72–97.
- Khalatbary, A. R., & Khademi, E. (2020). The green tea polyphenolic catechin epigallocatechin gallate and neuroprotection. *Nutritional neuroscience*, 23(4), 281–294.

References

- Khalid, M., Petroianu, G., & Adem, A. (2022). Advanced glycation end products and diabetes mellitus: Mechanisms and perspectives. *Biomolecules*, 12(4), 542. <https://doi.org/10.3390/biom12040542>
- Khatana, C., Saini, N. K., Chakrabarti, S., Saini, V., Sharma, A., Saini, R. V., & Saini, A. K. (2020). Mechanistic insights into the oxidized low-density lipoprotein-induced atherosclerosis. *Oxidative medicine and cellular longevity*, 2020, 5245308. <https://doi.org/10.1155/2020/5245308>
- Kimmel, R. A., Dobler, S., Schmitner, N., Walsen, T., Freudenblum, J., & Meyer, D. (2015). Diabetic pdx1-mutant zebrafish show conserved responses to nutrient overload and anti-glycemic treatment. *Scientific reports*, 5, 14241. <https://doi.org/10.1038/srep14241>
- Kirthi, A. V., Kumar, G., Pant, G., Pant, M., Hossain, K., Ahmad, A., & Alshammari, M. B. (2022). Toxicity of nanoscaled zero-valent iron particles on tilapia, *Oreochromis mossambicus*. *ACS omega*, 7(51), 47869–47879.
- Kishi, S., Slack, B. E., Uchiyama, J., & Zhdanova, I. V. (2009). Zebrafish as a genetic model in biological and behavioral gerontology: where development meets aging in vertebrates--a mini-review. *Gerontology*, 55(4), 430–441.
- Kong, M., Xie, K., Lv, M., Li, J., Yao, J., Yan, K., Wu, X., Xu, Y., & Ye, D. (2021). Anti-inflammatory phytochemicals for the treatment of diabetes and its complications: Lessons learned and future promise. *Biomedicine & pharmacotherapy*, 133, 110975. <https://doi.org/10.1016/j.biopha.2020.110975>
- Krawczyk, M., Burzynska-Pedziwiatr, I., Wozniak, L. A., & Bukowiecka-Matusiak, M. (2023). Impact of polyphenols on inflammatory and oxidative stress factors in diabetes mellitus: Nutritional antioxidants and their application in improving antidiabetic therapy. *Biomolecules*, 13(9), 1402. <https://doi.org/10.3390/biom13091402>
- Kuete, V. (2014). Physical, hematological, and histopathological signs of toxicity induced by African medicinal plants. In *Toxicological survey of African medicinal plants*, 635-657. <https://doi.org/10.1016/B978-0-12-800018-2.00022-4>
- Kumar, A., Aswal, S., Semwal, R. B., Chauhan, A., Joshi, S. K., & Semwal, D. K. (2019). Role of plant-derived alkaloids against diabetes and diabetes-related

References

- complications: a mechanism-based approach. *Phytochemistry Reviews*, 18, 1277-1298.
- Kumar, R., Saha, P., Kumar, Y., Sahana, S., Dubey, A., & Prakash, O. (2020). A review on diabetes mellitus: Type1 & type2. *World Journal of Pharmacy and Pharmaceutical Sciences*, 9(10), 838-850.
- Kurutas, E. B. (2015). The importance of antioxidants which play the role in cellular response against oxidative/nitrosative stress: current state. *Nutrition journal*, 15(1), 1-22.
- Lakra, K. C., Banerjee, T. K., & Lal, B. (2021). Coal mine effluent-induced metal bioaccumulation, biochemical, oxidative stress, metallothionein, and histopathological alterations in vital tissues of the catfish, *Clarias batrachus*. *Environmental science and pollution research international*, 28(20), 25300–25315.
- Latha, R. C., & Daisy, P. (2011). Insulin-secretagogue, antihyperlipidemic and other protective effects of gallic acid isolated from *Terminalia bellerica* Roxb. in streptozotocin-induced diabetic rats. *Chemico-biological interactions*, 189(1-2), 112–118.
- Lee, C. K., Liao, C. W., Meng, S. W., Wu, W. K., Chiang, J. Y., & Wu, M. S. (2021). Lipids and lipoproteins in health and disease: Focus on targeting atherosclerosis. *Biomedicines*, 9(8), 985.
<https://doi.org/10.3390/biomedicines9080985>
- Lee, Y., & Yang, J. (2021). Development of a zebrafish screening model for diabetic retinopathy induced by hyperglycemia: Reproducibility verification in animal model. *Biomedicine & pharmacotherapy*, 135, 111201.
<https://doi.org/10.1016/j.biopha.2020.111201>
- Legeay, S., Rodier, M., Fillon, L., Faure, S., & Clere, N. (2015). Epigallocatechin gallate: A review of its beneficial properties to prevent metabolic syndrome. *Nutrients*, 7(7), 5443–5468.
- Lei, P., Zhang, W., Ma, J., Xia, Y., Yu, H., Du, J., Fang, Y., Wang, L., Zhang, K., Jin, L., Sun, D., & Zhong, J. (2023). Advances in the utilization of zebrafish for assessing and understanding the mechanisms of nano-/microparticles toxicity in water. *Toxics*, 11(4), 380. <https://doi.org/10.3390/toxics11040380>

References

- Leris, I., Kalogianni, E., Tsangaris, C., Smeti, E., Laschou, S., Anastasopoulou, E., Vardakas, L., Kapakos, Y., & Skoulidakis, N. T. (2019). Acute and sub-chronic toxicity bioassays of Olive Mill Wastewater on the Eastern mosquitofish *Gambusia holbrooki*. *Ecotoxicology and environmental safety*, 175, 48–57.
- Li, J., & Ge, W. (2020). Zebrafish as a model for studying ovarian development: Recent advances from targeted gene knockout studies. *Molecular and cellular endocrinology*, 507, 110778.
<https://doi.org/10.1016/j.mce.2020.110778>
- Li, M., Xu, J., Shi, T., Yu, H., Bi, J., & Chen, G. (2016). Epigallocatechin-3-gallate augments therapeutic effects of mesenchymal stem cells in skin wound healing. *Clinical and experimental pharmacology & physiology*, 43(11), 1115–1124.
- Liew, W. C., Bartfai, R., Lim, Z., Sreenivasan, R., Siegfried, K. R., & Orban, L. (2012). Polygenic sex determination system in zebrafish. *PloS one*, 7(4), e34397. <https://doi.org/10.1371/journal.pone.0034397>
- Liu, B., Zhao, H., Wu, K., & Großhans, J. (2021). Temporal gradients controlling embryonic cell cycle. *Biology*, 10(6), 513.
<https://doi.org/10.3390/biology10060513>
- Liu, H., Guan, H., Tan, X., Jiang, Y., Li, F., Sun-Waterhouse, D., & Li, D. (2022). Enhanced alleviation of insulin resistance via the IRS-1/Akt/FOXO1 pathway by combining quercetin and EGCG and involving miR-27a-3p and miR-96-5p. *Free radical biology & medicine*, 181, 105–117.
- Longkumer, S., Jamir, A., & Pankaj, P. P. (2020). Development and appraisal studies of chemically induced zebrafish hyperglycemia model. *Journal of Experimental Zoology India*, 23(2), 1305-1310.
- Longkumer, S., Jamir, A., & Pankaj, P. P. (2022). Evaluation of lipid profile in streptozotocin induced diabetic zebrafish, treated with C-phycocyanin and Epigallocatechin gallate. *Biochemical & Cellular Archives*, 22(1), 1441-1446.
- Luzio, A., Parra, S., Costa, B., Santos, D., Álvaro, A. R., & Monteiro, S. M. (2021). Copper impair autophagy on zebrafish (*Danio rerio*) gill

References

- epithelium. *Environmental toxicology and pharmacology*, 86, 103674.
<https://doi.org/10.1016/j.etap.2021.103674>
- Lv, Y. Q., Yuan, L., Sun, Y., Dou, H. W., Su, J. H., Hou, Z. P., Li, J. Y., & Li, W. (2022). Long-term hyperglycemia aggravates α -synuclein aggregation and dopaminergic neuronal loss in a Parkinson's disease mouse model. *Translational neurodegeneration*, 11(1), 14.
<https://doi.org/10.1186/s40035-022-00288-z>
- Macirella, R., & Brunelli, E. (2017). Morphofunctional alterations in zebrafish (*Danio rerio*) gills after exposure to mercury chloride. *International journal of molecular sciences*, 18(4), 824. <https://doi.org/10.3390/ijms18040824>
- MacRae, C. A., & Peterson, R. T. (2023). Zebrafish as a mainstream model for *in vivo* systems pharmacology and toxicology. *Annual review of pharmacology and toxicology*, 63, 43–64.
- Mahjoubian, M., Naeemi, A. S., & Sheykhan, M. (2021). Toxicological effects of Ag₂O and Ag₂CO₃ doped TiO₂ nanoparticles and pure TiO₂ particles on zebrafish (*Danio rerio*). *Chemosphere*, 263, 128182.
<https://doi.org/10.1016/j.chemosphere.2020.128182>
- Mai, Y., Peng, S., Li, H., & Lai, Z. (2019). Histological, biochemical and transcriptomic analyses reveal liver damage in zebrafish (*Danio rerio*) exposed to phenanthrene. *Comparative biochemistry and physiology. Toxicology & pharmacology:CBP*, 225, 108582.
<https://doi.org/10.1016/j.cbpc.2019.108582>
- Mandal, S., Pal, S., Maiti, P., & Roy, S. (2022). Roles of reactive oxygen species in the pathogenesis of type 2 diabetes mellitus. *Journal of Pharmaceutical Negative Results*, 13(10), 5234-5245.
- Mangang, Y. A., & Pandey, P. K. (2021). Hemato-biochemical responses and histopathological alterations in the gill and kidney tissues of *Osteobrama belangeri* (Valenciennes, 1844) exposed to different sub-lethal unionized ammonia. *Aquaculture*, 542, 736887.
<https://doi.org/10.1016/j.aquaculture.2021.736887>
- Mansouri, B., Maleki, A., Davari, B., Johari, S. A., Shahmoradi, B., Mohammadi, E., & Shahsavari, S. (2016). Histopathological effects following short-term coexposure of *Cyprinus carpio* to nanoparticles of TiO₂ and

References

- CuO. *Environmental monitoring and assessment*, 188(10), 575.
<https://doi.org/10.1007/s10661-016-5579-6>
- Marlow F. L. (2020). Setting up for gastrulation in zebrafish. *Current topics in developmental biology*, 136, 33–83.
- Martagon, A. J., Zubirán, R., González-Arellanes, R., Praget-Bracamontes, S., Rivera-Alcántara, J. A., & Aguilar-Salinas, C. A. (2023). HDL abnormalities in type 2 diabetes: Clinical implications. *Atherosclerosis*, 117213.
<https://doi.org/10.1016/j.atherosclerosis.2023.117213>
- Mashi, S. K. (2017). Effect of *Eruca sativa* leaves extract on liver enzymes and lipid profile in phosphoric acid induced liver damage in male rabbits. *journal of entomology and zoology studies*, 5(6), 1011-1015.
- Mason, S. A., Parker, L., van der Pligt, P., & Wadley, G. D. (2023). Vitamin C supplementation for diabetes management: A comprehensive narrative review. *Free radical biology & medicine*, 194, 255–283.
- Mathieu, C., Martens, P. J., & Vangoitsenhoven, R. (2021). One hundred years of insulin therapy. *Nature reviews. Endocrinology*, 17(12), 715–725.
- Mathur, M. L., Gaur, J., Sharma, R., & Haldiya, K. R. (2011). Antidiabetic properties of a spice plant *Nigella sativa*. *Journal of Endocrinology and Metabolism*, 1(1), 1-8.
- Mehta, A. S., & Singh, A. (2019). Insights into regeneration tool box: an animal model approach. *Developmental biology*, 453(2), 111–129.
- Meneses, J.O., dos Santos Cunha, F., Dias, J.A., da Cunha, A.F., dos Santos, F.J., da Costa Sousa, N., do Couto, M.V., Paixão, P.E., Abe, H.A., dos Santos Lima, B., de Carvalho Neto, A.G., de Souza Araújo, A.A., da Costa, L., Cardoso, J.C., & Fujimoto, R.Y. (2020). Acute toxicity of hot aqueous extract from leaves of the *Terminalia catappa* in juvenile fish *Colossoma macropomum*. *Aquaculture International*, 28, 2379 - 2396.
- Mesquita, J., Castro-de-Sousa, J. P., Vaz-Pereira, S., Neves, A., Passarinha, L. A., & Tomaz, C. T. (2018). Vascular endothelial growth factors and placenta growth factor in retinal vasculopathies: current research and future perspectives. *Cytokine & growth factor reviews*, 39, 102–115.
- Meyers, J. R. (2018). Zebrafish: development of a vertebrate model organism. *Current Protocols Essential Laboratory Techniques*, 16(1), e19.

References

- <https://doi.org/10.1002/cpet.19>
- Milligan, P. A., Brown, M. J., Marchant, B., Martin, S. W., van der Graaf, P. H., Benson, N., Nucci, G., Nichols, D. J., Boyd, R. A., Mandema, J. W., Krishnaswami, S., Zwillich, S., Gruben, D., Anziano, R. J., Stock, T. C., & Lalonde, R. L. (2013). Model-based drug development: a rational approach to efficiently accelerate drug development. *Clinical pharmacology and therapeutics*, 93(6), 502–514.
- Misra, H. P., & Fridovich, I. (1972). The role of superoxide anion in the autoxidation of epinephrine and a simple assay for superoxide dismutase. *The Journal of biological chemistry*, 247(10), 3170–3175.
- Mohan, T., Velusamy, P., Chakrapani, L. N., Srinivasan, A. K., Singh, A., Johnson, T., & Periandavan, K. (2017). Impact of EGCG supplementation on the progression of diabetic nephropathy in rats: an insight into fibrosis and apoptosis. *Journal of agricultural and food chemistry*, 65(36), 8028–8036.
- Molina, L. C. P., Oliveira, P. F., Alves, M. G., & Martin-Hidalgo, D. (2021). Assisted reproductive technology outcomes in obese and diabetic men: lighting the darkness. *F&S Reviews*, 2(4), 317-329.
- Mostafa-Hedeab, G., Ewaiss Hassan, M., F Halawa, T., & Ahmed Wani, F. (2022). Epigallocatechin gallate ameliorates tetrahydrochloride-induced liver toxicity in rats *via* inhibition of TGF β / p-ERK/p-Smad1/2 signaling, antioxidant, anti-inflammatory activity. *Saudi pharmaceutical journal: the official publication of the Saudi Pharmaceutical Society*, 30(9), 1293–1300.
- Mukhtar, Y., Galalain, A., & Yunusa, U. (2020). A modern overview on diabetes mellitus: a chronic endocrine disorder. *European Journal of Biology*, 5(2), 1-14.
- Nazir, N., Zahoor, M., Ullah, R., Ezzeldin, E., & Mostafa, G. A. E. (2020). Curative effect of catechin isolated from *Elaeagnus Umbellata* Thunb. berries for diabetes and related complications in streptozotocin-induced diabetic rats model. *Molecules*, 26(1), 137. <https://doi.org/10.3390/molecules26010137>
- Neelima, P., Cyril, L., Arun, K. J., Rao, C. S., & Rao, N. G. (2015). Histopathological alterations in Gill, Liver and Kidney of *Cyprinus carpio* (Linn.) exposed to Cypermethrin (25% EC). *International journal of advanced research in biological sciences*, 2(2), 34-40.

References

- Neels, J. G., Leftheriotis, G., & Chinetti, G. (2023). Atherosclerosis Calcification: Focus on Lipoproteins. *Metabolites*, 13(3), 457.
<https://doi.org/10.3390/metabo13030457>
- Nimet, J., Neves, M. P., Viana, N. P., de Arruda Amorim, J. P., & Delariva, R. L. (2019). Histopathological alterations in gills of a fish (*Astyanax bifasciatus*) in neotropical streams: negative effects of riparian forest reduction and presence of pesticides. *Environmental monitoring and assessment*, 192(1), 58. <https://doi.org/10.1007/s10661-019-8030-y>
- Ohiagu, F., Chikezie, P., & Chikezie, C. (2021). Pathophysiology of diabetes mellitus complications: Metabolic events and control. *Biomedical Research and Therapy*, 8(3), 4243-4257.
- Oliveira, H. H. Q., Reis-Filho, J. A., Nunes, J. A. C. C., Dos Santos, R. M., de F Esteves Santiago, E., Aguilar, L., de Mello Affonso, P. R. A., & da Cruz, A. L. (2022). Gill histopathological biomarkers in fish exposed to trace metals in the todos os santos bay, Brazil. *Biological trace element research*, 200(7), 3388–3399.
- Olsen, A. S., Sarras, M. P., Jr, & Intine, R. V. (2010). Limb regeneration is impaired in an adult zebrafish model of diabetes mellitus. *Wound repair and regeneration*, 18(5), 532–542.
- Omara, E. A., Nada, S. A., Farrag, A. R., Sharaf, W. M., & El-Toumy, S. A. (2012). Therapeutic effect of *Acacia nilotica* pods extract on streptozotocin induced diabetic nephropathy in rat. *Phytomedicine: international journal of phytotherapy and phytopharmacology*, 19(12), 1059–1067.
- Organisation for Economic Co-operation and Development. Test guideline 203. Fish, acute toxicity test. OECD guidelines for the testing of chemicals, section 2. OECD publishing, Paris, France 1992.
- Ortiz-Delgado, J. B., Funes, V., Albendín, G., Scala, E., & Sarasquete, C. (2021). Toxicity of malathion during Senegalese sole, *Solea senegalensis* larval development and metamorphosis: Histopathological disorders and effects on type B esterases and CYP1A enzymatic systems. *Environmental toxicology*, 36(9), 1894–1910.
- Ouyang, T., Yin, H., Yang, J., Liu, Y., & Ma, S. (2022). Tissue regeneration effect of

References

- betulin via inhibition of ROS/MAPKs/NF- κ B axis using zebrafish model. *Biomedicine & pharmacotherapy*, 153, 113420.
<https://doi.org/10.1016/j.biopha.2022.113420>
- Packard, C. J., Boren, J., & Taskinen, M. R. (2020). Causes and Consequences of Hypertriglyceridemia. *Frontiers in endocrinology*, 11, 252.
<https://doi.org/10.3389/fendo.2020.00252>
- Pal, S., Kokushi, E., Koyama, J., Uno, S., & Ghosh, A. R. (2012). Histopathological alterations in gill, liver and kidney of common carp exposed to chlorpyrifos. *Journal of environmental science and health. Part. B, Pesticides, food contaminants, and agricultural wastes*, 47(3), 180–195.
- Palani, S., Joseph, N. M., Tegene, Y., Zacharia, A., & Marew, T. (2014). Gestational diabetes-a review. *Journal of global trends in pharmaceutical sciences*, 5(2), 1673-83.
- Pang, S., Gao, Y., Wang, F., Wang, Y., Cao, M., Zhang, W., Liang, Y., Song, M., & Jiang, G. (2020). Toxicity of silver nanoparticles on wound healing: a case study of zebrafish fin regeneration model. *The science of the total environment*, 717, 137178. <https://doi.org/10.1016/j.scitotenv.2020.137178>.
- Papachristoforou, E., Lambadiari, V., Maratou, E., & Makrilakis, K. (2020). Association of glycemic indices (hyperglycemia, glucose variability, and hypoglycemia) with oxidative stress and diabetic complications. *Journal of diabetes research*, 2020, 7489795. <https://doi.org/10.1155/2020/7489795>
- Paramanya, A.; Patel, N.; Kumar, D.; Kamal, F.Z.; Yiğit, B.M.; Sundarrajan, P.; Balyan, P.; Khan, J.; Ali, A. (2023). Preventive roles of phytochemicals from *Ficus carica* in diabetes and its secondary complications. In *Fig (Ficus carica): production, processing, and properties*; springer nature: Berlin/Heidelberg, Germany, pp. 539–559. Doi/10.1007/978-3-031-16493-4_24
- Parasuraman, S., Hui, L. C., Beng, J. Y., & Qin, B. N. (2021). Effect of epigallocatechin gallate on cadmium chloride-induced changes in behavior, biochemical parameters and spermatogenesis of male sprague dawley rats. *Tropical journal of natural product research*, 5(3), 549-554.
- Partoazar, A., Kianvash, N., & Goudarzi, R. (2022). New concepts in wound targeting

References

- through liposome-based nanocarriers (LBNs). *Journal of drug delivery science and technology*, 77, 103878.
<https://doi.org/10.1016/j.jddst.2022.103878>
- Pasupuleti, V. R., Arigela, C. S., Gan, S. H., Salam, S. K. N., Krishnan, K. T., Rahman, N. A., & Jeffree, M. S. (2020). A review on oxidative stress, diabetic complications, and the roles of honey polyphenols. *Oxidative medicine and cellular longevity*, 2020, 8878172. <https://doi.org/10.1155/2020/8878172>
- Patel, C. N., Kumar, S. P., Rawal, R. M., Patel, D. P., Gonzalez, F. J., & Pandya, H. A. (2020). A multiparametric organ toxicity predictor for drug discovery. *Toxicology mechanisms and methods*, 30(3), 159–166.
- Patel, S., Srivastava, S., Singh, M. R., & Singh, D. (2019). Mechanistic insight into diabetic wounds: pathogenesis, molecular targets and treatment strategies to pace wound healing. *Biomedicine & pharmacotherapy*, 112, 108615. <https://doi.org/10.1016/j.biopha.2019.108615>
- Pathak, N. H. & Barresi, M. J. F. (2020). Zebrafish as a model to understand vertebrate development. *The Zebrafish in Biomedical Research*, First Edition (eds S. Cartner, J. Eisen, S. Farmer, K. Guillemin, M. Kent and G. Sanders). Academic Press, London. (pp. 559-591). <https://doi.org/10.1016/B978-0-12-812431-4.00045-2>
- Paul, S., Ali, A., & Katare, R. (2020). Molecular complexities underlying the vascular complications of diabetes mellitus - A comprehensive review. *Journal of diabetes and its complications*, 34(8), 107613. <https://doi.org/10.1016/j.jdiacomp.2020.107613>
- Paula, V. G., Sinzato, Y. K., Gallego, F. Q., Cruz, L. L., Aquino, A. M., Scarano, W. R., Corrente, J. E., Volpato, G. T., & Damasceno, D. C. (2023). Intergenerational hyperglycemia impairs mitochondrial function and follicular development and causes oxidative stress in rat ovaries independent of the consumption of a high-fat diet. *Nutrients*, 15(20), 4407. <https://doi.org/10.3390/nu15204407>
- Pérez Gutiérrez, R. M., Soto Contreras, J. G., Martínez Jerónimo, F. F., de la Luz Corea Téllez, M., & Borja-Urby, R. (2022). Assessing the ameliorative effect of selenium *Cinnamomum verum*, *Origanum majorana*, and *Origanum*

References

- vulgare* nanoparticles in diabetic zebrafish (*Danio rerio*). *Plants*, 11(7), 893. <https://doi.org/10.3390/plants11070893>
- Pradeep, S. R., Barman, S., & Srinivasan, K. (2019). Attenuation of diabetic nephropathy by dietary fenugreek (*Trigonella foenum-graecum*) seeds and onion (*Allium cepa*) via suppression of glucose transporters and renin-angiotensin system. *Nutrition*, 67-68, 110543. <https://doi.org/10.1016/j.nut.2019.06.024>
- Pradhan, A., Sengupta, S., Sengupta, R., & Chatterjee, M. (2023). Attenuation of methotrexate induced hepatotoxicity by epigallocatechin 3-gallate. *Drug and chemical toxicology*, 46(4), 717–725.
- Pramila, K., & Julius, A. (2019). *In vitro* antioxidant effect of green tea polyphenol epigallocatechin-3-gallate (EGCG) in protecting cardiovascular diseases. *Research journal of pharmacy and technology*, 12(3), 1265-1267.
- Prasad, R. B., & Groop, L. (2015). Genetics of type 2 diabetes-pitfalls and possibilities. *Genes*, 6(1), 87–123.
- Rad, M. G., Sharifi, M., Meamar, R., & Soltani, N. (2022). The role of pancreas to improve hyperglycemia in STZ-induced diabetic rats by thiamine disulfide. *Nutrition & diabetes*, 12(1), 32. <https://doi.org/10.1038/s41387-022-00211-5>
- Rahmati, M., Silva, E. A., Reseland, J. E., Heyward, C. A., & Haugen, H. J. (2020). Biological responses to physicochemical properties of biomaterial surface. *Chemical society reviews*, 49(15), 5178-5224.
- Ramachandran, B., Jayavelu, S., Murhekar, K., & Rajkumar, T. (2016). Repeated dose studies with pure Epigallocatechin-3-gallate demonstrated dose and route dependant hepatotoxicity with associated dyslipidemia. *Toxicology reports*, 3, 336–345.
- Rao, H., Jalali, J. A., Johnston, T. P., & Koulen, P. (2021). Emerging roles of dyslipidemia and hyperglycemia in diabetic retinopathy: molecular mechanisms and clinical perspectives. *Frontiers in endocrinology*, 12, 620045. <https://doi.org/10.3389/fendo.2021.620045>
- Raposo, D., Morgado, C., Pereira-Terra, P., & Tavares, I. (2015). Nociceptive spinal cord neurons of laminae I-III exhibit oxidative stress damage during diabetic

References

- neuropathy which is prevented by early antioxidant treatment with epigallocatechin-gallate (EGCG). *Brain research bulletin*, 110, 68–75.
- Rashmi, P., Urmila, A., Likhith, A., Subhash, B., & Shailendra, G. (2023). Rodent models for diabetes. *3 Biotech*, 13(3), 80. <https://doi.org/10.1007/s13205-023-03488-0>
- Ratnani, S., & Malik, S. (2022). Therapeutic properties of green tea: a review. *Journal of multidisciplinary applied natural science*, 2(2), 90-102.
- Rawat, S. G., Tiwari, R. K., Sonker, P., Maurya, R. P., Vishvakarma, N. K., & Kumar, A. (2021). EGCG as anti-obesity and anticancer agent. *Obesity and Cancer*, 209-233. https://doi.org/10.1007/978-981-16-1846-8_11
- Reed, J., Bain, S., & Kanamarlapudi, V. (2021). A review of current trends with type 2 diabetes epidemiology, aetiology, pathogenesis, treatments and future perspectives. *Diabetes, metabolic syndrome and obesity: targets and therapy*, 14, 3567–3602.
- Regufe, V. M. G., Pinto, C. M. C. B., & Perez, P. M. V. H. C. (2020). Metabolic syndrome in type 2 diabetic patients: a review of current evidence. *Porto biomedical journal*, 5(6), e101. <https://doi.org/10.1097/j.pbj.0000000000000101>
- Rehman, H. U., Ullah, K., Rasool, A., Manzoor, R., Yuan, Y., Tareen, A. M., Kaleem, I., Riaz, N., Hameed, S., & Bashir, S. (2023). Comparative impact of streptozotocin on altering normal glucose homeostasis in diabetic rats compared to normoglycemic rats. *Scientific reports*, 13(1), 7921. <https://doi.org/10.1038/s41598-023-29445-8>
- Ren, Z., Yang, Z., Lu, Y., Zhang, R., & Yang, H. (2020). Anti-glycolipid disorder effect of epigallocatechin-3-gallate on high-fat diet and STZ-induced T2DM in mice. *Molecular medicine reports*, 21(6), 2475–2483.
- Robertson, G. N., McGee, C. A., Dumbarton, T. C., Croll, R. P., & Smith, F. M. (2007). Development of the swimbladder and its innervation in the zebrafish, *Danio rerio*. *Journal of morphology*, 268(11), 967–985.
- Rodrigues, S., Antunes, S. C., Nunes, B., & Correia, A. T. (2019). Histopathological effects in gills and liver of *Sparus aurata* following acute and chronic exposures to erythromycin and oxytetracycline. *Environmental science and pollution research international*, 26(15), 15481–15495.

References

- Roep, B. O., Thomaidou, S., van Tienhoven, R., & Zaldumbide, A. (2021). Type 1 diabetes mellitus as a disease of the β -cell (do not blame the immune system?). *Nature reviews. Endocrinology*, 17(3), 150–161.
- Roghani, M., & Baluchnejadmojarad, T. (2010). Hypoglycemic and hypolipidemic effect and antioxidant activity of chronic epigallocatechin-gallate in streptozotocin-diabetic rats. *Pathophysiology*, 17(1), 55–59.
- Romanowski, K. S., & Sen, S. (2022). Wound healing in older adults with severe burns: Clinical treatment considerations and challenges. *Burns open: an international open access journal for burn injuries*, 6(2), 57–64.
- Ross, J., Cotterill, S., Bower, P., & Murray, E. (2023). Influences on patient uptake of and engagement with the national health service digital diabetes prevention programme: Qualitative interview study. *Journal of medical Internet research*, 25, e40961. <https://doi.org/10.2196/40961>
- Sabarwal, A., Kumar, K., & Singh, R. P. (2018). Hazardous effects of chemical pesticides on human health-Cancer and other associated disorders. *Environmental toxicology and pharmacology*, 63, 103–114.
- Sabi, E. M., Mujamammi, A. H., Althafar, Z. M., Al-Shouli, S. T., Bin Dahman, L. S., & Sumaily, K. M. (2022). Protective effects of *Ficus benghalensis* in streptozotocin (STZ) induced diabetic zebrafish (*Danio rerio*) model. *Indian Journal of pharmaceutical education and research*, 56(3), 822-829.
- Sagoo, M. K., & Gnudi, L. (2020). Diabetic nephropathy: An overview. *Methods in molecular biology (Clifton, N.J.)*, 2067, 3–7.
- Salehpour, A., Rezaei, M., Khoradmehr, A., Tahamtani, Y., & Tamadon, A. (2021). Which hyperglycemic model of zebrafish (*Danio rerio*) suites my type 2 diabetes mellitus research? a scoring system for available methods. *Frontiers in cell and developmental biology*, 9, 652061. <https://doi.org/10.3389/fcell.2021.652061>
- Salgado, M. T. S. F., Fernandes E Silva, E., Matsumoto, A. M., Mattozo, F. H., Amarante, M. C. A., Kalil, S. J., & Votto, A. P. S. (2022). C-phycocyanin decreases proliferation and migration of melanoma cells: In silico and in vitro evidences. *Bioorganic chemistry*, 122, 105757. <https://doi.org/10.1016/j.bioorg.2022.105757>

References

- Salis, P., Lee, S. H., Roux, N., Lecchini, D., & Laudet, V. (2021). The real Nemo movie: Description of embryonic development in *Amphiprion ocellaris* from first division to hatching. *Developmental dynamics*, 250(11), 1651–1667.
- Samanta, P., Pal, S., Mukherjee, A. K., & Ghosh, A. R. (2014). Evaluation of metabolic enzymes in response to Excel Mera 71, a glyphosate-based herbicide, and recovery pattern in freshwater teleostean fishes. *BioMed research international*, 2014, 425159. <https://doi.org/10.1155/2014/425159>
- Samim, A. R., & Vaseem, H. (2023). Exposure to nickel oxide nanoparticles induces alterations in antioxidant system, metabolic enzymes and nutritional composition in muscles of *Heteropneustes fossilis*. *Bulletin of environmental contamination and toxicology*, 110(4), 79. <https://doi.org/10.1007/s00128-023-03714-8>
- Sampath, C., Rashid, M. R., Sang, S., & Ahmedna, M. (2017). Green tea epigallocatechin 3-gallate alleviates hyperglycemia and reduces advanced glycation end products via nrf2 pathway in mice with high fat diet-induced obesity. *Biomedicine & pharmacotherapy*, 87, 73–81.
- Sanati, M., Afshari, A. R., Ahmadi, S. S., Moallem, S. A., & Sahebkar, A. (2023). Modulation of the ubiquitin-proteasome system by phytochemicals: Therapeutic implications in malignancies with an emphasis on brain tumors. *BioFactors (Oxford, England)*, 49(4), 782–819.
- Satpathy, L., & Parida, S. P. (2020). Acute toxicity assessment and behavioral responses induced by kandhamal haladi in adult zebrafish (*Danio rerio*). *Biointerface research in applied chemistry*, 11(1), 7368-7381.
- Saucedo, R., Ortega-Camarillo, C., Ferreira-Hermosillo, A., Díaz-Velázquez, M. F., Meixueiro-Calderón, C., & Valencia-Ortega, J. (2023). Role of Oxidative Stress and Inflammation in Gestational Diabetes Mellitus. *Antioxidants (Basel, Switzerland)*, 12(10), 1812. <https://doi.org/10.3390/antiox12101812>
- Schmidt, F., & Braunbeck, T. (2011). Alterations along the Hypothalamic-Pituitary-Thyroid Axis of the Zebrafish (*Danio rerio*) after Exposure to Propylthiouracil. *Journal of thyroid research*, 2011, 376243. <https://doi.org/10.4061/2011/376243>
- Sen S. (2022). Liposome-encapsulated glycyrrhizin alleviates hyperglycemia and

References

- glycation-induced iron-catalyzed oxidative reactions in streptozotocin-induced diabetic rats. *Journal of liposome research*, 32(4), 376–385.
- Sesti, G., Antonelli Incalzi, R., Bonora, E., Consoli, A., Giaccari, A., Maggi, S., Paolisso, G., Purrello, F., Vendemiale, G., & Ferrara, N. (2018). Management of diabetes in older adults. *Nutrition, metabolism, and cardiovascular diseases*, 28(3), 206–218.
- Seth, A., Stemple, D. L., & Barroso, I. (2013). The emerging use of zebrafish to model metabolic disease. *Disease models & mechanisms*, 6(5), 1080–1088.
- Sfakianakis, D. G., Leris, I., & Kentouri, M. (2011). Effect of developmental temperature on swimming performance of zebrafish (*Danio rerio*) juveniles. *Environmental Biology of Fishes*, 90, 421–427.
<https://doi.org/10.1007/s10641-010-9751-5>
- Shahwan, M., Alhumaydhi, F., Ashraf, G. M., Hasan, P. M. Z., & Shamsi, A. (2022). Role of polyphenols in combating type 2 diabetes and insulin resistance. *International journal of biological macromolecules*, 206, 567–579. <https://doi.org/10.1016/j.ijbiomac.2022.03.004>
- Sharma, A. K., Singh, S., Singh, H., Mahajan, D., Kolli, P., Mandadapu, G., Kumar, B., Kumar, D., Kumar, S., & Jena, M. K. (2022). Deep insight of the pathophysiology of gestational diabetes mellitus. *Cells*, 11(17), 2672. <https://doi.org/10.3390/cells11172672>
- Sharma, D., Gandotra, R., Dhiman, S. K., Arif, M., Dogra, A., Lone, A., Choudhary, N., & Choudhary, P. (2021a). Ultrastructural biomarker responses in gill tissues of *Cirrhinus mrigala* (Hamilton, 1822) through SEM after exposure to zinc sulphate. *The Egyptian Journal of Aquatic Research*, 47(2), 157–162.
- Sharma, R., Jindal, R., & Faggio, C. (2021b). Impact of cypermethrin in nephrocytes of freshwater fish *Catla catla*. *Environmental toxicology and pharmacology*, 88, 103739. <https://doi.org/10.1016/j.etap.2021.103739>
- Sharma, V. K., Singh, T. G., Singh, S., Garg, N., & Dhiman, S. (2021c). Apoptotic Pathways and Alzheimer's disease: probing therapeutic potential. *Neurochemical research*, 46(12), 3103–3122.
- Shi, J., Liu, F., Zhang, W., Liu, X., Lin, B., & Tang, X. (2015). Epigallocatechin-3-gallate inhibits nicotine-induced migration and invasion by the suppression of angiogenesis and epithelial-mesenchymal transition in non-small cell lung

References

- cancer cells. *Oncology reports*, 33(6), 2972–2980.
- Shin, A., Connolly, S., & Kabytaev, K. (2023). Protein glycation in diabetes mellitus. *Advances in clinical chemistry*, 113, 101–156.
- Shreenidhi, K. S., & Bose, V. G. (2022). A preliminary investigation on the antihepatotoxic activity of *Artemisia pallens* leaves in the diclofenac-treated-Pangasius Sps. *Polish journal of environmental studies*, 31(5), 4837-4849.
- Singh, A., Kukreti, R., Saso, L., & Kukreti, S. (2022). Mechanistic Insight into oxidative stress-triggered signaling pathways and type 2 diabetes. *Molecules (Basel, Switzerland)*, 27(3), 950. <https://doi.org/10.3390/molecules27030950>
- Singh, B. N., Shankar, S., & Srivastava, R. K. (2011). Green tea catechin, epigallocatechin-3-gallate (EGCG): mechanisms, perspectives and clinical applications. *Biochemical pharmacology*, 82(12), 1807-1821.
- Singh, K., Devi, S., & Pankaj, P. P. (2016a). Diabetes associated male reproductive dysfunctions: prevalence, diagnosis and risk factors. *International journal of drug development and research*, 8, 7-10.
- Singh, N. A., Mandal, A. K., & Khan, Z. A. (2016b). Potential neuroprotective properties of epigallocatechin-3-gallate (EGCG). *Nutrition journal*, 15(1), 60. <https://doi.org/10.1186/s12937-016-0179-4>
- Singleman, C., & Holtzman, N. G. (2014). Growth and maturation in the zebrafish, *Danio rerio*: a staging tool for teaching and research. *Zebrafish*, 11(4), 396–406.
- Sinha A. K. (1972). Colorimetric assay of catalase. *Analytical biochemistry*, 47(2), 389–394.
- Skrypnik, D., Bogdański, P., Zawiejska, A., & Wender-Ożegowska, E. (2019). Role of gestational weight gain, gestational diabetes, breastfeeding, and hypertension in mother-to-child obesity transmission. *Polish archives of internal medicine*, 129(4), 267–275.
- Song, Q. X., Sun, Y., Deng, K., Mei, J. Y., Chermansky, C. J., & Damaser, M. S. (2022). Potential role of oxidative stress in the pathogenesis of diabetic bladder dysfunction. *Nature reviews. Urology*, 19(10), 581–596.
- Soussi, A., Gargouri, M., Aouedi, S., Akrouti, A., Magne, C., & Abdelfattah, E. (2020). The (–)-epigallocatechin gallate (EGCG) ameliorates hyperglycemia and hyperlipidemia-mediated oxidative stress in liver and kidney of alloxan

References

- induced diabetic mice. *Research Square*. <https://doi.org/10.21203/rs.3.rs-28586/v1>
- Soussi, A., Gargouri, M., Magné, C., Ben-Nasr, H., Kausar, M. A., Siddiqui, A. J., Saeed, M., Snoussi, M., Adnan, M., El-Feki, A., Chappard, D., & Badraoui, R. (2022). (-)-Epigallocatechin gallate (EGCG) pharmacokinetics and molecular interactions towards amelioration of hyperglycemia, hyperlipidemia associated hepatorenal oxidative injury in alloxan induced diabetic mice. *Chemico-biological interactions*, 368, 110230. <https://doi.org/10.1016/j.cbi.2022.110230>
- Suchana, S. A., Ahmed, M. S., Islam, S. M. M., Rahman, M. L., Rohani, M. F., Ferdusi, T., Ahmmad, A. K. S., Fatema, M. K., Badruzzaman, M., & Shahjahan, M. (2021). Chromium exposure causes structural aberrations of erythrocytes, gills, liver, kidney, and genetic damage in striped catfish *Pangasianodon hypophthalmus*. *Biological Trace Element Research*, 199(10), 3869-3885.
- Sugahara, M., Pak, W. L. W., Tanaka, T., Tang, S. C. W., & Nangaku, M. (2021). Update on diagnosis, pathophysiology, and management of diabetic kidney disease. *Nephrology (Carlton, Vic.)*, 26(6), 491–500.
- Sun, M., Xie, Q., Cai, X., Liu, Z., Wang, Y., Dong, X., & Xu, Y. (2020). Preparation and characterization of epigallocatechin gallate, ascorbic acid, gelatin, chitosan nanoparticles and their beneficial effect on wound healing of diabetic mice. *International journal of biological macromolecules*, 148, 777–784.
- Sun, W., Liu, X., Zhang, H., Song, Y., Li, T., Liu, X., Liu, Y., Guo, L., Wang, F., Yang, T., Guo, W., Wu, J., Jin, H., & Wu, H. (2017). Epigallocatechin gallate upregulates NRF2 to prevent diabetic nephropathy via disabling KEAP1. *Free radical biology & medicine*, 108, 840–857.
- Tan, M., & Armbruster, J. W. (2018). Phylogenetic classification of extant genera of fishes of the order Cypriniformes (Teleostei: Ostariophysi). *Zootaxa*, 4476(1), 6-39.
- Tanbek, K., & Sandal, S. (2023). An experimental study: Diabetic nephropathy and oxidative damage relationship. *Annals of medical research*, 30(4), 449–454.
- Thakur, S., Gupta, S. K., Ali, V., Singh, P., & Verma, M. (2021). Aldose reductase: a

References

- cause and a potential target for the treatment of diabetic complications. *Archives of pharmacal research*, 44(7), 655–667.
- Thangapandiyan, S., & Miltonprabu, S. (2014). Epigallocatechin gallate supplementation protects against renal injury induced by fluoride intoxication in rats: Role of Nrf2/HO-1 signaling. *Toxicology reports*, 1, 12–30.
- Thomas, H. Y., & Ford Versypt, A. N. (2022). Pathophysiology of mesangial expansion in diabetic nephropathy: mesangial structure, glomerular biomechanics, and biochemical signaling and regulation. *Journal of biological engineering*, 16(1), 19.
<https://doi.org/10.1186/s13036-022-00299-4>
- Thomas, N., & Ting, N. (2014). Minimum Effective Dose (MinED). *Wiley StatsRef: Statistics reference online*. doi:10.1002/9781118445112.stat07098
- Tran, N., Pham, B., & Le, L. (2020). Bioactive compounds in anti-diabetic plants: from herbal medicine to modern drug discovery. *Biology*, 9(9), 252.
<https://doi.org/10.3390/biology9090252>
- Trombini, C., Kazakova, J., Villar-Navarro, M., Hampel, M., Fernández-Torres, R., Bello-López, M. Á., & Blasco, J. (2022). Bioaccumulation and biochemical responses in the peppery furrow shell *Scrobicularia plana* exposed to a pharmaceutical cocktail at sub-lethal concentrations. *Ecotoxicology and environmental safety*, 242, 113845.
- Truong, V. L., & Jeong, W. S. (2021). Cellular defensive mechanisms of tea polyphenols: structure-activity relationship. *International journal of molecular sciences*, 22(17), 9109. <https://doi.org/10.3390/ijms22179109>
- Tsang, B., Zahid, H., Ansari, R., Lee, R. C., Partap, A., & Gerlai, R. (2017). Breeding zebrafish: A review of different methods and a discussion on standardization. *Zebrafish*, 14(6), 561–573.
- Tsang, V. H. M., McGrath, R. T., Clifton-Bligh, R. J., Scolyer, R. A., Jakrot, V., Guminski, A. D., Long, G. V., & Menzies, A. M. (2019). Checkpoint inhibitor-associated autoimmune diabetes is distinct from type 1 diabetes. *The Journal of clinical endocrinology and metabolism*, 104(11), 5499–5506.
- Uchiyama, Y., Suzuki, T., Mochizuki, K., & Goda, T. (2013). Dietary supplementation with (-)-epigallocatechin-3-gallate reduces inflammatory response in adipose

References

- tissue of non-obese type 2 diabetic Goto-Kakizaki (GK) rats. *Journal of agricultural and food chemistry*, 61(47), 11410–11417.
- Ugbomeh, A. P., Bob-manuel, K. N. O., Green, A., & Taylorharry, O. (2019). Biochemical toxicity of Corexit 9500 dispersant on the gills, liver and kidney of juvenile *Clarias gariepinus*. *Fisheries and Aquatic Sciences*, 22, 1-8.
- Unuofin, J. O., & Lebelo, S. L. (2020). Antioxidant effects and mechanisms of medicinal plants and their bioactive compounds for the prevention and treatment of type 2 diabetes: An updated review. *Oxidative medicine and cellular longevity*, 1356893. <https://doi.org/10.1155/2020/1356893>
- Vekic, J., Stefanovic, A., & Zeljkovic, A. (2023). Obesity and Dyslipidemia: A Review of Current Evidence. *Current obesity reports*, 12(3), 207–222.
- Vekic, J., Zeljkovic, A., Cicero, A. F., Janez, A., Stoian, A. P., Sonmez, A., & Rizzo, M. (2022). Atherosclerosis development and progression: the role of atherogenic small, dense LDL. *Medicina*, 58(2), 299. <https://doi.org/10.3390/medicina58020299>
- Verma, B., Singh, C., & Singh, A. (2021). Effect of hydro-alcoholic extract of centella asiatica on streptozotocin induced memory dysfunction in adult zebrafish. *Current research in behavioral sciences*, 2, 100059. <https://doi.org/10.1016/j.crbeha.2021.100059>
- Waltner-Law, M. E., Wang, X. L., Law, B. K., Hall, R. K., Nawano, M., & Granner, D. K. (2002). Epigallocatechin gallate, a constituent of green tea, represses hepatic glucose production. *The Journal of biological chemistry*, 277(38), 34933–34940.
- Wan, C., Ouyang, J., Li, M., Rengasamy, K. R. R., & Liu, Z. (2022). Effects of green tea polyphenol extract and epigallocatechin-3-O-gallate on diabetes mellitus and diabetic complications: Recent advances. *Critical reviews in food science and nutrition*, 19, 1–29.
- Wang, D., Wang, Y., Wan, X., Yang, C. S., & Zhang, J. (2015). Green tea polyphenol (-)-epigallocatechin-3-gallate triggered hepatotoxicity in mice: responses of major antioxidant enzymes and the Nrf2 rescue pathway. *Toxicology and applied pharmacology*, 283(1), 65–74.
- Wang, M., Tan, Y., Shi, Y., Wang, X., Liao, Z., & Wei, P. (2020). Diabetes and

References

- sarcopenic obesity: pathogenesis, diagnosis, and treatments. *Frontiers in endocrinology*, 11, 568. <https://doi.org/10.3389/fendo.2020.00568>
- Wang, S., Wang, H., Chen, Y., Liu, J., He, X., Huang, D., Wu, Y., Chen, Y., & Weng, Z. (2021). Protective effects of (-)-epigallocatechin gallate and curcumin against acrylamide toxicity. *Toxicological & environmental chemistry*, 103(2), 199-218.
- Wang, Y., Feng, F., He, W., Sun, L., He, Q., & Jin, J. (2022). miR-188-3p abolishes germacrone-mediated podocyte protection in a mouse model of diabetic nephropathy in type I diabetes through triggering mitochondrial injury. *Bioengineered*, 13(1), 774–788.
- Watts, S. A., Powell, M., & D'Abramo, L. R. (2012). Fundamental approaches to the study of zebrafish nutrition. *Institute for laboratory animal research journal*, 53(2), 144–160.
- Wen, J. J., Li, M. Z., Chen, C. H., Hong, T., Yang, J. R., Huang, X. J., Geng, F., Hu, J. L., & Nie, S. P. (2023). Tea polyphenol and epigallocatechin gallate ameliorate hyperlipidemia via regulating liver metabolism and remodeling gut microbiota. *Food chemistry*, 404, 134591. <https://doi.org/10.1016/j.foodchem.2022.134591>
- Wibowo, I., Utami, N., Anggraeni, T., Barlian, A., Putra, R. E., Indriani, A. D., Masadah, R., & Ekawardhani, S. (2021). Propolis can improve caudal fin regeneration in zebrafish (*Danio rerio*) induced by the combined administration of alloxan and glucose. *Zebrafish*, 18(4), 274-281.
- Wondmkun Y. T. (2020). Obesity, Insulin resistance, and Type 2 diabetes: Associations and therapeutic implications. *Diabetes, metabolic syndrome and obesity: targets and therapy*, 13, 3611–3616.
- World Health Organization. (1985). Diabetes Mellitus: Report of a WHO Study Group. *World Health Organization technical report series*, 727, 1–113.
- Wu, T., Ding, L., Andoh, V., Zhang, J., & Chen, L. (2023). The mechanism of hyperglycemia-induced renal cell injury in diabetic nephropathy disease: An update. *Life*, 13(2), 539. <https://doi.org/10.3390/life13020539>
- Xu, F. W., Lv, Y. L., Zhong, Y. F., Xue, Y. N., Wang, Y., Zhang, L. Y., Hu, X., & Tan, W. Q. (2021). Beneficial Effects of Green Tea EGCG on Skin Wound Healing: A Comprehensive Review. *Molecules*, 26(20), 6123.

References

- <https://doi.org/10.3390/molecules26206123>
- Yadav, U. C., & Ramana, K. V. (2013). Regulation of NF- κ B-induced inflammatory signaling by lipid peroxidation-derived aldehydes. *Oxidative medicine and cellular longevity*, 2013, 690545. <https://doi.org/10.1155/2013/690545>
- Yang, J., Zhong, C., & Yu, J. (2023). Natural monoterpenes as potential therapeutic agents against atherosclerosis. *International journal of molecular sciences*, 24(3), 2429. <https://doi.org/10.3390/ijms24032429>
- Yang, R., Chen, J., Jia, Q., Yang, X., & Mehmood, S. (2022). Epigallocatechin-3-gallate ameliorates renal endoplasmic reticulum stress-mediated inflammation in type 2 diabetic rats. *Experimental biology and medicine*, 247(16), 1410–1419.
- Yazdi, H. B., Hojati, V., Shiravi, A., Hosseinian, S., Vaezi, G., & Hadjzadeh, M. A. (2019). Liver dysfunction and oxidative stress in streptozotocin-induced diabetic rats: protective role of *artemisia turanica*. *Journal of pharmacopuncture*, 22(2), 109–114.
- Ye, M., & Chen, Y. (2020). Zebrafish as an emerging model to study gonad development. *Computational and structural biotechnology journal*, 18, 2373–2380.
- Yehualashet A. S. (2020). Toll-like receptors as a potential drug target for diabetes mellitus and diabetes-associated complications. *Diabetes, metabolic syndrome and obesity: targets and therapy*, 13, 4763–4777.
- Yildirim, M. Z., Benli, A. C., Selvi, M., Ozkul, A., Erkoç, F., & Koçak, O. (2006). Acute toxicity, behavioral changes, and histopathological effects of deltamethrin on tissues (gills, liver, brain, spleen, kidney, muscle, skin) of Nile tilapia (*Oreochromis niloticus* L.) fingerlings. *Environmental toxicology*, 21(6), 614–620.
- Yingrui, W., Zheng, L., Guoyan, L., & Hongjie, W. (2022). Research progress of active ingredients of *Scutellaria baicalensis* in the treatment of type 2 diabetes and its complications. *Biomedicine & pharmacotherapy*, 148, 112690. <https://doi.org/10.1016/j.biopha.2022.112690>
- Yoon, S. P., Maeng, Y. H., Hong, R., Lee, B. R., Kim, C. G., Kim, H. L., Chung, J. H., & Shin, B. C. (2014). Protective effects of epigallocatechin gallate (EGCG) on streptozotocin-induced diabetic nephropathy in mice. *Acta*

References

- histochemica*, 116(8), 1210–1215.
- Zhang, B. H., Yin, F., Qiao, Y. N., & Guo, S. D. (2022). Triglyceride and triglyceride-rich lipoproteins in atherosclerosis. *Frontiers in molecular biosciences*, 9, 909151. <https://doi.org/10.3389/fmolb.2022.909151>
- Zhang, C., Li, X., Hu, X., Xu, Q., Zhang, Y., Liu, H., Diao, Y., Zhang, X., Li, L., Yu, J., Yin, H., & Peng, J. (2021). Epigallocatechin-3-gallate prevents inflammation and diabetes -Induced glucose tolerance through inhibition of NLRP3 inflammasome activation. *International immunopharmacology*, 93, 107412. <https://doi.org/10.1016/j.intimp.2021.107412>
- Zhang, H., Shao, D., Wu, Y., Dai, B., Cai, C., Fang, W., Ye, B., Zhang, Y., Liu, J., & Jia, X. (2013). Regulation of nodularin-induced apoptosis by epigallocatechin-3-gallate on fish lymphocytes in vitro. *Fish & shellfish immunology*, 34(5), 1085–1093.
- Zhang, R., Zhang, J., Gao, Q., & Guo, N. (2018). Effects of EGCG and chlorpyrifos on the mortality, AChE and GSH of adult zebrafish: Independent and combination. In *IOP conference series: Materials science and engineering*, 301(1), 012168.
- Zhang, S., Xu, H., Yu, X., Wang, Y., Sun, F., & Sui, D. (2015). Simvastatin ameliorates low-dose streptozotocin-induced type 2 diabetic nephropathy in an experimental rat model. *International journal of clinical and experimental medicine*, 8(4), 6388–6396.
- Zhang, Y., Lin, H., Liu, C., Huang, J., & Liu, Z. (2020). A review for physiological activities of EGCG and the role in improving fertility in humans/mammals. *Biomedicine & pharmacotherapy*, 127, 110186. <https://doi.org/10.1016/j.biopha.2020.110186>
- Zhang, Y., Xia, Q., Wang, J., Zhuang, K., Jin, H., & Liu, K. (2022). Progress in using zebrafish as a toxicological model for traditional Chinese medicine. *Journal of ethnopharmacology*, 282, 114638. <https://doi.org/10.1016/j.jep.2021.114638>
- Zhang, Z., Huang, Q., Zhao, D., Lian, F., Li, X., & Qi, W. (2023). The impact of oxidative stress-induced mitochondrial dysfunction on diabetic microvascular complications. *Frontiers in endocrinology*, 14, 1112363. <https://doi.org/10.3389/fendo.2023.1112363>

References

- Zhong, J., Xu, C., Reece, E. A., & Yang, P. (2016). The green tea polyphenol EGCG alleviates maternal diabetes-induced neural tube defects by inhibiting DNA hypermethylation. *American journal of obstetrics and gynecology*, 215(3), 368.e1–368.e10. <https://doi.org/10.1016/j.ajog.2016.03.009>
- Zhong, R., Chen, Y., Ling, J., Xia, Z., Zhan, Y., Sun, E., Shi, Z., Feng, L., Jia, X., Song, J., & Wei, Y. (2019). The toxicity and metabolism properties of *Herba Epimedii* flavonoids on larval and adult zebrafish. *Evidence-based complementary and alternative medicine*, 3745051. <https://doi.org/10.1155/2019/3745051>
- Zhou, C., Yool, A. J., & Byard, R. W. (2017). Armanni–Ebstein lesions in terminal hyperglycemia. *Journal of forensic sciences*, 62(4), 921-925.
- Zohora, K. F. T., & Arefin, M. R. (2022). Tea and tea product diversification: A review. *Turkish journal of agriculture - Food science and technology*, 10(12), 2334–2353.
- Zon, L. I., & Peterson, R. T. (2005). In vivo drug discovery in the zebrafish. *Nature reviews Drug discovery*, 4(1), 35-44.
- Zwolak I. (2021). Epigallocatechin gallate for management of heavy metal-induced oxidative stress: mechanisms of action, efficacy, and concerns. *International journal of molecular sciences*, 22(8), 4027.

Appendix

List of publications

1. **Jamir, A.**, Longkumer, S., & Pankaj, P. P. (2023). Epigallocatechin gallate improves caudal fin regeneration in the streptozotocin-induced diabetic zebrafish model. *Journal of Pharmaceutical Negative Results*, 14(3), 1264-1270.
2. **Jamir, A.**, Longkumer, S., & Punj, P. (2024). Acute Toxicity of Epigallocatechin Gallate and C-Phycocyanin in Zebrafish (*Danio rerio*): Behavioral and Histopathological Studies. *Indian Journal of Pharmaceutical Sciences*, 86(2), 546-555.
3. **Jamir, A.**, Longkumer, S., Roy, V. K., Kharwar, R. K., & Pankaj, P. P. (2024). Feasibility study of foldscope microscope for selected mammalian endocrine glands. *Multimedia Tools and Applications*, 83(6), 16197-16203.
4. Longkumer, S., **Jamir, A.**, & Pankaj, P. P. (2020). Development and appraisal studies of chemically induced zebrafish hyperglycemia model. *Journal of Experimental Zoology, India*, 23(2), 1305-1310.
5. Kechu, M., Ezung, S., Longkumer, S., **Jamir, A.**, & Pankaj, P. P. (2020). Progress and Prospects for Sustainable Conservation of Threatened Cold Water Fishes of Northeast India with Special Reference to Nagaland State. *Journal of Experimental Zoology, India*, 24 (1), 27-33.
6. Ezung, S., Kechu, M., Longkumer, S., **Jamir, A.**, & Pankaj, P. P. (2020). A review on the ichthyofauna of Nagaland, North-East India. *World News of Natural Sciences*, 30 (2), 104-116.
7. Longkumer, S., **Jamir, A.**, Kechu, M., Ezung, S., & Pankaj, P. P. (2021). Alloxan monohydrate induced diabetes: A comprehensive review. *International Journal of Innovative Life Sciences*, 1 (1), 1-9.
8. Longkumer, S., **Jamir, A.**, & Pankaj, P. P. (2022). Evaluation of lipid profile in streptozotocin induced diabetic zebrafish, treated with C-phycocyanin and Epigallocatechin gallate. *Biochemical and Cellular Archives*, 22(1), 1441-1446.
9. Longkumer, S., **Jamir, A.**, & Pankaj, P. P. (2022). Maintenance and breeding of Zebrafish (*Danio rerio*) under laboratory condition. *Agricultural Science Digest*. DOI: 10.18805/ag.D-5599.

Book chapters in edited books

1. **Jamir, A.**, Longkumer, S., & Pankaj, P. P. (2022). Biomedical Applications of Epigallocatechin Gallate (EGCG) – A Potent Green Tea Extract. *Biological Spectrum of Northeast India. (Annual Bioscience Communication); Vol. I*, 2021, 11-18.
2. Longkumer, S., **Jamir, A.**, & Pankaj, P. P. (2020). In-vivo animal models for the study of diabetes mellitus. *Biological Spectrum of Northeast India* edited by Hemen Chandra Majumdar, ISBN 9789390434190: (Annual Bioscience Communication); Vol. I, 2021, 66-74.

Epigallocatechin Gallate Improves Caudal Fin Regeneration in the Streptozotocin-Induced Diabetic Zebrafish Model

Ajunlia Jamir¹, Sentianger Longkumer², Pranay Punj Pankaj³

^{1,2,3}Department of Zoology, Fish Biology and Fisheries Laboratory, Nagaland University, Lumami - 798627, India
Email: pranaypunj@gmail.com
DOI: 10.47750/pnr.2023.14.03.168

Abstract

Impaired wound healing is the leading manifestation of diabetes mellitus (DM). It is mainly triggered by chronic inflammation, hyperglycemia, hypoxia, and delayed neuropeptide signaling. The rising number of DM patients exhibiting poor healing of DM wounds has, thus, given rise to the need for therapeutic intervention. Natural extracts are said to contain high anti-oxidant and anti-inflammatory properties that decrease the pathogenesis of DM. It was recorded that epigallocatechin gallate (EGCG) can improve the blood glucose level and caudal fin regeneration in the streptozotocin-induced zebrafish model. The animals were categorized into four groups. The hyperglycemic state was maintained throughout the experiment for 21 days in the test subject. After the treatment with EGCG, the test zebrafish showed a decrease in blood glucose level from 295.5±14.7 mg/dl to 99.6±4.7 mg/dl on day 21. Results showed better regeneration of amputated caudal fin in the group treated with EGCG. The percentage regeneration in the caudal fin was 60% in diabetic subjects treated with EGCG and 66% in control subjects treated with EGCG, whereas diabetic zebrafish showed only 41% regeneration on day 21. It can be concluded that EGCG has the potency to treat impaired wounds in the DM model of zebrafish.

Keywords: Blood glucose level, diabetes mellitus, epigallocatechin gallate, fin regeneration, zebrafish.

INTRODUCTION

Diabetes mellitus (DM) is a metabolic dysregulation characterized by elevated blood glucose levels or hyperglycemia caused by disruption of glucose homeostasis in the blood. Ultimately several complications are accompanied, such as retinopathy, cardiovascular disease, stroke, delayed wound healing, and neuropathy [1,2]. Impaired wound healing is considered one of the leading manifestations of DM, a long-term complication that significantly degrades the quality of life [3]. Impaired wound healing is mainly triggered by chronic inflammation, hyperglycemia, hypoxia, sensory neuropathy, and delayed neuropeptide signaling [4,5]. DM is said to cause delayed wound healing by affecting the biological mechanisms of the patients [6]. Secondary complications such as the increased risk of infections, inflammatory phase around the wound, decreased cell number and growth factor response resulting in decreased local angiogenesis, inhibition of blood flow in peripheral blood vessels to chronic injuries, and amputations are prone to occur [7]. The rising number of DM patients exhibiting poor healing of the DM wound has, thus, given the need for therapeutic intervention [8]. Zebrafish (*Danio rerio*) is a well-established animal model used to study developmental biology, human disease, and regeneration [9]. It is considered a valuable model system for studying regenerative biology as it can restore poorly restored organs in other mammals [10]. The caudal fin of the zebrafish is considered the most convenient tissue approach experimentally due to its accessibility, simple structure, and fast regeneration [11]. Studies showed that streptozotocin (STZ) injection in adult zebrafish sustained hyperglycemia as the blood glucose level and biochemical properties were elevated [12]. Further, zebrafish consists of critical signaling pathways that play essential roles in regulatory pathways and are associated with wound healing, including Hedgehog (Hh), bone Morphogenetic Protein (BMP), and Wnt/catenin signaling pathways [13].

Although synthetic drug therapies are used to treat DM wounds to subdue chronic injury and restore tissue regeneration, side effects are always associated with it. Therefore, alternative therapies with minimal side effects showing positive results are a point of concern and a clinical challenge for researchers today. Natural extracts are said to contain high anti-oxidant and anti-inflammatory properties that decrease the pathogenesis of DM [14]. One such natural product is Epigallocatechin gallate (EGCG), an extract from green tea known for its high antioxidant and anti-inflammatory properties [15]. EGCG has been effectively used to treat cancer and cardiovascular diseases and has also emerged as a potent anti-diabetic agent [16,17]. In an

Journal of Pharmaceutical Negative Results | Volume 14 | Issue 3 | 2023

1264

Research Paper

Acute Toxicity of Epigallocatechin Gallate and C-Phycocyanin in Zebrafish (*Danio rerio*): Behavioral and Histopathological Studies

AJUNGLA JAMIR, SENTIYANGER LONGKUMER AND P. P. PUNJ*

Department of Zoology, Fish Biology and Fisheries Laboratory, Nagaland University, Lumami, Nagaland 798627, India

Jamir et al.: Acute Toxicity of Epigallocatechin Gallate and C-Phycocyanin in Zebrafish

Epigallocatechin gallate and C-phycocyanin are natural food supplements, gaining a lot of popularity in biomedical researches. The lethal concentration 50 value for the zebrafish model was determined using a 96 h semi-static acute toxicity test. Zebrafish were transferred into a 1 l water tank starting with a minimal dose of 8 mg of epigallocatechin gallate and 1 g of C-phycocyanin, which further increased to the concentration of 30 mg for epigallocatechin gallate and 5 g for C-phycocyanin. Lethal concentration 50 of epigallocatechin gallate and C-phycocyanin was calculated to be 21.37 mg/l and 2.45 g/l respectively at 96 h in the zebrafish model. At high doses above 12 mg of epigallocatechin gallate and 1 g of C-phycocyanin, the test fish displayed various behavior responses like erratic and jerky swimming, attempts to jump out of the water, frequent surfacing and swallowing of air, normal skin color change, decreased opercular movement and finally leading to death. Histological observations showed hypertrophy, atrophy and vacuolar degeneration in the liver whereas tubular degeneration, glomerular hyper cellularity, dilation of Bowman's space, hemorrhage, and necrosis were observed in the kidneys exposed to the high doses of epigallocatechin gallate and C-phycocyanin treated fish. The gills of the test animals also expressed lamellar synechia, hyperplasia, curling of lamellae, mucus secretion and shortening of the secondary lamella. The results demonstrated that doses above 30 mg/l and 5 g/l in the case of epigallocatechin gallate and C-phycocyanin respectively gave 100 % mortality and expressed organ-specific toxicity. Overall results revealed that exposure to high concentrations of epigallocatechin gallate and C-phycocyanin uninterruptedly may lead to severe alterations in the tissue of experimental animals.

Key words: Acute toxicity, behavior response, C-phycocyanin, zebrafish model, epigallocatechin gallate, histological observations

Toxicity is the leading cause of drug development failure and it is a key concentration and issue for current drug discovery^[1]. People assume that all-natural products are safe to consume and that no more research is required on toxicity. Offlate natural food supplements are gaining a lot of popularity; two such products are Epigallocatechin Gallate (EGCG) and C-Phycocyanin (C-PC). EGCG is one of the most studied and abundant catechins found in green tea extract. It is well known to exhibit antioxidant and anti-inflammatory properties and is marketed as a dietary supplement^[2]. Studies in model animals have shown that it inhibits the development and growth of tongue cancer cells in Keratin 14 (KRT14)/ERK1-Kirsten Rat Sarcoma Virus (Kras) transgenic mice^[3]. It induces apoptosis and inhibits the Phosphatidylinositol-3-Kinase (PI3K)/Protein Kinase B (Akt)/

mammalian Target of Rapamycin (mTOR) pathway progression in precancerous lesions of gastric carcinoma treated rats^[4]. It protects and improves the colon from chemically induced agents like N, N'-Dimethylhydrazine (DMH) in Wistar rats and protects the lung against fluoride-induced oxidative injury^[5]. However, findings suggest the use of EGCG as a pro-oxidant; a high dose of EGCG causes events of hepatotoxicity as well as suppresses the antioxidant enzyme in the liver^[7]. C-PC is a light-harvesting, water-soluble, protein-bound pigment obtained from some microalgae

This is an open access article distributed under the terms of the Creative Commons Attribution-NonCommercial-ShareAlike 3.0 License, which allows others to remix, tweak, and build upon the work non-commercially, as long as the author is credited and the new creations are licensed under the identical terms

Accepted 19 March 2024
Revised 16 April 2023
Received 04 September 2022
Indian J Pharm Sci 2024;86(2):946-955

*Address for correspondence
E-mail: pranaypunj@gmail.com
March-April 2024

Indian Journal of Pharmaceutical Sciences

548

Appendix

Multimedia Tools and Applications (2024) 83:16197–16203
https://doi.org/10.1007/s11042-023-16142-x



Feasibility study of foldscope microscope for selected mammalian endocrine glands

Ajungla Jamir¹ · Sentiyanger Longkumer¹ · Vikas Kumar Roy² ·
Rajesh Kumar Kharwar^{3,4} · Pranay Punj Pankaj¹

Received: 14 February 2022 / Revised: 29 May 2023 / Accepted: 3 July 2023 /
Published online: 13 July 2023
© The Author(s), under exclusive licence to Springer Science+Business Media, LLC, part of Springer Nature 2023

Abstract

Foldscope is a low cost, an origami-based optical microscope. It is extremely portable, durable, and can be assembled and constructed in minutes, achieving a magnification of 140X and a resolution of 2 μm . The objective of the present study is to evaluate the feasibility of foldscope by using mobile phone-based microscopy for class room study by selecting slides of mammalian endocrine glands (adrenal, thyroid, ovary, testis and pancreas), and to compare with the conventional microscope in the laboratory facility. Mobile phones were connected with the foldscope using a cassette and magnetic coupler to take images of the histology samples. The image acquired from both sources were edited further and put together for comparison. It was found that tissue sections of mammalian endocrine glands observed under foldscope were comparable to conventional light microscope images. The overall study of the images by the foldscope showed its potential use for classroom demonstration. It could also be stated that mobile phone-based portable microscopy with foldscope is feasible for histological sample investigations, especially in Limited-Resource Institutions.

Keywords Foldscope · Mobile phone-based microscopy · Endocrine glands, histology · Limited-resource institutions · Imaging

✉ Vikas Kumar Roy
vikasroy4araria@yahoo.co.in; vikasroy4araria@gmail.com

✉ Rajesh Kumar Kharwar
rkharwar1982@gmail.com

✉ Pranay Punj Pankaj
pranaypunj@gmail.com

¹ Department of Zoology, Nagaland University, Lumami, Zunheboto, Nagaland 798627, India

² Department of Zoology, Mizoram University, Aizawl, Mizoram 796004, India

³ Department of Zoology, Kutir Post Graduate College, Chakkey, Jampur, Uttar Pradesh, India

⁴ Department of Zoology, University of Lucknow, Lucknow, Uttar Pradesh 226007, India



J. Exp. Zool. India Vol. 23, No. 2, pp. 1305-1310, 2020

www.connectjournals.com/jez

ISSN 0972-0030

DEVELOPMENT AND APPRAISAL STUDIES OF CHEMICALLY INDUCED ZEBRAFISH HYPERGLYCEMIA MODEL

Sentiyanger Longkumer, Ajungla Jamir and Pranay Punj Pankaj*

Department of Zoology, Fish Biology and Fisheries Lab, Nagaland University, Lumami - 798 627, India.

*e-mail : pranaypunj@gmail.com

(Received 22 April 2020, Accepted 15 June 2020)

ABSTRACT : Diabetes mellitus (DM) is a metabolic disorder characterized by hyperglycemia and alterations in carbohydrate, fat and protein metabolism. Zebrafish (*Danio rerio*) exhibits many features of vertebrate models apart from physiological and anatomical characteristics of higher organisms that prompted scientists around the world to use it in biomedical research. In this study, we performed a validation study for the development of optimal hyperglycemia in zebrafish involving diabetogenic agents such as alloxan monohydrate (AM), streptozocin (STZ) and glucose water solution (GLU-W). Exposure of 100 mg of AM/dL and 200 mg of AM/dL for 30 mins were not capable of inducing DM in the subjects, whereas exposure of 300 mg of AM/dL and 400 mg of AM/dL for 30 mins were able to induce DM in the zebrafish. Mortality had also been recorded in the group treated with 400 mg of AM/dL. Overall, a dose of 300 mg of AM/dL for 30 mins was found to be suitable to induce DM in the subjects. Zebrafish showed diabetic when treated with AM then after exposure with 1% GLU-W minimum for 30 mins, but when the subjects left normal after induction, blood glucose level went down to time. It was also observed that when the subjects kept in different GLU-W (1%, 2% and 3%) for a minimum of 21 days then it took 21 days to induce DM in the subject treated with 1% GLU-W treated subjects whereas exposure with 1% and 2% GLU-W showed diabetes just after 7 days and 4 days onwards. Streptozocin (0.35 mg/gm of body weight) exposed with its booster doses was found to maintain diabetes in the subject for 21 days without any mortality which may be helpful for the researchers' working on secondary complications of DM taking zebrafish as a model.

Key words : Diabetes mellitus, zebrafish, alloxan monohydrate, streptozocin, glucose water solution.

INTRODUCTION

Diabetes mellitus (DM) is caused when blood glucose levels rise. Many complications, such as atherosclerosis, neuropathy, and cataract formation also accompany with DM (Pankaj, 2015; Devi *et al.*, 2016). 346 million people are currently affected by DM and it is projected to increase to 400 million by 2030. India's National Health Policy 2017 aims to increase screening and treatment of 80% of people with diabetes and reduce premature deaths from diabetes by 25% by 2025 (Lovic *et al.*, 2020). Evidence from both laboratory and large-scale clinical trials have revealed that diabetic complications progress unimpeded via the metabolic memory phenomenon even after achieving of glycemic control.

The diabetic models are chemically induced to destroy the beta cells, leading to hyperglycemia. Once diabetic complications are initiated, they continue to progress uninterruptedly even when glycemic control is achieved. Zebrafish is established as an appropriate animal model

for understanding vertebral-like physiological and pathological conditions (Maddison and Chen, 2012; Asaoka *et al.*, 2013; Stewart *et al.*, 2014). Due to its small size, fecundity, and output of optically clear embryos that undergo exceptionally rapid growth, zebrafish offers many advantages that make it an effective disease model (Amsterdam and Hopkins, 2006). As a vertebrate, the zebrafish's most important benefit is that it has a very close genome structure to that of humans, and is thus used for human genomic function studies (Dahme *et al.*, 2009; Ekker, 2008; Kinkel and Prince, 2009; Olsen *et al.*, 2010). Many laboratories have used zebrafish to perform studies on diabetes. These studies used an acute hyperglycemia model of zebrafish with glucose water only or streptozocin (Gleeson *et al.*, 2007; Kinkel and Prince, 2009; Olsen *et al.*, 2010). The diabetic zebrafish model induced with only glucose water required for a long time.

Zebrafish are freshwater teleosts which regulate their concentrations of internal water and total solute (Eames

Appendix

J. Exp. Zool. India Vol. 24, No. 1, pp. 27-33, 2021	www.connectjournals.com/jez	ISSN 0972-0030
DocID: https://connectjournals.com/03895.2021.24.27		eISSN 0976-1780

PROGRESS AND PROSPECTS FOR SUSTAINABLE PRODUCTION AND CONSERVATION OF THREATENED COLDWATER FISHES OF NORTH-EAST INDIA WITH SPECIAL REFERENCE TO NAGALAND STATE

Metevinu Kechu, Sophiya Ezung, Sentiyanger Longkumer, Ajungla Jamir and Pranay Punj Pankaj*

Department of Zoology, Nagaland University, Headquarters: Lumami -798 627, Nagaland, India.
*e-mail: pranaypunj@gmail.com

(Received 16 October 2020, Accepted 21 December 2020)

ABSTRACT : The geographic position of Northeast India with its captivating landscapes, climatic conditions of rivers or lakes to swift-running stream or rivulets makes it an ideal location for the existence of coldwater fishes in the region. Unfortunately, threatened coldwater fishes have declined in population because of overexploitation, destructive fishing methods, chemical toxins, and habitat fragmentation. It is highly recommended that the government and the local stakeholders adopt a more constructive technology-based approach and strengthened policies for enhancing sustainable fish production and conservation.

Key words : Northeast India, coldwater fishes, habitat fragmentation, constructive technology-based approach, sustainable fish production and conservation.

How to cite : Metevinu Kechu, Sophiya Ezung, Sentiyanger Longkumer, Ajungla Jamir and Pranay Punj Pankaj (2021) Progress and prospects for sustainable production and conservation of threatened coldwater fishes of North-East India with special reference to Nagaland State. J. Exp. Zool. India 24, 27-33. DocID: https://connectjournals.com/03895.2021.24.27

INTRODUCTION

A total number of 278 coldwater fish species consisting of 21 families and 76 genera are distributed in the peninsular plateau and the uplands of Himalayas (Singh *et al.*, 2015). Coldwater fishes consist of both the exotic and the indigenous fish species. The most common indigenous coldwater fish harbours the Mahseer viz. *Tor tor* and *Tor putitora*, schizothoracines like *Schizothorax richardsonii*, *Schizothorax progastus*, *Schizothorax curvifrons* and *Schizothorax esocinus* and *Schizothorax niger*. In contrast, the exotic coldwater fish consists of exotic trouts like *Oncorhynchus mykiss* and *Salmo trutta*. Among these fishes, *Schizothorax richardsonii*, *Schizothorax progastus* and *Tor putitora* are mostly preferred for aquaculture prospects for their wide range availability and distribution. Exotic trouts like *Salmo trutta fario* and *Oncorhynchus mykiss* were first transferred from Europe in 18th century during the British colonial rule in the cold waters of the Himalayan and Peninsular rivers. These exotic species have been closely associated with angling or sport fishing by British administrators (Schgal, 1989). Indigenous species taking into advantages of its wide distribution and consumer

preferences by the local people can boost its aquaculture production in Northeast and the country by further setting research interest on its thriving culture, health management, feeding nature, and breeding biology. The ICAR-Directorate of Coldwater Fisheries Research, Bhimtal, Uttarakhand, has recently chosen five species: *Semplotus semplotus*, *Labeo dero*, *Labeo dyocheilus*, *Neolissocheilus hexagonolepis* and *Osteobrama belangeri*, as upcoming candidate species for aquaculture.

India's north-eastern region has diversified physiographic landscapes ranging from numerous hill streams to major perennial rivers to varied mountain terrains, making it one among the 34 biodiversity hotspots globally by Conservation International (Roach, 2005). Northeast India is home to a wide variety of native and rheophilic fishes such as loaches, minor carps, minnows, catfishes, and mahseers to barbs, making it a biota hotspot for endemic freshwater fauna and flora. It is also contributing to the economy and livelihood of many local communities. There are about 0.92 lakh ha dams, 0.4 lakh ha mini barrages and small ponds in the north-eastern region that can be used effectively and productively for the production of coldwater fisheries (Sarma *et al.*, 2015).

Available online at www.worldnewsnaturalsciences.com



World News of Natural Sciences

An International Scientific Journal

WNOFNS 30(2) (2020) 104-116

EISSN 2543-5426

A Review on the Ichthyofauna of Nagaland, North-East India

Sophiya Ezung¹, Metevinu Kechu, Sentiyanger Longkumer, Ajungla Jamir & Pranay Punj Pankaj²

Department of Zoology, Nagaland University, Headquarters, Lumami 798627, India

^{1,2}E-mail address: sophiezung@gmail.com, pranaypunj@gmail.com

ABSTRACT

North-East India is a region with many native freshwater fishes and is one of the ichthyofaunal hotspots of the world. According to the current study, a total of 197 valid species of fish has been reported from Nagaland, India, which consists of 10 orders, 26 families and 87 genera, from various lotic and lentic habitats. Family Cyprinidae consists of the highest record of 75 fish species and Osphronemidae, Gobidae, Sciaenidae and Chacidae families with the lowest record of one fish species in each.

Keywords: North-East India, Ichthyofaunal hotspots, lotic and lentic habitat, Nagaland, Cyprinidae

1. INTRODUCTION

Northeast is known as one of the hot spots of the global biodiversity of freshwater fish that include substantial fish germplasm reserves. This region of India comprises eight states, viz: Assam, Arunachal Pradesh, Manipur, Meghalaya, Mizoram, Nagaland, Tripura and Sikkim. The abundance of ichthyofaunal diversity in this region is by forming part of the Himalayas and Indo-Burma. A total of 422 species belonging to 39 families is present in the Northeast region.

Nagaland is a small hilly mountainous state, in the northwestern corner of the country. It is situated between 25°6'-27°4' N latitudes and between 93°2'-95°1' E longitudes. The state of Nagaland has many rivers and hill streams blessed by the unusual exotic fish fauna.

(Received 10 March 2020; Accepted 01 April 2020; Date of Publication 02 April 2020)

Appendix



**International Journal of
INNOVATIVE
LIFE SCIENCES**
International Peer Reviewed Open
Access Referred Journal

Int. J. of Innovative Life
Sciences, 2021; 1 (1): Jan 2021

Available online at
<http://stjosephuniv.edu.in/ijils/ijils.html>

Original Article

Open Access

ALLOXAN MONOHYDRATE INDUCED DIABETES: A COMPREHENSIVE REVIEW

Sentiyanger Longkumer¹, Ajungla Jamir¹, Metevinu Kechu¹, Sophiya Ezung¹, & Pranay Punj Pankaj^{1*}

¹ Department of Zoology, Nagaland University, Headquarters: Lumami-798627
E-mail address: longkumersentiyanger@gmail.com

Abstract

Diabetes trials of alloxan monohydrate have been one of the most used diabetes chemicals. The action mechanism in β cells has been thoroughly studied and understood quite well. When given parentally (intravenously, intraperitoneally or subcutaneously), alloxan exercises its diabetic effect. Analogous to toxic glucose, alloxan typically accumulates through the existing glucose conveyor (GLUT2) in pancreatic β -cells. The dose requirement for alloxan differs to cause diabetes varies on choice of animal species and route of administration. Nutritional status of animals also plays a great role in creation of diabetic model. The analysis briefly explains the chemical properties of alloxan, the dosage used by different species and the mechanism of its action.

Keywords: Alloxan monohydrate, Diabetogenic chemicals, Glucose analogue, Glucose transporter.

Article History: Received : 26th December 2019; Accepted : 01st April 2020

©2020 | IJILS. All Rights Reserved |

6

Biochem. Cell. Arch. Vol. 22, No. 1, pp. 1441-1446, 2022
DocID: <https://connectjournals.com/03896.2022.22.1441>

www.connectjournals.com/bca

ISSN 0972-3073

eISSN 0976-1772

EVALUATION OF LIPID PROFILE IN STREPTOZOTOCIN-INDUCED DIABETIC ZEBRAFISH, TREATED WITH C-PHYCOCYANIN AND EPIGALLOCATECHIN GALLATE

Sentiyanger Longkumer, Ajungla Jamir and Pranay Punj Pankaj*

Department of Zoology, Fish Biology and Fisheries Laboratory, Nagaland University, Lumami - 798 627, India.
*e-mail : pranaypunj@gmail.com

(Received 10 January 2022, Revised 11 March 2022, Accepted 27 March 2022)

ABSTRACT : Of late, the use of natural products for various drug analyses and development has steadily increased. C-phycoerythrin (C-PC) and Epigallocatechin gallate (EGCG) are two natural products that are gaining much attention from researchers all over the globe for their diverse biomedical applications. The former is popularly used as a protein supplement and the later as a tea drink. In light of its strong biomedical potential, the present experiment was carried out to investigate the therapeutic roles of C-PC and EGCG in streptozotocin-induced diabetic zebrafish. Hyperglycemia was induced in the zebrafish model by streptozotocin (STZ) dose (0.35 mg/g of body weight) and then exposed to effective doses of 300 mg/L C-PC and 6 mg/L EGCG for 21 days. The serum lipid profile changes of normal, diabetic, and compound-treated zebrafish were analyzed. Diabetic zebrafish exhibited a significant ($p < 0.05$) increase in serum cholesterol, triglycerides, low-density lipoprotein, and very-low-density lipoprotein compared to the non-diabetic group, while high-density lipoprotein was affected contrarily as it was significantly ($p < 0.05$) decreased in diabetic subjects. On treatment with C-PC and EGCG for 21 days, the diabetic subjects were found to show profound improvement of the altered serum lipid profile, indicating their significant effect in countering the alterations caused in case of diabetic conditions and thus exhibiting its potential for possible supplement in the treatment of diabetes and its related complications.

Key words : C-phycoerythrin, epigallocatechin gallate, hyperglycemia, zebrafish, biomedical potential, lipid profile.

How to cite : Sentiyanger Longkumer, Ajungla Jamir and Pranay Punj Pankaj (2022) Evaluation of lipid profile in streptozotocin-induced diabetic zebrafish, treated with C-phycoerythrin and epigallocatechin gallate. *Biochem. Cell. Arch.* 22, 1441-1446.
DocID: <https://connectjournals.com/03896.2022.22.1441>

INTRODUCTION

Diabetes Mellitus (DM) is a metabolic disorder in which a person's blood sugar levels remain abnormally high, either as a result of insufficient insulin production by the body or as a result of insulin resistance in the cells. It is one of the costliest and most burdensome chronic diseases affecting people globally. 346 million people are currently affected by DM and it is expected to reach 400 million by 2030. The National Health Policy, 2017 of India seeks to detect and treat 80% of diabetics and reduce diabetes-related premature deaths by 25% by 2025 (Lovic *et al.*, 2020). Hyperglycemia is the main clinical symptom of DM, causing glycation of body proteins leading to several secondary complications affecting the eyes, nerves, sexual and reproductive functions, kidneys and blood vessels (Rodén, 2012; Pankaj, 2015; Devi *et al.*, 2016 and Singh *et al.*, 2016).

STZ is a naturally occurring chemical compound

obtained from the gram-positive bacterium *Streptomyces achromogenes*. STZ causes the death of pancreatic islet cells, and it is commonly employed in experimental settings to develop a type 1 diabetes mellitus (T1DM) model, while multiple low doses are used to induce type 2 diabetes mellitus (T2DM). The diabetic model in adult zebrafish through STZ induces pancreatic β -cell death, promoting diabetic complications such as a rapid increase in blood glucose levels, increased serum protein glycation, retinopathy, impaired regeneration in damaged areas, and decreased serum insulin levels (Olsen *et al.*, 2010). STZ is found to give reliable, stable, and highly effective hyperglycemia conditions. It has provided a suitable model for long-term diabetes complications studies with a single diabetogenic dose inducing DM within 24 hrs (Longkumer *et al.*, 2021).

Natural products are being used for various drug analyses and development. C-PC and EGCG are two such natural products. The bioactivity of *Spirulina platensis*

D-5599
[1-5]

RESEARCH ARTICLE

Agricultural Science Digest, Volume Issue, 1

Maintenance and Breeding of Zebrafish under Laboratory Conditions for Animal Research

Sentiyanger Longkumer, Ajungla Jamir, Pranay Punj Pankaj

10.18805/ag.D-5599

ABSTRACT

Background: Zebrafish is widely used in biomedical research to explore several diseases and abnormalities. A thorough understanding of husbandry is required to maintain effectively, breed and produce healthy and diversified colonies. Diet, age, size, light exposure, mating behaviour, tank temperature and time used for egg formation are all factors that influence the breeding process. **Methods:** The fishes were kept in the zebrafish housing system with frequent water quality checks and a breeding duration of 7 days. Developing eggs and larvae were photographed and further processed with image view software. The normal development of zebrafish goes through seven stages: ovulation, cleavage, blastula, gastrula, segmentation, pharyngula and hatching stage. **Result:** The average number of eggs deposited per female in the experiment was 3414.21, with 3181.4.81 viable eggs, 2984.00 eggs hatched after 72 hours and 2702.34 fingerlings survived was excluded after a week. The present paper discusses the care of zebrafish, setting up and maintenance in laboratory conditions. Once the system is standardized, it is easy to access healthy eggs, larvae and adults throughout the year for research and teaching purposes.

Key words: Biomedical application, Breeding biology, Embryonic development, Viable embryos, Water quality parameters.

INTRODUCTION

The zebrafish, formerly known as *Brachydanio rerio*, is a tropical freshwater teleost belonging to the Cyprinidae family and Cypriniformes order. No animal model is completely perfect for exploring human diseases. Because of ethical concerns, the search for new animal models has increased worldwide. The zebrafish *Danio rerio*, which has a fully sequenced genome and human-like features, is an effective animal model for studying human diseases. The zebrafish exhibits many features of vertebrate models apart from physiological and anatomical characteristics of higher organisms that attracted scientists worldwide for its use in biomedical research (Zhao *et al.*, 2015). It is very easy to handle and care for zebrafish because its short life cycle, small size, good fecundity and optical clarity of embryos make it suitable for toxicological, developmental and pathological research. Their transparency enables the monitoring of developmental processes using non-invasive imaging and tracking of protein/cell markers in the body system (Spitsbergen, 2007). Model zebrafish can be developed diabetes, lipid-related diseases (Longkumer *et al.*, 2022) and cancer as in human beings. Its embryo is an excellent vertebrate system for studying the cellular and molecular functions of genes associated with Alzheimer's disease (Kroehler *et al.*, 2018). It has also increasingly been used as a host for studies on infectious diseases. The behavioural responses of zebrafish to heavy metals and stress and catfish have been reviewed (Sahoo *et al.*, 2017; Huang *et al.*, 2021). Many drug compounds can be screened primarily through toxicological studies in carps, saving money and time (Kumar and Chand, 2021). For toxicity testing of water, the zebrafish embryo was included in the ISO test (ISO 15088:2007). Understanding and producing

Department of Zoology, Fish Biology and Fisheries Laboratory, Nagaland University, Lumami- 798 627, Nagaland.

Corresponding Author: Pranay Punj Pankaj, Department of Zoology, Fish Biology and Fisheries Laboratory, Nagaland University, Lumami-798 627, Nagaland. Email: pranaypunj@gmail.com

How to cite this article: Longkumer, S., Jamir, A. and Pankaj, P.P. (2022). Maintenance and Breeding of Zebrafish under Laboratory Conditions for Animal Research. Agricultural Science Digest. DOI: 10.18805/ag.D-5599.

Submitted: 11-04-2022 Accepted: 25-06-2022 Online: 31-08-2022

healthy stock in laboratory conditions becomes vital in light of the above utility of zebrafish and its ever-expanding application. A laboratory environment resembling zebrafish's natural habitat is necessary for optimal stock production. It has been shown that the agro-climatic conditions for zebrafish development can be maintained by utilising the zebrafish housing system (Model-NT-ZB-11; Make-Narshi Technologies). The increase in demand for zebrafish is mainly satisfied by wild catch; such housing systems are helpful in ensuring the long-term viability and sustainability of ichthyofaunal resources. The paper then illustrates the basic process involved in the successful breeding of zebrafish.

MATERIALS AND METHODS

Animals

Adult zebrafish of both sexes were procured in bulk from Aqua Fish and Pets, Jorhat, Assam, India. Then they were acclimatised and cultured in a zebrafish housing system (Model-NT-ZB-11; Make-Narshi Technologies). Polycarbonate

Volume Issue

1

2

Biomedical Applications of Epigallocatechin Gallate (EGCG) – A Potent Green Tea Extract

Ajungla Jamir
Sentiyanger Longkumer
Sophiya Ezung
Metevinu Kechu
Pranay Punj Pankaj

Abstract

Epigallocatechin Gallate (EGCG), a vital compound found in green tea, is believed to be responsible for many health benefits associated with green tea consumption. The compound EGCG showed to be potential in regulating many disease-specific molecular targets. EGCG has been shown to exhibit anticancer, antioxidant, antidiabetic properties and neurogenerative effects. The study on the efficacy of green tea extract - EGCG as a medicinal value is a new area for current scientists to verify the proposed claim with a suitable working model and research plan. Hence, further study with concrete observation and findings can be done using *in vitro*, *in vivo* or animal model. This review compiles the existing literature related to the biomedical applications of EGCG.

Keywords: Epigallocatechin gallate (EGCG), Anticancer effect, Antioxidant effect, Antidiabetic effect, Neurodegenerative diseases

8

In-vivo animal models for the study of diabetes mellitus

Sentiyanger Longkumer
Ajungla Jamir
Pranay Punj Pankaj

Abstract

Diabetes mellitus is a metabolic disorder characterised by hyperglycemia and alterations in carbohydrate, fat and protein metabolism. Animal models play an important role in diabetic research and make a significant contribution to it. They provide researchers with the ability to monitor the different genetic and environmental factors that affect the development and complications of diabetes mellitus, leading to potential curative and preventive steps. This review throws light into *in-vivo* animal models in the form of chemical, surgical and genetic-induced models used to study diabetes.

Keywords: *Diabetes mellitus, Animal models, Genetic and environmental factors, In-vivo animal models, Genetic induced model*

Introduction

Diabetes mellitus (DM) is caused when blood glucose levels rise. Many complications, such as atherosclerosis, neuropathy, and cataract formation, also accompany DM (Pankaj, 2015). DM is of 3 main types, namely Type 1 diabetes, known as juvenile-onset diabetes, representing 10% of all DM cases (Cefalu, 2006). It is linked with the destruction of pancreatic β cells which produces insulin. Type 2 diabetes is also known as adult-onset diabetes, representing about

Patents

1. **Jamir, A.**, Kumar, R., Longkumer, S., Pankaj, P., Phukan, M. (2024). Ein System zur Bewertung der restaurativen Wirkung von EGCG auf veränderte Stoffwechselenzyme in einem Streptozotocin-induzierten diabetischen Zebrafisch-Modell (German Patent No. 202024100859). German Patent and Trade Mark Office.
2. Pankaj, P., Longkumer, S., **Jamir, A.**, Giridharan, B., Phukan, M., Kumar, R. (2024). Laboratory System for Maintenance of Small Ornamental Fish. Indian Design No.: 406559-001. The Patent Office, Government of India.
3. Pankaj, P., **Jamir, A.**, Longkumer, S., Giridharan, B., Phukan, M., Kumar, R. (2024). Breeding Device for Fish. Indian Design No.: 406560-001. The Patent Office, Government of India.

Appendix

Bundesrepublik Deutschland

Urkunde

über die Eintragung des
Gebrauchsmusters Nr. 20 2024 100 859

Bezeichnung:
Ein System zur Bewertung der restaurativen Wirkung von EGCG auf veränderte
Stoffwechselenzyme in einem Streptozotocin-induzierten diabetischen
Zebrafisch-Modell

IPC:
C12Q 1/52

Inhaber/inhaberin:
Jamir, Ajungla, Kohima, Nagaland, IN
Kumar, Ranjit, Patna, Bihar, IN
Longkumer, Sentiyanger, Ungma, Nagaland, IN
Pankaj, Pranay, Bhagalpur, Bihar, IN
Phukan, Mayur, Dibrugarh, Assam, IN

Tag der Anmeldung:
22.02.2024

Tag der Eintragung:
04.03.2024

Die Präsidentin des Deutschen Patent- und Markenamts

Eva Schewior
Eva Schewior

München, 04.03.2024

Die Voraussetzungen der Schutzfähigkeit werden bei der Eintragung eines Gebrauchsmusters nicht geprüft.
Den aktuellen Rechtsstand und Schutzzumfang entnehmen Sie bitte dem DPMAregister unter www.dpma.de.

पेटेंट कार्यालय, भारत सरकार **The Patent Office, Government Of India**

डिजाइन के पंजीकरण का प्रमाण पत्र **Certificate of Registration of Design**

डिजाइन सं. / Design No. : 406559-001

तारीख / Date : 03/02/2024

पारस्परिकता तारीख / Reciprocity Date* :

देश / Country :

प्रमाणित किया जाता है कि संलग्न प्रति में वर्णित डिजाइन जो **LABORATORY SYSTEM FOR MAINTENANCE OF SMALL ORNAMENTAL FISH** से संबंधित है, का पंजीकरण, श्रेणी - 30-99 में 1.Pranay Pankaj 2. Sentiyanger Longkumer 3.Ajungla Jamir 4.Bupesh Girdharan 5.Mayur Phukan 6.Ranjit Kumar के नाम में उपर्युक्त संख्या और तारीख में कर लिया गया है।

Certified that the design of which a copy is annexed hereto has been registered as of the number and date given above in class 30-99 in respect of the application of such design to **LABORATORY SYSTEM FOR MAINTENANCE OF SMALL ORNAMENTAL FISH** in the name of 1.Pranay Pankaj 2. Sentiyanger Longkumer 3.Ajungla Jamir 4.Bupesh Girdharan 5.Mayur Phukan 6.Ranjit Kumar.

डिजाइन अधिनियम, 2000 तथा डिजाइन नियम, 2001 के अध्यायीन प्रावधानों के अनुसरण में।
In pursuance of and subject to the provisions of the Designs Act, 2000 and the Designs Rules, 2001.

जारी करने की तिथि : 02/04/2024

महाप्रमुख पेटेंट, डिजाइन और व्यापार चिह्न
Controller General of Patents, Designs and Trade Marks

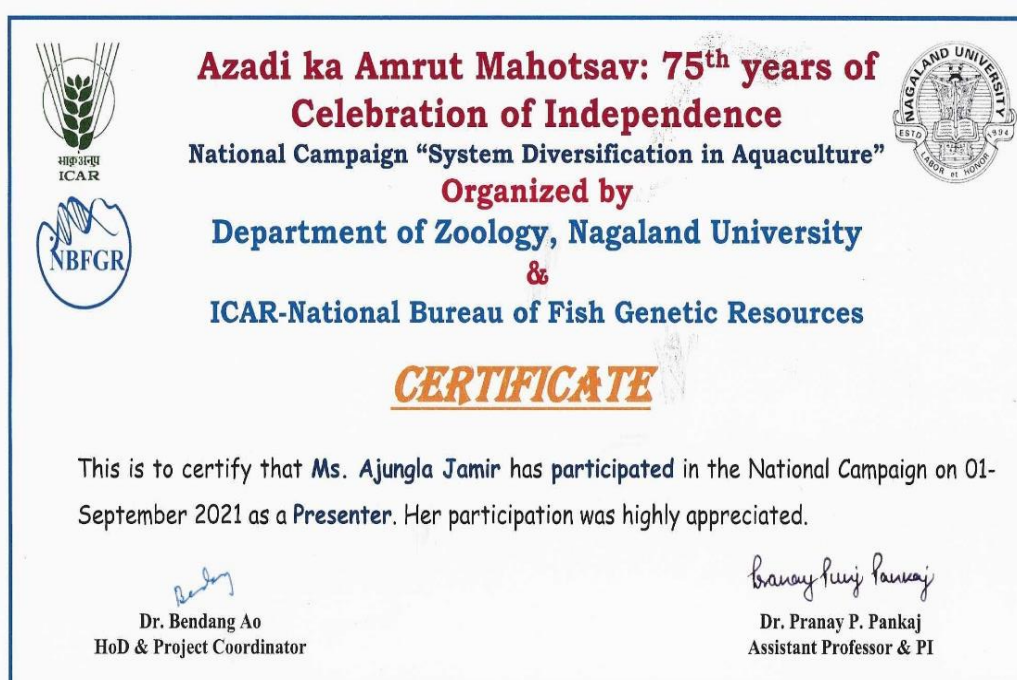
पारस्परिकता तारीख (यदि कोई हो) जिसकी अनुमति दी गई है तथा देश का नाम। डिजाइन का स्वतंत्रतापूर्वक पंजीकरण की तारीख से इस वर्षों के लिए लोग विपणन विस्तार, अधिनियम एवं नियम के नियमों के अधीन, पाँच वर्षों की अवधि के लिए किया जा सकेगा। इस प्रमाण पत्र का उपयोग विधिक कार्यवाही में अथवा विदेश में पंजीकरण प्राप्त करने के लिए नहीं हो सकता है।
The reciprocity date (if any) which has been allowed and the name of the country. Copyright in the design will subsist for ten years from the date of Registration, and may under the terms of the Act and Rules, be extended for a further period of five years. This Certificate is not for use in legal proceedings or for obtaining registration abroad.

Appendix

Himalayan Environment (GBNIHE) supported by Himalayan Knowledge Network, held on 31st March 2023.

International conferences

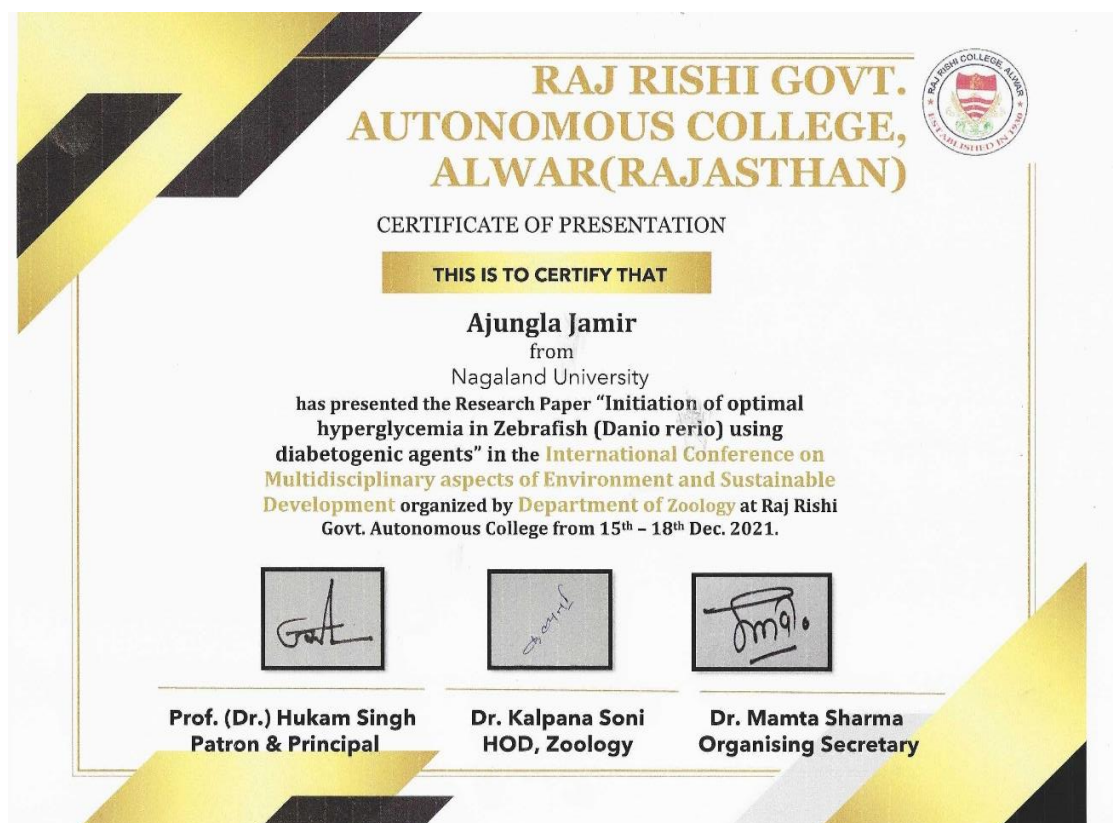
1. Oral presentation on the topic “Improvement of caudal fin regeneration in diabetic induced zebrafish (*Danio rerio*) using Epigallocatechin gallate (EGCG)” at International E-Conference on Sustainable and Futuristic Materials (SFM-2021), Organized by the international research center and department of chemistry Kalasalingam academy of research and education, Krishnankoil held from 29th -30th November 2021.
2. Oral presentation on the topic, “Initiation of Optimal Hyperglycemia in Zebrafish (*Danio rerio*) Using Diabetogenic Agents” at the International Conference on the Multidisciplinary Aspects of Environment and Sustainable Development after the Covid-19 Pandemic, organised by Raj Rishi (GOVT.) Autonomous College Alwar, 301001 (Rajasthan) Department of Zoology held from 15th -18th December 2021.
3. Oral presentation on the topic, “Assessment of Acute Toxicity and Histopathological Alteration in Liver and Gill of Zebrafish (*Danio rerio*) Exposed to Epigallocatechin gallate” at 3rd international conference on environmental, agricultural, chemical and biological sciences organised by Voice of India concern for the environment (VOICE) held from 22nd – 26th January 2022.



Appendix



Appendix



Appendix

VOICE- Virtual 3rd International Conference on ENVIRONMENTAL, AGRICULTURAL, CHEMICAL AND BIOLOGICAL SCIENCES

#ICEACBS2022

IN SUPPORT OF

UNITED NATIONS- SDGS
JANUARY 22, 23, 26, 2022



ORGANIZED BY

Voice Of Indian Concern for the Environment (VOICE) www.vvoice.weebly.com/ www.voiceindia.org.in
in association with
CAFRE & LINK-CAFRE, University of Pisa, Pisa, Italy
Murray State University, Murray, Kentucky, United States of America
The American College, Madurai, Tamilnadu, India
Kamaraj College, Thoothukudi, Tamilnadu, India
Vivekananda College of Arts and Sciences for Women, Tiruchengode, Tamilnadu, India
Rathinam College of Arts and Science, Coimbatore, Tamilnadu, India
Shree Venkateshwara Arts and Science College, Gobichettipalayam, Tamilnadu, India



Certificate of Presentation

This is to certify that

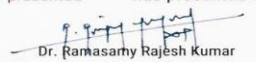
Ajungla Jamir * and Pranay Punj Pankaj

Department of Zoology, Nagaland University

Assessment of Acute Toxicity and Histopathological Alterations in Liver and Gill of Zebrafish (Danio rerio) exposed to Epigallocatechin gallate

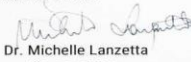
ppt

*author presented has presented in the above-said topic during the conference.


Dr. Ramesh Rajesh Kumar

Convener and Organizing Secretary

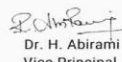
Founder- Voice Of Indian Concern for the Environment


Dr. Michelle Lanzetta

Co-organizer

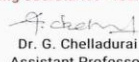
Director- CAFRE, University of Pisa, Italy

Co-organizing Secretaries - ICEACBS2022


Dr. H. Abirami

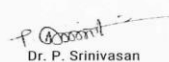
Vice Principal

Vivekananda College of Arts and Sciences for Women, Tamilnadu, India

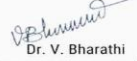

Dr. G. Chelladurai

Assistant Professor

PG and Research Dept of Zoology, Kamaraj College, Tamilnadu, India

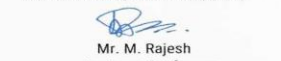

Dr. P. Srinivasan

Assistant Professor and Head
Dept of Microbiology, Rathinam College of Arts & Science, Tamilnadu, India


Dr. V. Bharathi

Assistant Professor and Head
Dept of Microbiology, Shree Venkateshwara Arts & Science College, Tamilnadu, India




Mr. M. Rajesh
Assistant Professor
PG Research Dept of Zoology, The American College, Tamilnadu, India

Appendix

Workshops & Seminars attended

1. National seminar on Chemistry in Interdisciplinary Research (NSCIR-2018) organised by the Department of Chemistry, Nagaland University from 9th – 10th November 2018.
2. National workshop on “Newer Frontier in Bioinformatics and Research Methodology” organised by Bioinformatics Infrastructure Facility (BIF) Centre, Nagaland University, Lumami, sponsored by Department of Biotechnology Ministry of Science and Technology, Government of India from 13th – 19th November 2018.
3. ICSSR sponsored National Seminar on “Writing Quality Research Papers: Preparation, Presentation, and Production” organised by Fazl Ali College, Mokokchung, Nagaland held on 22nd February 2019.
4. Sensitization workshop on DST- Women Scientist Scheme, organised by Department of Science and Technology, Government of India, New Delhi and Nagaland University at SASRD Medziphema, from 4th- 5th March 2019.
5. One-day workshop on “Importance of IPR in Academic Institutions” organised by IPR cell, Nagaland University, held on 29th May 2019.
6. Course on “Anti-inflammatory Life style for Prevention and Treatment of Cancer and Neurodegeneration: Facts and Fiction” by Global Initiative of Academic Networks (GIAN) at Zoology Department, Nagaland University, Lumami from 1st -5th October 2019.
7. Two Days Workshop on Intellectual Property Rights Organised by Fazl Ali College, Mokokchung in Collaboration with Patent Information Centre, Department of Science & Technology, Government of Nagaland, sponsored by Rajiv Gandhi National Institute of Youth Development, Sriperumbudur, Tamil Nadu held on 28th -29th January, 2021.
8. National webinar on “Recent Trends in Science and Technology” organised by Department of Computer Application, North-Eastern Hill University, Tura Campus, Meghalaya, India from 25th -26th February 2021.
9. Two-day workshop on “Quality Enhancement in Research” organised by IQAC Nagaland University held on 22nd -23rd March 2021.
10. National Seminar on “Contemporary Research in Biotechnology" Organized by the Department of Biotechnology & Bioinformatics, North-Eastern Hill University, Shillong-793022 on 25th March 2021.
11. Webinars on “Designing Rational Combination Therapies to treat Chemoresistant Breast and Ovarian Cancers; Crosstalk between Prostate Cancer and Microenvironment Reveals New Therapeutic Targets; Prostate Cancer Progression: Novel Signaling Mechanisms and Mouse Models” organized by Mizoram University on 6th September 2021.
12. Webinar on “Biotechnology in Drug discovery & Clinical applications” organized by Mizoram University on 7th September 2021.

Appendix

13. Webinar September Recent Advances in Cancer Research and Treatment: Conventional and Herbal methods organised by Department of Botany, Rajiv Gandhi University, Arunachal Pradesh, Tata Memorial Centre, ACTREC, Kharghar, Navi Mumbai and Mahatma Gandhi Institute of Medical Sciences, Sevagram held on 27th September 2021.
14. Eight Days International author workshop on “Academic Writing and Publishing” in collaboration with the renowned publishers (Elsevier, Taylor and Francis, Cambridge University Press, Springer Nature, Brill, Oxford University Press, Emerald, and Wiley) organized by Manipur University Library held during 21-29 October 2021.
15. Two days online workshop on “Recent Advancements in Biomedical Imaging and Image Processing” organized by Department of Biomedical Engineering, School of Technology, North-Eastern Hill University, Shillong, Meghalaya, INDIA, under the Azadi ka Amrit Mahotsav program held on 8th – 9th November, 2021.
16. Webinar on the topic ‘Transcranial Magnetic Stimulation to treat Obesity and Diabetes’organised by Department of Horticulture, Aromatic and Medicinal Plants, Mizoram University, Aizawl, held on 4th April 2022.